MEIRE ELLEN GORETE RIBEIRO DOMINGOS

Integrated production of chemicals and fuels in the pulp industry: techno-economic and environmental analysis of black liquor gasification-based processes

São Paulo
2023

MEIRE ELLEN GORETE RIBEIRO DOMINGOS

Integrated production of chemicals and fuels in the pulp industry: techno-economic and environmental analysis of black liquor gasification-based processes

Corrected version

Thesis presented to the Polytechnic School of the University of São Paulo to obtain the degree of Doctor of Science.

Concentration area: Chemical Engineering

Advisor: Prof. Dr. Moisés Teles dos Santos

São Paulo
2023

Este exemplar foi revisado e corrigido em relação à versão original, sob responsabilidade única do autor e com a anuência de seu orientador.

São Paulo, _____ de _____ de _____

Assinatura do autor: _____

Assinatura do orientador: _____

Catalogação-na-publicação

Domingos, Meire Ellen Gorete Ribeiro
Integrated production of chemicals and fuels in the pulp industry: techno economic and environmental analysis of black liquor gasification-based processes / M. E. G. R. Domingos -- versão corr. -- São Paulo, 2023.
216 p.

Tese (Doutorado) - Escola Politécnica da Universidade de São Paulo. Departamento de Engenharia Química.

1.Gaseificação 2.Integração de processos 3.Biorrefinarias 4.Otimização matemática 5.Descarbonização I.Universidade de São Paulo. Escola Politécnica. Departamento de Engenharia Química II.t.

DOMINGOS, M. E. G. R. - Integrated production of chemicals and fuels in the pulp industry: techno-economic and environmental analysis of black liquor gasification-based processes. Thesis (Doctor of Science in Chemical Engineering) - Polytechnic School, University of São Paulo, São Paulo, 2023.

Approved on _____

Examination board:

Prof. Dr. _____
Institution _____
Decision _____

Prof. Dr. _____
Institution _____
Decision _____

Prof. Dr. _____
Institution _____
Decision _____

Prof. Dr. _____
Institution _____
Decision _____

Prof. Dr. _____
Institution _____
Decision _____

"*Nothing in life is to be feared, it is only to be understood. Now is the time to understand more, so that we may fear less*."

Marie Curie

To my family, for the unconditional support to all my dreams.

Para minha família, pelo apoio incondicional a todos os meus sonhos.

Acknowledgments

At the end of my PhD journey, I really feel grateful to many people.

First, I would like to express my sincere gratitude to my supervisor, Prof. Dr. Moisés Teles, for giving me the opportunity to pursue my PhD studies under your guidance. Thank you very much for the trust, for the continuous support, the valuable comments and advices. You are not only a great scientist and mentor, but an even greater person and a true inspiration.

I would like to thanks Prof. Dr. Silvio de Oliveira Junior for enlightening my world perspective through the exergy concept and for all the discussions and feedbacks that deeply contributed to this thesis. I also would like to thank to Prof. Dr. François Maréchal for all the support and welcoming during my exchange in your lab at the École Polytechnique Fédérale de Lausanne. Thank you so much for your constant motivation, inspiring discussions and for the opportunity of interacting with a highly qualified team of scientists.

I am very grateful to all my professors from the University of Sao Paulo, in special Prof. Dr. Celma Ribeiro, Prof. Dr. Song Park, Prof. Dr. Galo le Roux, Prof. Dr. Ardson Vianna, Prof. Dr. Jorge Gut, Prof. Dr. Reinaldo Giudici and Prof. Dr. Erik Rego for the precious instructions received in your classes and discussions.

My deepest thanks to all the professors that contributed to my formation since the beginning!

I am wholeheartedly thank to my parents, Menir and Dario, and to my sister, Marcela, for always believing in me and for the endless support. I owe you everything, and I am very blessed to have you as my family. Thank you so much for the example, and for always encouraging me to do my best and face every difficult that may come. We made it!

My deepest thanks to my grandparents Nadir, Pedro*, Merice* and Orlando* (**in memoriam*) that always encouraged and supported me to pursue my studies. This thesis is also yours!

My special thanks to Daniel, for being present during this journey, for the endless support, fruitful discussions, for believing in me, and for the constant motivation to go further. I cannot fit all my gratitude for you in sentences, but your presence turned this adventure remarkable.

My warmest thanks to my friends, Lola, Chico, Kaccnny, Renata, Tallys, Talita e Marcela, for always encouraging me, sharing my happiness and for all the unforgettable memories. And their families that I also consider as mine, Janaina, Tulis, Wesley, Voninha, Theozinho, Denise. Thank you Lola, for being like a sister to me, I also don’t have words to express my gratitude to you, for always being there for me. Chico many thanks for your

friendship, support and unique sense of humor. Kacc and Renata thanks for being the best flatmates and share the life in SP. Tallys for teaching me that everything is gonna be allright. Talita and Marcela, thanks for the unconditional friendship and continuous support over the distances.

Many thanks to my colleagues and friends of the University of Sao Paulo, Alexandre, Priscilla, João, Rafael David, Tamires, Rafael Nakashima, Thamiris, Matheus, Maria, Bruno Theozzo, Elcio, Marcus, Ana, Larissa, Diego, and many others that I had the joyful opportunity to meet and share this journey.

I am very grateful to my colleagues of the Industrial Process and Energy Systems Engineering (IPESE) group. Many thanks for having the opportunity to know all of you and share valuable discussions and happy memories, Marie, Shivom, Xinyi, Yi, Cedric, Naveen, Eduardo, Luise, Ivan, Julia, Sylvie, Rafael, Luc, Jonas, Dorsan and Xiang.

I would like to acknowledge the valuable job of the personnel of the Department of Chemical Engineering of the University of Sao Paulo.

Thank you very much CNPq and the Swiss Government Excellence scholarship for the financial support.

Many thanks to everyone who contributed in some way to this work.

And God, for everything.

Resumo

O setor de celulose e papel é classificado como uma atividade intensiva em energia e vários esforços estão sendo feitos para mitigar as emissões atmosféricas, melhorar a recuperação do calor residual e capitalizar os seus subprodutos. O licor negro (LN) é um subproduto do processo de polpação kraft, que contém mais da metade da energia total da madeira alimentada no processo, representando assim uma importante fonte de energia renovável. O LN pode ser gaseificado e o gás de síntese pode ser usado para gerar eletricidade ou produzir produtos químicos e biocombustíveis, através do conceito de biorrefinaria. Neste trabalho, o cenário convencional do uso do LN (concentração e combustão) é comparado com o processo de gaseificação do LN para a produção de diferentes produtos (hidrogênio, gás natural sintético, metanol, dimetil éter, amônia, uréia e ácido nítrico), em termos de indicadores econômicos, eficiência exergética e impacto ambiental. Além disso, a integração energética combinada à análise exergética é usada para identificar as potenciais melhorias que poderiam permanecer ocultas se apenas a análise energética fosse feita, como a determinação e mitigação das irreversibilidades do processo. A síntese, modelagem e simulação dos processos químicos são realizadas no software Aspen Plus®. A determinação dos requisitos mínimos de energia e a solução do problema de integração energética são tratadas na plataforma OSMOSE Lua. Uma análise de sensibilidade da variação do INPV em função da taxa de carbono (0-100 EUR/t_{CO2}) e da taxa de juros (0-21%) também é feita. Inicialmente, assume-se que os preços da matéria-prima e dos produtos são constantes. Em seguida, a análise financeira incremental incorpora a incerteza relacionada aos custos de aquisição e venda das matérias-primas e combustíveis produzidos, quando inseridos em um mercado volátil, através do método de Monte Carlo. Como resultado, as eficiências exergéticas do cenário convencional e das plantas integradas são em média 40% e 43%, respectivamente; enquanto o balanço geral de emissões varia de 1.97 a -0.79 t_{CO2}/t_{Pulp}, respectivamente. Antecipando cenários futuros de taxação de carbono, a análise econômica incremental mostrou que a rota de produção de combustíveis e produtos químicos com importação parcial de eletricidade pode ter melhor performance econômica do que a planta de celulose kraft convencional para taxas de carbono moderadas (30-100 EUR/t_{CO2}), dependendo da taxa de juros adotada. Esses resultados reforçam a relevância da importação de eletricidade da matriz energética brasileira para aumentar a participação de recursos energéticos renováveis na produção de produtos químicos e combustíveis tradicionalmente de base fóssil, o que pode ser um importante fator a favor da exploração de biorrefinarias integradas.

Palavras-chave: Gaseificação, Integração de processos, Biorrefinarias, Otimização matemática, Descarbonização.

Abstract

The pulp and paper sector is classified as an energy intensive activity and several efforts are being made to mitigate its atmospheric emissions, improve the recovery of residual heat and capitalize on its byproducts. The black liquor (BL) is a byproduct of the kraft pulping process, which contains more than half of the energy content in the total woody biomass fed to the process, thus, representing a key supply of renewable energy to the pulping process. The BL can be gasified and the syngas can be used to generate electricity or produce chemicals and biofuels, through the broader biorefinery concept. In this work, the conventional scenario of the BL use (i.e. concentration and combustion) is compared with the BL upgrading gasification process for different chemicals and fuels (namely, hydrogen, synthetic natural gas, methanol, dimethyl ether, ammonia, urea and nitric acid) production, in terms of economics, exergy efficiency and environmental impact. A combined energy integration and exergy analysis is used to identify the potential improvements that may remain hidden to the energy analysis alone, namely, the determination and mitigation of the process irreversibility. The chemical processes synthesis, modelling and simulation are performed by using Aspen Plus® software. Meanwhile, the determination of the minimum energy requirements and the solution of the energy integration problem is handled by the OSMOSE Lua platform. A sensitivity analysis of the variation of the INPV as a function of the carbon taxation (0-100 EUR/t_{CO2}) and the interest rate (0-21%) is performed. Firstly, it is assumed that the present values of the feedstock and the products are constant. Next, the incremental financial analysis incorporates the uncertainty related to the acquisition and selling costs of the feedstock and fuels produced, when embedded in a volatile market, by using the Monte Carlo method. As a result, the exergy efficiencies of the conventional setup and the kraft pulp and the integrated plants average 40% and 43%, respectively; whereas the overall emission balance varies from 1.97 to -0.79 t_{CO2}/t_{Pulp}, respectively. In anticipation of future carbon taxation scenarios, the incremental economic analysis found that the fuels and chemicals production route with partial electricity import may economically outperform the conventional kraft pulp mill for moderate carbon taxations (30-100 EUR/t_{CO2}), depending on the interest rate adopted. These results reinforce the relevance of the electricity import from the Brazilian mix for pushing upwards the share of renewable energy resources in the production of traditionally fossil-based chemicals and fuels, which could be an important factor in favor to the exploration of integrated biorefineries.

Keywords: Gasification, Process integration, Biorefinery, Mathematical optimization, Decarbonization.

List of figures

List of tables

List of abbreviations and acronyms

ATR	autothermal reformer
BFW	boiler feedwater
BL	black liquor
BLG	black liquor gasification
BLGCC	black liquor gasification combined cycle
CAPE	Computer Aided Process Engineering
CAPEX	capital expenditure
CCS	carbon capture and storage
CFD	computational fluid dynamics
CW	cooling water
DC	distillation column
DCTIR_SC	deterministic carbon taxes and interest rates, stochastic prices of the commodities
DEPG	diethyl propylene glycol
DME	dimethyl ether
FEHE	feed-effluent heat-exchanger
HT	high temperature
INPV	incremental net present value
LCT_DIR_SC	linearly-increasing carbon taxes over the lifespan, deterministic interest rates and stochastic prices of commodities
LHT	liquor heat treatment
LHHW	Langmuir-Hinshelwood Hougen-Watson
LN	licor negro
LT	low temperature
MeOH	methanol
MEE	multiple effect evaporators
MER	minimum energy requirement
MILP	mixed integer linear programming
MINLP	mixed integer non-linear programming
Mt	millions of tons
MVR	mechanical vapor recompression
MTCI	Manufacturing and Technology Conversion International
NRTL-RK	nonrandom two liquid Redlich−Kwong
OPEX	operating costs
PC-SAFT	perturbed-chain statistical associating fluid theory
PEHT-BLG	pressurized entrained-flow, high temperature black liquor gasification
PPI	pulp and paper industry
PSA	pressure swing adsorption
RANS	Reynolds Averaged Navier-Stokes
SCTC_DIR	stochastic carbon taxes and variable prices of the commodities, deterministic interest rates.
SNG	synthetic natural gas
TRI	ThermoChem Recovery International
WGS	water gas shift
wt.	mass fraction (%)

Subscripts

AD	air dried
BL	black liquor
Dest.	destroyed
exp.	exported
imp.	imported
r	interval of temperature

Superscripts

CH	chemical exergy
K	kinetic
P	potential
PH	physical

List of symbols

Latin symbols

b	specific chemical exergy (kJ kg^{-1})
B	chemical exergy (kJ)
C	carbon mass fraction (%)
c	market costs and selling prices for feedstock and products (€ per kWh or kg)
C_0, C_1	cost at the reference scale (€)
C_p	specific heat at constant pressure (J kg^{-1} K^{-1})
E	activation energy (kJ/mol)
Exp	expenses (€)
f	unit load optimization factor (-)
g	standard molar energy of Gibbs, acceleration of gravity (m s^{-2})
h	specific enthalpy (kJ kg^{-1})
h_0	specific enthalpy at standard conditions (kJ kg^{-1})
h_{lv}	enthalpy of evaporation of water at standard conditions (kJ kg^{-1})
H	hydrogen mass fraction (%), enthalpy flow rate (kW)
HHV	higher heating value (kJ/kg)
i	interest rate (%)
K	reaction constant (m^3.mol^{-1}.min^{-1})
k_0	rate constant (kmol m^{-3} s^{-1} Pa^{-1}))
k	kinetic energy, thermal conductivity (J s^{-1} m^{-1} K^{-1})
LHV	lower heating value (kJ/kg)
M	molecular mass (kg $kmol^{-1}$)
MC_{eq}	equilibrium moisture content (%)
m	mass flow rate (kg/h)
N	number of utility units, temperature intervals, yearly periods, nitrogen mass fraction (%), number of effects
n	number of moles, total molar flow of the mixture (kmol h^{-1})
O	oxygen mass fraction (%)
P	partial pressure, total pressure (bar)

Q	heat flow (kW)
q	cooling or heating duty from the utility systems (kW)
R	universal gas constant, cascaded heat rate (kW)
Rev	revenues (€)
r	reaction rate (kmol m^{-3} s^{-1}), scale exponent
SN	stoichiometric number (-)
s	specific entropy (kJ $kg^{-1}K^{-1}$)
s_0	specific entropy at standard conditions (kJ $kg^{-1}K^{-1}$)
S_0	reference scale capacity (various)
S_1	actual scale capacity (various)
S_i	swirl number (-)
S_T	source term
T	temperature (°C, K)
t	time (s, h)
U	mean velocity (m s^{-1})
u'	fluctuating velocity (m s^{-1})
$\vec{v}$	velocity (vector) (m s^{-1})
W	power (kW), weight
x_i	mol fraction (%)
y	mass fraction (%), binary (existence) optimization factor
z	elevation (scalar) of the system (m)

Greek symbols

γ_i	activity coefficient (-)
δ	Kronecker delta
ε	dissipation (m^2 s^{-3})
η	exergy efficiency (%)
Θ	Carnot factor (-)
λ	renewability performance indicator (-)
ν	kinematic viscosity (m^2 s^{-1})
ρ	density (kg m^{-3})
σ_{ij}	stress tensor (kg m^{-1} s^{-2})
τ	Reynolds stress tensor (kg m^{-1} s^{-2})
φ	ratio of the chemical exergy to the lower heating (-)
ω	utility or process unit

TABLE OF CONTENTS

CHAPTER 1: INTRODUCTION

Due to increasing concerns about the environmental impact of the production of power, fuels and chemicals, many efforts are put to come up with alternatives to attend these demands in more sustainable ways. However, the adopted approaches must deal not only with the mitigation of emissions but also take into account the uncertainties about the prices of the energy supplies and carbon taxes likely adopted in future scenarios of more severe environmental regulations. To couple rigorous process models with economic analysis in uncertainty scenarios is a pathway to boost the bioeconomy.

The pulp and paper industry (PPI) can play an important role in the so-called decarbonization process, since it is a well stablished biomass-based activity worldwide and one of the most important economic activities. Brazil is the second largest pulp producer, only behind the United States, being responsible for more than 11% of the global production [1]. Even with the Covid-19 pandemic, the pulp production in Brazil presented a growth of 6.6% in 2020 compared to 2019 [2]. Brazilian competitiveness comes from highly favorable climate and soil conditions and from a long history of investment in research, development and forest innovation [3].

Moreover, this industry presents some industrial challenges. The PPI is considered one of the largest consumers of energy inputs in the industrial sector (fuel oil, natural gas, coal, wood for energy and electricity) [4]. According to the International Energy Agency and the Energy Research Office, this sector accounted for 5.3% of industrial energy consumption in 2020 at a global level [1], where the bioenergy and alternative fuels (mainly due to the use of the by-products such as black liquor) represent around only 30% of the total energy use [4]. The fossil fuels are primarily used for onsite utilities, and decarbonizing these utilities by switching to lower-carbon fuels allows to a significant impact. On the other hand, in the Brazilian scenario, the pulp and paper industry presents a high level of renewable energy resources, around 89% in 2020, but it ends up accounting for over 16% of the industrial energy consumption [1]. Thus, it very important to adopt measures to use energy more efficiently.

Despite the fact that biomass is the main material feedstock, the carbon emissions of the PPI sector amounts up to 2.3% of the global industrial direct CO_2 emissions, only behind cement, iron and steel, chemicals and petro-chemicals industries [5]. Accordingly, there is still room for improvement of its environmental performance, besides of being an opportunity to revise the business model of the PPI sector, enhancing its competitiveness by adding new

revenues streams [6]. The use of low-carbon electricity, together with the reduction of the heating requirement, the diversification of the fuel and feedstock with a secure supply of biomass, the increase of the component-wise efficiency, the enhanced waste heat recovery and the black liquor gasification, are potential strategies to decarbonize or improve the energy efficiency in this sector [7; 8].

A potential pathway for long-term sustainable growth of the pulp and paper industry that can improve its efficiency and profitability is the integration of biorefineries into the existing facilities [9]. The black liquor (BL) is a byproduct of the kraft pulping process, and it can be an important feedstock for alternatives assessments purposes, since it contains more than half of the energy content in the total woody biomass. The syngas produced from the gasification process of BL can be used either to generate electricity or produce chemicals and biofuels, such as hydrogen, ammonia, methanol, dimethyl ether and many others, thus, expanding the products portfolio and matching the biorefinery concept.

Although alternative pathways for hydrogen production, such as the use of electrolyzers working with solar or wind energy, and for the separation of nitrogen from air (cryogenic distillation, selective membranes, etc.), have been proposed [10], the upstream inefficiencies of these energy sources are usually not considered, not assuming them as sources of greenhouse gas emissions. Nevertheless, the overall CO_2 emissions balances should account for direct emissions as well as indirect emissions, derived from the previous stages of fuel processing, i.e. such as extraction, transportation, fabrication, construction, operation and decommissioning of the power plant. According to some authors, Brazilian electricity generation is 8 to 12 times less CO_2 intensive, if compared with USA and China electricity mixes, respectively [11]. Thus, a wholesome assessment must quantify the influence of the utilization of the electricity itself and other processed fuels in the different industrial production routes. In this context, the most promising alternative energy resources for hydrogen production remain to be the thermochemical conversion routes, especially for capitalizing on the underexploited biomass potential in tropical countries with a well-established biomass conversion expertise, such as Brazil.

Meanwhile, the main drawbacks of the biomass-based chemicals and fuels synthesis continue to be associated with the high investment risk, the availability of biomass and the scale-up of this technology, since it is still not as competitive as the capacities of the traditional commercial processes based on fossil sources. Despite this limitation, the larger pressurized biomass gasifiers are expected to aid increasing the performance of biomass conversion process [12]. Moreover, the limited access to fossil resources, such as natural gas and coal, mainly due to

shortage or unstable international prices, may turn this technology even more attractive [13]. Also, more stringent environmental regulations, along with increasing concerns about the market dependence, have led researchers to look for the use of the readily available biomass residues to produce commodities currently based on fossil resources [14; 15; 16]. In this context, black liquor gasification may be considered a more efficient and environmentally friendly alternative compared to current black liquor combustion, aside from promoting the diversification of the energy inputs, while requiring only a minimum additional investment cost.

In this work a holistic approach that considers thermodynamic and environmental performances, along with the economic implications of the feedstock and fuels price variation over the plant lifespan are addressed. The scenario of the conventional utilization of black liquor in a kraft pulp mill (i.e. concentration and combustion) is compared to the BL upgrading gasification process for power generation using gas turbines, and also for different chemicals and fuels production. Those fuels and chemicals are reported as potential low-carbon products that may help decarbonizing other sectors [17]. The exergy destruction and the cumulative CO_2 emissions are considered as criteria for assessing the sustainability of the energy conversion systems. In this way, the extended exergy method takes into account the inefficiencies of the different upstream supply chains, which provides a more accurate estimation of the environmental impacts. Finally, an incremental techno-economic assessment helps elucidating the effect of the uncertainty of the feedstock costs and the carbon taxes on the financial feasibility of the proposed process.

1.1 Relevance

The competitive pressure and environmental issues force pulp mills to continue reducing emissions, better manage resources and process residues, and also to reinvent themselves from production of a single commodity to offer multiple value-added chemicals and fuels. The IPCC recently published that to limit the global temperature to around 1.5 °C it is required to reduce the global greenhouse emissions by 43% by 2030 and reach net zero emissions in the early 2050s [18]. This is an opportunity not only to depletion emissions but also to decarbonize the processes of other commodities that may be produced in units integrated with the pulp industry. Furthermore, pulp and paper mills are logical sites for increased biomass use because of their experience in handling lignocellulosic materials and a readily available infrastructure (biomass feedstock transportation, utilities production and products logistics).

Due to its large territory, different climate areas and hosting one of the largest world's biodiversity, Brazil is also recognized as one of the countries able to lead the change for a low-carbon bio-based economy. Also, the pulp and paper sector already controls much of the raw material and infrastructure necessary to create Integrated Products Biorefineries and it is a very expressive economic sector in Brazil. In this context, forest-based biorefineries emerge as a technological solution to create value (renewable chemicals and energy) from biomass in Brazil. As biorefinery processes in Brazil are much focused on the sugarcane to produce ethanol, this work can widen the study of the biomass-based products in Brazil. Also, it is important to highlight that, the use of waste from agricultural and forestry activities in tropical countries like Brazil, with great biomass potential, can improve energy security and supply of strategic commodities for both agriculture (fertilizers) and chemical industries, which are traditionally based on fossil fuels, contributing to reduce their carbon footprint and also their dependence on the international market prices.

Literature survey [15; 19; 20; 21] shows a series of relevant findings in the field of modelling and analysis of black liquor upgrade strategies; however they mostly consist of specific scenarios and case study approaches. Notwithstanding, none of them proposes either a global superstructure-based approach or systematic tools for designing, assessing and optimizing an integrated black liquor upgrade biorefinery. Accordingly, the process synthesis and optimization allow for a more comprehensive comparison between the traditional process to other possible new integrated facilities in pulp mills. For this reason, this work aims to contribute to this gap in research and develop a generic approach (considering technical, economic and environmental aspects), using optimization techniques that could be widely applicable to the conversion of black liquor via thermochemical routes for the production of fuels, chemicals and electricity.

1.2 Objectives

The main objective of this thesis is the development and application of a systematic methodology consisting of industrial process simulation and integration, as well as optimization for proposing valorization strategies of black liquor based on the gasification route. The primary aim is to decarbonize chemicals and fuels production and compare the solutions in terms of thermodynamic, economic and environmental performance metrics.

The specific objectives of this thesis are:

- To develop and implement models for the black liquor gasification process as well as for different chemicals and fuels upgrading routes using the syngas, and also a methodology for analyzing those facilities with respect to multiple criteria (e.g. thermodynamic, environmental, economic).
- To implement an optimization framework that minimizes energy requirements of the alternative routes proposed by exploring the synergies via process integration, aiming to maximize the process performance and minimize the production costs.
- To apply the combined energy integration and exergy analysis that takes into account the upstream supply chains inefficiencies for the different energy inputs (electricity from the grid and chips) to identify the potential improvements that may remain hidden to the energy analysis alone, e.g. the mitigation of the process irreversibility.
- The use of an incremental financial analysis, which enlightens the influence of the uncertainty related to the feedstock prices and the carbon taxations on the viability of the novel integrated chemical plants.

1.3 Outline

This thesis is organized into five major parts: introduction and objectives, literature review, methodology, results and discussion, and conclusions. Chapter 2 presents the state-of-art literature review of: the kraft pulping process; the opportunities and challenges of integrated biorefineries in the pulp industry; the black liquor gasification modelling approaches; the process synthesis, integration and optimization techniques; and the exergy analysis for pulp mills. In Chapter 3 all the methods used to build, analyze and optimize the proposed routes for producing chemicals and fuels via black liquor gasification are presented. Chapter 4 addresses the results of the conventional scenarios of black liquor concentration and combustion (multiple effect evaporation or mechanical vapor recompression approaches), and also the black liquor gasification process for energy generation using gas turbines. In Chapters 5, 6 and 7 the black liquor gasification-based production routes for different chemicals and fuels are compared, divided as: hydrogen and synthetic natural gas in Chapter 5; methanol and dimethyl ether in Chapter 6; and ammonia, urea and nitric acid in Chapter 7. Lastly, the main conclusions, achievements and suggestions of future works are discussed in Chapter 8.

CHAPTER 2: LITERATURE REVIEW

This chapter addresses the state of the art of the main topics that guided the development of this work. First, the most traditional pulp production process, the kraft process, is presented. Then, the biorefineries opportunities applied to the pulp industry are generally discussed and, in sequence, the black liquor gasification within more details. A literature review on how the black liquor gasification is usually modelled as well as its commercial developments are also showed off. Next, the role of the process engineering tools for biorefineries and the main approaches to deal with this kind of problems are explored. Lastly, the exergy analysis applied to pulp mills is presented.

2.1 The kraft pulping process

The kraft process is currently the dominant technology employed in wood pulping. In this process, the cellulose is extracted from the wood chips under strong alkaline conditions. The simplified flowsheet of this process is represented in Figure 2.1. First, the logs are debarked, chipped, and classified. This process incurs 10% of losses of woody biomass, which will not be used as a feedstock in the digester, but as fuel in the biomass boilers [22]. Then, the white liquor (60% NaOH, 25% Na_2S, and 15% Na_2CO_3) is impregnated in the wood chips, which are subsequently fed to the digester, operating between 145 °C and 180 °C. The pulp yield varies between 45-55% of the input biomass, depending of the pulping conditions and wood quality [23; 24]. To avoid carrying over digestion chemicals to the downstream delignification unit, the pulp produced must be washed and separated from the black liquor. Next, a series of acidic and alkaline stages using hydrogen peroxide and ozone allows obtaining a bleached pulp [25]. Thereafter, the pulp moisture is reduced up to 10% and commercialized. The specific pulp yield commonly varies between 0.86 and 1.7 t_{BL}/t_{ADpulp} [19; 26].

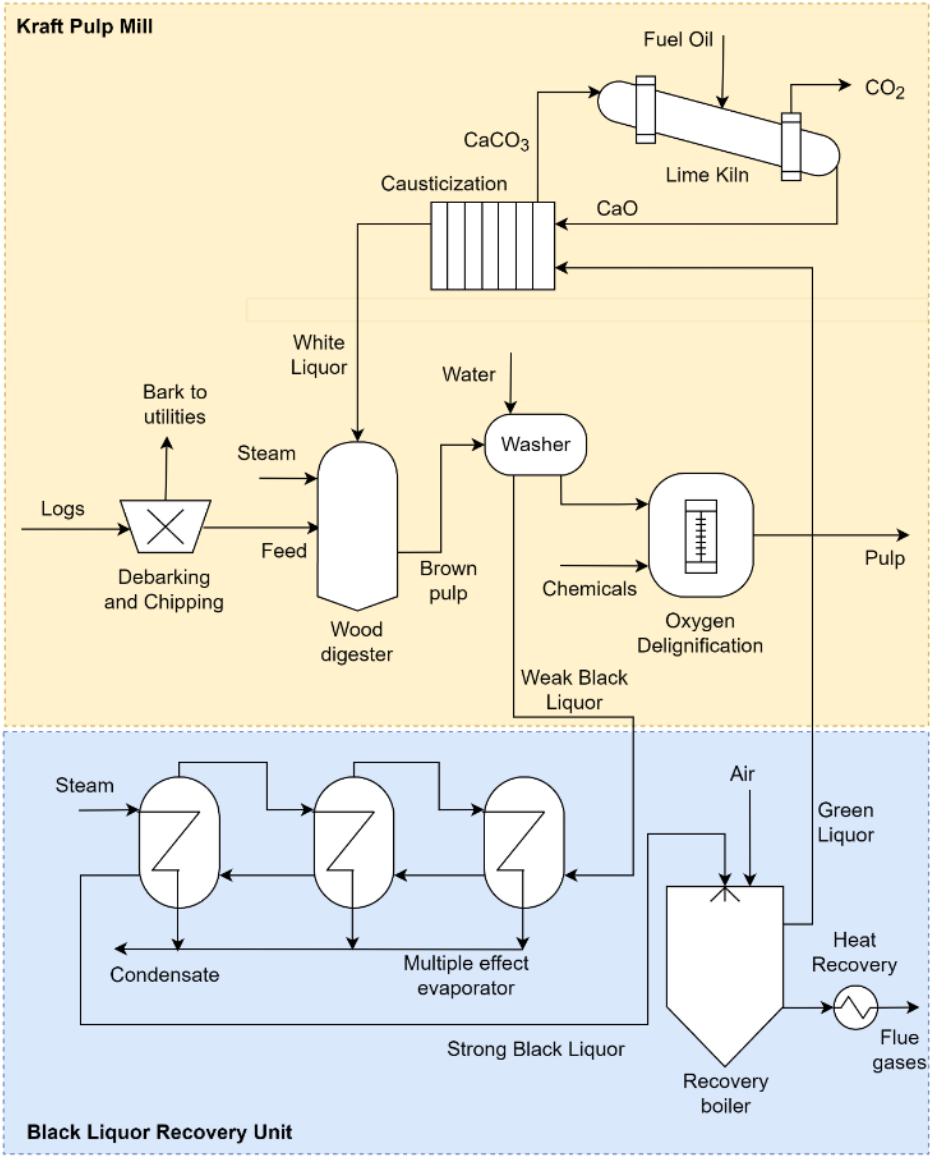

Figure 2.1 Kraft pulp mill process flowsheet with multiple effect evaporators.

The BL roughly contains half of the organic matter present in the wood, along with the chemicals used in the digestion process. In the conventional kraft pulp mill (see Figure 2.1), a series of multi-effect evaporators concentrates the weak BL coming from the digester, so it can be later burned in a recovery boiler to generate power and steam. In the combustion process, sodium sulfide and sodium carbonate are generated in the form of smelt, requiring a recausticizing process with lime in order to recuperate the chemicals that will compose the white liquor. This recovery process renders the pulp mill feasible in terms of economic and environmental points of view.

The 10% that represents the losses in the log debarking, chipping and chips classification are usually used in the biomass boiler as fuel. Due to the availability of fuel (black liquor and biomass), a modern kraft pulp mill tend to be self-sufficient in electricity (generating

90% to 100% of the electricity consumed), and the greater ones are able to produce and sell surplus electricity to local networks. The steam produced with black liquor in the recovery boilers accounts for about 80% to 100% of consumption in the pulp mill, and there is a need for supplementation in conventional boilers using biomass (bark, waste and wood chips generated for energy) [23]. Fuel oil or natural gas is widely used for lime kilns.

Figure 2.2 illustrates the steam distribution and the electric power for a pulp mill that produces 1200 t_{Pulp}/day. In this case, 220 t/h (60.11 kg/s) of steam (at 60 bar) is produced by burning 1,740 tdb/day (20.14 kg/s) of black liquor in the chemical recovery boiler, and an additional 60 t/h (16.67 kg/s) of steam is produced in the biomass boiler burning wood biomass. It can be seen that, for a cogeneration system with extraction and backpressure turbine, the mill is steam self-sufficiency with fuels derived entirely from wood (black liquor, bark and wood waste), but is not self-sufficient in electricity, needing to import 14 MW from the grid [23]. The mill is split into two steam levels i.e. medium pressure (MP) at 10-12 bar and low pressure (LP) at 4-5 bar.

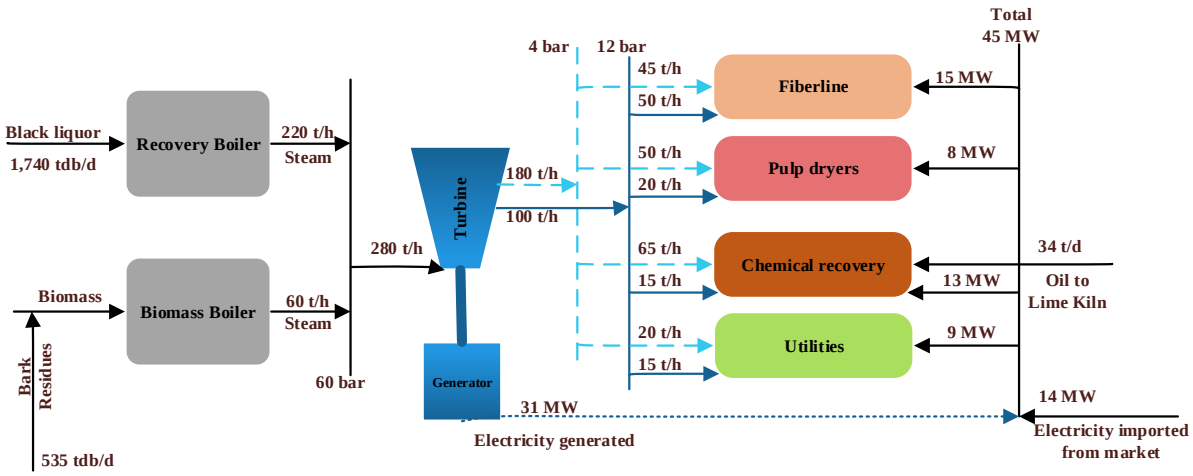

Figure 2.2 Overall mass and energy balance of a pulp mill producing 1200 t_{Pulp}/day and a cogeneration system with extraction/backpressure steam turbine. Source: adapted from [23].

An alternative consists in a cogeneration system using an extraction and condensation turbine (Figure 2.3), in which the biomass boiler needs to burn additional wood chips to make the installation self-sufficient [23]. In the process presented by Moraes (2011), the additional demand of wood to energy is 1000 m^3-solid/day, which represents 25% of the volume consumed for pulp production, in spite of saving 14 MW of electricity imported from the grid.

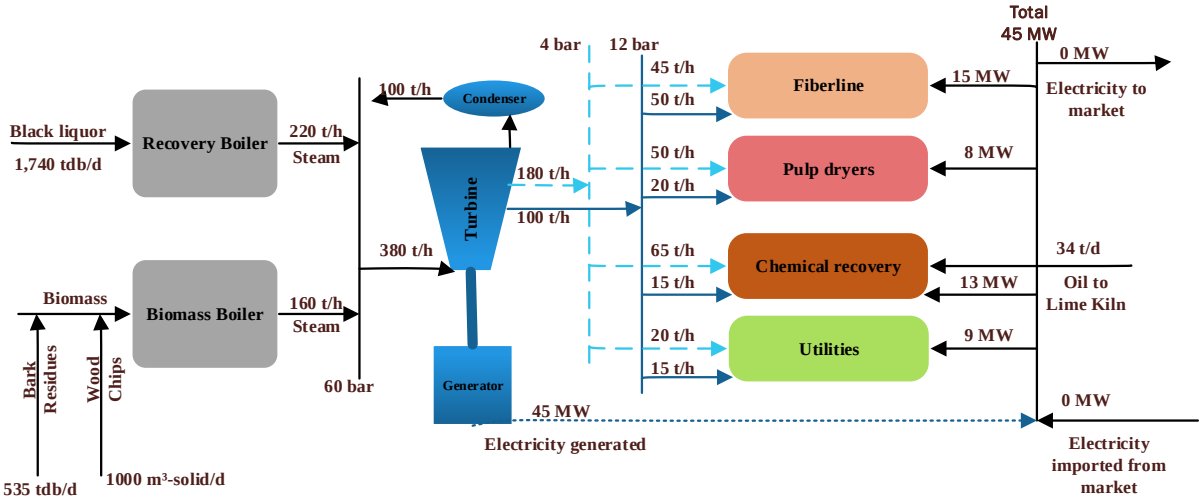

Figure 2.3 Overall mass and energy balance of a pulp mill producing 1200 t_{Pulp}/day and a cogeneration system with extraction/condensation turbine. Source: adapted from [23].

Notwithstanding, the conventional recovery boiler reportedly exhibits lower efficiency (9-14%) when used for electricity generation purposes [27]. In fact, due to the large share of exergy destruction in the digester and the recovery boiler, those components are often recognized as the least efficient energy systems in the kraft pulp mill [28]. Other systems, such as the existing multi-effect evaporation unit, also hold several drawbacks, such as fouling, foaming, and corrosion of the tubes. These problems exacerbate as the BL becomes more and more concentrated, leading to boilouts and low content of solids in the produced liquor, which greatly impacts the forthcoming processes [29]. The energy intensive BL evaporation system, responsible for nearly 50% of the steam used in the whole conventional kraft pulp mill, also represents an important source of process inefficiency, especially when dealing with the large number of hot condensates.

Regarding the environmental performance, the lime kiln, the recovery boiler, and the biomass boiler are reported as the most important sources of CO_2 emissions in the conventional kraft mill [29]. Since the introduction of CO_2 capture units in the pulp mills may increase the production cost about 30-40% [30], other strategies have been proposed to reduce their environmental impact. Those approaches include wastes energy recovery, synthesis of biofuels, fossil-fuel substitution, energy integration, and higher levels of pressures (100 bar) in the cogeneration units and the diversification of energy inputs (*e. g.* use of renewable sources of electricity) [31]. All in all, the discussed shortcomings in the conventional kraft pulp mills highlight in which direction efforts must be focused, so that the energy potential of residues can be fully exploited.

2.2 Biorefinery: opportunities and challenges for the pulp and paper sector

According to Hora et al. (2018) the pulp and paper industry is facing challenges to maintain competitiveness as a result of the high costs of wood production entailed by the low productivity of the forests, mainly in countries located in the Northern hemisphere. In contrast, in countries such as Brazil, with high forests profits and great availability of land, the future is more worthwhile. Although, considering the entry of large volumes of installed pulp capacity in low-cost regions, technological advances, and the real increase in wood production costs, the Brazilian companies should come up with new strategies aiming to improve their participation on the market, especially concerning the development of chemicals and fuels in pulp mills, with the potential to replace derivatives from fossil sources [3].

In times of growing concern about rising fuel prices, greenhouse gas emissions and oil shortages, the interest in technologies for sustainable energy production and fuel generation from renewable sources is strengthened. According to the International Energy Agency, "biorefining is the sustainable synergetic processing of biomass into a spectrum of marketable food and feed ingredients, products (chemicals, materials) and energy (fuels, power, heat)" [32]. The biorefinery approach aims to produce multiple types of fuels and products, integrating productive processes through chemical, thermochemical and biological conversion of biomass. This allows the efficient use of the full potential of raw materials, combining power generation and the production of a wide range of value-added products, such as chemicals, plastics, biogas, energy, carbon and a number of other fuels [33]. In other words, the integrated biorefinery could transform the typical pulp system (producing cellulose, steam and power) into a marketable multiple chemicals and fuels production system with sharing of raw materials, by-products, utilities, and infrastructure with the existing pulp mill [9].

Thus, the application of the concept of integrated biorefineries to pulp production plants can be the greatest potential for the future development and maintenance of competitiveness of the sector. As the pulp mills are already biomass-based plants, the introduction of new processes to convert biomass will not change to a great extent its key operations. Hence, the raw material used in these biorefineries would come from a biomass that, besides being a waste from a larger production process, would already be pre-treated, with great cost savings. Figure 2.4 illustrates the tendency of industrial configuration of the pulp mills in the past, present and future.

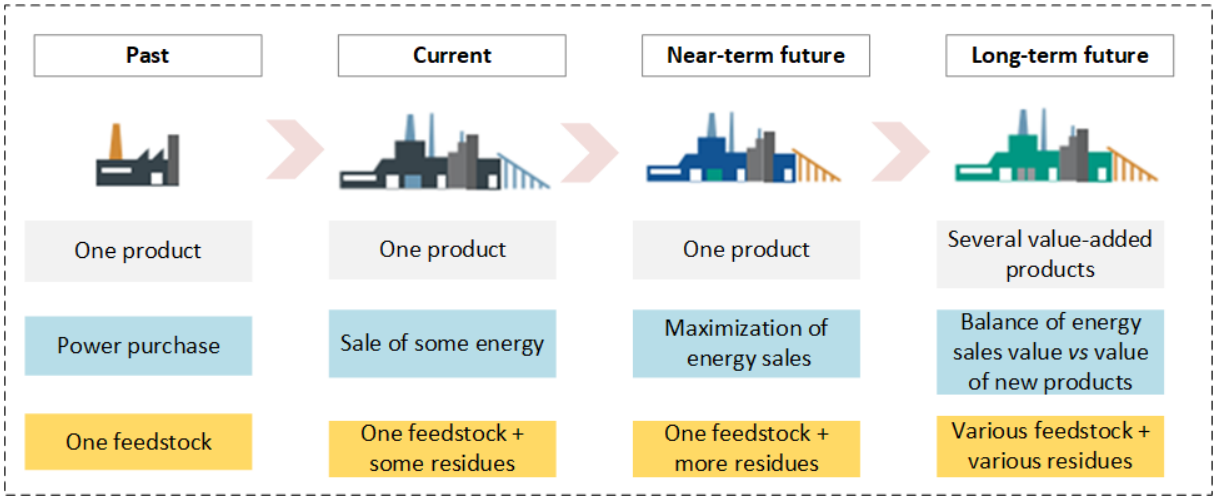

Figure 2.4 Current and future industrial configuration of the pulp mill. Source: Adapted from [3].

According to Figure 2.4, annexed plants can be a route to integrate new biomass-based processes (biorefineries) into a typical pulp mill. The integrated complex concept aims to obtain a zero-fossil fuel consumption, minimum utilities demand, reduced amounts of effluents and greenhouse gases emissions. The key challenge for this transformation consists in better comprehend the tradeoffs between the expansion of the pulp mills product portfolio and the impact in terms of economic, environmental and technical aspects. This industry has the potential to be a source of various innovative products and byproducts originating from wood, that could supply other industries, such as pharmaceuticals, chemicals, cosmetics, textiles, electronics and automotive [34]. Figure 2.5 illustrates possible biorefinery options in a kraft mill, using wood as feedstock (waste wood, bark and chips) or black liquor.

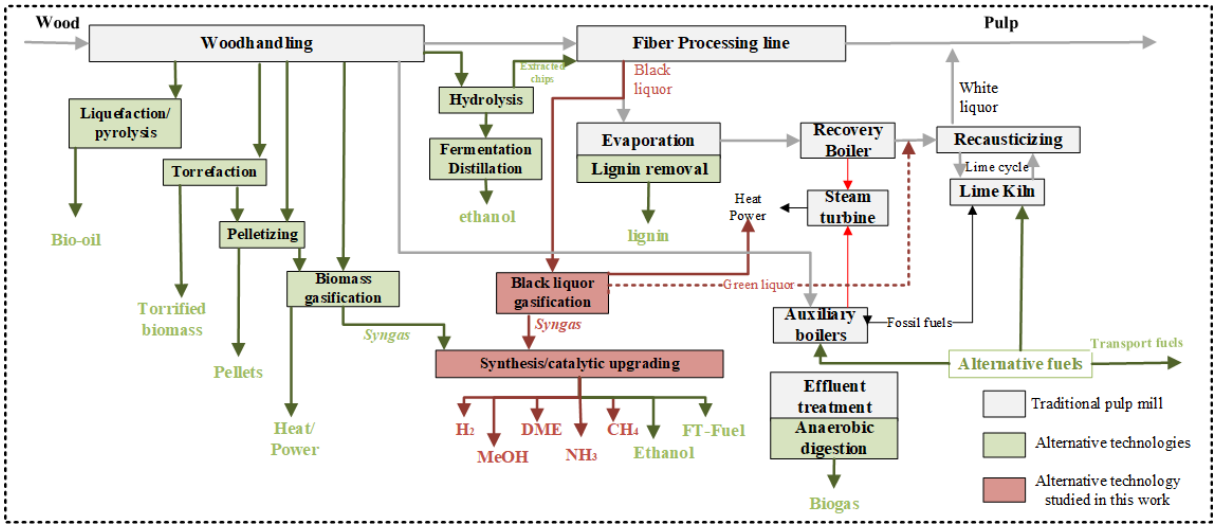

Figure 2.5 The kraft pulp mill and the alternative technologies for biofuels production. Source: adapted from [35].

The lignocellulosic biorefinery is normally based on two platforms: biochemical and thermochemical. The former is mainly based on sugars, consisting of the production of chemicals and fuels from cellulose and hemicellulose via biological processing of biomass, hydrolysis and fermentation. In case of decreasing paper demand, the pulp as well as the wood wastes from the mill could be also used as feedstock for the manufacturing of these new value-added products, such as ethanol, furfural and others [9].

On the other hand, in the thermochemical platform, biomass is converted to synthesis gas or pyrolysis oil via gasification or pyrolysis, respectively. In the pulp mill, the thermochemical platform consists of gasification of black liquor and/or biomass residues, and lignin extraction from black liquor [36]. Since the 1960s, the black liquor gasification (BLG) has gone through a step-wise development and now it is as an alternative chemical recovery technology for conventional boiler replacement [19]. The syngas produced by the BLG process consists mostly of carbon monoxide (CO), hydrogen (H_2) and carbon dioxide (CO_2) and it can be used in two main routes: a combined cycle (BLGCC) - where a gas turbine is applied to use the syngas for power generation-, and for chemicals and fuels production –where it is used to produce biofuels such as motor fuels, Fischer–Tropsch liquids (FTL), dimethyl ether (DME), methanol (MeOH) and mixed-alcohol, which has the potential for substituting fossil fuels [9].

Another strategy to improve the economy of the pulp and paper industry, is the extraction of lignin from the black liquor. According to Valmet (2020), the recovery boiler could be the limiting factor to increasing pulping capacity, and if 25% of the lignin in the black liquor is removed, the boiler capacity can be increased to enable 20-25% more pulp production [37]. Besides, lignin is a promising renewable raw material: in addition to have a high heating value, it can be potentially further converted into aromatic hydrocarbons, bio-oil via the cracking of lignin, and bio-materials such as activated carbon and carbon fiber [38]. The LignoBoost process is already commercially available, enabling high quality lignin precipitation at low cost [37].

In summary, among the most promising technological routes that can be applied to the pulp and paper industry considering the integrated biorefinery concept, the following alternatives can be highlighted [3]:

i) in current application: production of electricity and steam by cogeneration for use in the production processes and for sale;
ii) in the short and medium term: gasification of forest biomass and black liquor; biogas production from organic solid waste; fast pyrolysis of forest biomass to obtain fuel oil for use in the process or for co-processing with petroleum, in addition to fuel gas;

extraction of lignin from black liquor for internal use as fuel to the lime kiln and debottlenecking of the liquor recovery system, allowing to increase the productive capacity of the plant; pelletizing and briquetting of forest waste;

iii) in the medium and long term: use of lignin for the production of higher value-added products, such as carbon fiber, vanillin and aromatics.

As stated by the International Energy Agency, there are some innovation gaps in the technologies being developed for pulp and paper mills, for example [39]:

i) the fuel switching and the energy efficiency are considered as the primary mechanisms to cut CO_2 emissions, however innovation should also be taken into account;

ii) several technologies are still in the early stages of development, such as the deep eutectic solvents to dissolve wood into lignin, hemicellulose and cellulose. Also, alternative drying and paper forming processes can contribute to increase energy efficiency;

iii) the black liquor gasification, which can be the way to produce various carbon-neutral energy products, has already reached the initial stages of commercialization but still requires further development and deployment;

iv) the lignin extraction, which has been tested in both pilot at commercial scale, could make lignin available to be used as a biofuel or for new industrial products.

However, the implementation of these technological possibilities will only succeed if there is a transition in political will and in the future requirements of biofuels replacing fossil fuels. Notwithstanding, conceptual studies of cost-effective biorefinery synthesis and design strategies play a key role for development of practical and sustainable integrated biorefinery network, providing an overview and previous analysis needed for practical integration with existing pulping processes.

In the next section, the state of the art of black liquor gasification, the focus of this work, will be detailed.

2.3 Black liquor gasification

To contextualize, gasification is a complex process involving various chemical reactions, heat and mass transfer processes and pressure changes. The conversion of solid or liquid feedstock into useful gaseous fuel or chemicals requires a gasifying agent (air, oxygen or steam) [40]. The gasification process presents a certain complexity as a reactive system, consisting of several stages that occur simultaneously: drying, pyrolysis, gasification and

combustion. It also requires a significant amount of energy due to its endothermic nature. In addition, the production rate, composition and properties of the gas produced vary greatly according to the biomass properties, the gasification agent used (type and flow), equivalence ratio, the type of reactor used (fixed bed, fluidized bed or indirect gasifier), operating conditions (temperature, pressure, residence time) and the downstream processes used for gas cleaning and conditioning. Chemical reactions, fluid flow, molecular transport and radiation result in the modification of these properties at any point [40].

The BL gasification consists of the thermal conversion of the organic matter present in the concentrated BL into syngas (*i.e.* a gaseous mixture mainly composed of hydrogen and carbon oxides). The BL gasification process also allows recovering the inorganic sodium and sulfur-based compounds present in the cooking chemicals, which can be almost entirely recycled to the digester after going through a causticization treatment in the lime kiln [25].

The BL gasification processes can be divided into two main types. The first one occurs at relatively low temperatures in the range of 600–800 °C, which is below the melting point of the inorganic components. This condition avoids the liquor smelt formation and thus, the associated smelt-water explosion hazards. The second type of BL gasification operates at high temperatures above 800 °C and produces a molten smelt. A natural separation of sulfur from sodium is provided by both types, allowing pulping chemistry to perform better than in the current recovery boiler technology [41].

The BL gasification process involves various complex, multi-phase reaction mechanisms. Although BL is typically handled in a dense liquid form, the conversion reactions that take place in the gasifier are similar to those found in biomass and coal gasification units. According to Huang et al. (2011), the main reactions occurring during the BL gasification process can be represented by Equations (2.1-2.5):

Boudouard reaction: $C(s)+CO_2 \leftrightarrow 2CO \quad \Delta H_r = +172$ MJ/kmol (2.1)

Water gas primary reaction: $C(s)+H_2O \leftrightarrow CO+H_2 \quad \Delta H_r = +131$ MJ/kmol (2.2)

Methanation reaction: $C(s)+2H_2 \leftrightarrow CH_4 \quad \Delta H_r = -75$ MJ/kmol (2.3)

Water gas shift reaction: $CO+H_2O \leftrightarrow CO_2+H_2 \quad \Delta H_r = -41$ MJ/kmol (2.4)

Methane steam reforming reaction: $CH_4+H_2O \leftrightarrow CO+3H_2 \quad \Delta H_r = +206$ MJ/kmol (2.5)

Besides, the reactions showed in Equations (2.6-2.8), related with the inorganic compounds, are also present in the BL gasification reactor:

Sodium sulfate reduction:

$$2C(s)+Na_2SO_4(s,l) \rightarrow Na_2S(s,l)+2CO_2 \qquad \Delta H_r = +171 \text{ MJ/kmol } Na_2SO_4 \tag{2.6}$$

$$4C(s)+Na_2SO_4(s,l) \rightarrow Na_2S(s,l)+4CO \qquad \Delta H_r = +509 \text{ MJ/kmol } Na_2SO_4 \tag{2.7}$$

Reaction of sulfur solid-gas distribution:

$$Na_2S(s,l)+H_2O+CO_2 = Na_2CO_3(s,l)+H_2S \tag{2.8}$$

Where (s,l) denotes the solid and liquid (*i.e.* molten solution) phases, respectively. Equation (2.8) governs the distribution of the sulfur between gas phase (H_2S) and smelt (Na_2S). Other side-reactions, such as those occurred between thiosulfate present in the BL with some gaseous substances (CO, CO_2, and H_2O) may lead to carbonate formation.

The main modelling approaches to the black liquor gasification system reported in the literature are going to be presented in the next subsections.

2.3.1 Mathematical modelling

The predictive ability of a mathematical model for gasification depends on the model capacity of representing the variables as realistically as possible [40]. There are two main mathematical models that represent the gasification process, namely the kinetic and the thermodynamic equilibrium models [42]. The former is used to predict the progress of reactions and the composition of the reaction product at different reactor positions or over time. On the other hand, the equilibrium models are used to predict the maximum theoretical conversion that can be achieved if the system attains the thermodynamic equilibrium. Thus, the latter approach is useful to identify the ideal performance of the syngas production processes [43].

The highly non-linear nature of the modelled system and the presence of multiple tradeoffs between the energy consumption and the syngas yield reinforce the need for computational tools capable of predicting this behavior in order to improve the accuracy of the simulated scenarios. Many studies have been published on the subject of biomass gasification modelling [40; 43; 44; 45]. However, a limited amount of reported literature on black liquor gasification is available, despite the fact that the BL derived from pulp mills is one of the largest contributors to renewable energy in the industrial processes [46]. This can be partially explained

by the complexities associated with the phenomena. In this section, some basic and advanced models of black liquor gasification are summarized.

2.3.1.1 Equilibrium models

The modelling approaches based on equilibrium are classified either as stoichiometric or non-stoichiometric models. The end-gas composition calculated from the stoichiometric models is estimated based on equilibrium constants and specified chemical reactions. For this reason, some errors in the model prediction may arise if relevant reactions are omitted in the adopted list of reactions. This problem can be offset by using the non-stoichiometric modelling approaches based on the Gibbs free energy minimization, since it is not necessary to identify ahead the chemical reactions [40].

Aiming to define the thermodynamic constraints on pressurized black liquor gasification, Backman et al. (1993) studied the effect of the different operating conditions (air/fuel ratio, pressure, and temperature) on carbon conversion and sulfur and sodium distribution at equilibrium. The authors considered six chemical elements (*e.g.* C, H, O, S, Na, and N) in the system [47]. The authors pointed out that the complete gasification of the carbon in the BL is thermodynamically possible at temperatures above 700 °C and at low air-to-fuel ratios. The limit of the theoretical temperature for a complete gasification decreases when the pressure decreases and the air-to-fuel ratio increases. However, the product gas and the smelt equilibrium composition, as well as other gasification performance indicators, have been not reported.

Huang and Ramaswamy (2011) studied the effects of different operating conditions on the BL steam gasification using the thermodynamic equilibrium approach. The total Gibbs free energy of the gasification system is represented as in Equation (2.9).

$$G = \sum_{\substack{\text{pure}\\ \text{ideal}\\ \text{gas}}} n_i(g_i^0 + RT\ln P_i) + \sum_{\substack{\text{pure}\\ \text{condensed}\\ \text{phases}}} n_i g_i^0 + \sum_{\text{solution 1}} n_i(g_i^0 + RT\ln X_i + RT\ln\gamma_i) + \sum_{\text{solution 2}} n_i(g_i^0 + RT\ln X_i + RT\ln\gamma_i) + \ldots \quad (2.9)$$

Where n_i are the moles; g_i^0 is the standard molar energy of Gibbs; R is the constant of the ideal gases; T is temperature; P_i is gas partial pressure; X_i is mole fraction; and γ_i is the activity coefficient. Thereafter, P_i, X_i, and n_i are calculated by means of Gibbs free energy minimization.

At temperatures above 750 °C, Huang and Ramaswamy [48] observed full carbon conversion and no Na_2S formation. Moreover, as the temperature increases, both hydrogen and Na_2CO_3 fractions reportedly increase, reaching a maximum for later starting to decrease. Meanwhile, the amount of CO increases, while CO_2, CH_4, and H_2S fractions decrease as the temperature increases. By increasing the pressure, both H_2 and CO fraction slightly decrease, whereas the amounts of Na_2S and Na_2CO_3 decrease and increase, respectively. As it concerns the gasification agent, the H_2 and Na_2CO_3 fractions increase and the CO and Na_2S fractions decrease as the amount of steam input is increased [48]. These results are important for maximizing the recovery of the chemicals recycled to the kraft pulp process and also for understanding how the composition of the different phases change when the operation conditions are modified.

Larsson et al. (2006) considered the equilibrium-based modelling of a pressurized oxygen-blown gasification system to identify the effect that the inaccuracies in thermochemical data may have on the results of the process variables. A small impact on the formation of $H_2S(g)$ was observed by varying the operating pressure of the gasifier in the range of 25-32 bar. On the other hand, the uncertainties become more important for gasification temperatures above 1000 °C. Also, a high moisture content seems to favor the formation of NaOH(g) and KOH(g) for both recovery boiler and gasifier applications. The impact of the uncertainty about the sodium and potassium sulfide content on the equilibrium chemistry of sulfur has been also reported as extremely important. The results indicated that the largest impact of the uncertainties on the gas-phase alkali chemistry seem to be associated with NaOH(g) and KOH(g) production [49].

2.3.1.2 Kinetic models

Li and van Heiningen measured the kinetics of the gasification of chars derived from BL in a CO_2 rich environment at atmospheric pressure and temperatures ranging from 600 to 800 °C [50; 51]. The authors observed that BL chars are much more reactive than coal chars doped with sodium carbonate. This is can be explained by the finer and three-dimensional dispersion of the sodium in the char, which catalyzes the reactions occurring during the gasification process.

The gasification rates are described using a Langmuir–Hinshelwood mechanism [51]. Equation (2.10) defines the instantaneous rate of gasification.

$$-r_w = -\frac{1}{W}\frac{dW}{dt} \tag{2.10}$$

Where W is the carbon weight at time t. A differentiation of a polynomial fitted to the gasification weight loss curve is used to obtain the gasification rate [51]. Equation (2.11) describe the uncatalyzed and catalyzed CO_2 gasification of carbon.

$$-r_w = \frac{K[CO_2]}{1 + K_{CO2}[CO_2] + K_{CO}[CO]} \tag{2.11}$$

Where the reaction constant is represented by K ($m^3.mol^{-1}.min^{-1}$), and the equilibrium adsorption constants of CO_2 and CO are K_{CO2} ($m^3.mol^{-1}$) and K_{CO} ($m^3.mol^{-1}$), respectively. Moreover, the alkali-metal-catalyzed gasification rate of carbon by CO_2 can be described by Equation (2.12) [51].

$$-r_w = \frac{K'[CO_2]}{[CO_2] + K'_{CO}[CO]} \tag{2.12}$$

Where K' (min^{-1}) is the reaction constant, and K'_{CO} (dimensionless) is the equilibrium adsorption constant to CO [51].

Subsequently, Li and van Heiningen (1991) also studied the kinetics of BL char gasification with steam under atmospheric conditions [52]. The reactions reported in Equations (2.2-2.4) and in Equation (2.8) were considered under steam gasification conditions. As with CO_2 gasification, it was noticed that the Langmuir-Hinshelwood kinetics could be used to describe the measured rates [52]. The gasification rate is defined by Equation (2.13).

$$-r = -\frac{1}{W_{C,t}}\frac{dW_{C,t}}{dt} \tag{2.13}$$

Where $W_{C,t}$ denotes the carbon weight at time t. This rate is assessed using the measured concentration of CO and CO_2, as described in Equation (2.14). The methane concentration was not considered in the overall gasification rate, since its concentration was at least two times lower than the CO and CO_2 concentration. Also, the H_2S concentration accounts only for 5-10% of the carbon loss, and no correction was made for CO_2 consumed in the reaction of H_2S due to this fact.

$$-r = \frac{[p_{CO}(t) + p_{CO2}(t)]M_C Q / TR}{W_{C,0} - \frac{M_C Q}{TR}\int_0^t [p_{CO}(t) + p_{CO2}(t)]dt} \quad (2.14)$$

The influence of the composition of the gas on the gasification rate is assessed by two Langmuir-Hinshelwood kinetic expressions, described by Equation (2.15) and Equation (2.16).

$$-r = \frac{K[H_2O]}{1 + K_{H2O}[H_2O] + K_{H2}[H_2]} \quad (2.15)$$

$$-r = \frac{K'[H_2O]}{[H_2O] + K'_{H2}[H_2]} \quad (2.16)$$

Where K ($m^3.mol^{-1}.min^{-1}$) and K' (min^{-1}) are the reaction constants, and K_{H20} ($m^3.mol$), K_{H2} ($m^3.mol$), and K'_{H2} can be considered as the adsorption constants of H_2O and H_2, respectively. The authors observed that Equation (2.16) is the most appropriate to describe the BL char gasification process by using steam.

Whitty and collaborators (1996) investigated the kinetics of the gasification of the char derived from the BL by using steam. A pressurized thermogravimetric reactor operating between 600-675 °C and 1-30 bar has been used in that study. As a result, when the pressure is increased, the gasification rate decreases, more likely due to inhibiting effects caused by H_2 and CO content. The authors concluded that the rate of steam-blown gasification could be predicted by means of a model developed for carbon catalytic gasification [53].

2.3.1.3 Computational fluid dynamics (CFD) models

Marklund (2006) modelled the BL gasification process using the computational fluid dynamics technique. The refined modelling of the turbulent two-phase flow of gases and black liquor droplets in the pressurized entrained flow black liquor gasification (PEHT-BLG) reactor are based on an Eulerian-Lagrangian formulation [54]. The gasification process of BL droplets is modelled using this approach, similarly to the models for combustion of coal particles. The Reynolds Averaged Navier-Stokes equations (RANS) and energy equation for the continuous gas phase are solved using an Eulerian description. The Cartesian notation for these equations of the continuity equation for the mean flow, continuity equation for the turbulent field, mean momentum equations, and mean energy equation, are represented in Equations (2.17-2.20) [54].

$$\frac{\partial U_i}{\partial x_i} = \dot{m} \quad (2.17)$$

$$\frac{\partial u'_i}{\partial x_i} = 0 \tag{2.18}$$

$$\frac{\partial U_i}{\partial t} + U_j \frac{\partial U_i}{\partial x_j} + \frac{\partial}{\partial x_j}(\overline{u'_i u'_j}) = -\frac{1}{\rho}\frac{\partial P}{\partial x_i} - g\delta_{i3} + \nu \frac{\partial^2 U_i}{\partial x_j \partial x_j} + S_i \tag{2.19}$$

$$\rho C_p \left(\frac{\partial \overline{T}}{\partial t} + U_j \frac{\partial \overline{T}}{\partial x_j} \right) = \frac{\partial}{\partial x_j} \left(k \frac{\partial \overline{T}}{\partial x_j} - \rho C_p \overline{u_j T'} \right) + S_T \tag{2.20}$$

Where U is the mean velocity (m s^{-1}), $\dot{m}$ is the mass transfer rate (kg s^{-1}), x is the coordinate (m), u' is the fluctuating velocity (m s^{-1}), t is the time (s), P is the total pressure (Pa), g is the acceleration of gravity (m s^{-2}), δ is the Kronecker delta, ρ is the density (kg m^{-3}), v is the kinematic viscosity (m^2 s^{-1}), S_i is the swirl number, C_p is the specific heat at constant pressure (J kg^{-1} K^{-1}), T is the temperature (K), S_T is the source term, and k is the thermal conductivity (J s^{-1} m^{-1} K^{-1}). The mean momentum tensor equation can be rewritten as described in Equation (2.21).

$$\frac{DU_i}{Dt} = \frac{1}{\rho}\frac{\partial \overline{\sigma}_{ij}}{\partial x_i} - g\delta_{i3} + S_i \tag{2.21}$$

Where

$$\frac{DU_i}{Dt} = \frac{\partial U_i}{\partial t} + U_j \frac{\partial U_i}{\partial x_j} \tag{2.22}$$

$$\sigma_{ij} = -P\delta_{ij} + \mu\left(\frac{\partial U_i}{\partial x_j} + \frac{\partial U_j}{\partial x_i} \right) - \rho \overline{u'_i u'_j} \tag{2.23}$$

Equation (2.23) represents the stress tensor σ_{ij} (kg m^{-1} s^{-2}), and the last term is called the Reynolds stress tensor (τij). In this term, it usually lays the fundamental problem of turbulence using the RANS approach, and a model is necessary to compute this term in order to compute all the mean-flow properties of the turbulent flow. To complement the RANS equations, the k-ε turbulence model along with standard wall functions are used [54]. The k-ε model has been one of the most used models for turbulent flows, despite the fact that it is not very accurate close to the wall regions (*i.e.* the stagnation boundary), since the gradient of the variables involved rapidly grow. Adjustments on the coefficients of the k-ε models have reportedly improved the prediction capability of the models.

A brief description of the k-ε turbulence model is described in Equations (2.24-2.32) [54]. Equation (2.24) is the Reynolds-stress equation:

$$\frac{\partial \tau_{ij}}{\partial x_j} + U_k \frac{\partial \tau_{ij}}{\partial x_k} = -\tau_{ik} \frac{\partial U_j}{\partial x_k} - \tau_{jk} \frac{\partial U_i}{\partial x_k} + \varepsilon_{ij} - \Pi_{ij} + \frac{\partial}{\partial x_k}\left(\nu \frac{\partial \tau_{ij}}{\partial x_k} + C_{ijk} \right) \tag{2.24}$$

Where *τij* is the Reynolds-stress tensor and

$$\Pi_{ij} = \overline{p'\left(\frac{\partial u'_i}{\partial x_j} + \frac{\partial u'_j}{\partial x_i} \right)} \tag{2.25}$$

$$\varepsilon_{ij} = \overline{2\mu \frac{\partial u'_i}{\partial x_k} + \frac{\partial u'_j}{\partial x_k}} \tag{2.26}$$

$$C_{ijk} = \overline{\rho u'_i u'_j u'_k} + \overline{p u'_i}\delta_{jk} + \overline{p u'_j}\delta_{ik} \tag{2.27}$$

By performing mathematical manipulations, such as taking the trace of Equation (2.24) defining the turbulent kinetic energy *k* and dissipation *ε*, using the Boussinesq eddy-viscosity approximation, the authors obtained Equation (2.28) [54].

$$\tau_{ij} = \mu_T \frac{1}{2}\left(\frac{\partial U_i}{\partial x_j} + \frac{\partial U_j}{\partial x_i} \right) - \frac{2}{3}\rho k \delta_{ij} \tag{2.28}$$

Where the turbulent (eddy) viscosity is given by Equation (2.29).

$$\mu_T = C_\mu \rho \frac{k^2}{\varepsilon} \tag{2.29}$$

A closed system of the RANS equations is obtained via the equations for k and ε, shown in Equation (2.30) and Equation (2.31) [54].

$$\rho \frac{\partial k}{\partial t} + \rho U_j \frac{\partial k}{\partial x_j} = -\tau_{ij} \frac{\partial U_i}{\partial x_j} - \rho\varepsilon + \frac{\partial}{\partial x_j}\left[\left(\mu + \frac{\mu_T}{\sigma_k} \right) \frac{\partial k}{\partial x_j} \right] \tag{2.30}$$

$$\rho \frac{\partial \varepsilon}{\partial t} + \rho U_j \frac{\partial \varepsilon}{\partial x_j} = C_{\varepsilon 1} \frac{\varepsilon}{k} \tau_{ij} \frac{\partial U_i}{\partial x_j} - C_{\varepsilon 2} \rho \frac{\varepsilon^2}{k} + \frac{\partial}{\partial x_j}\left[\left(\mu + \frac{\mu_T}{\sigma_\varepsilon} \right) \frac{\partial \varepsilon}{\partial x_j} \right] \tag{2.31}$$

Where the corresponding closure constants are described in Equation (2.32) [54].

$$\begin{cases} C_{\varepsilon 1} = 1.44 \\ C_{\varepsilon 2} = 1.92 \\ C_{\mu} = 0.09 \\ \sigma_k = 1.0 \\ \sigma_{\varepsilon} = 1.3 \end{cases} \quad (2.32)$$

This derived k-ε model above is only valid for a certain distance away from the wall region, and other modelling approaches for the walls are required to deal with this problem [54]. In addition, the rates of the combustion reactions are controlled by the minimum of the Eddy dissipation rate and the chemical kinetic reaction rate [54]. According to Marklund et al. (2007), the most important parameters for modelling the Chemrec BL gasification reactor using CFD are: *(i)* volatile sulfur fraction, *(ii)* sulphide to sulphate ratio in the BL, *(iii)* volatile carbon fraction , and *(iv)* ratio of CO to CO_2 [55]. It was noticed that the amount of sulfur released to the gas phase as H_2S during devolatilization and the initial concentration ratio of Na_2S and Na_2SO_4 in BL solids have relatively large effects when compared to the other chosen performance response parameters. The CFD model validation of the PEHT-BLG against experimental data is greatly influenced by these parameters.

2.3.2 Scientific and technological issues

The research and development of commercially viable BL gasification technologies is based on the efforts of few companies over the last years [56]. Those enterprises are the Manufacturing and Technology Conversion International Company (MTCI) and the Chemrec company, whose technologies are based on atmospheric and pressurized gasification, respectively [57]. The main differences between these processes, as well as the detailed systems, are described in the following sections.

2.3.2.1 TRI process

This process was developed by MTCI and commercialized by ThermoChem Recovery International (TRI). TRI has two BL gasification facilities: Georgia-Pacific 200 t/day fluidized bed steam reformer system in Big Island, Virginia; and Norampac 100 t/day steam reformer in Trenton [58]. TRI technology is based on the indirect heating of BL in a bubbling fluidized bed steam reformer. It operates between 580-620 °C and at atmospheric pressure (see Figure 2.6), which are relatively milder operation conditions below the inorganic chemicals melting point.

The system consists of a steam reformer that is used as a gasifier, avoiding the use of air or oxygen. Synthesis gas and alkali salts as solids are the two main products of this process [59]. Some advantages of this system are the high combustion efficiency; the efficient transfer of heat with uniform heat flux; the low NO_x emissions and the absence of moving parts. Moreover, the pressure boost helps the exhaust gases to flow through a superheater and heat recovery steam generator. However, MTCI projects are running only in pulp mills with a Na_2CO_3 semi-chemical cooking process. During operation in the trial plants, it was also observed tar formation, incomplete conversion of carbon due to low temperature and carburization problems. Despite the progress made in the field of BL gasification, due to the technical problems appearing during the process, TRI has decided to turn back and use only conventional biofuels in its gasifier [59].

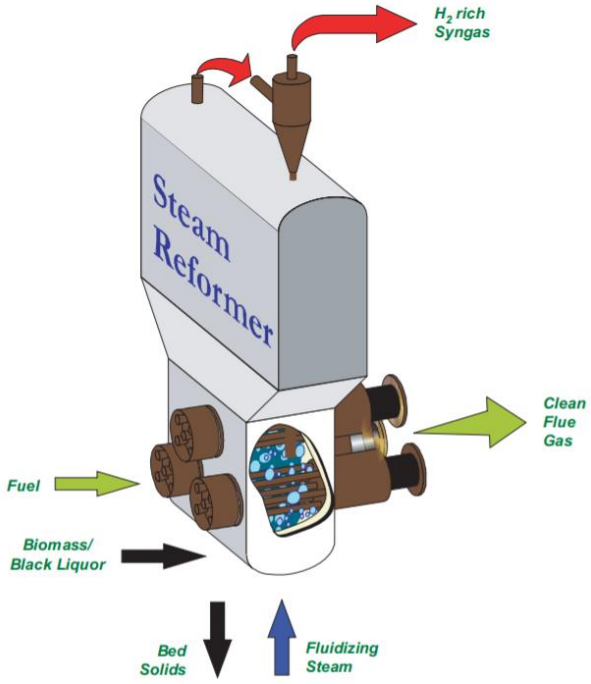

Figure 2.6 MTCI system configuration for kraft liquor. Source: [19].

2.3.2.2 Chemrec gasification

Chemrec has developed non-pressurized air-blown gasification systems and pressurized oxygen-blown gasification systems. The latter systems have the advantage of smaller equipment size and the capacity to produce low and medium pressure steam from syngas cooling [56]. It is reported that the pressurized entrained flow black liquor gasification has the potential to double the power output when compared to the traditional boiler, if it is

integrated to a combined cycle [60; 61]. Other advantages, such as a tar-free operation, uniform temperatures at turbulent conditions and low methane content, contribute to the increase of the conversion efficiency and the reaction rates [15; 59]. The trial plant started operation in 2005, in Piteå, Sweden, with a capacity of 3 MW black liquor (20 tds/day), corresponding approximately to 1% of the BL produced at the mill. The gasifier operating conditions are 1000 °C and 29 bar. A dry solid content of 73% for the black liquor is adopted [56].

As it can be seen from Figure 2.7, the Chemrec gasification system consists of an entrained flow reactor with the quench cooler, the countercurrent gas cooler, and heat exchangers for cooling the hot green liquor. This system allows the conversion of the carbonaceous materials in the BL into syngas (*i.e.* a mixture rich in CO, H_2, H_2O, and CO_2). Meanwhile, the smelt, mainly containing Na_2CO_3 and Na_2S, is formed in the bottom of the equipment. The syngas and the molten smelt flow downwards to a quench dissolver, where they are simultaneously separated. The smelt goes through a weak wash, where the green liquor is produced and subsequently pumped back to a dissolving tank. Finally, it is cooled from a quench temperature of 220 °C to about 90 °C [25]. The temperature and pressure of the gasifier usually vary between 900 °C and 1100 °C and 25-32 bar, respectively. Meanwhile, the oxygen-to-fuel ratio varies between 0.40-0.55. A residence time of about 5-10 s is often adopted [49]. The syngas produced in the gasifier is further cooled down and scrubbed with water, aiming to remove the impurities that otherwise could impact the downstream equipment.

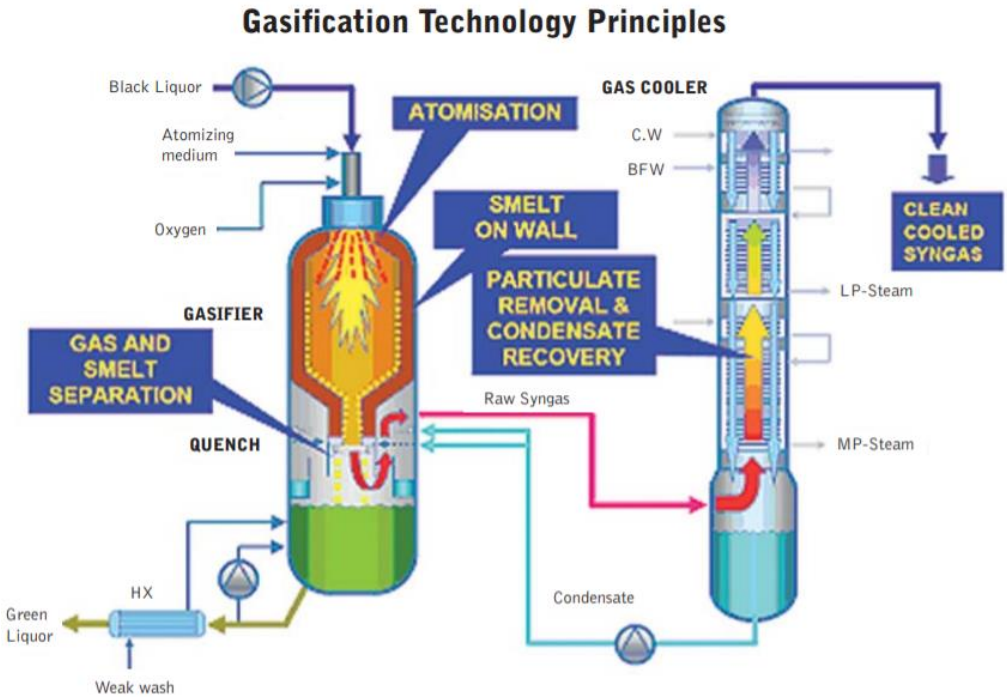

Figure 2.7 Chemrec gasifier. Source: [19].

2.4 Chemicals and fuels via black liquor gasification

Although the conventional recovery boiler is as a mature technology, its replacement by a BL gasification system has proved to be an attractive option to widen the product portfolio of the kraft pulp mills by manufacturing more value-added products [25]. Table 2.1 compares different studies that considered BL gasification for power and/or fuels production. As it can be seen from the comparison, usually the integration of fuels and chemicals production to the pulp mill leads to an energy deficit (new demands of electricity and steam) that must be fulfilled by importing additional biomass [25].

Table 2.1 Comparison of different studies considering black liquor gasification for power and fuels production.

Product	**Electricity**	**DME**	**FT fuels**	**Methanol**	**Hydrogen**	**Methane**
Pulp (AD t/day)	1600	1600	1600	2000	2000	1000
Black liquor (MW)	350.7	350.7	350.7	487.0	487.0	243.5
Biomass import (MW)	27.1	77.4	101.6	129.0	123.5	107.0
Electricity (MW) Import (-) /Export (+)	15.2	-99.6	-12.4	-45.9	-56.7	1.1
Fuel production (MW)	--	168.0	112.0	272.0	261.0	240.2
Reference	60; 62			63	64	65

A preliminary study investigating the potential of replacing conventional recovery boilers with hydrothermal BL gasification unit to optimize energy integration has been performed [66]. The authors used the LuaOsmose tool, aiming to satisfy the minimum energy requirements. The proposed system does not require the evaporation step, which reduces the overall heating demand. Moreover, BL gasification reportedly increases the energy efficiency and simultaneously generates syngas that can be further converted into biofuels. This analysis has shown the great potential of energy integration of the two processes [67], which points out the importance of the future evaluation of biofuels/chemicals plants integrated to pulp mills.

Another important aspect is the evaluation of the environmental performance, more specifically the CO_2 emissions. The Paris Agreement has set the goal to keep global warming below 2 °C. However, due to the current rates of CO_2 emissions (40 Gt_{CO2}/year), large-scale

removal of CO_2 from the atmosphere could be necessary, implying that negative emissions may play an important role in achieving this target. Nevertheless, over 90% of CO_2 emissions from a pulp mill are from biogenic origin, which represents a potential source of revenues if negative emissions could be marketable [31].

Petterson and Harvey (2010) studied how different assumptions with respect to systems surrounding the pulp mill, such as electricity generation and transportation systems, could affect the CO_2 emission balance for different BL gasification concepts aiming to produce electricity or fuels (MeOH, DME and FT fuels). The results show that a standalone pulp mill with a BL gasification unit has higher potential to reduce CO_2 emissions than an integrated pulp and paper mill. The global CO_2 emissions vary greatly depending on the electricity generation technology adopted. It was observed that, importing electricity from a grid intensive in CO_2 emissions, the electricity generation inside the mill is favored, whereas importing electricity with low associated CO_2 emissions would favor the production of the fuels. Higher drop in CO_2 emissions was achieved for the fuels production via BL gasification when the electricity generation technology was coal and a carbon capture and storage (CCS) unit was employed. In addition, the authors observed that the CO_2 emission balance may vary, depending on the fact that the biomass can be considered as CO_2 neutral or not [68].

The BL gasification concept is often weighed against the conventional recovery boiler in terms of energy, environmental, and economic advantages. Thus, it is important to offer a level playing field for rational comparisons and expose the pros and cons of the use of recovery boilers before implementing BL gasification plant. Those comparisons will be subject to the assumptions considered in the process, the type of the mill and the biomass availability, not to mention the technical and economic performance of the surrounding technologies [25]. Some process engineering tools that may help on understanding this kind of tradeoffs will be presented in the next section.

2.5 Process systems engineering for biorefineries

In the context characterized by many concerns related to the future energy supply and also economic competition, the process integration concept in modern chemical units can help to improve not only the efficiency of the energy and mass transfer, exploring the interactions among various process, but also can lead to reduce capital and operating costs as well as harmful emissions [69].

The design of a biorefinery involves a systematic approach to select and integrate processing units, and also analyze and optimize those facilities [70]. Process synthesis deals with the selection of the topology of the process, exploring the possible alternatives to come with flowsheetings with good design specifications aiming to meet the desired objectives [71; 72]. The process modelling and simulation can be very useful to analyze these different designs obtained in process synthesis for achieving optimal configurations.

In the next sections, the process systems engineering approaches are briefly presented.

2.5.1 Process synthesis

Process synthesis involve approaches that can be summarized as follows:

i) Methods using heuristics
ii) Methods using thermodynamic targets
iii) Methods using algorithmic

The heuristics methods are based in discover the solution of a problem by means of plausible guesses. It can be useful to do a preliminary screening and eliminate non-promising alternatives, however it can present some drawbacks that does not allow to establish the quality of the solution [73].

The thermodynamics approaches could be used to develop bounds and eliminate alternatives that do not present a good energy efficiency. Moreover, this approach can be used to determine the thermodynamic targets and the level of the utilities involved, and it can be very powerful if the quality of the bounds are good [73].

For the algorithmic approach the idea is to formulate the synthesis of a flowsheet as an optimization problem [73]. The scope of the superstructure, the physical data used, the objective function and its respective constraints, the uncertainties to consider, are the features that need to be decided [74]. Hierarchical decomposition [75] and pinch analysis [76] have been reported as major contributions of the first and second approaches, and have been successfully applied in different industrial applications [71].

The combination of some of these approaches by exploring their strength has proven to be a good strategy applied to synthesis problems. For example, heuristics can be used for doing a preliminary screening, then mathematical programming with algorithm methods based on optimization is applied to generate integrated flowsheets and optimum solutions. To do so, some steps should be followed: i) the development of a representation for the superstructure considering a set of alternatives from which the optimum solution can be selected; ii) the

formulation of a mathematical program that takes into account the discrete and continuous variables for the selection of the superstructure configuration and operating levels; iii) the solution of the optimization model to determine the optimum solution [77].

The main mathematical tool for this kind of methods is the mixed integer programming that is widely used for utility systems, heat recovery networks and processing systems [73]. In brief, the mixed integer programming deals with optimization techniques consisting of an objective function that is optimized subject to both equality and inequality constraints, where both continuous and discrete variables can be specified. The problems can be formulated as mixed integer linear programming (MILP) and as mixed integer non-linear programming (MINLP) [73]. The MILP problems are characterized for having linear functions and the typical procedure for solving is using the branch and bound method. On the other hand, the MINLP problems involve nonlinear objective function and/or nonlinear constraints, and can be solved by the branch and bound procedure and generalized benders decomposition method.

2.5.2 Process modelling

So far, the process modelling and simulation is one of the most used systems tools. Typical applications are related to the use of general flowsheeting software (e.g. Aspen Plus, Aspen HYSYS, Vali, gPROMS, DWSIM, EMSO, etc.) to generate configurations and perform techno-economic assessment and case-by-case analysis [70]. Modelling and simulation has great potential to assist the efficient operation of complex processes as well as to promote the deep understand of their behavior [78]. The mathematical models used for simulation consists of a set of variables for describing some properties and also of a set of equations that build the relationships between these variables and is able to predict the performance of the system. In process synthesis, many of these systems are very complex and characterized for nonlinear behavior. Then, it is very important that the model present a good accuracy to represent the processes. However, this high-fidelity models often come in expense of high computational effort. Some strategies, such as the development of surrogate models to replace the simulation flowsheeting, are gaining attention. This strategy is better discussed in the Appendix A of this thesis.

2.5.3 Process integration

Process integration corresponds to a holistic and systematic methodology that allow the combination of parts of processes or whole processes aiming to reduce the resources consumption or emissions to the environment. Consequently, it can contribute to improve the overall performance, increasing the energy efficiency, minimizing wastes and efficiently use the raw materials. Moreover, the process integration can contribute to understand the tradeoffs related to the implementation of biorefineries [70], as well as the possible synergies between processes. The process simulation can be a key tool to facilitate the process integration, since it can be used to develop general flowsheeting and understand the behavior of the process as well as its performance.

The process integration approach started mainly in the 1970s motivated by the energy crises, consisting by the pinch analysis based heat integration. The heat integration methodology is able to provide a systematic design procedure for energy recovery, since it investigates the potential for heat exchange between heat sources and sinks with the goal to reduce the amount of external utilities to the process, leading to a more effective and efficient use of the resources [79].

The application of the pinch analysis has proven to increase the energetic efficiency in industrial sites, such as chemical plants and refineries [80]. In addition, the Pinch technology applied to the pulp and paper mills, has shown a potential to contribute to decision-makers to decide on the implementation of new technologies, reduce the utilities consumption, going for alternatives with environmental compliance, considering make changes in the process such as the placement of heat pumps, and many others [81]. Thus, this approach allows identifying the best possibilities for process integration of new technologies and for defining cogeneration opportunities. The pinch analysis is described below.

Pinch analysis

The Pinch concept is a process systems tool that can provide important information of the plant regarding the heat integration potential. The composite curves, as illustrated in Figure 2.8a, states that the heat recovery between hot and cold streams is restricted by the shape, and the overlap between the composite curves represents the maximum amount of heat recovery possible within the process [82]. The minimum amount of external cooling required is represented by the “overshoot” in the bottom of the hot composite curve, whereas the minimum amount of

external heating consists of the "overshoot" at the top of the cold composite curve. *ΔTmin* corresponds to the minimum allowed temperature difference in exchangers (heaters and coolers). The point where we can observe the smallest vertical distance (equal to *ΔTmin*) is known as the Pinch point [76].

The overall heating and cooling demands can also be represented as in Figure 2.8b that corresponds to the plot of the net heat flow at each respective temperature interval. This plot is a graphical representation of the heat cascade, and it is very important for identifying the interface between the process and the utility system. The heat balance is made for each temperature interval, and any heat surplus from that interval is cascaded to the next interval at lower temperatures [79]. Moreover, the pinch point is also easily visualized, consisting of the point where the heat flow is zero, and it is not possible to have any hot utility below the pinch and also any cold utility above the pinch. This pinch point thus represents the bottleneck to energy recovery within the process.

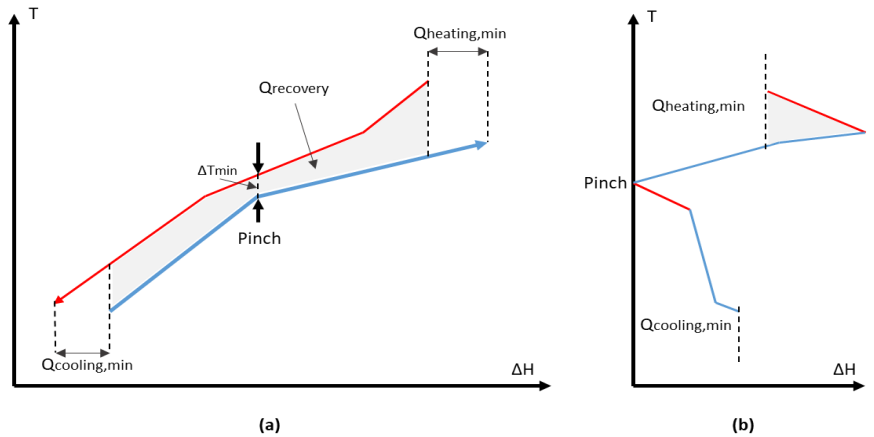

Figure 2.8 Example of: a) Hot and Cold composite curves and b) Grand composite curves. Adapted from [79].

Maréchal and Kalitventzeff (1996) proposed a new composite curve definition, known as integrated composite curve (Figure 2.9), that is based in the integration of the utility system. To build this curve, first the pinch analysis is used to propose the set of utilities that might satisfy the Minimum Energy Requirement (MER); then, the MILP optimization is used to select in this set of utilities the ones that are going to be used and calculate their optimal flowrates, based on the characteristics of the utilities (e.g. pressures, temperatures, compositions) [83]. The integrated composite curve is generated and allows to visualize in the same plot the heat and power aspects of a process or industrial site and how it is possible to improve the integration of the utilities systems. This representation is very useful to explore the results of the optimization

approach and also open the possibility to verify if the choices were consistent or if there is how to improve the utilities systems.

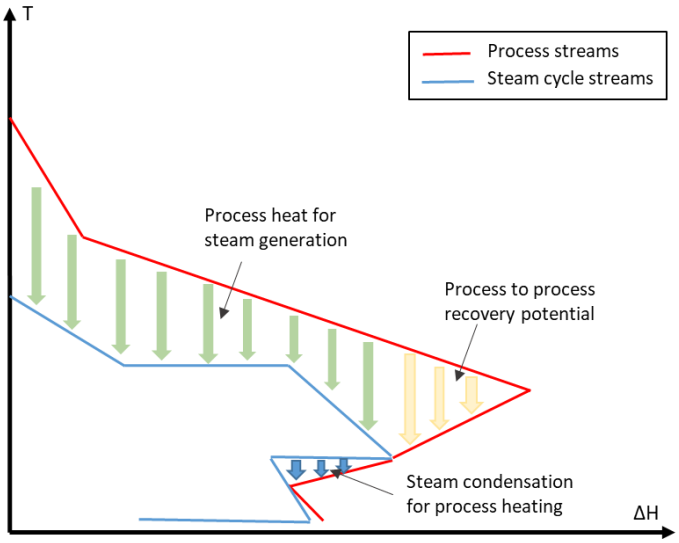

Figure 2.9 Example of Integrated Composite Curve.

2.6 Exergy analysis applied to the pulp and paper mills

To assess the technical performance of industrial chemical processes, several methods based on the First and Second Laws of Thermodynamics have been developed. The combination of these two laws led to the concept of exergy. Exergy is related to the quality of energy. It is defined as the maximum available work that can be obtained from a thermodynamic system when it interacts with the environment by means of reversible processes until the equilibrium state is attained (mechanical, thermal and chemical) [84]. The exergy balance applied to a particular process unit or to a whole chemical process reveals how much of the maximum available energy capacity provided by the feedstock is being utilized in a useful way by the system [85].

The exergy method demonstrates the practical application of the Second Law of Thermodynamics in the analysis of industrial processes, revealing how and where exergy is used or destroyed and provides directions for improvements in the efficiency of the use of available resources. Moreover, the exergy analysis can contribute to obtain optimal configurations, since it can be used as a measurement of environmental [86] and economic aspects [87]. This is due to the fact that the exergy destruction can be the major driver of expenses, and the possibility of measurement of the difference between the system and the ambient allows, for example, to visualize the effects of waste streams in the environment.

In the traditional kraft pulp mill process, the recovery boilers and the digester are reported as the least efficient conversion processes due to the higher exergy destruction presented by these units [28; 88; 89], which emphasizes the need for further process improvements. Lime kiln is an energy-intensive process and its heat losses also contribute to the large extent of irreversibility in the kraft pulp mill.

Some authors suggest that the exergy efficiency of the chemical recovery boiler can be increased by harnessing the exergy of the exhaust gases to preheat the combustion air or water demineralized. The increase in the concentration of the black liquor, which leads to a decrease in the percentage of water and consequently a reduction in the flow of generated gases, can also reduce the heat loss from inside the boiler [90].

The exhaust gases and damp air in the recovery boilers and bark/fuel oil boilers are the main waste flows associated to exergy losses. The temperature of these exhaust gases are between 70-180 °C, which can be suitable for preheating purposes or possible as a heat source in heat pumping systems [28].

The BL drying system also shows an important contribution that influence the overall exergy efficiency of the system. The literature reports that, the higher the number of effects in the MEE evaporator system, the higher will be the exergy efficiency [91]. Other authors also demonstrated that the use of a mechanical vapor recompression system based in the exergy recovery could contribute to improve the performance of the drying BL system compared to the traditional MEE system [92].

It is also very important to understand the impact in the overall process performance when new technologies are considered to be integrated in the existing mills. Notwithstanding, only few studies reported this type of analysis considering the black liquor gasification system. Ferreira et al. (2015) presented an exergy analysis for assessing the potential of BLGCC with and without CCS unit. The BLGCC without CCS achieved an exergy efficiency of 30%, whereas the inclusion of a CCS system decreased in 6% this performance [93]. However, no analysis taking into account the extended exergy performance of the supply chains involved to run those systems was evaluated. Rahman and Yang (2009) studied the influence of the temperature of the black liquor gasification process in the exergy efficiency and in the power generation. The authors found that the higher is the operation temperature, the higher is the exergy efficiency and the higher will be the power generation [94]. The largest share of the exergy destruction in this combined system of black liquor gasification with power generation occurs in the gasifier, achieving around 23.5% of loss.

2.7 Conclusion

Due to its particular composition and physical properties, as well as its large availability in pulp mills, the BL can be a key feedstock for gasification systems. The syngas produced by the BL gasification process can be used in two main routes, namely, for power generation in a combined cycle or a gas turbine, and for fuels and chemicals production such as hydrogen, synthetic natural gas, methanol, dimethyl ether, ammonia and many others. The implementation of these technologies for replacing the conventional recovery boiler may depend on several aspects, such as the type of the host pulp mill, the biomass availability, the technical and economic performance, among other criteria. But, despite the advances in the last years, the black liquor gasification technology still copes with technological gaps that hinder its fully commercial availability. Thus, the feasibility of the advanced configurations must still be further evaluated. To this end, robust process simulation aligned with optimization tools and structured performance indicators are helping in the decision-making of whether implementing or not those energy technologies. To reduce the exergy loss, the process integration is an important strategy that can be used to facilitate the use of heat and minimize the total exergy loss in the integrated system.

CHAPTER 3: METHODOLOGY

The graphical representation of the methodology adopted in this work is summarized in Figure 3.1. In this section, the methods and tools used in the process modelling and simulation are firstly presented. These computer-aided tools help calculating the stream properties and the energy demands of the main equipment. Next, the performance indicators are defined from environmental, economic and thermodynamic perspectives. Then, the optimization problem that minimizes the energy requirements, while maximizing the waste heat recovery and the operating revenues, is shown. Lastly, the hypotheses considered for carrying out the incremental comparative assessments and perform the uncertainty analysis via Monte Carlo simulations are also discussed.

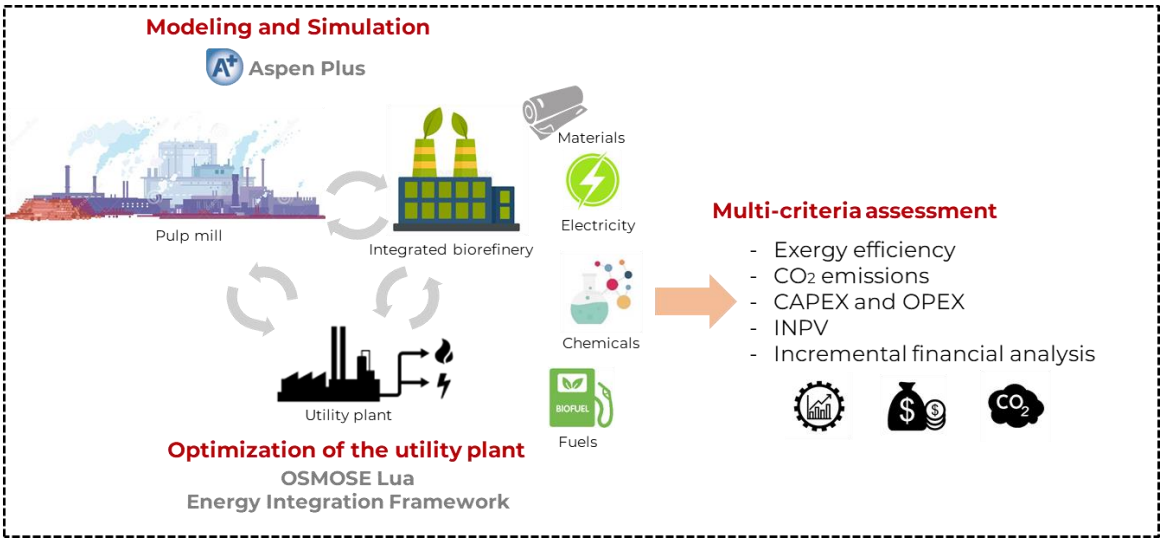

Figure 3.1 Graphical abstract of the methodology adopted in this work.

3.1 Process modelling and simulation

A conceptual process design was performed to represent the main process steps for each processing route. The mass, energy and exergy balances of each process unit are evaluated using Aspen Plus® v8.8 software [95]. The approach considered is based on the integration of a mechanical vapor recompression (MVR) system for alternative black liquor concentration followed by the gasification of the black liquor, syngas purification and conditioning to produce hydrogen, synthetic natural gas, methanol, dimethyl ether, ammonia, urea and nitric acid. Each unit of the proposed integrated flowsheets as well as the assumptions considered for modelling these systems will be described in the following sections.

Regarding the thermodynamic models, the Peng-Robinson equation of state with Boston-Mathias modifications (PR-BM), recommended for nonpolar or mildly polar mixtures, gas-processing and refinery is mostly used [96]. The Perturbed-Chain Statistical Associating Fluid Theory (PC-SAFT) is used to model the physical absorption of CO_2 with dimethyl ethers of polyethylene glycols (DEPG) as in [97]. The NRTL-RK property method (nonrandom two liquid (NRTL) activity-coefficient model and Redlich−Kwong equation of state for the vapor phase) is used for modelling the distillation section of MeOH and DME, since it is suitable for describe the phases presented in these systems [98]. The SR-POLAR thermodynamic model is used for the urea conversion unit, which is suitable for the high pressure, high-temperature conditions. The thermodynamic models NRTL-RK, ELECNRTL and STEAMNBS are considered for the nitric acid section, depending on the characteristic of the stream.

3.1.1 Kraft pulp mill

Considering the kraft pulping process described in section 2.1, a pulp yield of 46.51% with respect to the total amount of digested biomass and a black liquor production rate of 1.44 t_{BL}/t_{pulp} are adopted [22]. The power and steam demands are adapted from [23; 93] to produce about 880 air dried (AD) tons of pulp per day.

The ultimate and proximate composition (mass basis) for BL and other complex materials of interest are obtained by averaging the values found in the literature (see Table 3.1). The other stream properties and assumptions will be addressed in the next sections.

Table 3.1 Ultimate and proximate analyses of wood, bark, black liquor, oil and pulp.

	Wood	**Bark**	**Black liquor**	**Oil**	**Pulp**
Ultimate analysis					
Carbon	49.90	48.58	29.86	85.10	44.44
Hydrogen	6.14	5.52	3.27	10.90	6.17
Oxygen	42.85	41.19	29.05	-	49.39
Nitrogen	0.27	0.36	0.10	-	-
Sulphur	0.00	0.03	4.09	4.00	-
Chlorine	-	0.09	0.90	-	-
Proximate analysis					
Ash	0.83	4.23	32.73	-	-
Fixed Carbon	-	-	10.21	-	-
Volatiles	-	-	57.06	-	-
Moisture	40	50	85	2	10
References*	99; 100; 101; 102	103; 104	105	106	107

*The reported values are an average of the cited literature.

3.1.2 Black liquor evaporation

Differently from the conventional kraft pulp mill (see Figure 2.1), in which multiple effect evaporators are used; in this work, an alternative drying process consisting of a mechanical vapor recompression system (MVR) is adopted. The Mechanical Vapor Recompression (MVR) substitutes the large steam requirement in the BL concentration in multi effect evaporators by a demand of electrical energy, resulting in a very low operating cost compared to a multiple effect operation and higher efficiency, while reducing the moisture of BL to about 15% wt. [92]. This alternative concentration process is composed of three consecutive stages, namely BL preheating, evaporation and steam superheating (see Figure 3.2) [92]. In the first stage, BL is preheated using the compressed vapor before it enters in the steam tube rotary evaporator, wherein the weak BL evaporates in countercurrent heat exchange with the compressed steam. The heavy BL (85% wt. solids) leaves the evaporator, whereas the extracted moisture is divided into a recycled stream and a purged steam. The first is recirculated back to the evaporator in order to improve the heat transfer performance and the exhausted steam flows to the superheating stage. The saturated purge is superheated first in a heat exchanger that guarantees the vapor state and then it is recompressed in order to supply the energy required for evaporation [92; 108].

The solid content of the dried BL has a great influence in the viscosity, especially for concentrations above 60%, leading to pumping issues, formation of large liquor droplets, cracking and corrosion [109]. To overcome these drawbacks, some authors proposed a liquor heat treatment (LHT) [110], a thermal method consisting of the depolymerization of polysaccharides and lignin by raising the temperature of BL to 180-190 °C, allowing to obtain highly concentrated BL in a pumpable form [110; 111].

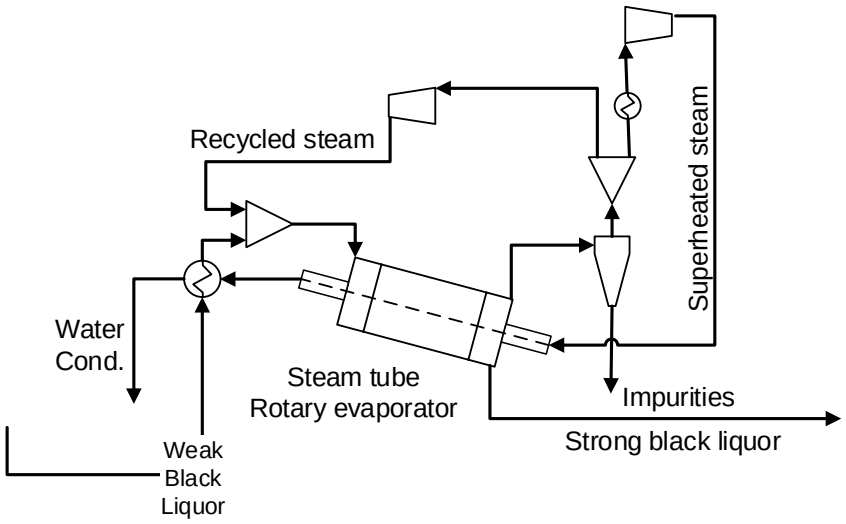

Figure 3.2 Mechanical Vapor Recompression (MVR) system for black liquor evaporation. Source: adapted from [92].

The moisture amount removed in the steam tube rotary evaporator $m_{H_2O,removed}$(kg/h) is determined in terms of the initial black liquor moisture $\psi_{H_2O,as-received}$(%), the desired black liquor moisture at the inlet of the gasifier $\psi_{H_2O,dried\ BL}$(%) and the feed mass flow rate of the weak black liquor, $m_{weak\ BL}$ (kg/h), according to Equation (3.1):

$$m_{H_2O,removed} = \left(\psi_{H_2O,as-received} - \frac{1-\psi_{H_2O,as-received}}{\psi_{H_2O,dried\ BL}}\ \psi_{H_2O,dried\ BL}\right) m_{weak\ BL} \quad (3.1)$$

The evaporation temperature (T, in °C) is estimated by Equation (3.2) which considers the concept of equilibrium moisture content, MC_{eq}, under the superheated steam condition [92; 108].

$$MC_{eq}(wt\%\ wet\ basis) = 54.678e^{-0.046T} \quad (3.2)$$

3.1.3 Black liquor gasification

The conceptual black liquor gasification with oxygen unit is represented in Figure 3.3. The concentrated BL coming from the evaporation unit follows to a pressurized entrained-flow, high temperature black liquor gasification process. Several stages, namely drying, pyrolysis, gasification and combustion, are taken into account to simulate the gasification process. The gasification pressure and temperature are set as 30 bar and 1000 °C [112], respectively. As black

liquor is a non-conventional component in Aspen Plus, so its properties were calculated based on the ultimate and proximate analysis reported in Table 3.1. The HCOALGEN and DCOALGEN models were selected for enthalpy and density solids calculations, respectively [113].

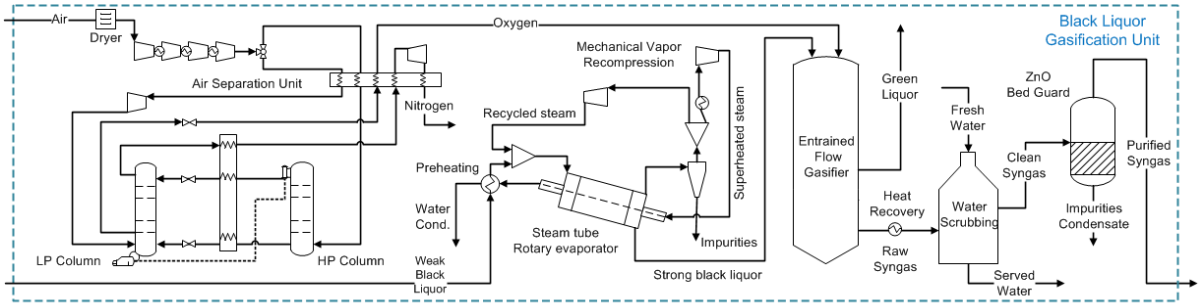

Figure 3.3 Black liquor gasification unit.

The RYield reactor is used to simulate the decomposition unit where black liquor is break down into its main constituent components, namely C, S, O_2, H_2, Cl_2, N_2 and ash. After being decomposed, the black liquor follows to the equilibrium reactor where C, H_2, CO_2, CO, CH_4, H_2S, NH_3, H_2O and HCl were fixed as the main products [113]. The H_2S and NH_3 were split from the main fuel stream before enters the other equilibrium reactor, where gasification takes place [113]. The reactions involved in gasification are summarized below in Equations (3.3-3.7):

Water gas: $C + H_2O \leftrightarrow CO + H_2 \quad \left(\Delta H^{o}_{298K} = 131 kJ/mol\right)$ (3.3)

Water gas shift: $CO_2 + H_2 \leftrightarrow CO + H_2O \quad \left(\Delta H^{o}_{298K} = -41.21 kJ/mol\right)$ (3.4)

Steam reforming: $CH_4 + H_2O \leftrightarrow CO + 3H_2 \quad \left(\Delta H^{o}_{298K} = 206 kJ/mol\right)$ (3.5)

Boudouard: $C + CO_2 \leftrightarrow 2CO \quad \left(\Delta H^{o}_{298K} = 172 kJ/mol\right)$ (3.6)

Tar forming: $6CO + 9H_2 \leftrightarrow 6H_2O + C_6H_6 \quad \left(\Delta H^{o}_{298K} = -158.3 kJ/mol\right)$ (3.7)

In the quench zone of the gasifier, the smelt is separated, diluted with water and recycled back to the causticization plant in the form of green liquor to regenerate the chemicals used in the kraft process. The combustion oxygen-rich of a fraction of the char produced in the pyrolysis step of black liquor supplies the energy required by the endothermic drying, pyrolysis

and reduction reactions. The heat and power demands associated with the air separation unit that provides the necessary oxygen for this gasification process were adapted from [114].

After the syngas produced leaves the gasifier, it is cooled down to 35 °C and scrubbed with water, in order to remove the impurities that may affect the downstream equipment. Finally, a zinc oxide (ZnO) guard bed, modelled as an ideal separator, is used to remove the sulfurous compounds. The syngas obtained after these steps presents the following composition in mole% : H_2 (36.71%), CO (26.75%), CO_2 (33.21%) and other minor compounds (CH_4, H_2O, O_2). This composition is in agreement with the one reported in the literature using a similar system [92], presenting an average error of 5%.

3.1.4 Synthesis gas treatment and purification processes

The syngas conditioning and purification processes are splitted into two units here, namely “syngas treatment unit” and “gas purification unit”. These units will be described in details below, since the syngas that leaves the gasifier needs to be treated and its composition must be adjusted considering the requirements for each specific fuel and chemical that is going to be produced further.

<u>Syngas treatment unit</u>

For the ammonia production, the H_2:N_2 molar ratio needs to be 3:1, so it is necessary that the syngas passes through an autothermal reformer (ATR) (governed by Equations (3.5, 3.8-3.9)), followed by shift reactors (Figure 3.4). As for the synthetic natural gas production, the syngas also passes through an autothermal reformer, however shifting the equilibrium aiming to increase the CH_4 content. Meanwhile, for hydrogen, methanol and dimethyl ether production, the syngas follows directly to the shift reactors (Figure 3.5).

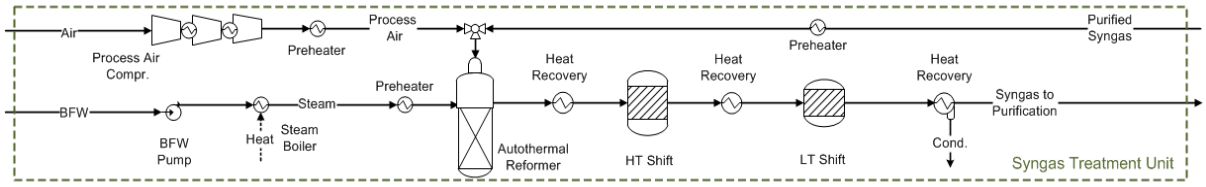

Figure 3.4 Syngas Treatment Unit for ammonia and synthetic natural gas production.

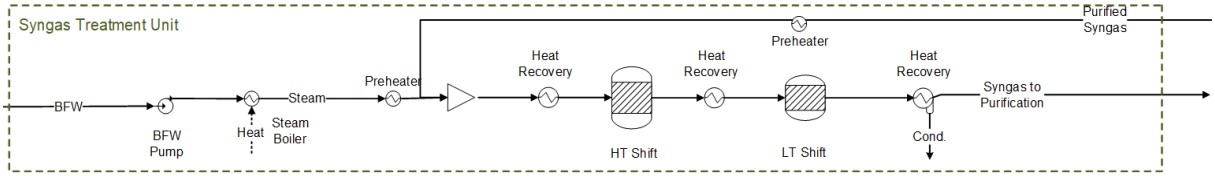

Figure 3.5 Syngas Treatment Unit for hydrogen, methanol and dimethyl ether production.

In the ATR, a portion of the reformed mixture is burnt with air in order to provide the energy to the reforming reactions as well as to attain a H_2/N_2 3:1 ratio, suitable for ammonia production [115]. The syngas reacts with an air stream that is previously compressed and preheated (35 bar, 540 °C) and with a saturated steam inside of an autothermal reformer. Therein, the syngas partial combustion increases the reactants temperature to 970 ºC, leading to the required H_2/N_2 ratio and meeting the reactor heat balance. The mixture passes through a heterogeneous reaction zone filled with a catalyst that is resistant to high temperature in order to reform the hydrocarbons and increase the hydrogen production [116]. The reactor effluent is then cooled down from 970 °C to approximately 350 °C in order to achieve a suitable feed temperature for the high temperature shift (HT Shift) reactor.

$$CO + H_2O \leftrightarrow CO_2 + H_2 \qquad \left(\Delta H^{o}_{298K} = 41.21\,\text{kJ/mol}\right) \tag{3.8}$$

$$CH_4 + 2O_2 \leftrightarrow CO_2 + 2H_2O \qquad \left(\Delta H^{o}_{298K} = -890\,\text{kJ/mol}\right) \tag{3.9}$$

At the HT Shift reactor filled with iron chromium catalyst, more hydrogen can be produced at the expense of the CO and water still present in the syngas (Equation 3.4) [116]. The exothermic water gas shift (WGS) reaction is equilibrium-limited but kinetically favored at higher temperatures which results in an incomplete conversion of carbon monoxide. So, the WGS reaction is preferably achieved in two shift reactors: a high temperature shift reactor and a low temperature shift reactor (LT Shift) reactors. After the mixture is partially converted in the HT Shift, the syngas is once again cooled down to 220 °C and fed to a LT Shift (copper-zinc catalyst) reactor, wherein the concentration of CO is reduced and the temperature rises to 232 °C [116]. The intercooling of the HT Shift and LT Shift reactors as well as the condensation of the excess steam is provided by preheating the boiler feedwater (BFW) and by using cooling water (CW). For methanol and dimethyl ether, this unit is modelled considering a design specification (Flowsheeting Options | Design Spec) setting the H_2:CO mole ratio equal to 2 (tolerance 0.1), varying the BFW input, in order to begin fitting the syngas composition to that required to enter the methanol loop. The same strategy is used for the synthetic natural gas

production, but setting the H_2:CO mole ratio equal to 3:1, in order to meet the requirements for this fuel synthesis. For hydrogen production, it was designed (Flowsheeting Options | Design Spec) to maximize H_2 mole fraction. The cold syngas produced (30 °C) will be sent to the Gas Purification Unit.

Gas purification unit

All the oxygenated compounds (CO, CO_2, O_2 and H_2O) should be removed before the syngas proceeds to the ammonia synthesis loop to avoid poisoning the catalyst used in this process The gas purification unit for ammonia production is composed of a CO_2 capture system and a methanator (Figure 3.6). For the other chemicals production processes, this unit is composed only by the CO_2 capture system.

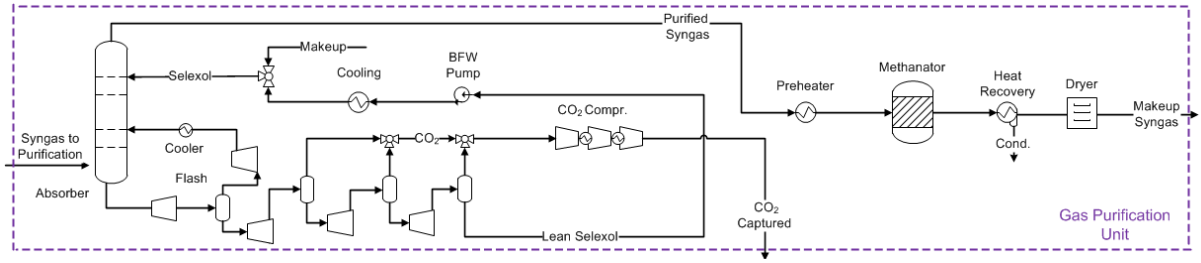

Figure 3.6 Gas Purification Unit.

Syngas purification based on the physical absorption is normally favored over chemical solvents if the process presents very high CO_2 concentrations and partial pressures [117], and the absorption of CO_2 in the solvent significantly increases at high pressure and low temperature. This system consists of a high pressure absorber (30 bar) where a mixture of dimethyl ethers of polyethylene glycol (DEPG) contacts the syngas, producing a CO_2-rich solution in the bottom. The rich DEPG solution is regenerated with a gradual pressure reduction that can also recover the energy derived from the expansion. The use of DEPG include some advantages, such as: i) the fact that the solvent regeneration demands a lower energy consumption due to the absence of a reboiler component; ii) during the absorption processes the DEPG performs a partial gas dehydration and the temperature for the CO_2 separation is near to the ambient conditions; and iii) the operating conditions for the DEPG process is more stable and non-corrosive, which take off the need of a special metallurgy, relatively reducing the capital and operating costs [118].

After the CO_2 removal, the syngas may still contain CO and CO_2, which should be removed for the purity requirements of the ammonia synthesis (this step is not necessary for the other chemicals). So, the syngas follows to the methanation system to remove the remaining oxygen compounds at expense of the consumption of a fraction of the hydrogen produced, converting oxygen compounds into inert methane over a nickel catalyst [116]. Downstream the methanator reactor, the syngas is cooled down and the moisture is removed.

As for the methanol and dimethyl ether synthesis, the syngas composition must be adjusted considering the stoichiometric number (SN), defined in Equation (3.10) (Flowsheeting Options | Design Spec), where y_i represents the mole fraction of the component *i*.

$$SN = \frac{y_{H_2} - y_{CO_2}}{y_{CO} + y_{CO_2}} \tag{3.10}$$

The literature reports that the SN should be slightly above 2, that is considered the best condition for entering the methanol loop [98; 119]. This condition also satisfies the commercial practice of maintaining a high $CO:CO_2$ ratio to increase the reaction rate and the CO_x conversion to methanol [119]. For the synthetic natural gas production, the SN needs to be approximately equal to 3 which is suitable for the later synthesis [120].

3.1.5 Production of bio-based fuels and chemicals

Finally, the purified syngas will be sent to each chemical or fuel synthesis process evaluated in this work: hydrogen, synthetic natural gas, methanol, dimethyl ether, ammonia, nitric acid and urea. The conditions and assumptions for the modelling and simulation of each of these products are described in the following subsections.

3.1.5.1 Hydrogen production

Due to the high grade requirements, the hydrogen purification step is mandatory, usually performed in batteries of adsorption columns known as pressure swing adsorption (PSA). This system is represented in Figure 3.7. The principle of this process is the internal pressure modulation of the column. The pressure swings that occur during an operation cycle determine the degree of retention of each gas [121]. PSA is an adsorption process onto the surface

of porous materials, such as activate carbon, zeolites, among others, that produces higher quality hydrogen (99.99%) at feedstock pressure [122].

After the CO_2 capture process, the purified syngas follows to the PSA system to separate hydrogen from other components. The CO_2 removal before the hydrogen purification reduces the size of the PSA system. The PSA unit was simulated as ideal separators, working at realistic pressure and temperature (30 bar and 35 °C, respectively) [123], assuming a hydrogen recovery efficiency of 80% mol [124]. The power consumption of the adsorption system is assumed as negligible compared to the power consumption in the downstream processes. The PSA unit is assumed as isothermal [124]. Pure hydrogen exits the PSA unit as the main product, whereas the purge gas produced can be burnt to recover its energy. Then, the purified hydrogen stream is compressed up to 200 bar for its exportation [125].

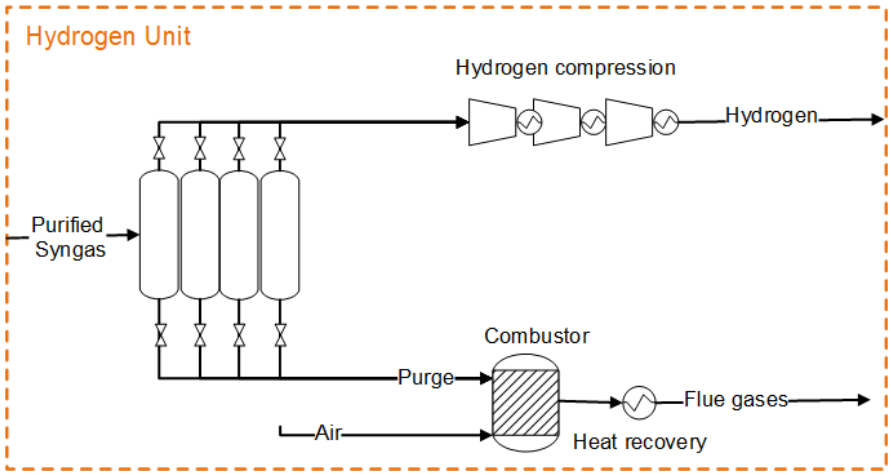

Figure 3.7 Flowsheet of the hydrogen unit production via pressure swing adsorption.

3.1.5.2 Synthetic natural gas

The synthetic natural gas production (Figure 3.8) is driven by the methanation reactions shown in Equations (3.11-3.12). The methanation process consists of three sequential reactor beds wherein the catalytic conversion of hydrogen, CO and CO_2 into methane and water occurs at temperatures between 250-700 °C [120], and pressure equal to 30 bar. Since the methanation reaction is exothermic, an efficient heat recovery is essential for any industrial methanation technology, and a bed intercooling and flow recycling are required to avoid catalyst deterioration. The gaseous mixture produced in the methanator has a high methane (> 97%) and moisture content, thus, an additional desiccation process is required in order to achieve commercial standards [124].

$$CO+3H_2 \longleftrightarrow CH_4+H_2O \qquad \Delta H = -206\,kJ\,mol^{-1} \tag{3.11}$$

$$CO_2+4H_2 \longleftrightarrow CH_4+2H_2O \qquad \Delta H = -165\,kJ\,mol^{-1} \tag{3.12}$$

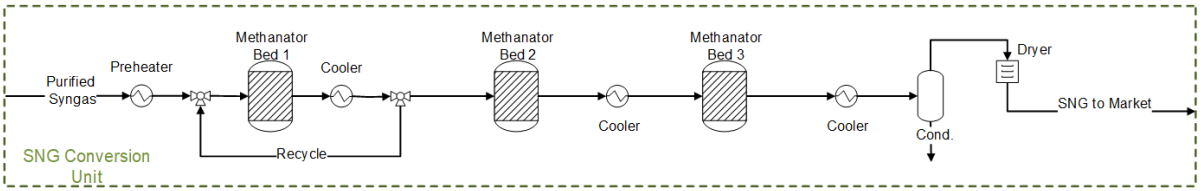

Figure 3.8 Flowsheet of the synthetic natural gas unit production.

3.1.5.3 Methanol synthesis

The flowsheet of the integrated kraft pulp process and methanol production plant is illustrated in Figure 3.9. Commercial methanol synthesis processes are carried out with a $CuO/ZnO/Al_2O_3$ catalyst at temperatures ranging from 200-300 °C and pressures at 50-100 bar [126]. There are different reactor configurations, but fixed bed reactor with quench or multi-tubular reactor with cooling are mainly used for industrial applications [127]. Commercially, the most used technology is the Lurgi externally-cooled multi-tubular reactor, with catalyst inside the tubes [127]. Methanol is obtained by syngas and the reaction is limited by chemical equilibrium, where a higher methanol yield is obtained at higher pressure and lower temperature [128]. So, the recycle of unreacted gas is necessary in order to turn the process feasible achieving higher conversions [129].

The methanol synthesis is modelled using the LHHW (Langmuir-Hinshelwood Hougen-Watson) kinetic model developed by (Graaf et al., 1988) and reformulated by [98] to be implement in Aspen plus (see Appendix B). The model considers three main equilibrium reactions, Equations (3.13-3.15).

$$CO + 2H_2 \leftrightarrow CH_3OH \qquad \left(\Delta H^{o}_{298K} = -90.77\,kJ/mol\right) \tag{3.13}$$

$$CO_2 + H_2 \leftrightarrow CO+H_2O \qquad \left(\Delta H^{o}_{298K} = +41.21\,kJ/mol\right) \tag{3.14}$$

$$CO_2 + 3H_2 \leftrightarrow CH_3OH + H_2O \qquad \left(\Delta H^{o}_{298K} = -49.16\,kJ/mol\right) \tag{3.15}$$

The corresponding rate equations for the kinetic model are represented in Equations (3.16-3.18). The detailed description of the parameters are in [98].

$$r_{CH_3OH} = k_A \frac{K_{CO}[f_{CO} f_{H_2}^{3/2} - f_{CH_3OH} / (K_A \sqrt{f_{H_2}})]}{(1 + K_{CO} f_{CO} + K_{CO_2} f_{CO_2})[\sqrt{f_{H_2}} + (K_{H_2O} / \sqrt{K_H}) f_{H_2O}]} \quad (3.16)$$

$$r_{CO} = r_{H_2O} = k_B \frac{K_{CO_2}[f_{CO_2} f_{H_2} - f_{H_2O} f_{CO} / K_B]}{(1 + K_{CO} f_{CO} + K_{CO_2} f_{CO_2})[\sqrt{f_{H_2}} + (K_{H_2O} / \sqrt{K_H}) f_{H_2O}]} \quad (3.17)$$

$$r_{CH_3OH} = r_{H_2O} = k_C \frac{K_{CO_2}[f_{CO} f_{H_2}^{3/2} - f_{H_2O} f_{CH_3OH} / (K_C f_{H_2}^{3/2})]}{(1 + K_{CO} f_{CO} + K_{CO_2} f_{CO_2})[\sqrt{f_{H_2}} + (K_{H_2O} / \sqrt{K_H}) f_{H_2O}]} \quad (3.18)$$

The kinetic model validation was performed using the data and conditions described in [98]. A sensitivity analysis at the reactor unit was performed, varying the temperature in the range of 200-300 °C and the pressure between 50-100 bar with the objective to evaluate the operation conditions. It was observed that the formation of methanol is favored at higher pressures. Kiss et al. (2016) found the same behavior explaining that this phenomenon occurs due to the fact that CO_2 and CO hydrogenation reactions proceed with a decrease of the total number of moles, so as more CO is converted to methanol at higher pressures, the CO yield decreases when the pressure is increased.

Yang et al. (2013) observed experimentally that, depending on the reaction temperature, the carbon atom incorporated into the MeOH molecule can originate from either CO or CO_2. As the temperature is lowered (below 240 °C), the preferred carbon source for the reaction changes from CO_2 to CO. In the same experiment, as the temperature is increased above 240 °C, the CO_2 carbon becomes the dominant reactant [130]. So, as the syngas obtained from BLG contains a higher fraction of CO than CO_2, it was noticed that the behavior is in agreement with the one described in literature, because the methanol formation is favored at lower temperatures. Based on a sensitivity analysis, a temperature of 210°C and a pressure of 90 bar were chosen.

Before the methanol synthesis loop, the purified syngas is compressed up to 90 bar. Therein, the syngas is firstly heated up by the reactor outlet stream in a feed-effluent heat-exchanger (FEHE). Then, the syngas is fed to an isothermal reactor operating at 90 bar and 210 °C. The reactor outlet stream comprises a gaseous mixture containing methanol, water and unconverted reactants. This mixture is cooled and flashed twice, first to 30 °C and 45 bar, and then to 3.5 bar, in order to separate the condensable products and the non-condensable reactants [98]. The condensed stream continues to a distillation column (DC) operating at atmospheric pressure, wherein methanol is produced with purity over 99% wt. A fraction of the non-

condensable stream is purged to avoid the built up of inerts, whereas the remainder is recycled back to the methanol synthesis loop.

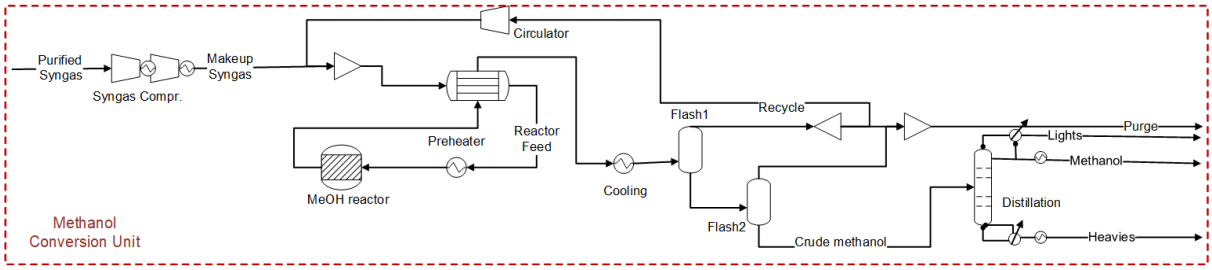

Figure 3.9 Flowsheet of the methanol conversion unit.

3.1.5.4 Dimethyl ether synthesis

The flowsheet of the integrated kraft pulp process and dimethyl ether production process is presented in Figure 3.10. The DME synthesis occurs via the indirect route, i.e. methanol dehydration as in Equation (3.19) over an acid zeolite catalyst.

$$2CH_3OH \leftrightarrow CH_3OCH_3 + H_2O \quad \left(\Delta H^{o}_{298K} = -23.4\,\text{kJ/mol}\right) \tag{3.19}$$

The purified syngas initially passes through the same processes previously described for methanol synthesis, namely, syngas is firstly compressed up to 90 bar and converted to methanol. Next, it continues to the DME synthesis loop, wherein an adiabatic DME reactor is used, since the DME reaction is not highly exothermic and the temperature can be maintained by preheating the feed and running the reactor adiabatically [131]. In the temperature range of normal operation for DME synthesis (250–400 °C), there are no significant side reactions. Catalyst is significantly deactivated at temperatures above 400 °C, and for this reason the reactor is designed for this temperature not to be exceeded. Therefore, the feed temperature of methanol was varied using a design specification that limits the outlet temperature of the DME reactor to the aforementioned limit aiming to maximize the DME production. The reaction rate equation represented by Equation (3.20) is given by [132], which was adapted to Aspen Plus form by [131; 133]. For further details, the reader must check in Appendix B.

$$-r_{CH_3OH} = k_0 \exp(E/RT)\, p_{CH_3OH} \tag{3.20}$$

Where k_0 = 0.336111 kmol/(m^3.s.Pa), E = 80.48 kJ/mol, and p_{CH3OH} is the partial pressure of methanol.

The outlet stream of the reactor is a mixture of water, DME and methanol, that is fed to a first DC, which removes DME as the distillate, with purity over 98.5% wt., meeting the standards defined by the International DME Association [134]. Meanwhile, the bottoms stream is a mixture of water and methanol that is subsequently fed to a second DC. The methanol that exits the second column as the distillate is recycled back to the reactor, while the water exits from the bottom.

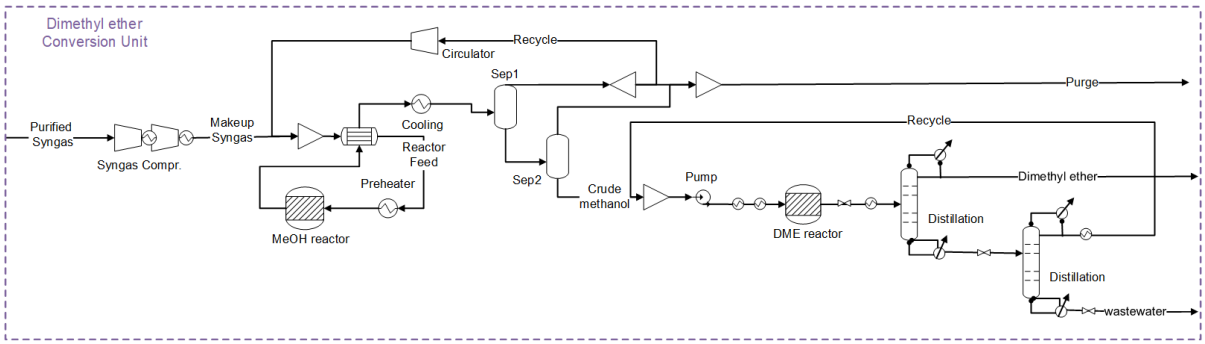

Figure 3.10 Flowsheet of the dimethyl ether conversion unit.

3.1.5.5 Ammonia synthesis

The model for the ammonia production process from synthesis gas is adapted from the work of [116]. The purified syngas coming from the purification process has the desired H_2/N_2 ratio and contains a small percentage of inerts. This mixture follows to the last stage, where it is compressed and fed to the ammonia synthesis loop above 150 bar (Figure 3.11). As the reactants are not fully converted, the unreacted mixture should be recompressed together with the makeup syngas, and recycled back to the ammonia converter. Before enters the converter, the mixture of the recycled and fresh syngas at 200 bar and 35 °C is preheated. The reaction (Equation 3.21) occurs in the presence of an iron based catalyst, obtaining conversions between 10-30%. More details regarding the kinetics of this synthesis is presented in Appendix B.

$$N_2 + 3H_2 \rightarrow 2\,NH_3 \qquad \left(\Delta H^{o}_{298K} = 92\,kJ/kmol\right) \tag{3.21}$$

The ammonia synthesis is highly exothermic. In practice, moderate temperatures (350-550 ºC) are used to achieve acceptable reaction rates and suitable equilibrium conversions [116], since higher temperatures could rapidly increase the loss of the catalyst activity, and lower

temperatures does not favor the exothermic reactor. Thus, it is often recommended the use of sequence of three or more catalytic beds with intercooling aiming to control the catalyst temperature and increase the per-pass conversion. It is also important to mention that the enthalpy of reaction of the ammonia synthesis corresponds to approx. 8.8% (2.72 GJ/t_{NH3}) of the overall fuel consumption in the conventional ammonia plants, which reinforces the importance of recovering as much as possible of this waste heat.

The ammonia produced is preliminarily condensed by using cooling water and then removed in the first flash vessel. However, the ammonia condensation by this method is not complete, being necessary that the recycled stream (joining the makeup syngas) be refrigerated to approximately -20 °C using a two-stage ammonia vapor compression refrigeration system. Although small fractions of inerts are present, the excessive accumulation of such components needs to be controlled, as they can contribute to increase the rate of circulation and reduce the conversion of reagents. A strategy to maintain the overall concentration of inerts down in an acceptable level (< 8% mol) is to purge a portion of the hydrogen-rich recycled gas [116].

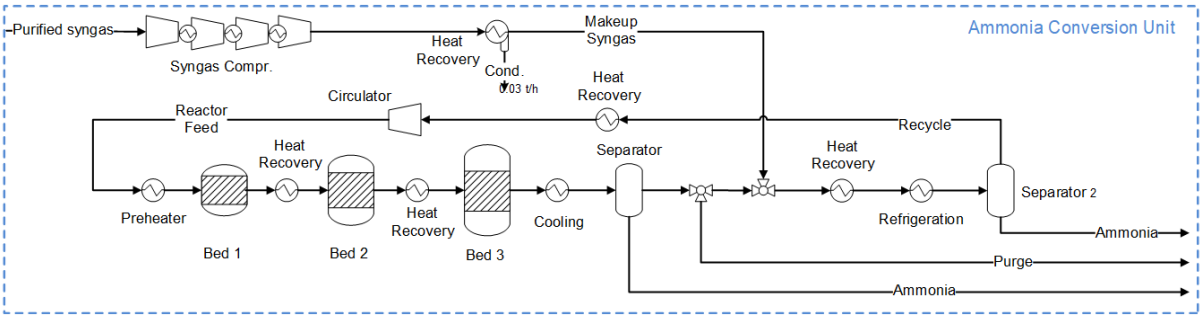

Figure 3.11 Flowsheet of the ammonia conversion unit.

The ammonia produced can be commercialized as it is or be used as a feedstock either to synthesize urea or nitric acid. The process for each of these chemicals will be described in the sequence.

3.1.5.6 Urea production

The commercial urea synthesis is based on the Basarov reaction (Equation 3.22) at 125 – 250 bar and 170 – 220 °C with two reactions: the formation of ammonium carbamate (NH_2COONH_4) (Equation 3.23) and the dehydration of ammonium carbamate to generate urea ($CO(NH_2)_2$) (Equation 3.24). The ammonium carbamate formation is highly exothermic and fast, and the chemical equilibrium is reached under the operating conditions in the reactor. On

the other hand, the dehydration of ammonium carbamate is endothermic and its rate is slow and equilibrium is usually not reached in the reactor. The base simulation approach for the urea model is described in [135].

$$2\,NH_3 + CO_2 \longleftrightarrow CO(NH_2)_2 + H_2O \tag{3.22}$$

$$2\,NH_3 + CO_2 \longleftrightarrow NH_2COONH_4 \quad \left(\Delta H^{o}_{298K} = -136.2\,kJ/kmol\right) \tag{3.23}$$

$$NH_2COONH_4 \longleftrightarrow CO(NH_2)_2 + H_2O \quad \left(\Delta H^{o}_{298K} = +17.6\,kJ/kmol\right) \tag{3.24}$$

The CO_2 coming from the gas purification unit reported in Figure 3.6 is compressed to 141 bar and fed to the CO_2 stripper to strip the urea solution coming from the reactor. In the stripper, ammonium carbamate decomposes, releasing more NH_3 and CO_2 to be stripped out. The outlet liquid solution from the stripper is rich in urea and goes to the low pressure (LP) urea purification section, obtaining an urea solution of 77 wt%. The mixture from the top of the urea purification is sent to the LP carbamate condenser again to compound ammonium carbamate, which is further cooled to pass through a high pressure (HP) ammonium carbamate circulating pump to follow to the Scrubber and eventually go back to the urea reactor to complete the loop.

In the adiabatic urea reactor, an aqueous solution of NH_3 and CO_2 (the major part in the form of ammonium carbamate) and vapors flow upward through the reactor volume to minimize back-mixing and provide sufficient residence time for urea formation. In the reactor, the occurs the condensation of the remaining gases and also the decomposition of the carbamate to provide heat for the slightly endothermic reaction of carbamate to urea. The urea solution overflows from the top of the reactor back to the Stripper, while the unreacted gases pass out the top of the reactor and follows to the Scrubber, where the recycled carbamate solution absorbs the unreacted NH_3 and CO_2, while inert gases go out in the off-gas stream. The solution of the bottom of the scrubber is then mixed with the top vapor stream from the stripper together with the ammonia feed stream.

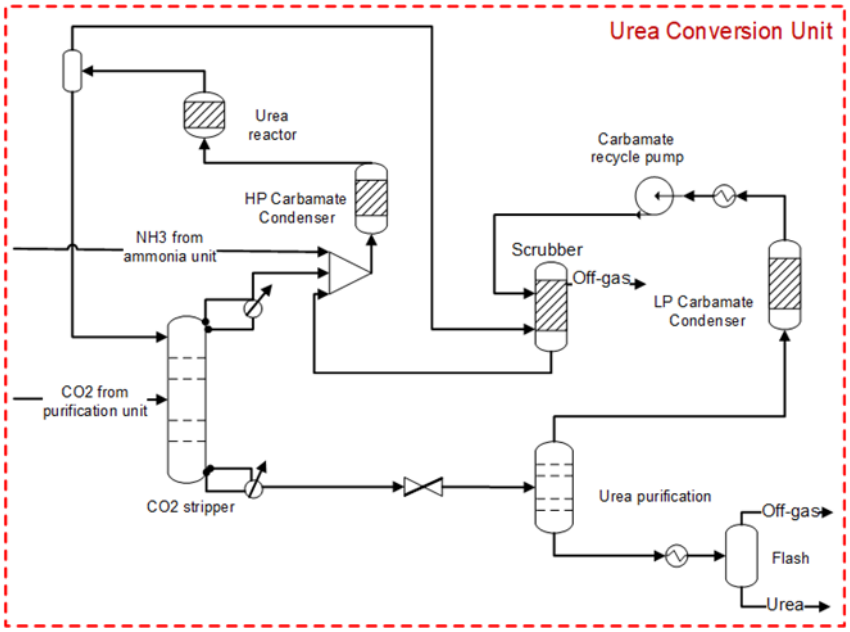

Figure 3.12 Flowsheet of the urea production.

3.1.5.7 Nitric Acid synthesis

Figure 3.13 illustrates the flowsheet of the nitric acid production. It occurs via the Ostwald process. First, ammonia is oxidized to nitric oxide (Equation 3.25) in the converter, in the presence of platinum or rhodium gauze catalyst at a high temperature of about 500 K and a pressure of 9 atm. Nitric oxide is then reacted with oxygen in air to form nitrogen dioxide (Equation 3.26) carried out by gas cooling shifts equilibrium toward NO_2 formation, whereas giving the sufficient residence time to allow the homogeneous oxidation reaction to complete this process [136]. An increase of the rate of NO oxidation at temperatures around 300 °C could result in an additional recovery of the heat of reaction at temperatures where high-pressure steam can be produced. Then, NO_2 is subsequently absorbed in water to form nitric acid and nitric oxide (Equation 3.27) in the absorption tower. The solution of nitric acid obtained is about 65 wt%, which is in agreement with the commercial grade. The tail gas of the absorption column is treated in the tail gas reactor before being discharged [136].

$$4NH_3 + 5O_2 \rightarrow 4NO + 6H_2O \quad \left(\Delta H^o_{298K} = -905.2\,kJ/mol\right) \tag{3.25}$$

$$2NO + O_2 \rightarrow 2NO_2 \quad \left(\Delta H^o_{298K} = -114\,kJ/mol\right) \tag{3.26}$$

$$3NO_2 + H_2O \rightarrow 2HNO_3 + NO \quad \left(\Delta H^o_{298K} = -117\,kJ/mol\right) \tag{3.27}$$

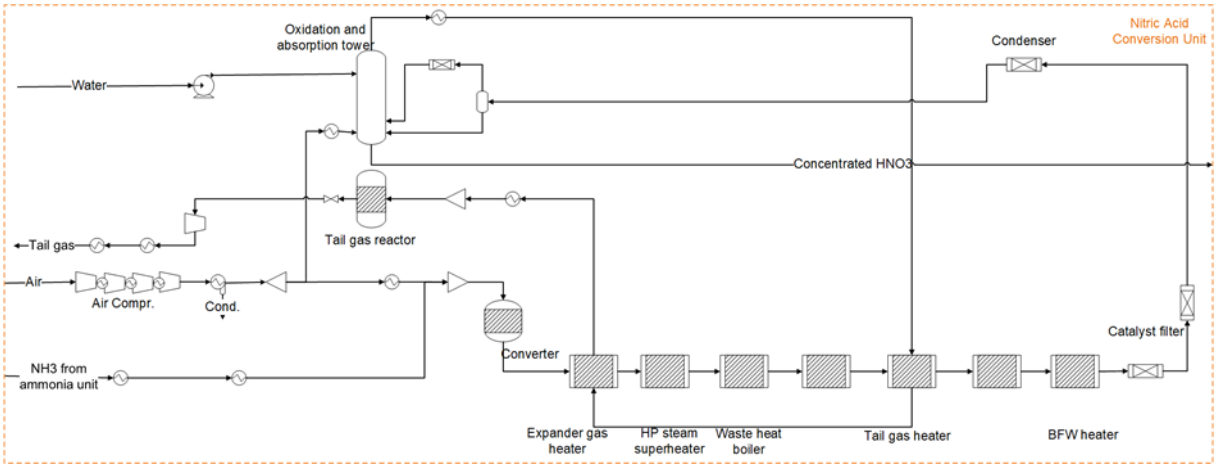

Figure 3.13 Flowsheet of the nitric acid production.

3.2 Performance indicators

The indicators used to evaluate and compare the conventional and alternative chemical plants are defined bearing in mind different perspectives. The base case consists of an existing kraft pulp mill equipped with a typical recovery boiler, whereas the alternative chemicals and fuels production routes rely on the pressurized gasification technology and on the integration thereof within a conventional kraft pulp mill. Since additional energy consumption is required to guarantee the utilities supply to the integrated plants, two operational modes are analyzed. The first operation mode makes use of intensive electricity import from the grid (i.e. 'mixed' mode), whereas the second mode runs without electricity import (i.e. 'autonomous' mode).

3.2.1 Exergy analysis indicators

Total exergy, B [kW] (Equation 3.28), accounts for four exergy components, the kinetic (K), potential (P), thermo-mechanical or physical (PH) and chemical (CH) [84], calculated by using Equations (3.29-3.32), respectively:

$$B = B^K + B^P + B^{PH} + B^{CH} \tag{3.28}$$

$$B^K = 0.5 \cdot m \cdot \left|\vec{\upsilon}\right|^2 \tag{3.29}$$

$$B^P = mgz \tag{3.30}$$

$$B^{PH} = m \cdot [h - h_0 - T_0(s - s_0)] \tag{3.31}$$

$$B^{CH} = n_{mix}\bar{b}^{CH} = n_{mix}\left[\sum_i x_i\, b_i^{CH} + R_u T_O \sum_i x_i\, \ln \gamma_i\, x_i\right] \tag{3.32}$$

Where $\vec{v}$ and z are the velocity (vector) and elevation (scalar) of the system, respect to a stationary reference; m is the mass flow rate; h and s are the specific enthalpy and entropy, respectively; h_0 and s_0 are the specific enthalpy and entropy at standard conditions, respectively; x_i and γ_i are the mol fraction and the activity coefficient of the component i in the mixture; b_i^{CH} is the standard chemical exergy of component i; R_u is the universal constant of gases, and n_{mix} is the total molar flow of the mixture.

Solid and liquid industrial fuels and other substances, such as biomass, are often mixtures of numerous chemical compounds, and the ratio of the chemical exergy to the lower heating value is defined as $\varphi = b^{CH}/LHV$ for pure chemical substances having the same ratios of chemicals constituents (H/C, O/C, N/C). Szargut et al. (1988) derived correlations that express the dependence of φ on those atomic ratios [84]. For biomass and other solid and dry organic substances composed of C, H, O and N, and 0.5 < O/C < 2, the value of φ can be calculated using Equation (3.33), at standard conditions (T_o = 298 K and P_o = 1 bar).

$$\varphi_{dry} = \frac{1.044 + 0.0160\left(H/C\right) - 0.3493\left(O/C\right)\left(1 + 0.0531\left(H/C\right)\right) + 0.0493\left(N/C\right)}{1 - 0.4124\left(O/C\right)} \tag{3.33}$$

Meanwhile, the LHV is estimated based on the correlations reported by [137], Equation (3.34).

$$LHV = 349.1y_C + 1178.3y_H + 100.5y_S - 103.4y_O - 15.1y_N - 21.1y_{ash} - 0.0894y_H h_{lv} \tag{3.34}$$

Where y_i are the mass fractions of carbon (C), hydrogen (H), sulfur (S), oxygen (O), nitrogen (N) and ashes (A) in the dry biomass, and h_{lv} is the enthalpy of evaporation of water at standard conditions (2442.3 kJ/kg).

The calculated lower heating value (LHV) and specific chemical exergy (b^{CH}) of the materials considered in this work, are presented in Table 3.2.

Table 3.2 Calculated lower heating value (LHV) and specific chemical exergy (b^{CH}) for wood, bark, black liquor, oil and pulp.

Material	LHV (MJ/kg dry)	b^{CH} (MJ/kg dry)
Wood	18.85	21.23
Bark	17.90	20.13
Black Liquor	10.28	12.08
Oil	40.56	43.38
Pulp	16.32	19.80

The exergy balance formulation applied to a control volume operating in steady state allows to calculate the overall amount of irreversibility generated in the system, B_{dest}, according to Equation (3.35):

$$B_{dest} = \sum_{e} m \cdot b - \sum_{s} m \cdot b + \int \left(1 - \frac{T_O}{T}\right) \delta Q - W_{useful} \tag{3.35}$$

Where *b* is the specific exergy of the mass flows going through the control volume, Equation (3.36):

$$b = \left(h - h_O\right) - T_O\left(s - s_O\right) + 1/2\left(m\upsilon^2\right) + mgz + b^{CH} \tag{3.36}$$

Where *h* is the specific enthalpy, and *s* is the specific entropy. The terms related to the kinetic and potential exergy in Equation 3.36 can be often neglected in comparison with the chemical and physical exergy of the mass flows. Furthermore, Q and W_{useful} are the rate of heat transfer and useful power, respectively, used to calculate the exergy related to the heat and work that enter or exit the control volume.

In order to compare the different configurations, two exergy efficiency indicators are proposed, namely the rational exergy efficiency (Equation 3.37) and the relative exergy efficiency (Equation 3.38). The rational exergy efficiency defined in Equation (3.37) assumes that the useful output of the integrated energy systems is the total exergy (*B in kW*), not only of the valuable products (chemicals and fuels produced, and cellulose), but also of the by-products (CO_2, purge gas, power).

$$\eta_{\text{Rational}} = \frac{B_{useful,output}}{B_{input}} = 1 - \frac{B_{Dest}}{B_{input}} = 1 - \frac{B_{Dest}}{B_{oil} + B_{wood} + B_{chips} + W_{net}} \tag{3.37}$$

On the other hand, Equation (3.38) quantifies the deviation from the minimum theoretical exergy consumption necessary to make up the main industrial products, i.e. pulp and chemicals or fuels.

$$\eta_{\text{Relative}} = \frac{B_{consumed,\,ideal}}{B_{consumed,\,actual}} = \frac{B_{chemical/\,fuel} + B_{pulp}}{B_{oil} + B_{wood} + B_{chips} + W_{net}} \tag{3.38}$$

In Equations (3.37-3.38), the overall exergy input corresponds to all the energy resources consumed, as depicted in Figure 3.14. Moreover, the term B_{Dest} stands for the irreversibility rate, owed to the imperfection of the actual processes. This indicator can be estimated based on the unit and plant-wise level, considering all the subunits that compose the conventional pulp mill and the integrated chemical plants. The calculation of the physical and chemical exergies is performed via Excel add-ins embedded in Aspen Plus®.

An additional exergy-based indicator evaluated is the *Renewability Performance* defined in Equation (3.39) [138].

$$\lambda = \frac{\sum B_{product}}{B_{fossil} + B_{destroyed} + B_{deactivation} + \sum B_{emissions}} \tag{3.39}$$

Where $B_{product}$ represents the net exergy associated with the renewable products; B_{fossil} is the non-renewable exergy consumed in the production process and supply chain (for biofuels production it considers growing, transport and chemical plant); $B_{deactivation}$ is the deactivation exergy for treating wastes, when they are carried to equilibrium conditions with the environment; $B_{emissions}$ is the exergy of wastes that are not treated or deactivated; and $B_{destroyed}$ is the exergy destroyed inside the system, penalizing the process for its inherent inefficiencies. Depending on the value of this renewability exergy index, it indicates that:

- Processes with $0 \leq \lambda < 1$ are environmentally unfavorable.
- For internal and externally reversible processes with nonrenewable inputs, $\lambda = 1$.
- If $\lambda > 1$, the process is environmentally favorable; and increasing λ implies that the process becomes ever more environmentally friendly.
- When $\lambda \rightarrow \infty$, it means that the process is reversible with renewable inputs and no wastes are generated.

It is worthy to notice that, from a pure energy conservation perspective, bio-based fuels and chemicals production processes are usually considered renewable and environmentally friendly. However, only an analysis based on the Renewability performance indicator addresses the issues associated with the degradation of the energy quality. In fact, the use of renewable resources does not guarantee that the process will be *fully renewable* inasmuch as they could not be used in a rational manner or still require a large amount of fossil resources for its exploitation. In other words, even solely using renewable resources (i.e. no B_{fossil}), a very inefficient conversion process (i.e. large $B_{destroyed}$) could fit into the category of non-renewable process. Contrarily, although a production process uses fossil resources to efficiently convert biomass into a relative large amount of renewable product, the environmental footprint of this last configuration may be lower and its renewability indicator could become higher than that of a totally biomass-based setup.

Thus, the Renewability performance indicator aims to quantify the potential to (i) compensate for the utilization of the fossil resources and the exergy destruction in the whole industrial process, as well as to (ii) mitigate the environmental impact using the renewable energy of the biomass-derived products. Consequently, since all real processes are inherently irreversible, this indicator aims to evaluate not only the extent of process irreversibility (closeness to ideal operating condition), but also the potential offset of those negative effect by working out means of producing bio-based fuels and chemicals that are more sustainable, efficient and less dependent on fossil-fueled supply chains.

The contribution related to fossil fuel consumption (B_{fossil}) is calculated by considering the non-renewable unit exergy costs of the resources consumed, i.e. by including the upstream supply chains of oil 1.0298 kJ/kJ_{oil}, biomass 0.059 $kJ/kJ_{biomass}$ and electricity 0.3329 $kJ/kJ_{electricity}$ as reported by [11; 139]. $B_{deactiviation}$ considers the treatment of the wastewater streams, with an specific electrical energy consumption of 1.7 kJ/kg_{H2O} [140].

3.2.2 CO_2 emissions assessment

Two CO_2 emissions balances were performed: the overall CO_2 emissions and the net one. The overall CO_2 balance (Equation 3.40) is calculated by assuming that the emitted CO_2 (either fossil or biogenic) can be compensated by the avoided CO_2 that is captured by the syngas purification unit. In this case of the overall CO_2 emissions balance, biogenic emissions are accounted in the emissions balance of the plant, so that the more conservative case can be analyzed and means for mitigating these emissions can be also suggested. On the other hand,

the net CO_2 balance (Equation 3.41) assumes that the CO_2 incorporated by the crops ($Biogenic_{emissions}^{direct}$) represents circular emissions, thus, it is subtracted from the overall emissions. The indirect non-renewable CO_2 emissions take into account those generated at the upstream supply chains of the electricity (62.09 g_{CO2}/kWh), wood (0.0043 g_{CO2}/kJ_{Wood}) and oil (0.0029 g_{CO2}/kJ_{Oil}), according to the Brazilian electricity mix profile as reported in [11; 139]. The biogenic emissions comprise those derived from the combustion of woody biomass (bark and chips), depending on the carbon content thereof.

$$\text{Overall } CO_{2emissions} = Fossil_{emissions}^{direct} + EE_{emissions}^{indirect} + Wood_{emissions}^{indirect} + Oil_{emissions}^{indirect} + Biogenic_{emissions}^{direct} - CO_{2captured} \quad (3.40)$$

$$\text{Net } CO_{2emissions} = Fossil_{emissions}^{direct} + EE_{emissions}^{indirect} + Wood_{emissions}^{indirect} + Oil_{emissions}^{indirect} - CO_{2captured} \quad (3.41)$$

Equation (3.42) and Equation (3.43) illustrate how the indirect and direct emissions are calculated, respectively.

$$m_{emissions}^{indirect}[kg_{CO2}/s] = (m_{Fuel}[kg_{Fuel}/s]) * b_{Fuel}[kJ_{Fuel}/kg_{Fuel}] * \frac{r_{Fuel}[g_{CO2}/kJ_{Fuel}]}{1000} \quad (3.42)$$

$$m_{emissions}^{direct}[kg_{CO2}/s] = (m_{Fuel}[kg_{Fuel}/s]) * C_{Fuel}[kg_{C}/kg_{Fuel}] * \frac{M_{CO2}[kg_{CO2}/kg_{C}]}{M_{C}} \quad (3.43)$$

Where r (g_{CO2}/kJ_{fuel}) is the indirect CO_2 emissions factor, M is the molecular mass (kg/kmol), and C_{Fuel} (%) is the percentage of carbon for each fuel reported in Table 3.1. The consumption of the biomass and fuels are calculated considering the LHV and b^{ch} ($\varphi = b^{ch}$ /LHV) presented in Table 3.2.

3.3 Optimization problem definition

In modern industrial chemical processes, there are several processes streams and unit operations interconnected by recycle loops and an extensive waste heat recovery network. Moreover, as long as electricity can be imported from the grid, a trade-off between additional fuel consumption for in-plant cogeneration and the extent of grid electricity purchase is expected. Since both resources can be used to supply the energy demand of the whole plant, the choice will be strongly influenced by the performance of the cogeneration and waste heat recovery systems, as well as by the cost of the electricity and fuel consumed [141]. Thus, when competing energy resources are involved, the conventional utility process flowsheet may be drastically modified and additional or very different demands may be created. This

circumstance requires a complete redesign of the energy integration between the main chemical process and the supporting utility systems, so that the power and steam requirements remain satisfied.

Thus, depending on the availability and cost of the energy resources and on the choice of producing various value-added products, cheaper energy resources (e.g. wood chips) may be favored over more expensive energy inputs, such as electricity [142]. On the other hand, by importing electricity in lieu of generating it in-plant, the energy, economic and environmental impacts are transferred to the outside of the process limits. Thus, depending on the electricity mix, importing electricity from the grid may bring more energy and environmental benefits than using wood chips as fuel in the cogeneration system. All these issues render the determination of the optimality a cumbersome task, if a systematic approach is not adopted.

For instance, the selection of the most suitable alternatives for the utility systems from a resourceful set of energy technologies allows reshaping the integrated curves of the chemical process, aiming to minimize the exergy destruction by reducing the inherent driving forces through the optimization of the waste heat recovery and power generation. This procedure relies on an efficient mathematical programming approach in which the potential energy technologies, resources and production routes are included (see Figure 3.14).

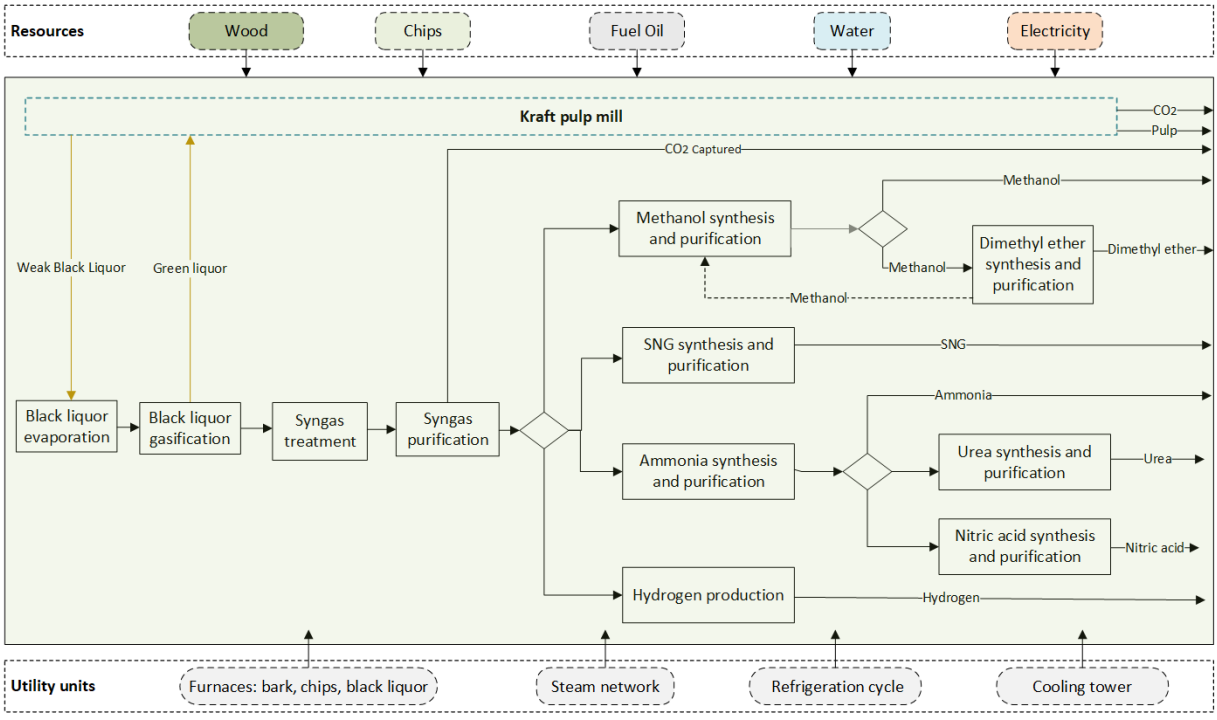

Figure 3.14 Flowsheet of the kraft pulp mill integrated to various chemicals production processes via black liquor upgraded gasification.

Additionally, by separating the chemical process simulation from the energy integration problem, the calculation of the mass and energy balances and the simulation of the complex energy conversion systems can be handled using the Aspen® Plus modeler [95]. Meanwhile, the determination of the minimum energy requirements (MER) and the solution of the energy integration problem is handled by the OSMOSE Lua platform, developed by the IPESE group at EPFL, in Switzerland [66].

The MER is calculated considering the contribution of each hot and cold streams to the overall heat balance, combined into the respective hot and cold composite curves [143]. A physical constraint, namely the minimum temperature approach ΔT_{min}, is used to guarantee that these composite curves would be shifted away from each other, so a reasonable heat transfer rates can be ensured. ΔT_{min} will depend on the nature of each stream, being used 8 °C, 5 °C and 2 °C for gas, liquid and two phases streams, respectively [76]. Equations (3.44-3.46) shows the optimization problem set to find the MER:

$$\min_{R_r} R_{N_r+1} \tag{3.44}$$

Subject to:

Heat balance of each interval of temperature r $$\sum_{i=1}^{N} Q_{i,r} + R_{r+1} - R_r = 0 \quad \forall r = 1 .. N \tag{3.45}$$

Feasibility of the solution $$R_r \geq 0 \tag{3.46}$$

Where N is the number of temperature intervals defined, considering the supply and target temperatures of the entire set of streams; Q is the heat exchanged between the process streams ($Q_{i,r} > 0$ for hot stream, $Q_{i,r} < 0$ for cold stream) and R is the heat cascaded from higher ($r+1$) to lower (r) temperature intervals (kW).

This framework allows to determine the most suitable utility systems (e.g. furnaces, refrigeration, steam network and cogeneration systems, described within more details in the next section) and their operating conditions that lead to the lowest resources consumption and optimal operating cost [143]. The computational framework manages the data transfer with the ASPEN Plus® software and builds the mixed integer linear programming (MILP) problem described in Equations (3.47-3.51) that minimizes the operating cost of the chemical plant. In other words, the optimization problem consists of finding the integer variables, y_w, associated to the existence or absence of a given utility unit, ω, and its corresponding continuous load factor, f_w, that minimizes the objective function given by Equation (3.47):

$$\min_{\substack{f_\omega,\ y_\omega \\ R_r, W}} \begin{bmatrix} f_{Chips}\,(B\cdot c)_{Chips} + f_{Wood}\,(B\cdot c)_{Wood} + f_{Oil}\,(B\cdot c)_{Oil} + f_{Power}\,(W\cdot c)_{Power} \\ -f_{Pulp}\,(B\cdot c)_{Pulp} - f_{chemicals/\,fuels}\,(B\cdot c)_{chemicals/\,fuels} - f_{CO_2}\,(\dot{m}\cdot c)_{CO_2} \end{bmatrix} \tag{3.47}$$

Subject to:

Heat balance at the temperature interval *(r)*

$$\sum_{\omega=1}^{N_\omega} f_\omega q_{\omega,r} + \sum_{i=1}^{N} Q_{i,r} + R_{r+1} - R_r = 0 \quad \forall r = 1..N \tag{3.48}$$

Balance of produced/consumed power

$$\sum_{\omega=1}^{N_\omega} f_\omega W_\omega + \sum_{\substack{chemical \\ units}} W_{net} + W_{imp} - W_{\exp} = 0 \tag{3.49}$$

Existence and size of the utility unit

$$f_{\min,\omega} y_\omega \le f_\omega \le f_{\max,\omega} y_\omega \qquad \forall \omega = 1..N_\omega \tag{3.50}$$

Feasibility of the solution (MER)

$$R_1 = 0,\ R_{N+1} = 0,\ R_r \ge 0 \text{ and } W_{imp} \ge 0,\ W_{\exp} \ge 0 \tag{3.51}$$

Where N is the number of temperature intervals defined by considering the supply and the target temperatures of the entire set of streams; Q is the heat flow rate exchanged between the process streams ($Q_{i,r} > 0$ for hot stream, $Q_{i,r} < 0$ for cold stream) and R is the heat flow rate cascaded from higher ($r+1$) to lower (r) temperature intervals (kW); N_w is the number of units in the set of utility systems; B is the exergy flow rate (kW) of the resources going in and out of the plant; c stands for the purchasing cost (euro per kWh, m^3 or kg) of the feedstock and electricity consumed, or the selling price of the marketable pulp, chemical or fuel (hydrogen, synthetic natural gas, methanol, dimethyl ether, ammonia, urea or nitric acid), surplus power and CO_2 produced; q is the heating/cooling flow rates supplied by the utility systems (kW); and W is the power produced by either the utility systems, the chemical processes themselves or imported from/exported to the grid (kW).

It is important to emphasize that the process modelling and simulation of the chemical plant is performed using Aspen® Plus software. Meanwhile, the utility units are modelled via equation-oriented subroutines written in the Lua programming language [66]. Therefore, the

additional equations required for the mass and energy balances of those units rely on the concept of layer (water, biomass, syngas, chemicals, fuels, power, carbon dioxide, heat).

Representative market costs for wood, chips, oil and electricity consumed, as well as the selling prices of pulp, hydrogen, synthetic natural gas, methanol, dimethyl ether, ammonia, urea, nitric acid and CO_2 produced, are used and are presented in Table 3.3.

Table 3.3 Market costs and selling prices for feedstock and products.

	Market cost/selling price	**Reference**
Wood	0.013 euro/kWh	[23; 144]
Chips	0.016 euro/kWh	[23; 144]
Oil	0.018 euro/kWh	[23]
Electricity	0.06 euro/kWh	[23]
Pulp	0.144 euro/kWh	[145]
Hydrogen	0.072 euro/kWh	[124]
Synthetic natural gas	0.032 euro/kWh	[146]
Methanol	0.065 euro/kWh	[147]
Dimethyl ether	0.07015 euro/kWh	[148]
Ammonia	0.098 euro/kWh	[14]
Urea	0.291 euro/kWh	[149]
Nitric Acid	1.68 euro/kWh	[150]
CO_2	0.0084 euro/kg	[151]

3.3.1 Technologies considered for the utility system

The set of technologies considered in the optimization problem is pointed in Figure 3.15. The steam network is responsible for recovering the waste heat produced in the chemical plant, which impacts directly in the fuels consumption by the utility systems. The steam network superstructure contains a set of superheated steam headers and different draw-off levels of steam, so the recovery and distribution of the waste heat in the chemical plant is allowed. The optimal steam levels are determined by consulting the grand composite curves profile of the chemical processes. Thus, the thermodynamic potential associated to the waste heat exergy can be optimally profited. The decision between importing electricity from the grid or purchase of additional fuel will depend on the performance of this waste heat recovery and cogeneration systems, and also on the respective cost associated to the electricity and wood chips.

As for the furnace model with preheating, the adiabatic flame temperature is changed according to the fuel (bark, chips, oil and black liquor) as well as its respective characteristics such as: molecular weight and LHV in mass basis; the stoichiometric molar air to fuel ratio; and the heat capacity. Also, the temperature of preheating of the air (generally below the pinch point) is provided. The model consists of three heat streams, two hot (radiative and convective) and one cold (preheating), as well as one material stream for fuel demand.

The cooling tower is modelled considering T_{in} equal to 12 °C, T_{out} equal to 40 °C, with a respective consumption of electric power per unit of reject heat as 0.021 kW_{el}/kW_{th} [152]. The refrigeration system is defined considering its exergy efficiency (50%), and also the condenser and evaporator temperatures [97].

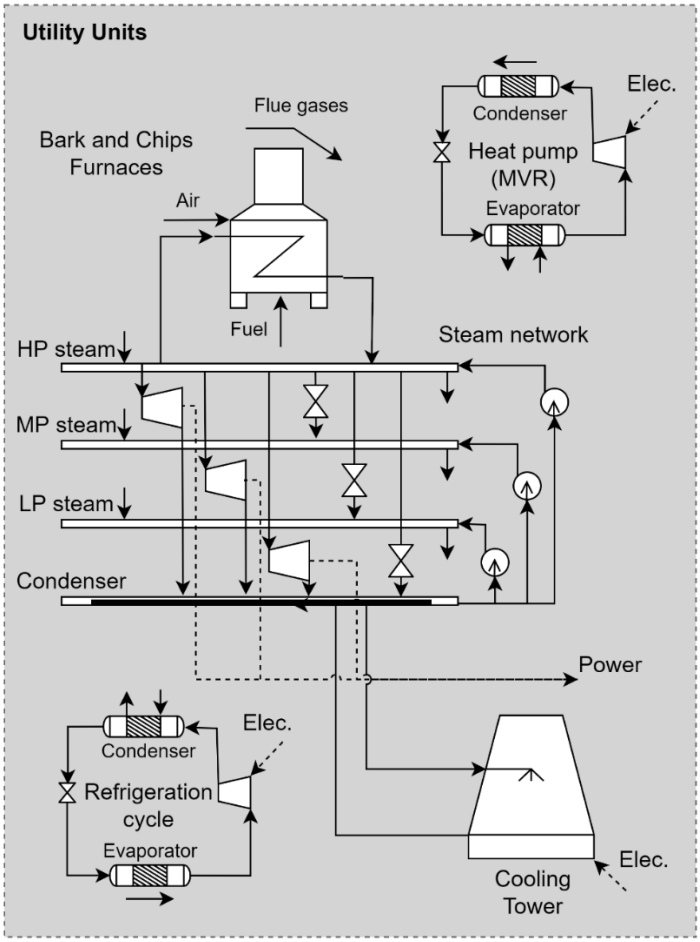

Figure 3.15 Set of technologies considered for the optimization of the utility system.

3.4 Economic analysis

The capital expenditure (CAPEX) of the main plant equipment is estimated by correlating the capacity of each unit to a reference capacity for which cost is known and using power scaling factors as in Equation (3.52) [153]. The references used to estimate the CAPEX of the main units are reported in Appendix C. For the other equipment, such as heat exchangers, pumps, compressors and furnaces the CAPEX is estimated considering the bare module factor methodology reported in [153]. The specific investment costs for the Rankine cycle, cooling tower and refrigeration are 2000 USD/kW [154], 18 USD/kW [155] and 854 USD/kW [156], respectively.

$$C_1 = C_0 \left(\frac{S_1}{S_0} \right)^r \tag{3.52}$$

Where S_0 represents the reference capacity with known capital cost C_0 and S_1 represents the actual capacity for which the capital cost C_1 is unknown. In addition, r is the power scaling factor, which may vary between 0.5 and 0.9 based on the type of process considered.

For the cash flow calculations, a plant lifetime of 20 y is considered. The total CAPEX is splitted among the first (60%) and second (40%) years, assuming a decommissioning cost of 6% of the overall CAPEX. The operating costs (OPEX) are calculated by the methodology suggested in reference [153]. As suggested in reference [157], the OPEX for the kraft pulp mill is considered as 4% of CAPEX. Due to the risk level associated with the technologies, it is assumed 20% as a contingency cost increment [153].

3.4.1 Incremental financial analysis under uncertainty of the commodities prices

The attractiveness of new investments only arises when the new technologies bring benefits over the conventional kraft pulp mill. Then, an incremental financial assessment must be addressed to elucidate the marginal gains and the conditions in which those gains are more likely to be achieved. To this end, some financial indicators are used, including the incremental net present value (INPV) assessed by Equation (3.53) [158]:

$$INPV = \sum_{n=1}^{N} \frac{\left[(\text{Rev-Exp})_{n,option\ B} \right] - \left[(\text{Rev-Exp})_{n,option\ A} \right]}{(1+i)^n} \tag{3.53}$$

Where (Rev-Exp), *i.e.* revenues minus expenses, is the net cash flow evaluated at each (n) of the N yearly periods, in which the reference (A) and the new (B) setups will work. Moreover, i is the average interest rate.

The impact of the variation of the carbon taxes (0-100 EUR/t_{CO2}) and the interest rate (0-21%) on the INPV has been analyzed by means of a sensitivity analysis, aiming to explore the effect of higher risk perception related to the new technologies and also to take into account more stringent environmental regulations.

Firstly, it has been considered that the costs of the feedstock and the products do not vary. In a second analysis, the uncertainty associated to the costs is incorporated to the

incremental financial analysis, simulating the effect of a volatile market. For this reason, the Monte Carlo method is used to simulate the stochastic variation of the prices of the commodities. Normal distributions with mean prices (mentioned in Section 3.3) and standard deviation of 30% are assumed for the commodities prices. In this way, the INPV of the integrated pulp and chemical plants can be estimated in the lifetime of those facilities, considering the probability of achieving a negative value, here denominated 'likelihood of loss'. Table 3.4 presents the three scenarios assessed in this work.

Table 3.4 Scenarios with the respective variation of the carbon taxes, interest rate and prices of commodities considered in the incremental financial analysis.

Scenario	Carbon taxes	Interest rate	Prices of commodities
i. DCTIR_SC	Deterministic (0-100 EUR/t_{CO2})	Deterministic (0-21%)	Stochastic
ii. LCT_DIR_SC	Linear increasing (0-100 EUR/t_{CO2})	Deterministic (0-21%)	Stochastic
iii. SCTC_DIR	Stochastic	Deterministic (0-21%)	Stochastic

In this regard, the "likelihood of loss" will rely on the values of the interest rates, the market prices fluctuations, and the carbon taxations which are representative of risk perception, governmental subventions, and technology readiness levels, also bearing in mind the effect of the money depreciation over time.

3.5 Schematic of the systematic framework used for the chemical process synthesis

Figure 3.16 presents the graphical summary of the systematic framework used for the chemical process synthesis conducted in this work based on the methodology described on the previous sections. The approach relies on the use of heuristics, thermodynamics and algorithmic methods for identifying, assessing and ranking the generated configurations and solutions. Different Computer Aided Process Engineering (CAPE) tools are combined considering solvers for algebraic and differential equations, optimization routines, along with thermophysical properties databases and visualization tools.

In brief, a first literature review is made in order to identify the promising chemicals and fuels available in the market that could be produced using black liquor as feedstock. The mass, energy and exergy balances for each processing route and its respective design specifications are performed in flowsheeting software (Aspen Plus). The energy integration

problem is then defined and solved using the OSMOSE framework, considering the chemical process energy demands identified when the models simulation was performed. A resourceful utility superstructure is proposed for closing the energy balance of the chemical process. The optimal solution is identified based on the minimization of the operating costs. If no solution is retrieved, two actions can be taken: either the utilities system is revisited to verify if some technology should be added or the sizes and conditions are adequate; or some modifications in the flowsheeting are needed in order to enhance its performance. With the optimal solution for the energy integration of the studied scenario identified, the setup is assessed considering the thermodynamic, economic and environmental performance. This process creates a solution database that is further going to be ranked using the TOPSIS method considering multiple objectives such as efficiency, CO_2 emissions, economic performance. This results in recommendations for the market (implementation of the processing route is attractive and under which conditions).

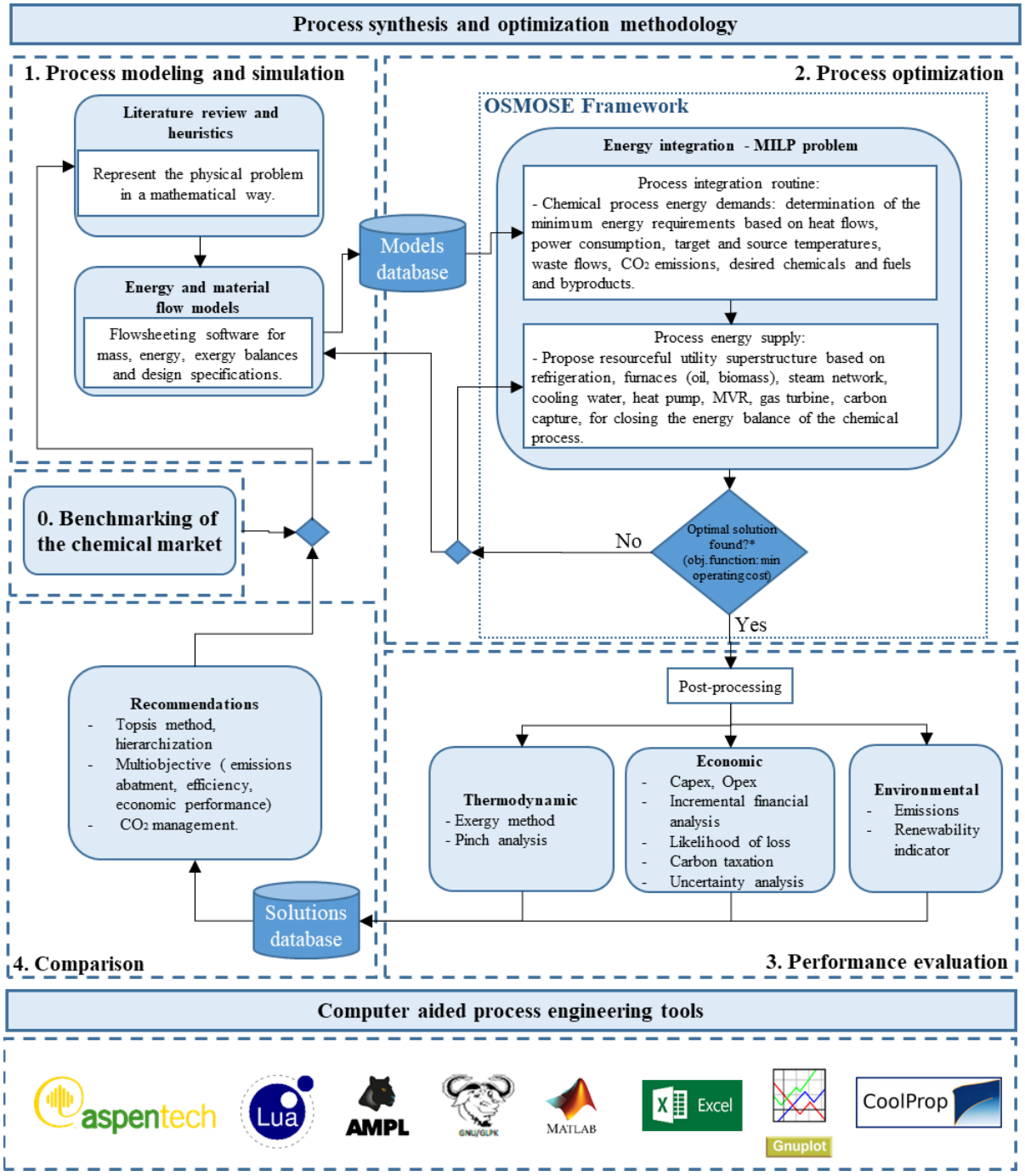

Figure 3.16 Graphical representation of the systematic framework used for chemical processes synthesis.

CHAPTER 4: BLACK LIQUOR DRYING, GASIFICATION AND INTEGRATED COMBINED CYCLE

As pointed out in the literature review, there is a large room for improvement the black liquor handling and use in the traditional kraft pulp mill. According to some authors [19], the conventional scenario based on outdated recovery boilers (60 bar) may be improved by implementing various energy integration approaches. They consist of (i) the utilization of steam networks operating at higher pressures (100 bar), (ii) the substitution of older technologies, such recovery boilers, by gasification systems handling black liquor with higher solids contents and (iii) the diversification of the energy inputs and products, such as the utilization of biorefinery residues and electricity generated from a more efficient electricity mix (e.g. Brazilian mix).

Although the BL gasification is still under development, some studies evaluated the potential to couple this scheme with a combined cycle aiming to obtain a better performance of the BL energy recovery [92; 93; 108; 159; 160; 161]. The black liquor gasification combined cycle (BLGCC) has been successfully demonstrated in a pilot scale [162], presenting high carbon conversion efficiency (>98%). Other authors showed that the implementation of this technology can change the status of the pulp from electricity importer to exporters, due to the surplus produced [160], and also reduces the heat surplus of the mill. Ferreira et al. (2015) found that the BLGCC present an exergy efficiency of 30%, but when this system is coupled to a carbon capture and storage (CCS) system, it decreases to 24%. Despite of the interesting exergy efficiency, the BLGCC integrated to a CCS did not prove to be attractive and requires major incentives [93].

A case of study considering three scenarios, namely the *conventional MEE* case (based on a recovery boiler with the multiple effect evaporation system), *conventional MVR* (based on a recovery boiler with the mechanical vapor recompression system) and the *BLGICC* application (*i.e.* black liquor gasification integrated with combined cycle), is presented. For the sake of considering all the scenarios in a leveling playing field, the steam network is already improved operating at higher pressures. The aim is to analyze the performance of the BL drying systems and also the process integration of the BL gasification system in a kraft pulp mill (Figure 4.1). The results considering the methodology described in Chapter 3 are presented in the next sections.

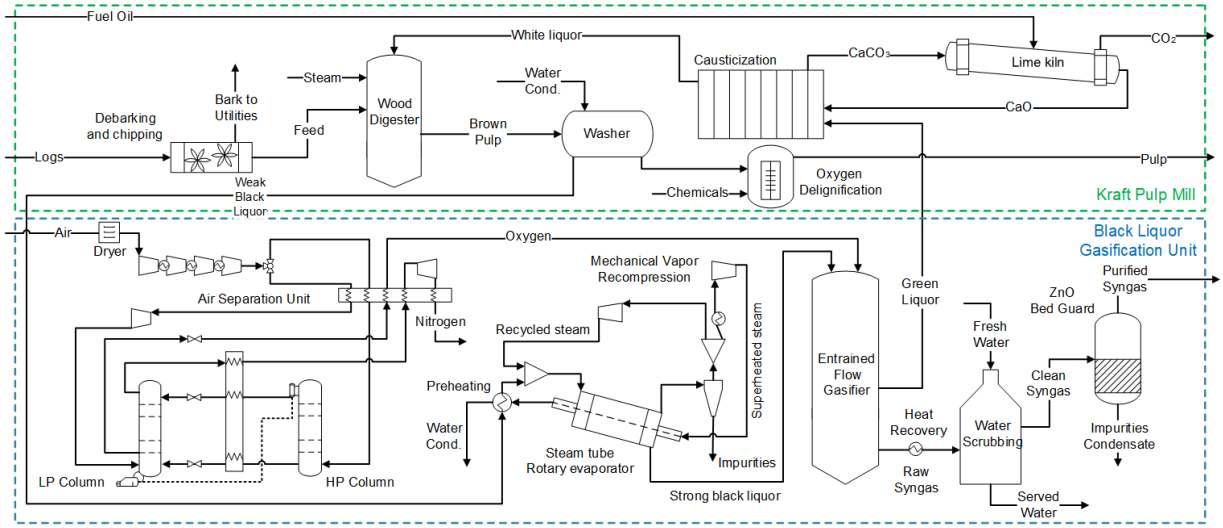

Figure 4.1 Integrated kraft pulp mill and black liquor gasification units.

4.1 Exergy consumption remarks and energy integration

Table 4.1 summarizes the optimal process variables for the three scenarios studied. The efficiency of the upstream supply chains, namely the electricity generation (55.68%), and oil (95.20%) and biomass (86.13%) production and transportation steps, are considered in the *Extended Exergy Consumption* indicator [11; 139]. The addition of the upstream inefficiencies increases the plant consumption in up to 16% in the studied cases. This analysis is important to be considered in the early stages of design, since it evidences a holist scenario, which is useful to support decision-makers and public policies makers towards more efficient and environmentally-friendly production routes.

Table 4.1 Energy consumption remarks for the Conventional MEE, Conventional MVR and BLGICC scenarios.

Parameter	Conventional MEE	Conventional MVR	BLGICC
Fuel input	--	--	Chips
Feedstock consumption (GJ/t_{Pulp})	41.15	41.15	41.15
Utility chips consumption (GJ/t_{Pulp})	0.00	0.00	0.30
Utility electricity consumption (GJ/t_{Pulp})	0.00	0.00	0.00
Oil consumption (GJ/t_{Pulp})	1.05	1.05	1.05
Overall plant consumption (GJ/t_{Pulp})	***42.20***	***42.20***	***42.50***
Extended plant consumption (GJ/t_{Pulp})	***48.87***	***48.87***	***49.22***
Rankine cycle power generation (GJ/t_{Pulp})[1]	3.82	4.26	1.47
Process power consumption (GJ/t_{Pulp})			
- *Kraft Pulp Mill*	2.84	2.84	2.84
- *Black Liquor Treatment and Gasification*	0.00	1.20	1.20
Cooling and refrigeration power consumption (GJ/t_{Pulp})	0.07	0.14	0.07
Min. cooling requirement (GJ/t_{Pulp})[2]	2.81	1.40	1.63
Min. heating requirement (GJ/t_{Pulp})[2]	12.80	8.3	4.36
Biomass consumption (t_{Wood}/t_{Pulp})	3.23	3.23	3.25
Syngas production (GJ/t_{Pulp})	0.00	0.00	9.36
Pulp production (t/day)	877.83	877.83	877.83
Electricity export (kW)	9301	880	12764

1. Steam pressure levels 100, 12, 4 and 0.10 bar, steam superheating 200 °C; 2. Heating requirements of the chemical processes (energy basis) determined from the composite curves.

It can be seen from Table 4.1 that in the conventional MEE and conventional MVR cases, the combustion of the black liquor and the residual bark are enough to supply the utilities requirements, and also export a surplus of electricity. In fact, the exergy efficiency (Table 4.2) and the power balance shows that the integration of a mechanical vapor recompression to this facility becomes slightly less efficient (~2 percentage points) than the conventional MEE approach. This fact evidences a sensible relationship between the amount of power consumed in the mechanical vapor recompression system and the value of the exergy of low pressure steam consumed, namely $Q_{drying} \times \Theta \times N_{effects} \sim W_{MVR}$, where Q_{drying} is the heat flow provided by the steam network to the first effect of the multiple effect evaporator, Θ is the Carnot factor thereof, $N_{effects}$ is the number of effects in the multiple effect evaporator, and W_{MVR} is the power consumed by the mechanical vapor recompression system. As the number of effects increases, the relation becomes an inequality in favor of the multiple effect evaporation system, provided that the steam consumption drops ($Q_{drying} \times \Theta \times N_{effects} < W_{MVR}$). The number of effects is normally maintained between four and six for economic purposes.

On the other hand, as the number of effects reduces, the integration of the MVR unit becomes more and more attractive, as the exergy of the steam used in the first evaporator increases to the point that all the exergy required for concentrating the black liquor would be supplied by the low temperature steam produced in the steam network ($Q_{drying} \times \Theta > W_{MVR}$). Briefly, a large excess of waste heat available in the kraft pulp mill, due to the burning of the

bark and strong black liquor, favors the generation of low pressure steam to provide the exergy required by the drying process over a surplus power generation to drive the mechanical recompression unit. Yet, the performance of both options do not differ significantly in terms of exergy efficiency, thus alternative kraft pulp mills with a heat pumping system (MVR) still seem to be competitive vis-à-vis the conventional layout. Mechanical vapor recompression units have other advantages, e.g. faster and reliable steam superheating using cheap electricity imported or generated by the mill.

According to Figure 4.2, the kraft pulp mill is the major consumer of the power generated. The BL MVR evaporation system is responsible for 25% of the overall power consumed. Unlike the MVR system, in the traditional multiple effect evaporation, the black liquor concentration is performed at the expense of a large amount of steam. Thus, MVR system not only allows reducing the excess steam consumption (with the subsequent condensate management), but also reduces the large driving forces arisen from the comprehensive heat exchange of steam generation and condensation. This maximizes the recovery of the thermodynamic potential by transforming low-grade waste heat into power via a heat recovery network.

In the case of the BLGICC scenario, the air separation unit consumes 13% of the total power produced in the utility system (Figure 4.2c). The integration of a gas turbine to the combined cycle aims to improve the energy integration capabilities at higher temperatures and also boost the electricity generation. In effect, it can be noticed that the use of this technology significantly increases the electricity export compared to the conventional cases.

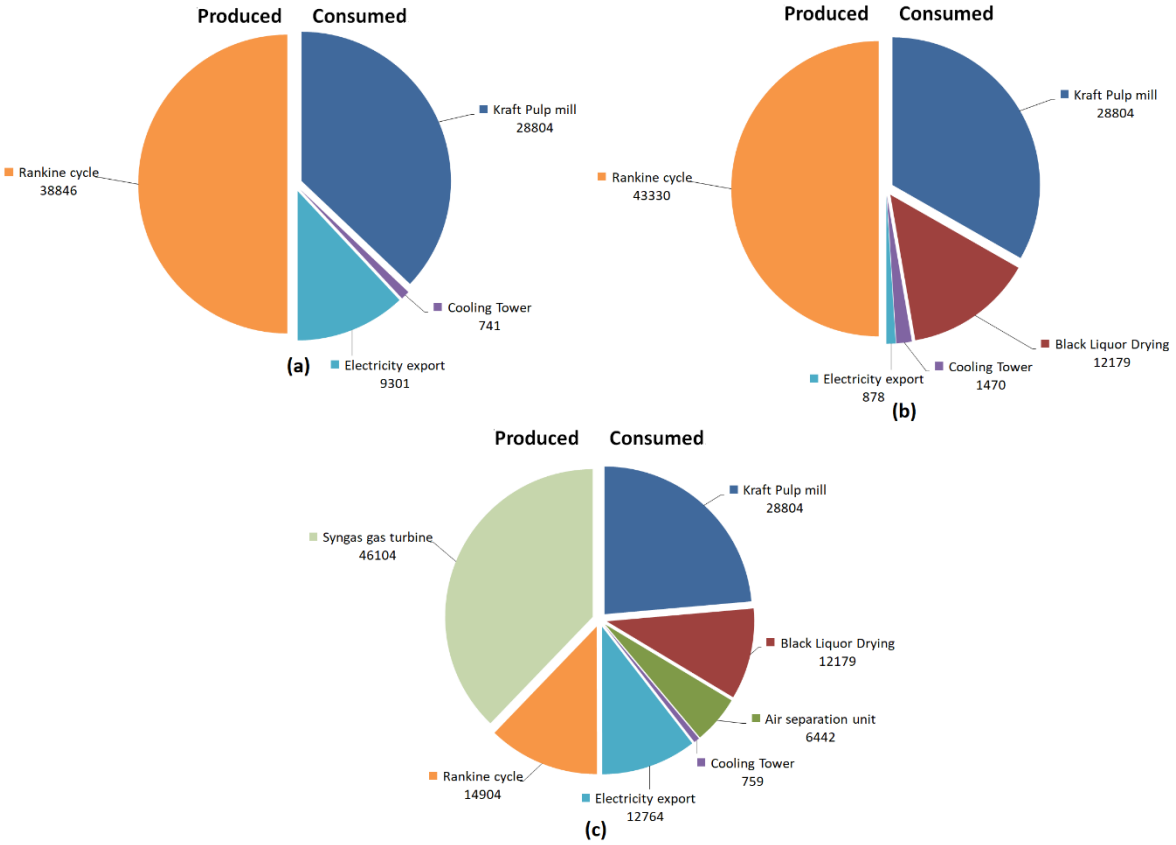

Figure 4.2 Breakdown of the power consumption (in kW): (a) conventional application with multiple effect evaporator (MEE); (b) conventional application with mechanical vapor recompression (MVR); (c) BLGICC-Black liquor gasification integrated to combined cycle.

According to Table 4.2, the BLGICC scenario presents slightly higher exergy efficiencies in comparison to both conventional cases. The consideration of additional upstream sources of irreversibility reduces the exergy efficiency by around 14% for all the studied scenarios (see the Extended exergy efficiency indicators).

Table 4.2 Exergy destruction and efficiencies for the two studied scenarios.

Process parameter	Conventional MEE	Conventional MVR	BLGICC
Rational exergy efficiency (%)	44.4	42.5	44.9
Extended rational exergy efficiency (%)	38.4	36.7	38.8
Relative exergy efficiency (%)	42.3	42.3	42.0
Extended relative exergy efficiency (%)	36.5	36.5	36.2
Exergy destruction (GJ/t_{Pulp})	23.4	24.3	23.4
Extended exergy destruction (GJ/t_{Pulp})	30.1	30.9	30.1

The integrated curves for the conventional MEE, conventional MVR and the BLGICC cases are presented in Figure 4.3. In Figure 4.3b, the heat exchange rate occurring in the four falling film evaporators (as in Figure 4.3a) is represented by the plateau-like extension to the

right, wherein the superheated steam raised using a mechanical vapor recompression is used to concentrate the black liquor. This manoeuvre allows reducing the amount of steam consumed in the concentration process of BL using the waste heat available at lower temperatures to preheat the boiling feed water of a Rankine cycle that, in turn, drives the compression system of the alternative MVR drying technology. Notably, the black liquor gasification with integrated gas turbine (Figure 4.3c) helps maximizing the waste heat recovery. Consequently, the irreversibility associated to the extensive heat transfer rate is reduced, as demonstrated by the shorter span in the abscissa (*H*) of the integrated curves.

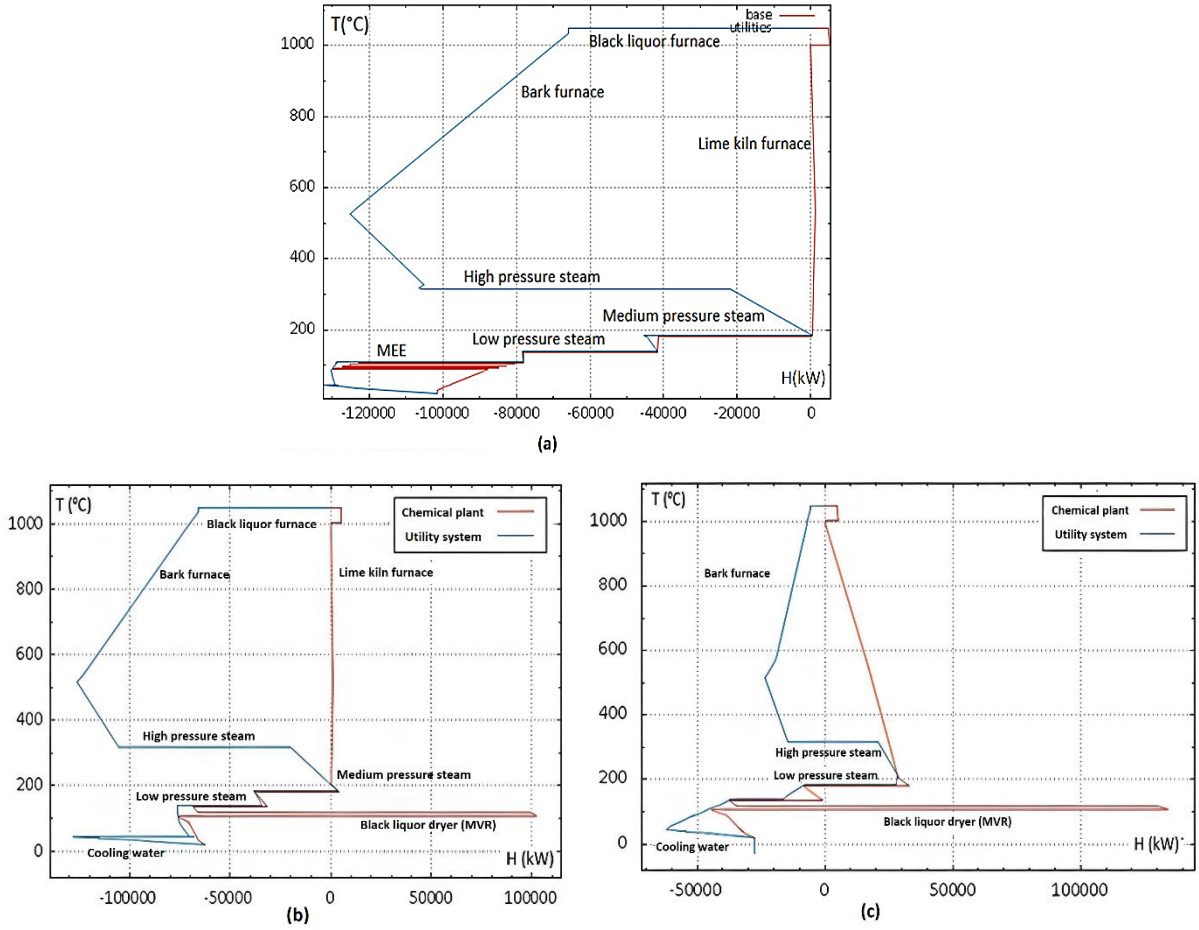

Figure 4.3 Integrated composite curves: (a) conventional application with multiple effect evaporator (MEE); (b) conventional application with mechanical vapor recompression (MVR); (c) BLGICC-Black liquor gasification integrated to combined cycle.

4.2 Economic and environmental assessment

Table 4.3 shows the incomes, costs and revenues of the conventional MEE, conventional MVR and BLGICC scenarios. In fact, the higher power consumption by the MVR system renders the alternative pulp mill equipped with a mechanical vapor recompression

slightly less attractive (2%) than the conventional MEE setup. On the other hand, the BLGICC may lead to higher operating revenues, being an interesting alternative boosted by the fact that it is expected that the capital expenditure of the gas turbines will decrease in the upcoming years [163]. Moreover, the opportunity to install an integrated black liquor gasification combined cycle in order to increase the efficiency and, thus, the profiting of the thermodynamic potential at high temperature, would result in a higher power self-generation efficiency, electrification of the heating requirements and further electricity exportation.

Table 4.3 Operating incomes, costs and revenues of the conventional MEE, conventional MVR and BLGICC scenarios.

Parameter	**Conventional MEE**	**Conventional MVR**	**BLGICC**
Operating Incomes (euro/ t_{Pulp})	728.43	715.00	734.11
Operating Costs (euro/t_{Pulp})	-153.49	-153.50	-154.84
Operating Revenues (euro/t_{Pulp})	575.94	561.12	579.27

Finally, Table 4.4 summarizes the emissions balance as well as the renewability indicator of the studied scenarios. The balance does not vary significantly since no additional fuel was imported in the conventional cases, and only a small amount of fuel chips (see Table 4.1) was needed in the BLGICC case. It is worthy to notice that the direct biogenic emissions are assumed as circular emissions; thus, they do not contribute to the net emission balance. The direct fossil CO_2 emissions are related to the oil consumption in the lime kiln, whereas the indirect fossil CO_2 emissions are associated to the biomass, electricity and oil supply chains. It can be seen that the largest share of indirect emissions belongs to the biomass acquisition and transportation steps, even higher than those directly emitted by the fuel oil consumption in the lime kiln. In fact, the supply chains of the biomass-based route have been already recognized as being important contributors to environmental impact, despite the renewable nature of the feedstock used at the plant-wide level.

Lastly, the renewability performance indicator followed the same behavior of the exergy efficiency, being slightly higher for the BLGICC case when compared to the conventional black liquor combustion due to the better performance of the black liquor gasification with integrated combined cycle using gas turbine technology, which increased the amount of electricity produced. Pellegrini and Oliveira Junior (2011) also demonstrated the biomass integrated combined cycle could achieve higher values for the renewability performance compared to conventional backpressure steam systems and condensing-extraction steam systems [164].

Table 4.4 Fossil, biogenic, direct and indirect CO_2 emissions and renewability indicator of the conventional MEE, conventional MVR and BLGICC scenarios.

Emissions	**Conventional MEE**	**Conventional MVR**	**BLGICC**
Fossil CO_2 emitted –direct (t_{CO2}/t_{Pulp})	0.08	0.08	0.08
Fossil CO_2 emitted – indirect (t_{CO2}/t_{Pulp})	0.18	0.18	0.18
- *CO_2 emitted indirect – EE grid (%)*	0.00	0.00	0.00
- *CO_2 emitted indirect – Biomass (%)*	98.31	98.31	98.32
- *CO_2 emitted indirect – Oil (%)*	1.69	1.69	1.68
Total fossil CO_2 emitted (t_{CO2}/t_{Pulp})	0.26	0.26	0.26
Biogenic CO_2 emissions avoided (t_{CO2}/t_{Pulp})	0.00	0.00	0.00
Biogenic CO_2 emitted – direct (t_{CO2}/t_{Pulp})	1.71	1.71	1.71
Total atmospheric emissions (t_{CO2}/t_{Pulp})	1.97	1.97	1.97
Overall CO_2 emissions balance (t_{CO2}/t_{Pulp})	**1.97**	**1.97**	**1.97**
Net CO_2 emissions balance (t_{CO2}/t_{Pulp})	**0.26**	**0.26**	**0.26**
Renewability performance	**0.69**	**0.64**	**0.71**

4.3 Conclusion

The integration of a mechanical vapor recompression system for drying the black liquor has proven to be an interesting solution to avoid the excess steam generation. The implementation of the BLGCC increased in 37% the potential to generate power compared to the conventional MEE scenario. This potential can be even higher if the steam network is not as efficient as the one considered in this work. Moreover, the BLGCC presented higher exergy efficiency, operating revenues and renewability performance. However, regarding the BL evaporation systems, the large amount of waste heat in the pulp mill makes the integration of a heat pumping technology slightly less attractive, if compared to the case in which a series of multiple effect evaporators are implemented. Although installing a heat pump is not a warranty of higher efficiencies or revenues, it may bust efficiency in certain applications.

CHAPTER 5: HYDROGEN AND SYNTHETIC NATURAL GAS

Indeed, many decarbonization pathways consider that hydrogen plays an important role as either chemical input or energy carrier. It is largely used as feedstock in various refineries and chemicals plants and, and it is drawing recent attention due to its decarbonization potential for the transport sector [165]. In practice, about 95% of the hydrogen is currently produced using coal, oil or natural gas via steam reforming [165], whereas only a small fraction is produced using alternative routes, such as water electrolysis or biomass gasification [125]. Anyhow, the production of biomass-derived synthetic natural gas has been also labeled as an interesting opportunity to drop the CO_2 emissions of the hydrogen production routes, and also be a key element for energy security [166; 167; 168]. Even the synthetic natural is a versatile energy resource, since it can be used for domestic, heating and transportation applications [169]. Moreover, according to the International Energy Agency, in the present context of market uncertainty, the natural gas prices are foreseen to remain extremely volatile [170], which reinforces the need of alternative pathways to overcome its limited availability, guaranteeing the supply of this important commodity.

Naqvi et al. (2010) studied the methane production via black liquor catalytic hydrothermal gasification, considering two scenarios, namely biofuel production with and without import of additional biomass to meet the power requirements. According to the authors, the alternative production route generally improves the plant performance, compared to the existing design that uses a Tomlinson recovery boiler [65]. Since the produced biofuel is partially consumed in the power boiler, a significant reduction in the synthetic natural gas yield (43%) was observed in the second scenario. Later, Naqvi et al. (2012) also studied the production of synthetic natural gas via oxygen-blown black liquor gasification process and direct causticization in order to replace the traditional recovery boiler. The import of additional biomass is required, so that the lack of fuel in the utility plant due to the increase of biofuel production can be offset [171]. Moreover, an important quantity of biogenic CO_2 can be captured. Unlike the present work, in Naqvi et al. (2012), neither the CO_2 emissions associated with the upstream supply chains (*i.e.* the cultivation and transportation of the biomass), nor the effect of the electricity import were assessed.

Andersson and Harvey (2006) studied the potential reduction of CO_2 emissions when using the black liquor gasification to integrate the production of hydrogen, methanol or electricity in pulp mills. The results showed that hydrogen has a significantly higher potential

of reduction of the CO_2 emissions, compared to methanol or electricity co-production routes [64]. An even higher reduction of the CO_2 emissions could be achieved if additional carbon capture is considered. This reduction potential depends on the assumptions regarding the nature of the electricity and the transport of the energy resources [64]. Nonetheless, suggestions on how to improve its attractiveness under more stringent environmental regulations and the uncertain variation of feedstock prices have not been performed. Darmawan and collaborators (2019) investigated the hydrogen and power coproduction via supercritical water gasification to convert the black liquor into syngas. The syngas chemical looping has been also implemented. As result, a relatively high efficiency (80% energy basis) highlighted that the black liquor gasification is a very promising energy technology [16]. However, thermodynamic performance alone does not suffice to ensure financial attractiveness of these upgraded routes.

Despite the relevance of thermodynamic performance for revealing potential actions that may improve the pulp and paper production processes, the previous works fall short of depicting a broader window of feasible operating conditions and, thus, they may lead to misleading conclusions, especially if future implementations of carbon taxations and changing market scenarios are not suitably considered. Thus, in view of the gaps in the revised literature, in this work, the co-production of pulp and either hydrogen or synthetic natural gas via black liquor gasification is evaluated and compared with the conventional kraft pulping processes. The integrated flowsheet proposed is represented in Figure 5.1, where it also depicts the energy resources (*e.g.* chips, wood, fuel oil and electricity) available to be consumed. The products and byproducts that can be manufactured and marketed (pulp, electricity, SNG, H_2 and CO_2) in those facilities are shown. Figure 5.1 also illustrates the utility units used for the combined heat and power production in the cogeneration system. As previously mentioned in the methodology chapter, the integration and sizing of those utility units and the selection of the operating conditions (*i.e.* levels of steam generation, internal power generation, auxiliary boiler activation, extent of electricity import, etc.) may radically impact the extent of the waste heat recovery, the economics and the environmental impact of those facilities, which will be discussed in the next sections.

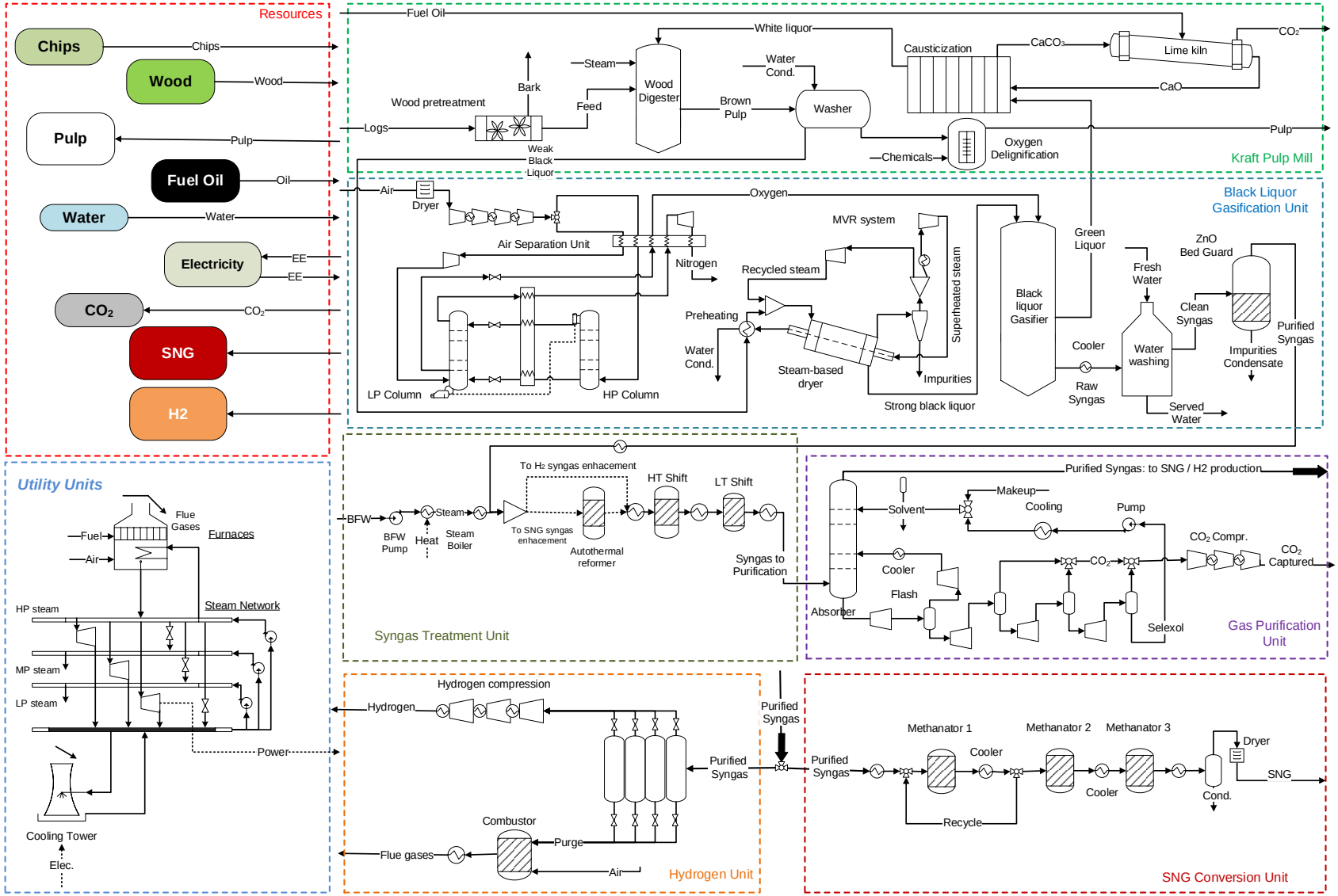

Figure 5.1 Integrated flowsheet for simultaneous pulp and chemicals (H_2 or SNG) production plants.

5.1 Energy and exergy consumption remarks

Table 5.1 presents the processes parameters results corresponding to the integrated hydrogen (H_2) and synthetic natural gas (SNG) plants, working under the mixed and autonomous modes. As it can be seen, the amount of chips fuel consumed to drive the utility systems of the integrated plants running under autonomous mode is sevenfold higher than the amount consumed when the mixed mode is considered. In the mixed operation mode, the electricity import from the grid is favored to supply the utility system. In this way, depending on the emissions footprint of the electricity mix involved, the partial import of electricity may become more or less favorable than cogenerating power and heat in the internal utility system. Anyhow, the minimum energy requirements of a kraft pulp mill can be better supplied when a chemical plant is integrated. It can be justified by an enhanced utilization of the waste heat and by the capitalization on the biorefinery residues, in order to produce value-added products whereas satisfying the utilities demands.

According to Table 5.1, the overall exergy consumption of the integrated plants varies depending on whether the mixed or the autonomous operation mode is enabled. For instance, taking as a reference the conventional case with MVR reported in Chapter 4, the scenarios that considered the integrated chemical plants working under the mixed mode presented an increase of 10-12% of exergy consumption, while the scenarios working under the autonomous mode exhibit up to 35% higher exergy consumption. This increment can be explained by newly created exergy demands of the H_2 and SNG production routes. Table 5.1 also reports the *Extended Exergy Consumption*, which can be up to 20% higher, due to the inclusion of the upstream supply chain inefficiencies. This outcome is important when comparing the performance of integrated kraft mill and chemicals plants with other chemical sectors, as the indirect exergy consumption is typically neglected during early stages of design.

Table 5.1 Process parameters calculated for the conventional and the integrated kraft pulp mill and chemical production plants, considering the operation under autonomous and mixed modes.

Process parameter	**Operative configuration**			
Operating mode	Mixed	Autonomous	Mixed	Autonomous
Integrated plant value-added product	H_2	H_2	SNG	SNG
Fuel input of the utility system	Electricity/Chips	Chips	Electricity/Chips	Chips
Feedstock wood consumption (GJ/t_{Pulp})	41.15	41.15	41.15	41.15
Consumption of chips by utility systems (GJ/t_{Pulp})	2.13	14.95	1.19	13.24
Import of electricity as utility (GJ/t_{Pulp})	3.05	0.00	2.89	0.00
Consumption of oil in the lime kiln furnace (GJ/t_{Pulp})	1.05	1.05	1.05	1.05
Overall plant exergy consumption (GJ/t_{Pulp})	47.37	57.14	46.28	55.44
Extended plant exergy consumption (GJ/t_{Pulp})	56.81	66.23	55.45	64.25
Power generated by the Rankine cycle (GJ/t_{Pulp})[1]	2.07	5.28	1.97	5.02
Power demand of the kraft pulp mill and the integrated chemical plants (GJ/t_{Pulp}):				
• *Kraft pulp mill*	2.84	2.84	2.84	2.84
• *Black liquor treatment and gasification*	1.20	1.20	1.20	1.20
• *Syngas conditioning and H_2/SNG plant*	0.38	0.38	0.13	0.13
Ancillary power demand (GJ/t_{Pulp})[2]	0.06	0.22	0.06	0.21
Minimum cooling requirement (GJ/t_{Pulp})	2.67	2.67	1.95	1.95
Minimum heating requirement (GJ/t_{Pulp})	2.04	2.04	1.99	1.99
Consumption of biomass ($t_{Wood}/t_{(H2\ or\ SNG)+Pulp}$)	3.22	4.17	2.97	3.82
Production of syngas (GJ/t_{Pulp})	9.36	9.36	9.36	9.36
Production of H_2 or SNG (t/day)	46.96	46.96	101.40	101.40
Production of pulp (t/day)	877.00	877.00	877.00	877.00
Production of marketable CO_2 (kg/h)	49,590	49,590	38,362	38,362
Electricity export (kW)	0.00	0.00	0.00	0.00

1. High pressure steam 100 bar, intermediate pressure steam 12bar, low pressure steam 4 and very low pressure steam 0.10 bar, 200°C superheating increment; 2. Vapor compression refrigeration unit and cooling tower system.

As for the breakdown of the power generated and consumed in the production facilities, Figure 5.2 evidences that the kraft pulp mill alone account for about half of the total power demand, regardless of the setup. The mechanical vapor recompression (MVR) and the air separation unit are responsible for 23% and 13% of the overall power consumed, respectively. It can be also observed that the Rankine cycle for the scenarios working under the autonomous mode entails a larger capacity (5.02-5.28 GJ/t_{Pulp}) to meet both the chemical plants demands and the ancillary power consumption. For the hydrogen production (Figures 5.2a and 5.2b), the hydrogen compression for commercialization up to 200 bar represents around 4% of the power consumption. Another important aspect is that the CO_2 capture system for the SNG production (see Figures 5.2c and 5.2d) demands lower power compared to the H_2 production, which can be explained by the requirements for adjusting its composition, dictated by the SN number. For SNG synthesis, both CO and CO_2 are used as resource for methanation, whereas for H_2 production the goal is to maximize the H_2 content.

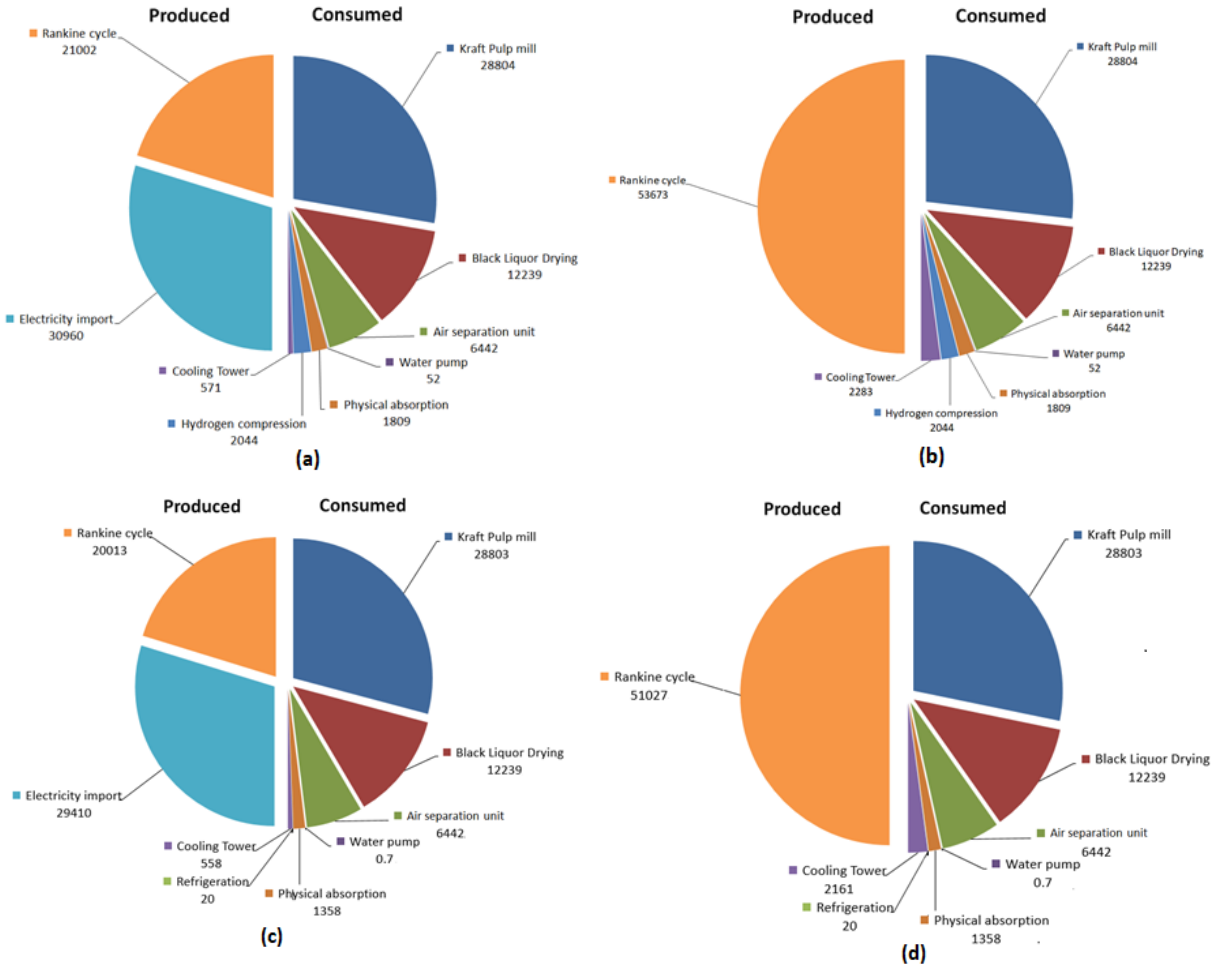

Figure 5.2 Power generation and consumption (in kW): (a) pulp and hydrogen production running on mixed mode, (b) pulp and hydrogen production running on autonomous mode, (c) pulp and synthetic natural gas production running on mixed mode, (d) pulp and synthetic natural gas production running on autonomous mode.

5.2 Energy integration analysis

The energy integration could be an important approach to enlighten opportunities for enhancing the overall performance of the processes. Moreover, it can significantly contribute to the design of a more efficient integration of processes in existing facilities in terms of energy and cost [167]. The heat cascading is a very important strategy for short-term decarbonization scenarios [172]. Figures 5.3a-d show the modifications in the *integrated composite curves* of the integrated pulp and hydrogen and synthetic natural gas production plants. Some studies have suggested this thermodynamic potential, however the details on how this integration can be performed are not presented [67; 173].

The waste heat produced along the chemical plants is represented by the pockets. This waste heat can be recovered either for preheating or raising high pressure steam. This strategy helps shortening the amount of chips used as fuel. As for the configurations working under the

autonomous mode (see Figure 5.3b and Figure 5.3d), supplementary chips must be used to fully supply the energy demands of the chemical plants. For the configurations running under the mixed mode (Figure 5.3a and Figure 5.3c), the quantity of chips is sharply reduced by maximizing the recovery of waste heat, whereas the largest share of the power used in the chemical plants is imported from the grid. As a consequence, the large irreversibility rates associated to the autonomous scenarios can be avoided, as the heat transfer rates are minimized (observe the shorter horizontal span in Figures 5.3a and 5.3c). It is clear that the advantages of the electricity import are subject to the availability of more efficient and environmentally friendly electricity mixes, which is the case of the highly renewable Brazilian electricity mix [11].

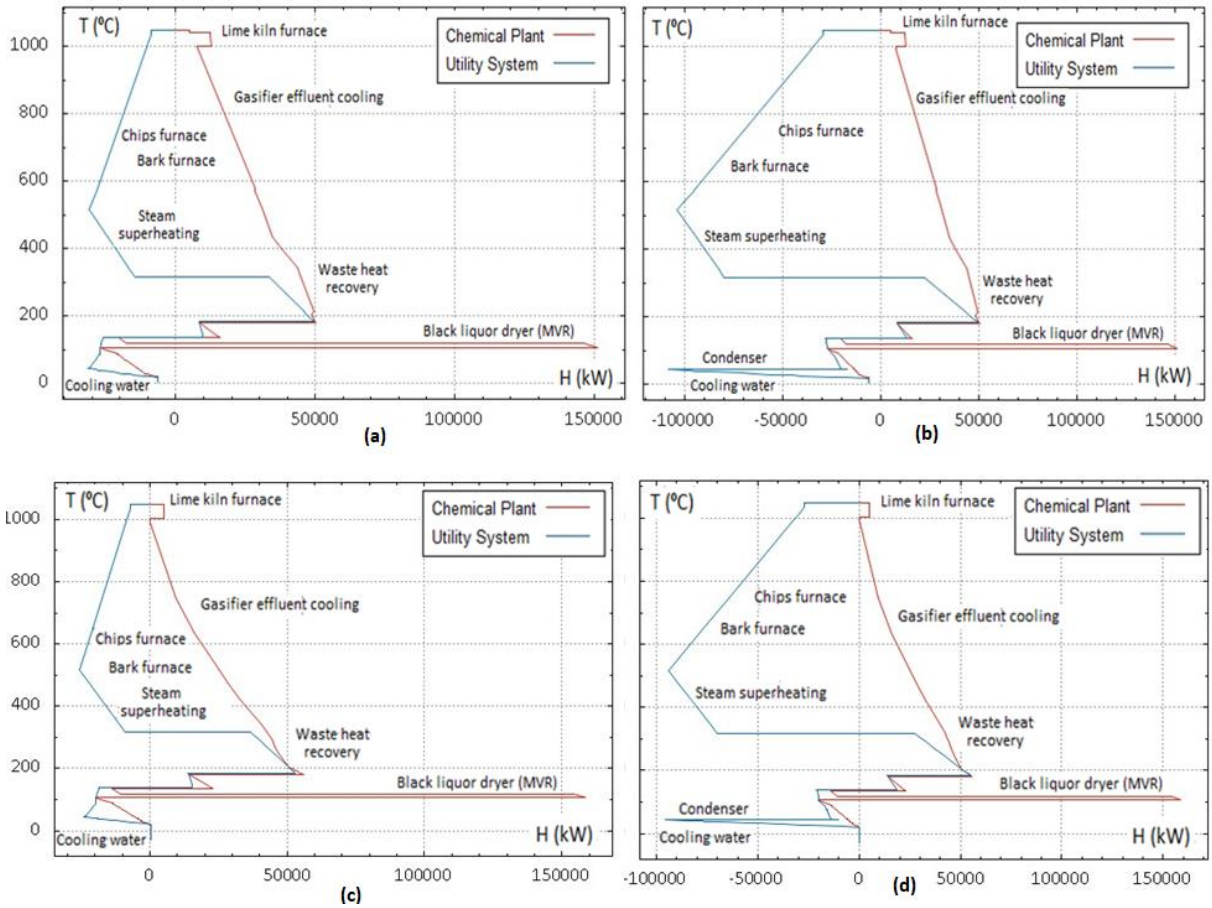

Figure 5.3 Integrated composite curves: (a) pulp and hydrogen production running on mixed mode, (b) pulp and hydrogen production running on autonomous mode, (c) pulp and synthetic natural gas production running on mixed mode, (d) pulp and synthetic natural gas production running on autonomous mode.

5.3 Exergy efficiencies

The previous results are in agreement with the exergy efficiencies summarized in Table 5.2. In effect, the value calculated for the conventional kraft pulp mill (39.46%, average exergy efficiency of Table 4.2) is slightly lower than the average values found for the integrated chemical plants, producing pulp and synthetic natural gas (44.16%) or pulp and hydrogen (43.59%). More interestingly, when we look to the exergy efficiency values of the mixed and the autonomous operation modes, it is observed an average of 47% and 40%, respectively, regardless the value-added product. In addition, concerning to the overall exergy destruction, the integrated plants running under the mixed mode also outperformed the remaining scenarios. According to Table 5.2, when the irreversibility associated to the supply chains is considered, it leads to an important reduction (up to 19%) of the exergy efficiency for all the studied scenarios. Regarding the extended exergy destruction, the supply chains have an impairing effect on the performance of the integrated plants, when compared to the conventional case (30.9 GJ/t_{Pulp}). It can be explained by the need for less energy inputs in the conventional case, but at the same time it lacks of value-added products. The conventional case also leads to increased overall emissions, as it will be discussed in the next section.

Table 5.2 Exergy efficiencies and overall exergy destruction for the H_2 and SNG scenarios.

Operation mode	**Mixed**	**Autonomous**	**Mixed**	**Autonomous**
Value-added product	H_2	H_2	SNG	SNG
Rational exergy efficiency (%)	52.26	43.32	52.62	43.92
Extended rational exergy efficiency (%)	43.57	37.38	43.91	37.90
Relative exergy efficiency (%)	50.97	42.25	51.59	43.07
Extended relative exergy efficiency (%)	42.49	36.45	43.06	37.16
Exergy destruction (GJ/t_{Pulp})	22.61	32.39	21.93	31.09
Extended exergy destruction (GJ/t_{Pulp})	32.06	41.47	31.10	39.90

5.4 Environmental assessment

The results of the overall and net balances of CO_2 emissions, including the breakdown of indirect and direct emissions, are presented in Figure 5.4. Strikingly, the fossil indirect CO_2 emissions related to the supply of wood and chips represents the largest contribution to the indirect emissions (77-99% out of 0.24 t_{CO2}/t_{Pulp}), surpassing the contribution of the fossil direct emissions in the lime kiln. This fact can be justified by a large biomass requirement, which is subsequently converted by means of low efficiency energy technologies, such as bark and chip boilers and waste heat steam generators in the Rankine cycle. These emissions can be sharply

dropped if biomass integrated gasification combined cycles were implemented. Yet, the use of combined cycles would only add complexity and render the initial investments prohibitively high.

The biogenic emissions avoided are linked to the syngas purification unit integrated into the chemical production plants. This capture represents an opportunity to decarbonize the hydrogen and synthetic natural gas production, aside from promoting the indirect carbon capture from atmosphere. In effect, in view of the negative net CO_2 emissions balance obtained (-1.03 t_{CO2}/t_{Pulp}), it is expected a withdrawal of one ton of CO_2 from the environment per ton of pulp produced in the integrated plants. Although the net CO_2 emissions balance of the production routes of synthetic natural gas it is a bit higher than the hydrogen production route, it is also negative (-0.73 t_{CO2}/t_{Pulp}).

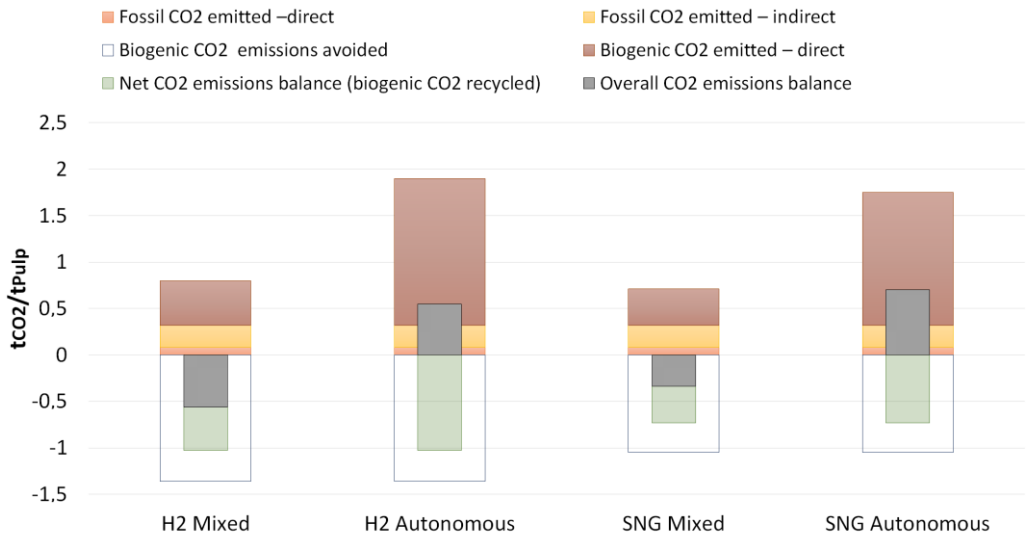

Figure 5.4 Balance of CO_2 emissions for the H_2 and SNG scenarios.

For the conventional kraft pulp mill, the renewability indicator can be as low as 0.64, which contrast against the values for the integrated chemical plants (0.91-0.92) (see Figure 5.5). The literature also reports lambda values lower than the unity for other biorefineries, such as the ethanol production from banana and its respective lignocellulosic residues [174]. This fact suggests that the exergy of the products would not be enough to compensate for the fossil fuel exergy, the losses and the irreversibilities associated to the productive system, including the supply chains. It must be underlined that renewability indicator increases as more electricity is imported from the grid (*i.e.* mixed case). This behavior is consistent with the trend shown by the exergy efficiency. This result reinforces the idea that the use of resources with a large share

of renewable contribution, may favor the adoption and deployment of the production of biofuels in integrated biorefineries.

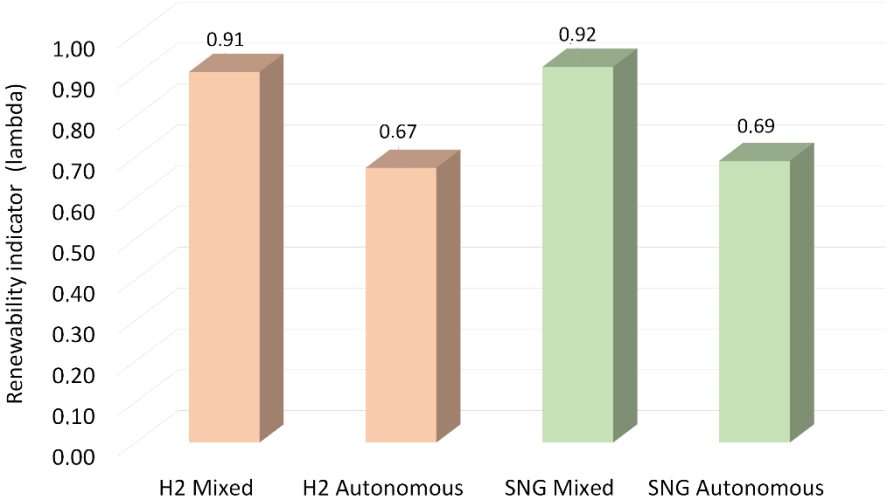

Figure 5.5 Renewability indicator for the H_2 and SNG scenarios.

5.5 Economic analysis

A technical analysis would be incomplete if only thermodynamic and environmental performance is considered. Actually, the new investment could be only justified if the proposed configurations translate into higher operating revenues coming from the drop of fuel consumption, the increase of yield of value-added products or the reduction of the atmospheric emissions, in view of the potential implementation of carbon markets and more severe environmental regulations.

Table 5.3 shows the annualized investment costs and the net plant revenues calculated for the hydrogen and synthetic natural gas scenarios. As it can be seen, all the integrated chemicals production plants have higher operating revenues (1-14%), compared to the conventional scenario due to the expansion of the product portfolio. However, as it concerns the net plant revenues, *i.e.* after discounting the higher capital costs of the newly integrated chemical plants, only the integrated pulp and hydrogen production routes achieve marginal gains compared to the conventional scenario, regardless of the operation mode. It is worth noticing that, despite the import of costlier electricity from the grid, the hydrogen production under the mixed operation mode is seemingly favored by a relatively higher efficiency of the Brazilian electricity mix. On the other hand, the net revenues of the integrated kraft pulp mill and synthetic natural gas production plants drop between 11-20% in comparison to the conventional case.

Table 5.3 Operating incomes, costs and revenues and annualized investment cost for the H_2 and SNG scenarios.

Operation mode	**Mixed**	**Autonomous**	**Mixed**	**Autonomous**
Value-added product	H_2	H_2	SNG	SNG
Operating incomes (EUR/t_{Pulp})	850.80	850.80	775.73	775.73
Operating costs (EUR/t_{Pulp})	-213.72	-219.92	-207.01	-212.34
Operating revenues (EUR/t_{Pulp})	637.08	630.89	568.73	563.40
Annualized investment cost (EUR/t_{Pulp})	-321.59	-347.53	-320.77	-340.78
Net Plant Revenues (EUR/t_{Pulp})	315.49	283.36	247.96	222.61

The breakdown of the CAPEX for the integrated chemicals production plants (Figure 5.6) indicates that running the integrated plants under an autonomous mode demands larger chips furnaces and Rankine cycles for producing either synthetic natural gas or hydrogen. In fact, since electricity import is not enabled, the heat recovery steam generators and the heat exchanger network must be oversized, compared to both the conventional and the integrated plants running under the mixed mode. This fact has direct influence in the financial feasibility of the alternative production routes.

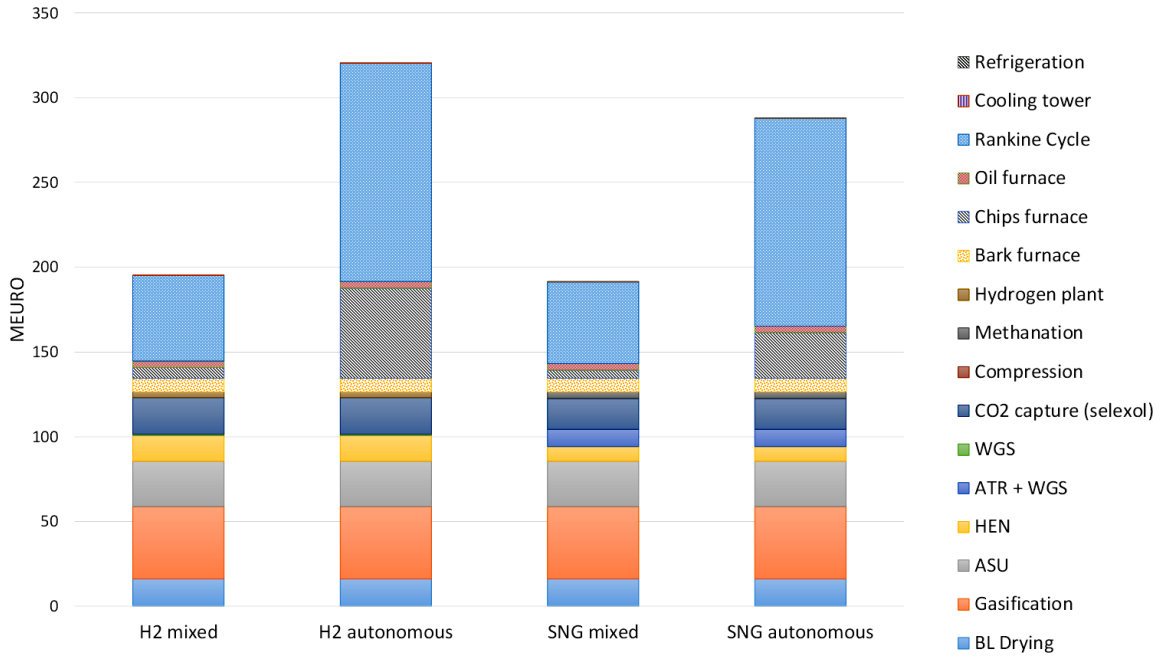

Figure 5.6 CAPEX breakdown for the integrated chemicals production plants. WGS: water gas shift reactors, ATR: autothermal reformer, HEN: heat exchanger network, ASU: air separation unit.

Other parameters that may influence the financial feasibility are the adopted carbon taxation and the interest rate. For this reason, in the next section, the effect of the two financial parameters is studied using a sensitivity analysis, but considering that the carbon tax and prices of the commodities do not change over the project lifespan. This assumption is challenged in the last section, in which the sensitivity analyses consider the uncertainty of the commodities

prices and the carbon taxes, aiming to shed light on the *likelihood of the loss* for each productive route.

5.5.1 Sensitivity analysis of the incremental net present value to carbon tax and interest rate

The net revenues of the integrated kraft pulp mills and chemical production plants rather depend on uncertain financial parameters which may drastically influence the behavior of the INPV. The INPV variation subject to the carbon taxes and interest rate varying in the range of 0-100 EUR/t_{CO2} and 0-21%, respectively, is reported in Figures 5.7a-d. As expected, better INPV are attained when higher carbon taxes and lower the interest rates are assumed. From Figure 5.7a, a positive INPV can be achieved for the integrated kraft pulp mill and hydrogen production plant when the mixed operation mode is adopted and the carbon taxes range between 30-60 EUR/t_{CO2}. For the autonomous operation mode (Figure 5.7b), positive INPV is only reached for carbon taxes above 85 €/t_{CO2} and interest rates lower than 6%. Meanwhile, for the integrated kraft pulp mill and synthetic natural gas production plants, the INPV is always negative, regardless of the operation mode (*i.e.* mixed and autonomous), the carbon tax and the interest rate adopted.

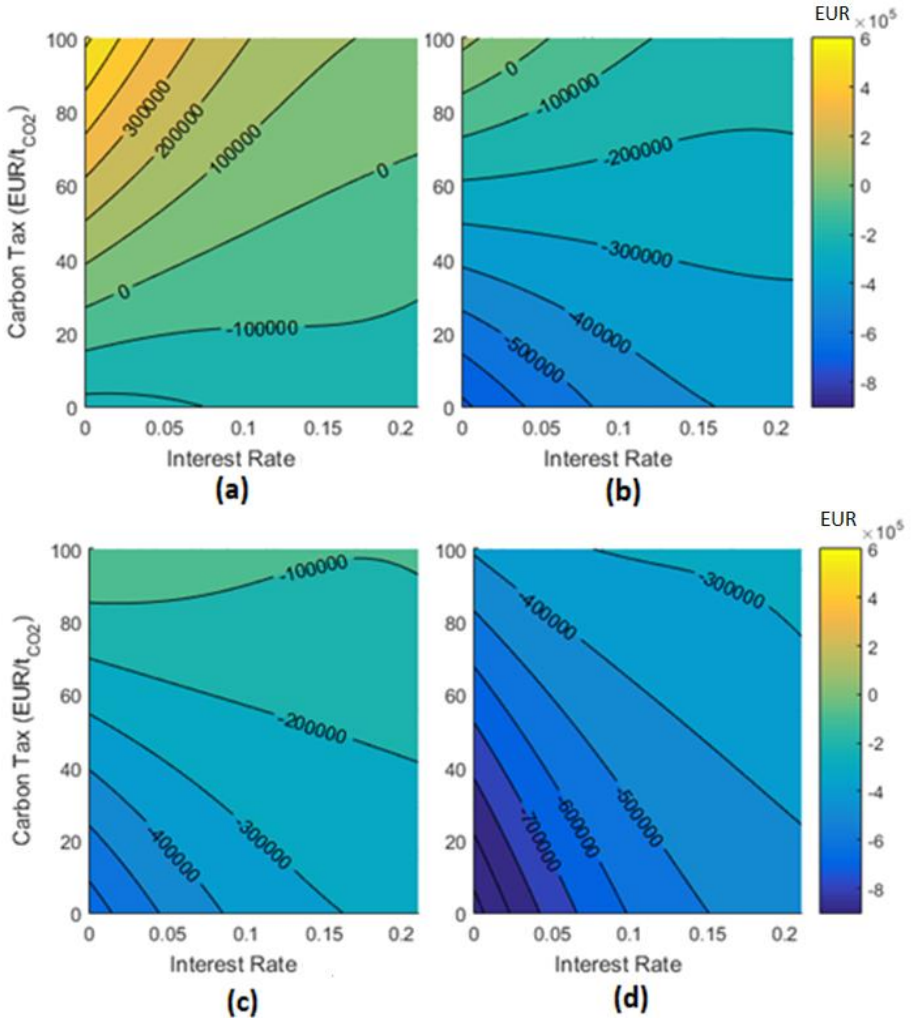

Figure 5.7 INPV variation (in EUR) represented in contour plots for: (a) pulp and hydrogen production running on mixed configuration, (b) pulp and hydrogen production running on autonomous configuration, (c) pulp and synthetic natural gas production running on mixed configuration, (d) pulp and synthetic natural gas production running on autonomous configuration.

5.5.2 Estimation of the effect of the uncertain commodities prices using incremental financial analysis

In practice, the prices of the commodities are subjected to the market volatility. In order to consider their stochastic variation, a series of Monte Carlo simulation are performed. These incremental financial analyses rely on the concept of *likelihood of loss*, defined as the probability that the incremental net present value of the integrated production routes is negative, taking as reference the net present value of a conventional kraft pulp mill.

Tables 5.4-5.7 present the heat maps with the results for the scenario *(i)* proposed in Section 3.4.1. In this scenario, it is assumed that the carbon taxes and the interest rates remain constant over time, whereas the commodities prices vary stochastically. As reported in Table 5.4, for the integrated kraft pulp mill and chemical plant simultaneously producing pulp and

hydrogen running in the mixed mode, the probability that the INPV is positive is very high for carbon taxes higher than 60 EUR/t_{CO2}, subjected to the interest rate assumed. Yet, as the carbon tax drops and the interest rate increases, a set of Fischer interceptions becomes evident. This region demarcates the financially unfeasible operating conditions of the integrated biorefinery concept. These tax values are in line with the current carbon taxes adopted for example by Finland or Switzerland (~70-100 EUR/t_{CO2}) [175], and in attendance with the median forecast of 100 EUR/t_{CO2} suggested by climate economists to meet the 1.5 °C goal [176]. In contrast, the production of hydrogen under autonomous operation mode (Table 5.5) becomes financially attractive only for the condition of the highest carbon taxes and the lowest interest rates. Meanwhile, for the integrated kraft pulp mills and synthetic natural gas production routes (Tables 5.6-5.7), the scenario is much less favorable, which can be explained by a lower market price of that value-added product in comparison to the price of hydrogen.

Table 5.4 Effect of the interest rate and the carbon tax on the likelihood of loss (in %) for the scenario (i) DCTIR_SC (see section 3.4.1) in which an integrated kraft pulp mill and hydrogen production plant operates under the mixed mode.

CO_2 tax (EUR/t_{CO2}) →	**0**	**10**	**20**	**30**	**40**	**50**	**60**	**70**	**80**	**90**	**100**
i (%) 0%	100.00	99.46	85.71	35.84	4.19	0.16	0.00	0.00	0.00	0.00	0.00
3%	100.00	99.94	96.41	63.80	14.24	0.76	0.00	0.00	0.00	0.00	0.00
6%	100.00	100.00	99.37	87.10	41.01	6.00	0.21	0.00	0.00	0.00	0.00
9%	100.00	100.00	99.94	96.86	71.41	23.47	2.09	0.04	0.00	0.00	0.00
12%	100.00	100.00	100.00	99.37	90.27	53.76	13.64	1.10	0.01	0.00	0.00
15%	100.00	100.00	100.00	99.84	97.14	78.64	37.23	7.30	0.46	0.00	0.00
18%	100.00	100.00	100.00	99.97	99.20	92.26	64.14	24.36	4.33	0.23	0.00
21%	100.00	100.00	100.00	99.97	99.89	97.37	83.20	47.30	13.97	2.16	0.14

Table 5.5 Effect of the interest rate and the carbon tax on the likelihood of loss (in %) for the scenario (i) DCTIR_SC (see section 3.4.1) in which an integrated kraft pulp mill and hydrogen production plant operates under the autonomous mode.

CO_2 tax (EUR/t_{CO2}) →	**0**	**10**	**20**	**30**	**40**	**50**	**60**	**70**	**80**	**90**	**100**
i (%) 0%	100.00	100.00	100.00	100.00	100.00	100.00	99.96	97.40	71.34	20.30	1.29
3%	100.00	100.00	100.00	100.00	100.00	100.00	100.00	99.94	96.70	68.69	18.83
6%	100.00	100.00	100.00	100.00	100.00	100.00	100.00	100.00	99.81	96.79	69.91
9%	100.00	100.00	100.00	100.00	100.00	100.00	100.00	100.00	100.00	99.91	97.19
12%	100.00	100.00	100.00	100.00	100.00	100.00	100.00	100.00	100.00	100.00	99.93
15%	100.00	100.00	100.00	100.00	100.00	100.00	100.00	100.00	100.00	100.00	100.00
18%	100.00	100.00	100.00	100.00	100.00	100.00	100.00	100.00	100.00	100.00	100.00
21%	100.00	100.00	100.00	100.00	100.00	100.00	100.00	100.00	100.00	100.00	100.00

Table 5.6 Effect of the interest rate and the carbon tax on the likelihood of loss (in %) for the scenario (i) DCTIR_SC (see section 3.4.1) in which an integrated kraft pulp mill and synthetic natural gas production plant operates under the mixed mode.

CO_2 tax (EUR/t_{CO2}) →	0	10	20	30	40	50	60	70	80	90	100
i (%) 0%	100.00	100.00	100.00	100.00	100.00	100.00	100.00	100.00	100.00	97.47	44.97
3%	100.00	100.00	100.00	100.00	100.00	100.00	100.00	100.00	100.00	99.93	88.51
6%	100.00	100.00	100.00	100.00	100.00	100.00	100.00	100.00	100.00	100.00	99.40
9%	100.00	100.00	100.00	100.00	100.00	100.00	100.00	100.00	100.00	100.00	99.97
12%	100.00	100.00	100.00	100.00	100.00	100.00	100.00	100.00	100.00	100.00	100.00
15%	100.00	100.00	100.00	100.00	100.00	100.00	100.00	100.00	100.00	100.00	100.00
18%	100.00	100.00	100.00	100.00	100.00	100.00	100.00	100.00	100.00	100.00	100.00
21%	100.00	100.00	100.00	100.00	100.00	100.00	100.00	100.00	100.00	100.00	100.00

Table 5.7 Effect of the interest rate and the carbon tax on the likelihood of loss (in %) for the scenario (i) DCTIR_SC (see section 3.4.1) in which an integrated kraft pulp mill and synthetic natural gas production plant operates under the autonomous mode.

CO_2 tax (EUR/t_{CO2}) →	0	10	20	30	40	50	60	70	80	90	100
i (%) 0%	100.00	100.00	100.00	100.00	100.00	100.00	100.00	100.00	100.00	100.00	100.00
3%	100.00	100.00	100.00	100.00	100.00	100.00	100.00	100.00	100.00	100.00	100.00
6%	100.00	100.00	100.00	100.00	100.00	100.00	100.00	100.00	100.00	100.00	100.00
9%	100.00	100.00	100.00	100.00	100.00	100.00	100.00	100.00	100.00	100.00	100.00
12%	100.00	100.00	100.00	100.00	100.00	100.00	100.00	100.00	100.00	100.00	100.00
15%	100.00	100.00	100.00	100.00	100.00	100.00	100.00	100.00	100.00	100.00	100.00
18%	100.00	100.00	100.00	100.00	100.00	100.00	100.00	100.00	100.00	100.00	100.00
21%	100.00	100.00	100.00	100.00	100.00	100.00	100.00	100.00	100.00	100.00	100.00

Meanwhile, Tables 5.8 and 5.9 present the results of the likelihood of loss for scenarios *(ii)* and *(iii)*, respectively, defined in Section 3.4.1. The scenario *(ii)* envisages a smooth transition from zero to maximum carbon tax over time, with the commodities price still varying in a stochastic way. On the other hand, the scenario *(iii)* assumes that the carbon tax varies stochastically over time along with the prices of the commodities. These analyses are performed for certain interest rates. According to Tables 5.8 and 5.9, only the integrated kraft pulp mill and hydrogen production plant running under the mixed mode has relatively more favorable results for the likelihood of loss. Anyhow, for both scenarios *(ii)* and *(iii)*, the co-production of hydrogen will be only favored at very low interest rates (>> 5%). Thus, the chemicals and fuels production through renewable biomass resources will be only boosted if other measures of incentives are combined, since their implementation is still dictated the technology maturity, costs, market conditions, and lack of regulatory commitments.

Table 5.8 Effect of the interest rate and the carbon tax on the likelihood of loss (in %) for the scenario (ii) LCT_DIR_SC (see section 3.4.1) in which a smooth transition from zero to maximum carbon tax is assumed over the lifespan of the integrated kraft pulp mill and H_2 or SNG production plants.

Operation mode		mixed	autonomous	mixed	autonomous
Value-added product		H_2	H_2	SNG	SNG
i (%)	**0%**	0.06	100.00	100.00	100.00
	1%	0.24	100.00	100.00	100.00
	2%	1.43	100.00	100.00	100.00
	3%	4.79	100.00	100.00	100.00
	4%	11.66	100.00	100.00	100.00
	5%	26.20	100.00	100.00	100.00
	6%	42.40	100.00	100.00	100.00
	7%	63.37	100.00	100.00	100.00
	8%	78.06	100.00	100.00	100.00
	9%	88.60	100.00	100.00	100.00
	10%	95.14	100.00	100.00	100.00
	11%	97.71	100.00	100.00	100.00
	12%	98.93	100.00	100.00	100.00
	13%	99.61	100.00	100.00	100.00
	14%	99.91	100.00	100.00	100.00
	15%	99.96	100.00	100.00	100.00
	16%	99.99	100.00	100.00	100.00
	17%	99.99	100.00	100.00	100.00
	18%	100.00	100.00	100.00	100.00
	19%	100.00	100.00	100.00	100.00
	20%	100.00	100.00	100.00	100.00
	21%	100.00	100.00	100.00	100.00

Table 5.9 Effect of the interest rate and the carbon tax on the likelihood of loss (in %) for the scenario (iii) SCTC_DIR, (see section 3.4.1) in which a stochastic variation of the carbon tax is assumed over the lifespan of the integrated kraft pulp mill and H_2 or SNG production plants.

Operation mode		mixed	autonomous	mixed	autonomous
Value-added product		H_2	H_2	SNG	SNG
i (%)	**0%**	0.36	99.99	100.00	100.00
	1%	0.44	100.00	100.00	100.00
	2%	1.19	100.00	100.00	100.00
	3%	1.70	100.00	100.00	100.00
	4%	3.81	100.00	100.00	100.00
	5%	6.40	100.00	100.00	100.00
	6%	10.47	100.00	100.00	100.00
	7%	14.57	100.00	100.00	100.00
	8%	20.44	100.00	100.00	100.00
	9%	28.90	100.00	100.00	100.00
	10%	36.60	100.00	100.00	100.00
	11%	46.60	100.00	100.00	100.00
	12%	53.66	100.00	100.00	100.00
	13%	62.13	100.00	100.00	100.00
	14%	69.70	100.00	100.00	100.00
	15%	77.57	100.00	100.00	100.00
	16%	82.00	100.00	100.00	100.00
	17%	85.31	100.00	100.00	100.00
	18%	88.81	100.00	100.00	100.00
	19%	91.83	100.00	100.00	100.00
	20%	93.71	100.00	100.00	100.00
	21%	95.69	100.00	100.00	100.00

5.6 Conclusion

In this chapter, thermodynamic, environmental and financial indicators are used to compare the performance of a standalone kraft pulp mill to that of an integrated kraft pulp mill that also produce hydrogen or synthetic natural gas. The integration of the chemical plants and the manufacture of the value-added products are possible thanks to the black liquor upgraded gasification system that replaces the recovery boiler. An important finding is that the possibility of importing electricity helps reducing the irreversibility, the biomass consumption, and the overall CO_2 emissions, apart from increasing the renewability performance of the integrated chemical plants. In fact, the exergy efficiency of the conventional system (40%) is calculated as four percentage points lower than the average exergy efficiency of the integrated routes (44%). Other advantage of the integrated kraft pulp and chemical production plants is that negative overall CO_2 emissions balances (up to -0.56 t_{CO2}/t_{Pulp}) suggest a decarbonization pathway for typically fossil-based commodities through the use of biomass. The analysis

included the extended and indirect exergy consumption as well as the related atmospheric emissions, which may be helpful when comparing to other chemical manufacturing routes. In fact, the techno-environomic performance exhibited a marked dependence of the indirect CO_2 emissions and the import of greener electricity in the Brazilian scenario. Moreover, due to the commercialization of the valuable hydrogen, higher operating revenues were obtained for the integrated pulp and hydrogen production plants. The uncertainty of the market prices for the commodities has been also considered, revealing that the use of constant inputs costs may lead to misleading results regarding the likelihood of loss of risky projects. The implementation of more rigorous carbon taxes and the technologies maturation may reduce the financial risks and give support to decision-makers in implementing biorefineries and exploring new business opportunities to trigger the decarbonization of important commodities.

CHAPTER 6: METHANOL AND DIMETHYL ETHER

Methanol is a very important chemical in the energy sector, where it can be used directly as fuel or blended with gasoline. Also, it can be used as an intermediate molecule for various chemical syntheses, such as olefins, amines, acetic acid, dimethyl ether and formaldehyde [177]. Dimethyl ether has remarkable properties that make it useful in different fields such as power generation, household, transport, as refrigerant fluid and as feedstock to synthesize other products. DME is considered as non-toxic, non-corrosive, colorless and environmentally friendly compound. It also has the advantage to be easily transportable, to have a high cetane number and similar properties do the liquefied petroleum gas [178].

Traditionally, the methanol and dimethyl ether industrial processes are based on fossil sources, such as coal and natural gas, which present some disadvantages such as high energy and water consumption and high level of pollutant emissions, not to mention their nonrenewability and future depletion [179]. Alternative routes are being investigated aiming to decarbonize their production supply chains, such as the biomass thermochemical conversion via gasification [179; 180].

The methanol and dimethyl ether production via black liquor gasification has been studied by several authors [63; 65; 180; 181; 182; 183]. Häggström et al. (2012) successfully synthesized methanol from syngas generated via black liquor gasification. In their work, the syngas passes through a catalytic reactor at 25 bar which yields 0.16–0.19 $g_{methanol}/(g_{catalyst}.h)$. This experience was an important step towards demonstrating the feasibility of methanol synthesis from a bench scale for subsequent scale-up processes.

As previously mentioned, when a conventional kraft pulp mill is integrated to biofuels production, the existing cogeneration unit falls short to supply the increased utilities requirements. This energy deficit should be fulfilled by importing additional biomass to compensate for the energy withdrawn from the black liquor [25]. Ekbom et al. (2003) studied the technical and economic feasibility of BL gasification for motor fuels production (MeOH and DME). The authors evaluated the marginal energy efficiency of methanol and dimethyl ether production by considering additional biomass consumption. The biomass-to-fuel conversion efficiency was 66% and 67%, for methanol and dimethyl ether, respectively. In both cases, the energy efficiency is enhanced due to the increased energy flows of both biomass and motor biofuels produced.

Carvalho et al. (2018) compared the conventional BL combustion to an integrated methanol production via BL gasification and other blended feedstock. The integrated system

resulted in a higher efficiency (60%) compared to the conventional combustion of BL to generate steam and electricity (below 40%). The pure BL gasification case also presented higher energy efficiency compared to the co-gasification scenarios, partly due to the increased energy demands of these latter cases [180].

Fornell and collaborators (2013) performed a techno-economic analysis of a biorefinery built upon the integration of a kraft pulp-mill and ethanol and dimethyl ether production plants. The pulp is sent to an ethanol production process, while the BL is gasified and refined to produce dimethyl ether. The results of this study indicated that the process can be self-sufficient in terms of hot utility demand (i.e. fresh steam). However, a deficit of electricity is expected.

Pettersson and Harvey (2012) compared the BL gasification and downstream production of DME or electricity to other pulping biorefinery concepts, considering different energy market scenarios. The authors observed that BL gasification with DME production has the best economic performance for both pulp mills and integrated pulp and paper mills. The carbon capture and storage was also considered in this study, and it pointed to improved process profitability.

Despite the relevance of the previous works, they only considered either thermodynamic or environmental indicators. In this work, the holistic approach mentioned in Chapter 3 that considers both performances along the economic implications of the feedstock and fuels price variation over the plant lifespan is used to compare the BL upgrading gasification process for methanol (MeOH) and dimethyl ether (DME) production with the scenario of the conventional utilization of black liquor in a kraft pulp mill (i.e. concentration and combustion). The results are presented in the next sections. Different energy resources can be consumed in the integrated chemical plants shown in Figure 6.1 in order to manufacture the marketed products (e.g. pulp, electricity, MeOH and DME). The utility systems involved are also shown in Figure 6.1.

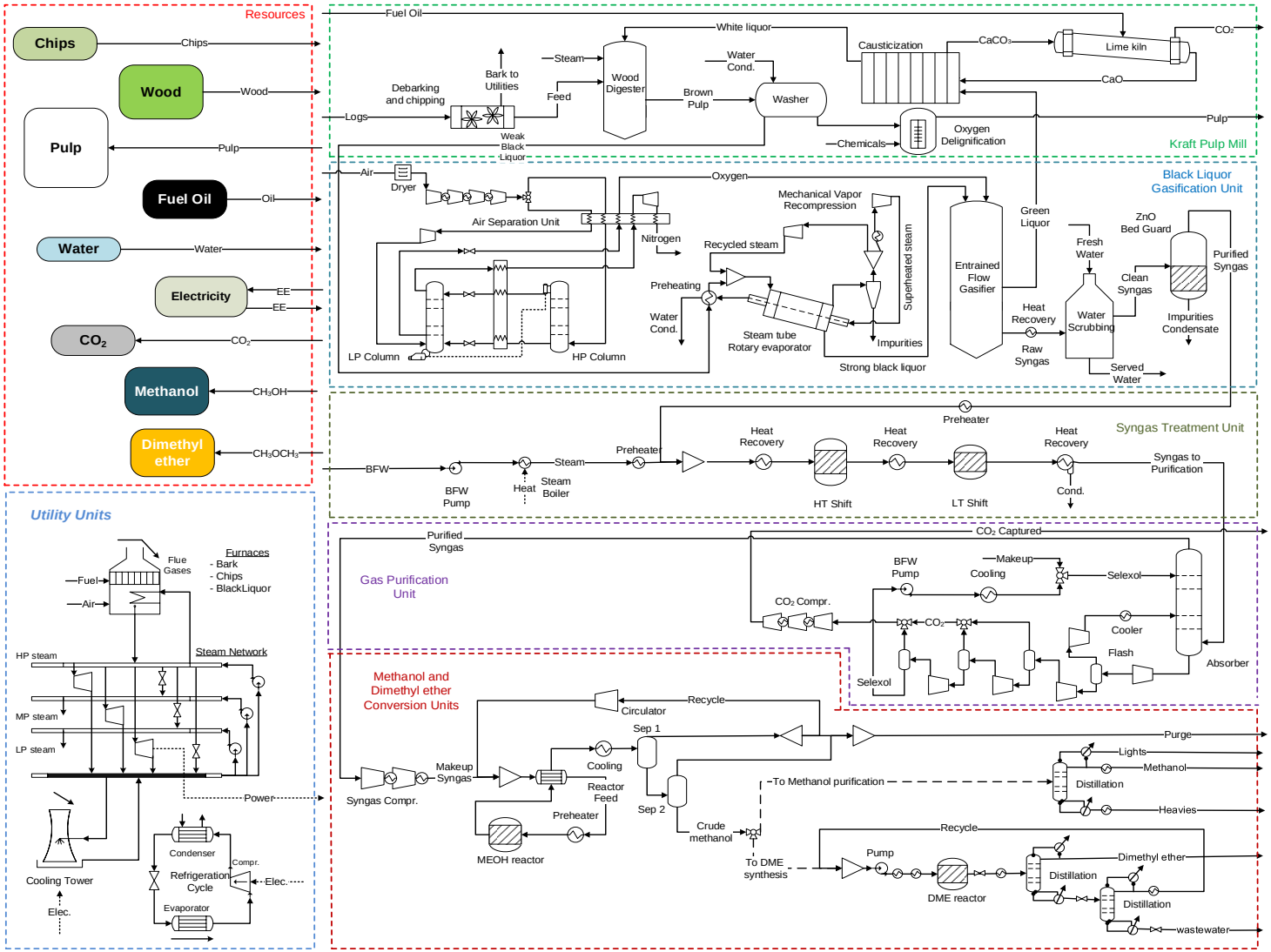

Figure 6.1 Integrated flowsheet of kraft pulp mill and the methanol or dimethyl ether production plants.

6.1 Energy and exergy consumption remarks

The optimal process variables of the three chemical plants are compared in Table 6.1. According to these results, the integrated plants operating in autonomous mode present a consumption of fuel (wood chips) between five and seven times higher than in the cases in which the chemical plants operate in mixed mode. However, this lower chips consumption only comes at the expense of a considerable import of electricity when operating in the mixed mode. Accordingly, depending on the cost and the embodied emissions of the electricity generated in the electricity mix, there will be a trade-off between the self-generation of the utilities and the purchase of electricity from the grid. The MER of the conventional kraft pulp mill can be drastically cut down if a chemical plant is integrated, which can be explained by the large extent of waste heat recovery and valorization of the residues, so that value added co-products can be produced.

According to Table 6.1, the integrated chemical plants operating under the mixed and autonomous modes present energy consumptions 14% and 38% higher than that of the conventional case (42.20 GJ/t_{Pulp}), respectively. This fact can be explained by the increased biomass and electricity consumptions necessary to drive the compressors and other auxiliary equipment in the integrated chemical plants. More interestingly, an intensive import of Brazilian electricity during the mixed mode operation renders the MeOH and DME production less energy intensive if compared to the autonomous cases (see Table 6.1, cf. overall plant consumption). Furthermore, when the upstream supply chains of the feedstock consumed are accounted for, the extended exergy consumption increases up to 20%, compared to the plant-wide energy consumption. Those extended results are useful to issue public policies and decision-makers, since holistic comparisons of the impact of the supply chains in the bioproducts manufacturing sectors may be achieved, thus, ensuring a level playing field for comparisons between different MeOH or DME and pulp production routes.

Table 6.1 Optimal process variables of the studied production facilities.

	Integrated chemical plants			
Chemical plant	**Pulp + MeOH**		**Pulp + DME**	
Operation mode	Mixed	Auto	Mixed	Auto
Fuel input of the utility system	Electricity/Chips	Chips	Electricity/Chips	Chips
Feedstock wood consumption (GJ/t_{Pulp})	41.15	41.15	41.15	41.15
Consumption of chips for utility(GJ/t_{Pulp})	2.32	16.06	2.96	16.23
Consumption of electricity for utility (GJ/t_{Pulp})	3.3	0	3.18	0.00
Consumption of oil (GJ/t_{Pulp})	1.05	1.05	1.05	1.05
Overall plant consumption (GJ/t_{Pulp})	47.81	58.26	48.34	58.42
Extended plant consumption (GJ/t_{Pulp}) [1]	57.48	67.52	58.03	67.71
Power generation of rankine cycle (GJ/t_{Pulp})[2]	1.74	5.22	1.86	5.22
Power demand of the chemical processes (GJ/t_{Pulp})				
- *Kraft Pulp Mill*	2.84	2.84	2.84	2.84
- *Black Liquor Treatment and Gasification*	1.20	1.20	1.20	1.20
- *Syngas Conditioning and MeOH/DME Synthesis*	0.30	0.30	0.31	0.31
Demand of ancillary power (GJ/t_{Pulp})[3]	0.06	0.24	0.07	0.24
Min. Cooling requirement (GJ/t_{Pulp})[4]	3.19	3.19	3.62	3.62
Min. Heating requirement (GJ/t_{Pulp})[4]	2.12	2.12	2.52	2.52
Consumption of biomass ($t_{Wood}/t_{Bioproduct+Pulp}$)	2.56	3.37	2.79	3.64
Syngas production (GJ/t_{Pulp})	9.36	9.36	9.36	9.36
MeOH or DME production yield (t/day)	289.62	289.62	208.19	208.19
Pulp production (t/day)	877.83	877.83	877.83	877.83
Marketable CO_2 production (kg/h)	32714	32714	32714	32714
Electricity export (kW)	0	0	0	0

1. It considers the extended efficiency of the generation of electricity (55.68%), and the oil (95.20%) and biomass (86.13%) production [11; 139]; 2.Steam pressure levels 100, 12, 4 and 0.10 bar, steam superheating 200°C; 3. Refrigeration and cooling tower; 4. MER of the chemical processes.

As for the power consumption breakdown (Figure 6.2), the electricity import in the integrated chemical plants that operate under the mixed mode (Figures 6.2a and 6.2c), can be as high as 63% of the total power demand in the plant. In addition, the power generation in the Rankine cycle is 22% higher for the autonomous cases when compared to the conventional case (Figures 6.2b and 6.2d). In the mixed cases, due to the diversification in the resources, the total power generation is reduced. This fact consequently affects other utility units, such as the cooling tower, which has a greater demand for autonomous operating modes due to the size of the Rankine cycle required. Looking specifically to the additional demands due to the integration of the methanol and dimethyl ether production plants, it can be seem that the syngas compression up to 90 bar may accounts for almost 3% of the total energy consumption. Another observation is that, similarly to the SNG production, the MeOH and DME synthesis also use both CO and CO_2 as resources, but with a different requirement for the SN number, which

increase the demand for the CO_2 capture unit compared to SNG, but it is still lower compared to the required for H_2 production.

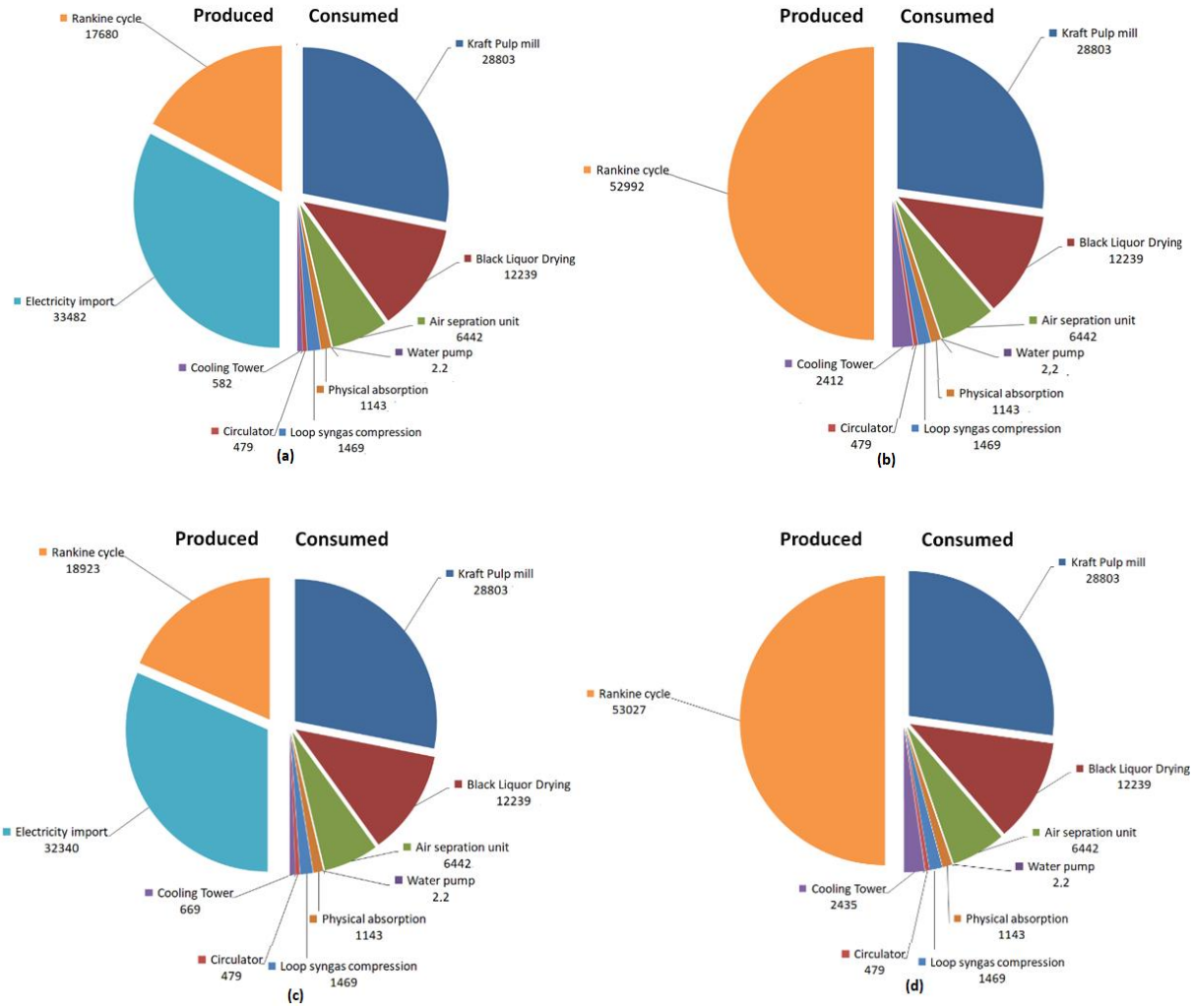

Figure 6.2 Breakdown graphics of the power consumption (kW): (a) pulp&MeOH - Mixed op. mode, (b) pulp&MeOH - Autonomous op. mode, (c) pulp&DME - Mixed op. mode, (d) pulp&DME - Autonomous op. mode.

6.2 Energy integration analysis

Figures 6.3a-d shows the energy integration results for all the chemical plants. Due to the introduction of additional energy conversion processes, a sharp modification of these curves is observed for the integrated chemical plants (Figures 6.3a-d) if compared to the curves of the conventional kraft pulp mill (Figure 4.3b). Moreover, compared to the previous evaluated chemicals, H_2 and SNG (see section 5.2), the differences between the chemicals plants are evidenced in the energy integration analysis, such as the steam demands at specific temperatures for the methanol and dimethyl ether production due to the need of one and two distillation

columns, respectively. In fact, due to the recovery of most of the waste heat available throughout the chemical plants, an otherwise rejected source of energy can be used for other purposes.. Accordingly, there is an opportunity for reducing the energy import when integrating the conventional kraft process to the MeOH/DME chemical plants via the BL gasification process.

Although the heating requirements of the conventional kraft pulp mill are fully supplied by the residual bark and black liquor combustion, it only comes at the expense of a heightened quantity of exergy destruction per unit of product (pulp), if compared to the integrated plants operating under the mixed mode (Figures 6.3a and 6.3c). The effect of surplus chips fuel consumption can be also observed in the curves corresponding to the integrated kraft pulp and MeOH or DME plants (Figures 6.3b and 6.3d), as the span of heat exchange (abscissa H) becomes wider than in the case of electricity import (Figures 6.3a and 6.3c).

It is worth noticing that these results are location-dependent, since more economically and environmentally friendly electricity mixes should be involved to take advantage of their higher generation efficiency.

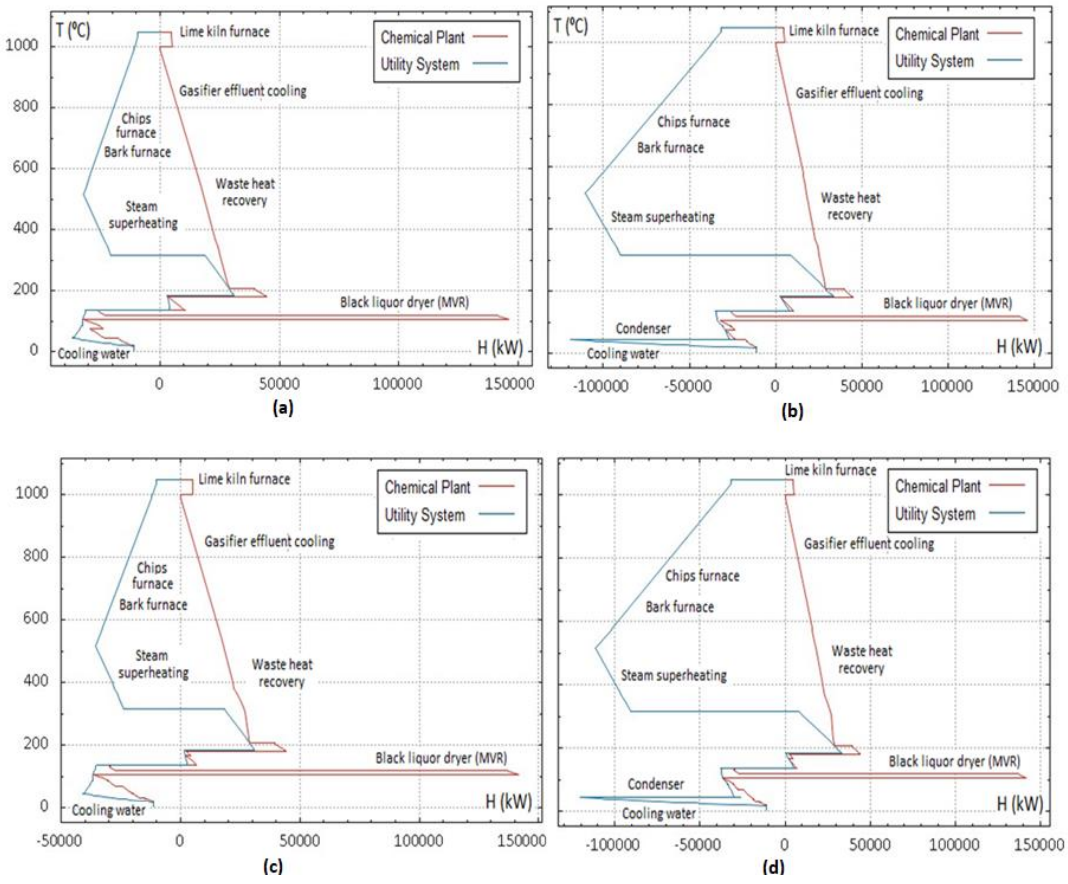

Figure 6.3 Integrated composite curves: MeOH production under mixed (a) or autonomous (b) operating modes; and DME production under mixed (c) or autonomous (d) operating modes. Enthalpy flow rate (H in kW), Temperature (T in °C).

6.3 Exergy-based indicators

Table 6.2 shows the breakdown of the exergy destruction for the two integrated chemical plants (*i.e.* with MeOH or DME co-production), excluding the utility systems. It is noteworthy that the distribution of the exergy destruction in the utility systems depends on the operation mode adopted (mixed or autonomous).

Table 6.2 Exergy destruction share for each unit of both methanol and dimethyl ether integrated plants (the utility systems are not included)

Units	**MeOH**	**DME**
Kraft pulp mill	73.52%	73.13%
Black liquor gasification unit	24.20%	24.07%
Syngas treatment unit	0.14%	0.14%
Gas purification unit	0.99%	0.98%
MeOH or DME conversion unit	1.15%	1.68%

As it can be observed from Table 6.2, the kraft pulp mill holds the highest share of the exergy destruction, which can be explained by energy intensive chemical processes necessary to separate pulp from wood and convert it into a commercial product. The black liquor gasification unit accounts for about 24% of the exergy destruction in the integrated plants, due to the reduction and oxidation reactions, while burning char at high temperatures to provide the energy demanded by those reactions [184]. In the syngas purification unit, the exergy destruction can be explained by the throttling for solvent regeneration, and the CO_2 separation and subsequent intercooled recompression. Finally, the exergy destruction in the methanol and dimethyl ether loops are mainly owed to the chemical reactions, recycled streams mixing and intercooling.

According to Table 6.3, the average exergy efficiencies calculated for the conventional scenario is lower than that calculated for the integrated plants for MeOH and DME co-production. These results are strongly in agreement with those reported by Van Rens et al. (2011), who performed an exergy analysis for production of MeOH and DME using wood as feedstock via gasification process [185].

Among all the configurations studied, the integrated chemical plants operating under the mixed mode present the highest exergy efficiencies. These findings reinforce the idea that the electricity import, whether available, may help reducing the irreversibility in the manufacturing of bioproducts. Although intensive industrial utilization of the Brazilian electricity mix may bring about further challenges to electricity generation companies, the

intensive electricity import in the integrated biorefineries has many opportunities that have not been fully exploited.

Meanwhile, a radical drop of up to 20% in the exergy efficiency is expected when incorporating the performance of the upstream supply chains due to the inclusion of the irreversibility associated to the feedstock and fuels acquisition. Looking at the extended exergy destruction of the conventional kraft pulp mill and the integrated chemical plants operating in mixed operation mode (around 31 GJ/t_{Pulp}), it becomes evident that the intensive consumption of biomass of the designs operating under autonomous mode becomes a decisive factor, as it influences both the irreversibilities (41 GJ/t_{Pulp}) and the carbon footprint related to the co-production of chemicals. In other words, the apparent benefits of the biorefinery concepts must be always weighed in the light of the extended production route, and not only from the plant-wide perspective.

Table 6.3 Exergy performance indicators for the conventional and the integrated chemicals production plants.

	Integrated chemical plants			
Chemical plant	**Pulp + MeOH**		**Pulp + DME**	
Operation mode	Mixed	Auto	Mixed	Auto
Rational exergy efficiency (%)	55.0	45.1	54.0	44.7
Extended rational exergy efficiency (%)	45.7	38.9	45.0	38.6
Relative exergy efficiency (%)	52.8	43.3	52.0	43.0
Extended relative exergy efficiency (%)	43.9	37.4	43.3	37.1
Exergy destruction (GJ/t_{Pulp})	21.5	32.0	22.2	32.3
Extended exergy destruction (GJ/t_{Pulp})	31.2	41.2	31.9	41.6

6.4 Environmental assessment

Table 6.4 shows a detailed CO_2 emissions balance for all the configurations studied. In fact, the largest share of indirect emissions belongs to the biomass acquisition and transportation steps, even higher than those directly emitted. Thus, the present analysis reveals environmental issues that otherwise may remain unveiled if the biomass and electricity use were wrongly considered *emissions free*.

As a result, the overall emission balance achieves 1.97 t_{CO2}/t_{Pulp} in the conventional mill (reported in Chapter 4). Those values are much lower, even negative, in the case of the combined pulp and MeOH production plant (-0.07 t_{CO2}/t_{Pulp}), and the facilities coproducing pulp and DME (-0.02 t_{CO2}/t_{Pulp}) when running under the mixed operating mode. The negative values point towards a potential depletion of the CO_2 in the atmosphere by co-producing other

chemicals in the integrated kraft pulp mills. In other words, the captured biogenic emissions offsets both the indirect CO_2 emissions from the feedstock supply chains with the aid of the intensive import of electricity in the Brazilian scenario.

Table 6.4. Fossil, biogenic, direct and indirect CO_2 emissions of the integrated chemicals production facilities.

	Integrated chemical plants			
Chemical plant	**Pulp + MeOH**		**Pulp + DME**	
Operation mode	Mixed	Auto	Mixed	Auto
Direct fossil CO_2 emitted (t_{CO2}/t_{Pulp})	0.08	0.08	0.08	0.08
Indirect fossil CO_2 emitted(t_{CO2}/t_{Pulp})	0.25	0.25	0.25	0.25
Total fossil CO_2 emitted (t_{CO2}/t_{Pulp})	0.33	0.33	0.33	0.33
Avoided biogenic CO_2 emissions (t_{CO2}/t_{Pulp})	-0.89	-0.89	-0.89	-0.89
Direct biogenic CO_2 emitted (t_{CO2}/t_{Pulp})	0.49	1.67	0.55	1.69
Overall CO_2 emissions balance(t_{CO2}/t_{Pulp})	**-0.07**	**1.11**	**-0.02**	**1.13**
Net CO_2 emissions balance (t_{CO2}/t_{Pulp})	**-0.57**	**-0.56**	**-0.57**	**-0.56**

Figure 6.4 summarizes the results for the renewability index. Compared to the conventional kraft pulp mill, in which this indicator achieves 0.64 the scenarios based on the integrated chemical plants running either on mixed (0.97) or autonomous (0.71) modes achieve higher renewability indexes, with the co-production of pulp and methanol attaining a renewability index of 1. These lambda values are similar to those reported in the literature for ethanol and sugar production from sugarcane in Brazil (0.66 to 0.72) [86; 186]. For this reason, the exergy embodied in the production of MeOH or DME by using BL gasification would not suffice to compensate for exergy losses, irreversibility and fossil fuel consumption in the chemical plants studied. Similarly to the exergy efficiency behavior, the larger the electricity import, the higher the lambda index, which supports the use of electricity from the Brazilian electricity mix as a major driver of more sustainable biorefineries.

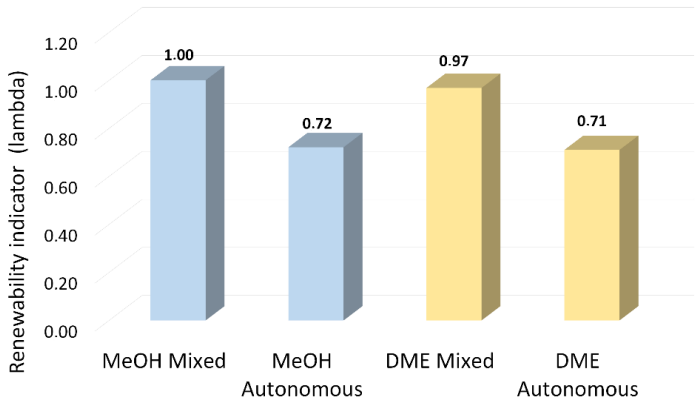

Figure 6.4 Renewability performance indicator for the kraft mill integrated to MeOH and DME production plants.

6.5 Economic analysis

According to Table 6.5, the integrated pulp and chemicals production plants running either on mixed and autonomous operating modes have 12-15% higher operating revenues owed to the additional value-added products (i.e. apart from the pulp).

The breakdown of the capital expenditure shown in Figure 6.5 implies that the operation under the autonomous mode requires bulkier equipment, such as larger chips furnaces and steam network components, compared to the plants running on the mixed operating mode. For this reason, the intensive use of electricity seems to be the most promising approach in terms of capital expenditure, provided that inexpensive and environmentally friendly energy resources are used in its generation.

Table 6.5 Annualized capital costs and net plant revenues for the studied cases.

	Integrated chemical plants			
Chemical plant	**Pulp + MeOH**		**Pulp + DME**	
Operation mode	Mixed	Auto	Mixed	Auto
Operating Incomes (€/ t_{Pulp})	854.12	854.12	863.07	863.07
Operating Costs (€/t_{Pulp})	-218.72	-224.89	-219.69	-225.62
Operating Revenues (€/t_{Pulp})[1]	635.40	629.24	643.37	637.45
Annualized capital cost (€/t_{Pulp})[2]	-320.86	-345.55	-322.26	-327.16
Net Plant Revenues (€/t_{Pulp})[3]	**314.54**	**283.69**	**321.12**	**310.29**

1. The operating revenues are estimated as the difference between the gross operating incomes minus the operating cost; 2. The investment costs of pulp mill are scaled (0.6 factor) according to [20], other CAPEX costs calculated by the described methodology [153]; 3. The net revenues are calculated as the operating revenues subtracting the yearly investment cost.

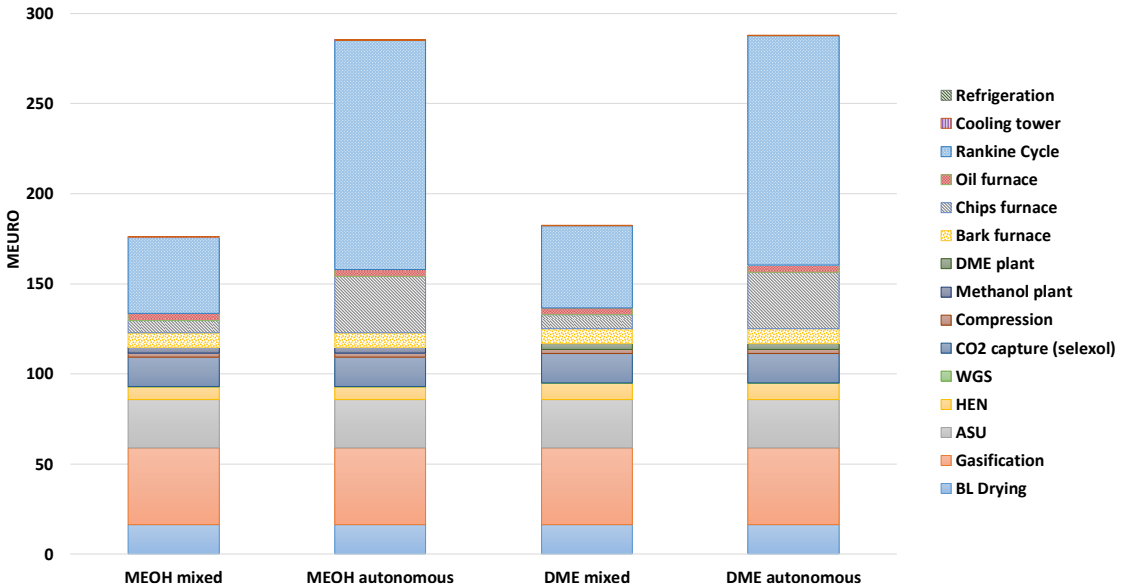

Figure 6.5 Capital investment costs breakdown for the integrated chemical production plants - 20% of contingency considered.

6.5.1 Sensitivity analysis to carbon tax and interest rate

The attractiveness of the proposed setups will depend on certain financial parameters that affect the incremental net present value (INPV). For instance, even if the price of the commodities were considered as constant, any change in the carbon taxations and interest rates may alter the economic feasibility of a formerly viable solution. Accordingly, Figures 6.6a-d show the variation of the INPV for all the integrated chemical plants as a function of the carbon tax (0-100 €/t_{CO2}) and the interest rate (0-21%).

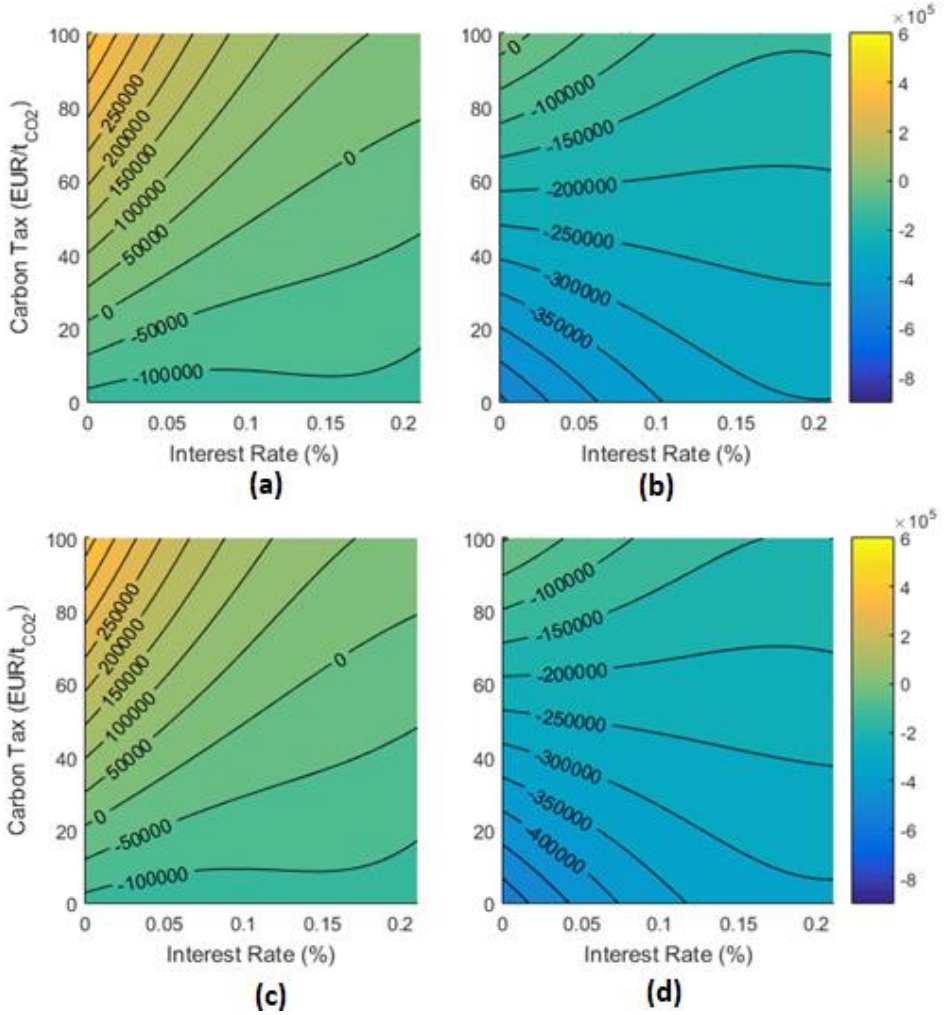

Figure 6.6 Contour plots of INPV (€) variation: (a) integrated pulp and MeOH production operating in mixed mode, (b) integrated pulp and MeOH production operating in autonomous, (c) integrated pulp and DME production operating in mixed mode (d) integrated pulp and DME production operating in autonomous mode.

As expected, more attractive financial conditions can be achieved for lower interest rates and higher carbon taxations. More specifically, for the integrated plants co-producing MeOH or DME and operating under the mixed mode, positive INPV values can be found for carbon taxes ranging between 20-70 €/t_{CO2}, depending on the interest rate adopted (see Figure

6.6a and Figure 6.6c). On the other hand, for the same integrated plants operating under the autonomous mode, the INPV cannot achieve positive values for DME production (Figure 6.6d), whereas for the MeOH production, the INPV is positive only when the carbon tax becomes higher than 95 €/t_{CO2} and the interest rate is lower than 3%.

In this regard, middle-to-high carbon taxations (20-100 €/t_{CO2}) may render MeOH or DME co-production attractive in the Brazilian context of a highly renewable electricity mix. This feasibility range is in agreement with that suggested by the High-Level Commission on Carbon Prices, which estimated that a global CO_2 price of 50-100 USD/t_{CO2} would be needed by 2030 [187] to achieve the goals of the Paris Agreement.

6.5.2 Incremental financial analysis under uncertainty of the prices of the commodities

The aforementioned results assumed that the prices of the commodities could be considered as constant. However, in practice, those values are not deterministically defined, since they depend on the volatility of the market. In view of this circumstance, it is desirable to assess the effect of the stochastic variation of the price of those commodities on the financial attractiveness of the proposed plants. This analysis relies on the Monte Carlo simulations developed for the scenarios *(i)* to *(iii)* described in Section 3.4.1.

The heat maps given in Tables 6.6-6.9 summarize the results obtained for the integrated chemical plant scenarios in which prices of the commodities vary in a stochastic way, for a series of carbon tax values (0-100 €/t_{CO2}) and interest rates (0-21%). According to Table 6.6, for the integrated plant co-producing pulp and MeOH and operating under the mixed mode, there exists a large probability of the INPV being positive, depending on the interest rate adopted and for a region of middle to stringent carbon taxations (70-100 €/t_{CO2}). For the integrated plant co-producing pulp and DME and operating under the mixed mode, Table 6.8 shows that an economically feasible carbon tax starts at a higher carbon tax level (80-100 €/t_{CO2}). The set of Fischer interceptions (*i.e.* the transition region from green to yellow in the heat map of Tables 6.6 and 6.8) indicates the conditions at which the shift from a null likelihood of loss (i.e. financially feasible region) to a positive one (i.e. likely unfeasible region) occurs. In this way, the heat maps allow bounding the financially interesting conditions of the integrated biorefineries.

In this regard, at very low carbon taxes (< 10 €/t_{CO2}) typically found in the regional economies [188], even a very low interest rate would not be enough to shift the INPV to positive

values. Meanwhile, at moderate carbon taxations, such as those imposed by Norway and Finland (~40-80 €/t_{CO2}) [188], the integrated chemical plant starts to bring about better INPV values if MeOH or DME are produced under the mixed operation mode. For the sake of comparison, Tables 6.7 and 6.9 shows that the integrated chemical plants co-producing MeOH or DME operating under the autonomous mode present relatively unfavorable INPVs, regardless of the value of the interest rates.

Table 6.6 Probability that the INPV is negative (likelihood of loss in %) as a function of the interest rate, for deterministic carbon taxes and stochastic prices of the commodities (scenario *i*) for an integrated pulp and MeOH chemical plant operating under the mixed mode.

CO_2 tax (€/t_{CO2}) →	0	10	20	30	40	50	60	70	80	90	100
i (%) 0%	97.70	85.81	59.07	25.93	6.44	0.76	0.07	0.00	0.00	0.00	0.00
3%	99.59	95.26	78.46	46.97	17.63	3.83	0.47	0.00	0.00	0.00	0.00
6%	99.90	98.77	91.19	70.77	38.40	13.86	3.19	0.40	0.01	0.00	0.00
9%	99.99	99.57	97.34	87.64	64.73	36.11	12.40	2.59	0.33	0.01	0.00
12%	100.00	99.90	99.47	95.70	84.00	59.30	31.13	11.66	2.81	0.46	0.01
15%	100.00	100.00	99.83	98.51	93.44	79.50	54.66	28.61	11.37	2.61	0.37
18%	100.00	100.00	99.91	99.53	97.44	89.57	74.84	50.96	25.69	9.76	2.77
21%	100.00	100.00	99.97	99.87	99.06	95.53	86.96	69.01	45.61	23.50	9.31

Table 6.7 Probability that INPV is negative (likelihood of loss in %) as a function of the interest rate, for deterministic carbon taxes and stochastic prices of commodities (scenario *i*) for an integrated pulp and MeOH chemical plant operating under the autonomous mode.

CO_2 tax (€/t_{CO2}) →	0	10	20	30	40	50	60	70	80	90	100
i (%) 0%	100.00	100.00	100.00	100.00	100.00	99.94	99.77	97.40	85.81	59.10	27.77
3%	100.00	100.00	100.00	100.00	100.00	100.00	99.97	99.83	98.10	89.86	67.20
6%	100.00	100.00	100.00	100.00	100.00	100.00	100.00	100.00	99.89	99.14	93.99
9%	100.00	100.00	100.00	100.00	100.00	100.00	100.00	100.00	99.99	99.93	99.56
12%	100.00	100.00	100.00	100.00	100.00	100.00	100.00	100.00	100.00	100.00	100.00
15%	100.00	100.00	100.00	100.00	100.00	100.00	100.00	100.00	100.00	100.00	100.00
18%	100.00	100.00	100.00	100.00	100.00	100.00	100.00	100.00	100.00	100.00	100.00
21%	100.00	100.00	100.00	100.00	100.00	100.00	100.00	100.00	100.00	100.00	100.00

Table 6.8 Probability that the INPV is negative (likelihood of loss in %) as a function of the interest rate, for deterministic carbon taxes and stochastic prices of commodities (scenario *i*) for an integrated pulp and DME chemical plant operating under the mixed mode.

CO_2 tax (€/t_{CO2}) →	0	10	20	30	40	50	60	70	80	90	100
i (%) 0%	96.37	83.77	55.69	25.79	6.61	0.81	0.09	0.01	0.00	0.00	0.00
3%	98.87	94.10	76.47	47.96	18.24	4.39	0.53	0.03	0.00	0.00	0.00
6%	99.74	98.19	90.60	70.89	41.34	15.74	3.66	0.47	0.03	0.00	0.00
9%	99.97	99.57	97.03	88.16	65.70	37.47	14.79	3.80	0.63	0.04	0.00
12%	100.00	99.80	99.26	95.20	84.31	61.04	35.03	15.44	3.23	0.67	0.09
15%	100.00	99.96	99.80	98.40	93.61	80.60	59.00	33.30	13.44	3.93	0.86
18%	100.00	100.00	99.89	99.47	97.61	90.87	76.11	55.40	31.86	14.57	4.70
21%	100.00	99.99	99.96	99.90	98.97	96.24	88.41	72.19	52.03	28.90	13.41

Table 6.9 Probability that INPV is negative (likelihood of loss in %) as a function of the interest rate, for deterministic carbon taxes and stochastic prices of commodities (scenario *i*) for an integrated pulp and DME chemical plant operating under the autonomous mode.

i (%) \ CO_2 tax (€/t_{CO2}) →	0	10	20	30	40	50	60	70	80	90	100
0%	100.00	100.00	100.00	100.00	100.00	100.00	99.94	98.30	92.16	73.71	43.64
3%	100.00	100.00	100.00	100.00	100.00	100.00	100.00	99.84	99.09	94.69	80.36
6%	100.00	100.00	100.00	100.00	100.00	100.00	100.00	100.00	99.93	99.59	97.20
9%	100.00	100.00	100.00	100.00	100.00	100.00	100.00	100.00	100.00	99.97	99.81
12%	100.00	100.00	100.00	100.00	100.00	100.00	100.00	100.00	100.00	100.00	100.00
15%	100.00	100.00	100.00	100.00	100.00	100.00	100.00	100.00	100.00	100.00	100.00
18%	100.00	100.00	100.00	100.00	100.00	100.00	100.00	100.00	100.00	100.00	100.00
21%	100.00	100.00	100.00	100.00	100.00	100.00	100.00	100.00	100.00	100.00	100.00

Meanwhile, the heat maps shown in Tables 6.10 and 6.11 summarize the results obtained for scenarios *(ii)* and *(iii)*, described in Section 3.4.1. The former scenario *(ii)* aims to represent the situation in which the carbon taxes linearly increase from 0 to 100 €/t_{CO2}, to allow for a smooth transition between the current and the future carbon taxed scenario. Similarly to the previous analyses, the prices of commodities are stochastically varied over the project lifespan. In the second scenario *(iii)*, all the previous assumptions remain the same, except for the carbon taxation, which turn out be also stochastic in nature (i.e. randomly varied between 0 to 100 €/t_{CO2}). In both scenarios, the analysis is performed for an interest rate varying from 0% to 21%.

According to Tables 6.10 and 6.11, only the integrated chemical plants producing MeOH or DME operating under the mixed mode and at very low interest rates (~0%) presented close to favorable results in terms of likelihood of loss (i.e. the probability that INPV is negative). As a final remark, only the confluence of several factors, such as (*i*) equipment maturation and deployment; (*ii*) advantageous economies of scale; (*iii*) more stringent regulatory commitments pointing towards the decarbonization of chemicals and fuels; as well as (*iv*) attractive fiscal incentives and international cooperation may boost the integration of chemicals and fuels production via black liquor gasification in pulp and paper industries. These factors become more relevant if uncertainties are considered for the carbon taxations and the price of the commodities. The optimistic scenario is not at all unrealistic, considering that by 2040, more than two thousand large-scale CCS facilities are necessary to reach sustainable development goals, as stated by the International Energy Agency [189].

Table 6.10 Probability that the INPV is negative (likelihood of loss in %) as a function of the interest rate considering linearly increasing carbon taxes and stochastic prices of the commodities (scenario *ii*).

i (%)	pulp&MeOH - mixed mode	pulp&MeOH - autonomous mode	pulp&DME - mixed mode	pulp&DME - autonomous mode
0%	1.00	100.00	1.24	100.00
1%	2.37	100.00	2.16	99.99
2%	4.79	100.00	5.17	100.00
3%	9.37	100.00	10.46	100.00
4%	17.46	100.00	18.56	100.00
5%	27.77	100.00	29.49	100.00
6%	41.91	100.00	42.26	100.00
7%	56.33	100.00	55.40	100.00
8%	67.77	100.00	68.56	100.00
9%	77.80	100.00	78.61	100.00
10%	85.34	100.00	85.87	100.00
11%	91.99	100.00	91.20	100.00
12%	95.07	100.00	94.63	100.00
13%	96.93	100.00	96.69	100.00
14%	98.34	100.00	98.33	100.00
15%	99.11	100.00	98.89	100.00
16%	99.47	100.00	99.47	100.00
17%	99.69	100.00	99.66	100.00
18%	99.77	100.00	99.79	100.00
19%	99.89	100.00	99.81	100.00
20%	99.96	100.00	99.91	100.00
21%	99.97	100.00	99.97	100.00

Table 6.11. Probability that the INPV is negative (likelihood of loss in %) as a function of the interest rate, considering stochastic carbon taxes and prices of the commodities (scenario *iii*).

i (%)	pulp&MeOH - mixed mode	pulp&MeOH - autonomous mode	pulp&DME - mixed mode	pulp&DME - autonomous mode
0%	1.49	99.96	1.67	99.96
1%	2.14	99.99	2.36	100.00
2%	3.24	100.00	3.64	99.99
3%	5.24	100.00	6.21	99.99
4%	8.37	100.00	8.89	100.00
5%	11.63	100.00	13.00	100.00
6%	16.81	100.00	18.30	100.00
7%	21.74	100.00	23.29	100.00
8%	28.81	100.00	31.86	100.00
9%	36.17	100.00	39.30	100.00
10%	44.74	100.00	47.31	100.00
11%	52.09	100.00	55.40	100.00
12%	60.14	100.00	61.77	100.00
13%	66.36	100.00	67.71	100.00
14%	72.81	100.00	75.71	100.00
15%	77.93	100.00	79.84	100.00
16%	82.31	100.00	84.59	100.00
17%	86.00	100.00	87.14	100.00
18%	88.89	100.00	89.96	100.00
19%	91.44	100.00	92.49	100.00
20%	92.83	100.00	93.80	100.00
21%	94.61	100.00	94.99	100.00

6.6 Conclusion

The thermoenvironomic performance of two proposed chemical production plants (MeOH or DME) integrated to a kraft pulp mill via the black liquor gasification process are compared to the performance of a conventional kraft pulp mill. By using the combined exergy and energy integration analyses, it was possible to work out the best alternatives of the utility systems. As a result, the exergy efficiencies of the conventional and integrated cases average 40% and 45%, respectively, whereas the overall emission balance varies from 1.97 to -0.07 t_{CO2}/t_{Pulp}, respectively. These negative emissions highlight the benefits of using alternative energy sources, such as biomass and electricity, in integrated chemical plants. The renewability factor turns out to be higher for the integrated chemical plants operating under the mixed mode, due to the reduction of the fossil energy consumption and the intensive import of the Brazilian electricity. The results pointed that the environmental and economic performances are highly related to the indirect emissions due to the consumption of energy resources and are subjected to the adopted market prices for the commodities. The introduction of more stringent carbon taxes and more affordable biomass conversion technologies may encourage the deployment and diminish the financial risks associated to breakthrough technologies. Anyhow, the integrated BL gasification prove to be feasible to co-produce methanol and dimethyl ether in existing pulp mills sites.

CHAPTER 7: FERTILIZERS SECTOR- AMMONIA, UREA AND NITRIC ACID

Ammonia is one of the several chemicals that can produced from syngas and it is one of the most demanded bulk chemicals in the world. In 2016, the ammonia production reached 175 million tons, and the trend from 2006 to 2016 shows a growth rate of 1.9% per year [190]. Around 70% of the total ammonia produced worldwide is used for the production of fertilizers for the agricultural sector [191]. The urea production is the largest-volume derivative of ammonia, accounting for more than 50% of the ammonia demand, being widely used in fertilizers as a source of nitrogen and it is also an important material for the food and chemical industry. The nitric acid and ammonium nitrate are the second major users of the ammonia demand. About 75-80% of nitric acid is utilized for fertilizer production [191]. Thus, the decarbonization of the fertilizers sector is directly related to the decarbonization of the ammonia supply chain, as it can be used directly or as feedstock to other chemicals.

Currently, almost 100% of ammonia production obtains the required hydrogen from fossil fuel feedstock. The literature reports that the ammonia production accounts for around 2% of total final energy consumption and 1.3% of CO_2 emissions from the energy system, since it is heavily based on fossil fuels [191]. The pursuit of alternative sources for the nitrogen fertilizers sector has recently earned renewed interest due to increasing concerns regarding the world dependence on non-renewable resources and also motivated by the more stringent environmental regulations. The decarbonization of this sector might help not only improving its carbon footprint, but also reducing its dependence on international market prices of natural gas. The use of cheaper biomass resources has been suggested as an alternative to address the partial or complete decarbonization of the fertilizers production [14].

For instance, reference [14] developed a detailed evaluation of the economic and environmental impacts of the *partial* or *total* substitution of the natural gas in conventional ammonia production plants, calculating the exergy efficiencies of natural gas and biomass-based (bagasse as feedstock) ammonia production routes. Those results show that the exergy efficiencies of the conventional and the alternative production routes average 65.8% and 41.3%, respectively. Meanwhile, the overall CO_2 emission balance attained 0.5 to -2.3 t_{CO2}/t_{NH3}, for the fossil and alternative production routes, respectively. For the biomass-based ammonia production, the indirect emissions of the biomass supply are the largest share of indirect emissions (85–100%). Thus, the availability on site and the large distance for transportation

may contribute to higher carbon footprint in the ammonia supply chain, due to the increase of indirect emissions.

Andersson and Lundgren [21] performed a techno-economic evaluation of the simultaneous pulp and ammonia production in a kraft pulp mill via integrated gasification of bark (30 bar and 1200 °C). The authors compared the performance of a stand-alone ammonia production plant operating separately from the kraft pulp mill, both plants consuming external wood as fuel. In a second scenario, the authors considered the energy integration of both facilities, so that the bark from the kraft pulp mill can be used as the gasification feedstock by replacing the original bark boiler. Meanwhile, the black liquor produced is still consumed in a typical recovery boiler. The results showed that the overall efficiency calculated in terms of what the authors defined as 'electricity equivalents' (analogous to the exergy concept, but strongly reliant on arbitrary power conversion factors) for the stand-alone ammonia production plant achieves 44%, whereas for the integrated system an efficiency of 54% is obtained. According to the authors, this increment in the electricity equivalents-based efficiency is a consequence of the enhanced utilization of bark in the gasification system and the integration of both plants. In any case, the utilization of the 'electricity equivalents' is largely subjective, as it depends on arbitrary conversion factors, unlike exergy, which is based on physical principles and the Second law of Thermodynamics.

In this work, the use of black liquor gasification in the integrated syngas and ammonia production plant (Figure 7.1) is proposed. Moreover, the ammonia produced can be used either to synthesize urea or nitric acid following the flowsheets reported in Figures 3.12 and 3.13. These integrated plants are compared with the performance of the conventional kraft mill in light of thermodynamic, economics and environmental impacts, applying the optimization framework for the utility plant following the methodology described in Chapter 3. The results are presented in the next sections.

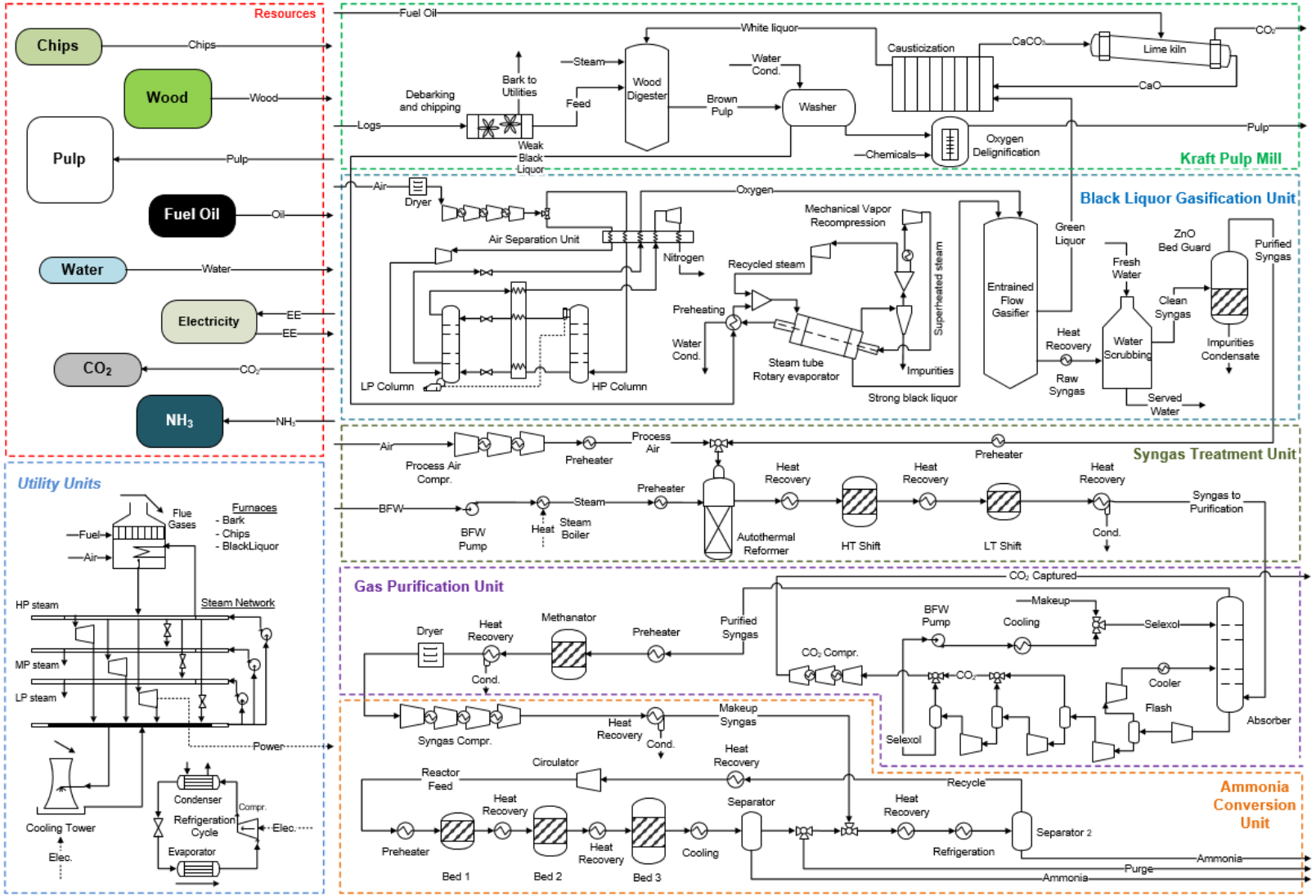

Figure 7.1 Flowsheet of the integrated kraft pulp process and ammonia production plant.

7.1 Energy and exergy consumption remarks

Table 7.1 summarizes the exergy consumption remarks of the kraft mill integrated to the plants producing either ammonia, nitric acid or urea. A first remark relies on the fact that the integrated plants have an increment between 5-36% in the overall exergy consumption compared to the conventional MVR case, due to the new demands required by the integration of the new facilities. In addition, the *Extended Exergy Consumption* presented an increase of the exergy consumption between 16-21%. Compared to the ammonia plant, the urea and nitric acid plants presented lower resources consumption for utility purposes, since they are highly exothermic processes.

Akbari and co-workers [15]studied the ammonia production process from black liquor gasification at 27 bar and 1050 °C, obtaining an energy yield of 31.07%, defined as the ratio between the higher heating value (HHV) of ammonia and BL. For the sake of comparison, the integrated setups evaluated on the current study achieved 31.94% for this indicator. However, in Akbari's work, neither the kraft pulp mill responsible for the production of the BL nor the utility systems that must satisfy the overall energy requirements of both pulp and ammonia production are explicitly modelled. In this way, the energy yield indicator is only based on the amount of black liquor consumed, not in the overall energy consumption of the chemical and utility system. This circumstance renders difficult the comparison with the proposed systems studied in this paper, since the interrelation between the waste heat recovery, the cogeneration system and the chemical plants is not explicit. In other words, the irreversibility associated with the conversion of the energy resources required for supplying the steam and power of the integrated systems is missing, once the proposed energy yield by [15] should also account for the extended framework of specific energy consumption.

Table 7.1 Optimal process variables of the conventional and the integrated kraft pulp process and ammonia production plants.

Process parameter	**NH_3 Mixed**	**NH_3 Auto**	**Urea Mixed**	**Urea Auto**	**Nitric Acid Mixed**	**Nitric Acid Auto**
Utility system fuel input	Electricity/Chips	Chips	Electricity/Chips	Chips	Electricity/Chips	Chips
Feedstock wood consumption (GJ/t_{Pulp})	41.15	41.15	41.15	41.15	41.15	41.15
Utility chips consumption (GJ/t_{Pulp})	0.88	15.31	0.00	11.96	0.00	6.23
Utility electricity consumption (GJ/t_{Pulp})	3.43	0.00	4.08	0.00	2.13	0.00
Oil consumption (GJ/t_{Pulp})	1.05	1.05	1.05	1.05	1.05	1.05
Overall plant consumption (GJ/t_{Pulp})	***46.51***	***57.51***	**46.28**	**54.15**	**44.32**	**48.43**
Extended plant consumption (GJ/t_{Pulp}) [1]	***56.06***	***66.65***	**56.21**	**62.76**	**52.70**	**56.11**
Rankine cycle power generation (GJ/t_{Pulp})[2]	2.05	5.67	2.02	6.26	3.64	5.85
Chemical process power demand (GJ/t_{Pulp})						
- *Kraft Pulp Mill*	2.84	2.84	2.84	2.84	2.84	2.84
- *Black Liquor Treatment and Gasification*	1.20	1.20	1.20	1.20	1.20	1.20
- *Syngas Conditioning and Ammonia Synthesis*	0.58	0.58	1.19	1.19	0.77	0.77
Ancillary power demand (GJ/t_{Pulp})[3]	0.22	0.41	0.24	0.39	0.32	0.41
Min. Cooling requirement (GJ/t_{Pulp})[4]	2.68	2.68	2.74	2.74	7.60	7.60
Min. Heating requirement (GJ/t_{Pulp})[4]	2.33	2.33	0.45	0.45	0.00	0.00
Biomass consumption ($t_{Wood}/t_{fertilizer+Pulp}$)	2.64	3.54	2.37	3.06	1.67	1.93
Syngas production (GJ/t_{Pulp})	9.36	9.36	9.36	9.36	9.36	9.36
Chemical production (t/day)	218.93	218.93	316.34	316.34	812.77	812.77
Pulp production (t/day)	877.83	877.83	877.83	877.83	877.83	877.83
Marketable CO_2 production (kg/h)	50,518	50,518	37,883	37,883	50,518	50,518
Electricity export (kW)	0	0	0.00	0.00	0.00	0.00

1. The overall exergy consumption increases if the extended efficiency of the electricity generation (55.68%), as well as of the oil (95.20%) and biomass (86.13%) supply chains are considered as [11; 139]; 2.Steam pressure levels 100, 12, 4 and 0.10 bar, steam superheating 200°C; 3. Cooling tower and vapor compression refrigeration systems; 4.Heating requirements of the chemical processes (energy basis) determined from the composite curves;

According to Figure 7.2, in all the integrated production facilities (i.e. mixed and autonomous scenarios), the kraft pulp mill continues to be the major consumer of the power generated or imported. However, the autonomous case upholds the highest total power generation (5.67-6.26 GJ/t_{Pulp}) in the Rankine cycle, 33-47% higher than that of the conventional MVR case. On the other hand, in the mixed mode configuration, there is a reduction in the power generation due to the diversification of the resources consumed, namely, a major proportion of the power demand is supplied by the electricity grid.

It is also important to notice that the air separation unit consumes about 12% of the total power generation in the utility system. In spite of this, air enrichment avoids the dilution of the gasification syngas with nitrogen, which otherwise would require the integration of a downstream nitrogen separation system in order to control the suitable ratio of H_2 to N_2 required for the ammonia synthesis.

From Figure 7.2 it can be observed the syngas compression and the refrigeration demands required for the ammonia production and consequently for the other ammonia-derived fertilizers. For the urea production (Figures 7.2c and 7.2d) the physical absorption unit presents a larger power demand since part of the absorbed CO_2 needs to be compressed to be used in the urea synthesis loop. As for the nitric acid production (Figures 7.2e and 7.2f) there is a power consumption associated with the air that should be compressed to enter this chemical synthesis.

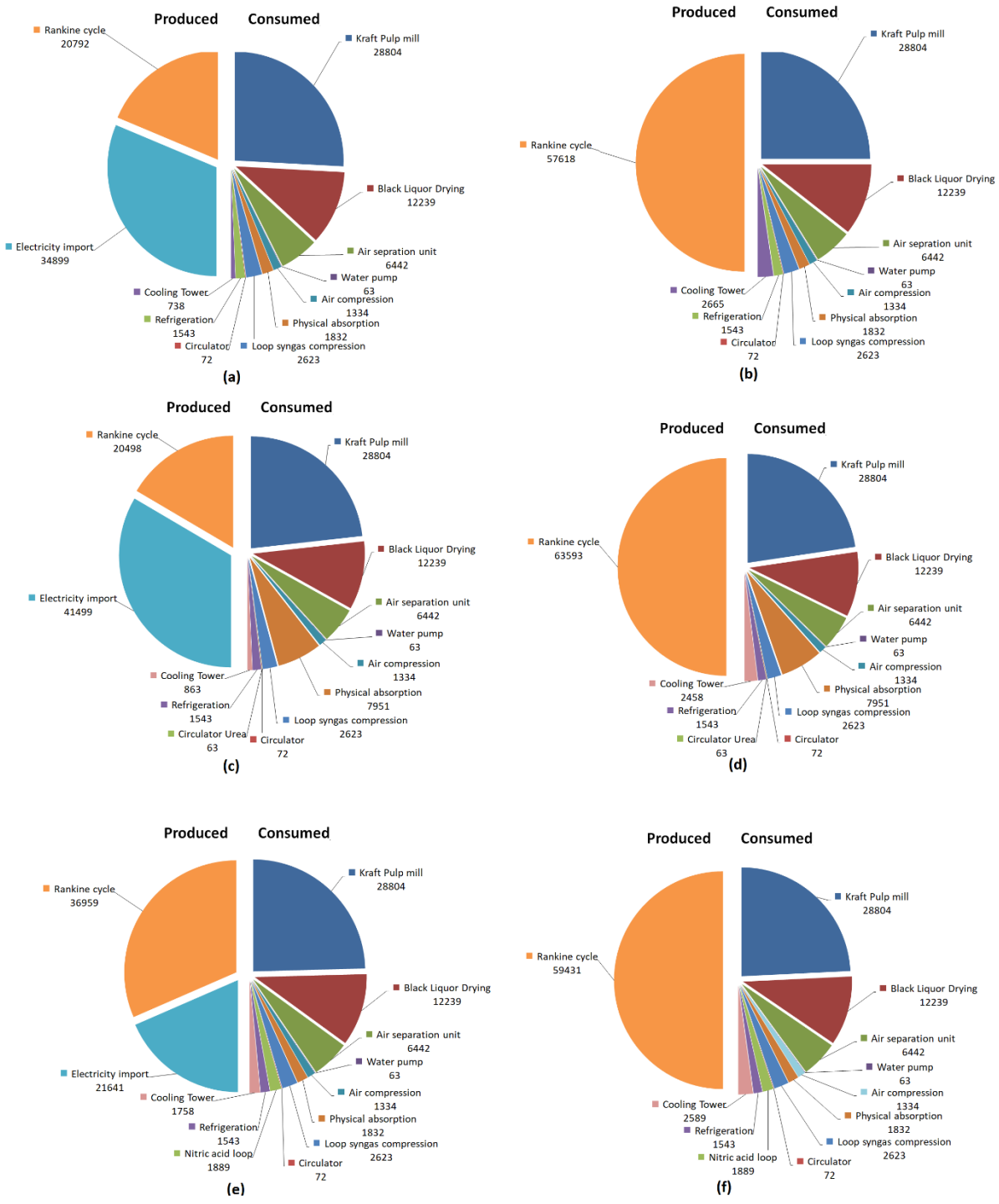

Figure 7.2 Power consumption breakdown (in kW): *Ammonia production under* mixed (a) or autonomous (b) operating modes*; Urea production under* mixed (c) or autonomous (d) operating modes; and *Nitric Acid production under* mixed (e) or autonomous (f) operating modes.

7.2 Energy integration analysis

Regarding the energy integration analysis, it can be observed a radical modification of the integrated curves due to the integration of any associated fertilizer plant (Figure 7.3) when compared with the conventional kraft pulp mill curve (Figure 4.3b). Actually, a large amount

of waste heat (*pockets*) is produced throughout the chemical plants, and this fact is even more pronounced for the urea and nitric acid integrated plants, due to the high exothermic nature of the reactions involved, favoring the waste heat recovery. For the autonomous cases, a large amount of chips must be burned to balance the energy requirements, resulting in an increased amount of exergy destruction. Finally, in the mixed mode configuration, the amount of chips is dramatically reduced by maximizing the waste heat recovery and also importing the major part of the power consumed in the plant. This solution is responsible for the reduction of the irreversibility linked to the extensive heat transfer rates inherent to the autonomous scenarios, as it can be evidenced by the shorter span of the integrated curves along the abscissa (H) of the plots in Figures 7.3a, 7.3c and 7.3e. Clearly, the most suitably solution might not be only related to the reduction of the irreversibility and chips consumption rates, since there may be a trade-off that potentially favours the electricity import only if this condition is both economical and environmentally friendly, e.g. considering the highly renewable Brazilian electricity and the energy intensive biomass and oil supply chains.

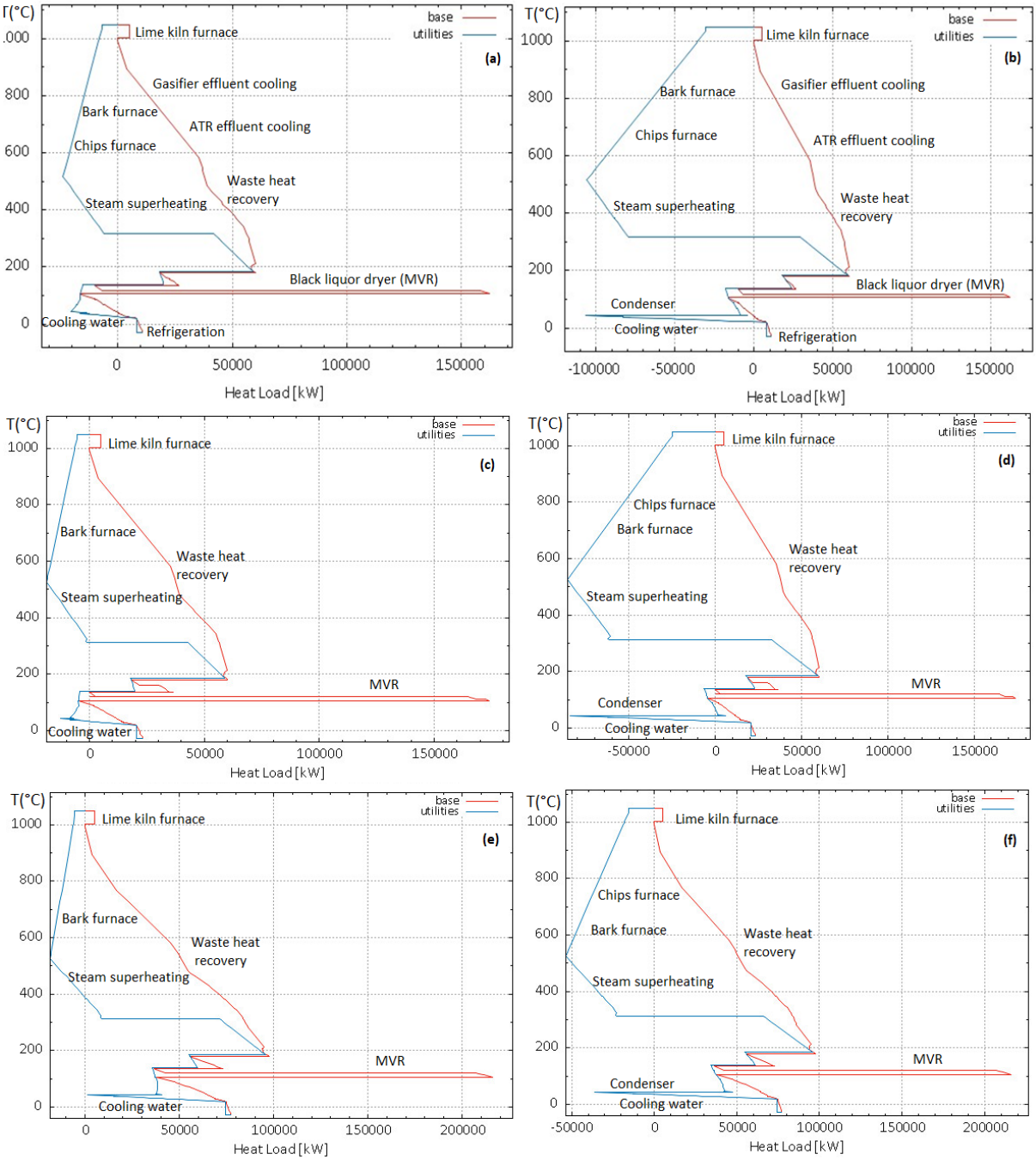

Figure 7.3 Integrated composite curves: *Ammonia production under* mixed (a) or autonomous (b) operating modes*; Urea production under* mixed (c) or autonomous (d) operating modes; and *Nitric Acid production under* mixed (e) or autonomous (f) operating modes. MVR: Mechanical Vapor Recompression.

7.3 Exergy efficiencies

According to Figure 7.4 and Table 7.2, there is a significant reduction of the exergy efficiency for all the studied scenarios compared to the chemicals and fuels evaluated in chapters 5 and 6. Ammonia synthesis requires other steps such as methanation after CO_2

capture, syngas compression up to 150 bar, refrigeration, that may impact on its exergy efficiency performance.

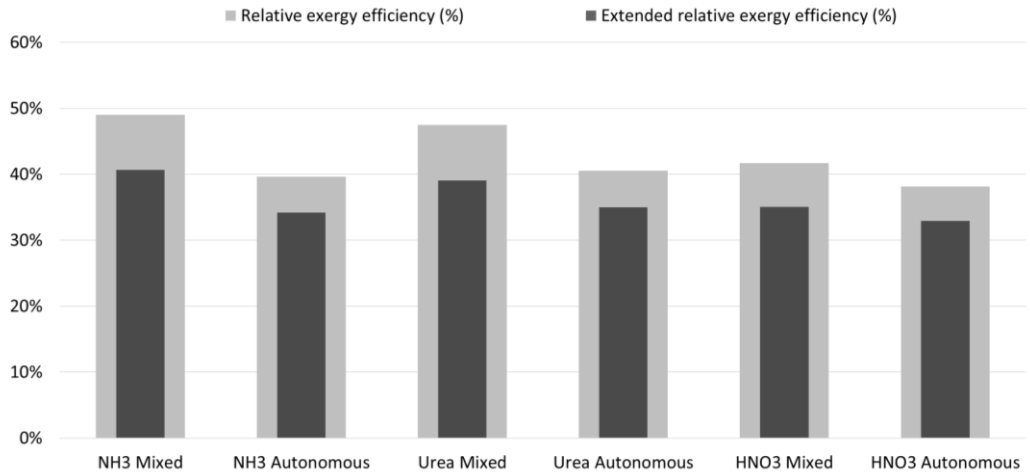

Figure 7.4 Comparison between the relative and extended relative exergy efficiency of the integrated kraft pulp process and chemicals production plants.

Concerning the exergy destruction (Table 7.2), the mixed mode seems to outperform the other scenarios. However, by looking to the extended exergy destruction indicator, an apparently more efficient process becomes deteriorated by the intensive consumption of raw materials with an important carbon footprint associated to its production, which finally results in a slightly better performance of the conventional case (as reported in Table 4.2). As a result, better plant configurations may be offset by the worse performance of the extended production process.

Table 7.2 Exergy destruction and exergy efficiencies for the integrated kraft pulp process and chemicals production plants.

Process parameter	**NH_3 Mixed**	**NH_3 Auto**	**Urea Mixed**	**Urea Auto**	**Nitric Acid Mixed**	**Nitric Acid Auto**
Rational exergy efficiency (%)	51.6	41.8	49.8	42.5	44.4	40.7
Extended rational exergy efficiency (%)[1]	42.8	36.0	41.0	36.7	37.4	35.1
Relative exergy efficiency (%)	49.0	39.6	47.5	40.6	41.7	38.1
Extended relative exergy efficiency (%)[1]	40.6	34.2	39.1	35.0	35.0	32.9
Exergy destruction (GJ/t_{Pulp})	22.5	33.5	23.2	31.1	24.6	28.7
Extended exergy destruction (GJ/t_{Pulp})[1]	32.0	42.6	33.2	39.7	33.0	36.4

1.Overall exergy consumption increases if the cumulative efficiency of the electricity generation (55.68%), as well as of the oil (95.20%) and biomass (86.13%) supply chains are considered as reported by [11; 139]

7.4 Environmental assessment

7.4.1 CO_2 emissions

The direct and indirect CO_2 emissions (i.e. related to the supply chains of the electricity, oil and biomass) are shown in detail in Table 7.3 and in Figure 7.5. For instance, the large amount of wood and chips required in some of the integrated plants, not only takes a toll to the efficiency of the overall plant as it will be shown latter, but also proportionally increases the indirect CO_2 emissions produced.

The avoided CO_2 emissions are related to the carbon capture system in the syngas purification section of the ammonia production plant. The negative values indicate an overall positive impact towards the depletion of the CO_2 present in the atmosphere, meaning that for each ton of ammonia produced, around one ton of CO_2 is withdrawn from the environment when the alternative routes are used. For the urea production, since part of the CO_2 from the ammonia purification unit is used to synthesize the urea, the potential for CO_2 depletion is slightly lower. It is known that the CO_2 amount used in the urea production, is released when this fertilizer is applied in the soil, however the volume control in this work does not take into account any end-use.

Table 7.3 Fossil, biogenic, direct and indirect CO_2 emissions of the integrated chemicals production facilities.

Process parameter	NH_3 Mixed	NH_3 Auto	Urea Mixed	Urea Auto	Nitric Acid Mixed	Nitric Acid Auto
Fossil CO_2 emissions avoided (t_{CO2}/t_{Pulp})[1]	0.00	0.00	0.00	0.00	0.00	0.00
Fossil CO_2 emitted –direct (t_{CO2}/t_{Pulp})	0.08	0.08	0.08	0.08	0.08	0.08
Fossil CO_2 emitted – indirect (t_{CO2}/t_{Pulp})[2]	0.24	0.25	0.25	0.23	0.22	0.21
- CO_2 emitted indirect – EE grid (%)	24.38	0.00	28.1	0.0	17.0	0.0
- CO_2 emitted indirect – Biomass (%)	74.37	98.76	70.7	98.7	81.6	98.5
- CO_2 emitted indirect – Oil (%)	1.25	1.24	1.2	1.3	1.4	1.5
Total fossil CO_2 emitted (t_{CO2}/t_{Pulp})	0.32	0.33	0.33	0.31	0.30	0.29
Biogenic CO_2 emissions avoided (t_{CO2}/t_{Pulp})[1]	-1.38	-1.38	-1.04	-1.04	-1.38	-1.38
Biogenic CO_2 emitted – direct (t_{CO2}/t_{Pulp})	0.37	1.61	0.29	1.32	0.29	0.83
Total atmospheric emissions (t_{CO2}/t_{Pulp})	0.69	1.94	0.62	1.63	0.59	1.12
Overall CO_2 emissions balance[3](t_{CO2}/t_{Pulp})	**-0.69**	**0.56**	**-0.41**	**0.60**	**-0.79**	**-0.26**
Net CO_2 emissions balance[3] (t_{CO2}/t_{Pulp})	**-1.06**	**-1.05**	**-0.70**	**-0.72**	**-1.08**	**-1.09**

1.CO_2 emissions captured through a physical absorption system; 2. It considers the indirect emissions due to the upstream supply chains of electricity (62.09 g_{CO2}/kWh), wood (0.0043 g_{CO2}/kJ_{Wood}) and oil (0.0029 g_{CO2}/kJ_{Oil}) [11; 139]; 3. The overall CO_2 balance considers overall CO_2 emitted (either fossil or biogenic) minus CO_2 captured, whereas the net value subtracts the amount of CO_2 embodied by the crops, assumed as circular emissions;

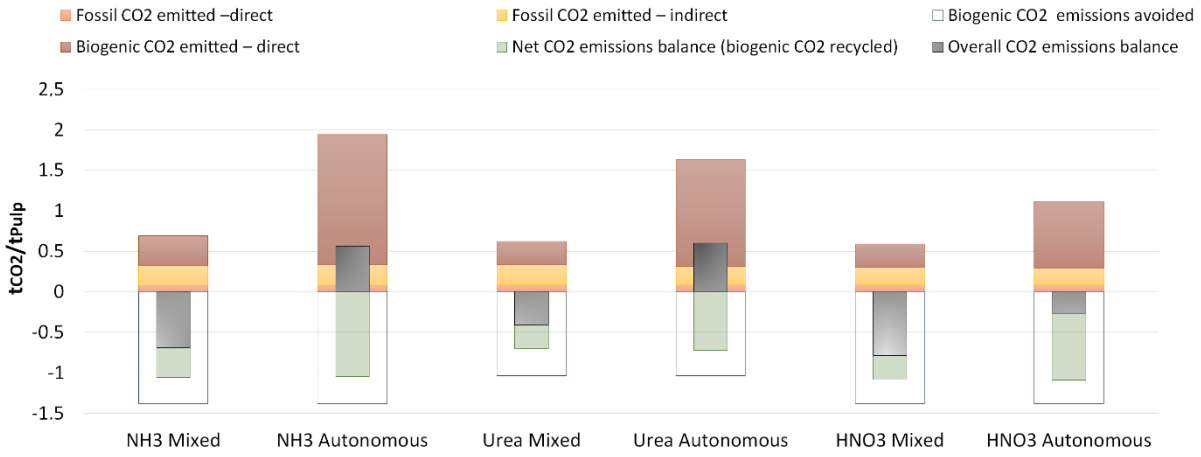

Figure 7.5 Overall and detailed (biogenic and fossil, directly and indirectly emitted, and avoided) CO_2 emissions for the integrated kraft pulp process and chemicals production plants.

7.4.2 Renewability Performance

Meanwhile, the Renewability performance indicator achieves 0.64 for the conventional case (as in Chapter 4), 0.68-0.88 for the mixed mode configuration and 0.60-0.65 for the autonomous configuration (see Figure 7.6). By definition, processes with $0 < \lambda < 1$ are considered non-renewable indicating that the exergy of the products is insufficient to compensate for the fossil exergy consumption and process irreversibility, as well as the emissions and waste treatment expenditure. These results are very much alike to those reported for a first and second generation sugarcane-based ethanol production, also determined as nonrenewable processes, even though considering different levels of integration between these two processes [192]. It can be observed that, similarly to the exergy efficiency behavior, the mixed mode presents the highest value for the renewability indicator, since the electricity import from the Brazilian mix push upwards the consumption of renewable energy source, which reinforces that it could be an important decision variable for the exploration of integrated biorefineries.

Other practices that may help increasing the renewability indicator in the integrated pulp and fertilizers production is the substitution of diesel consumption in the supply and transportation stages of biomass by ethanol or biodiesel [140] or even introducing electric trucks for wood transportation. The replacement of the lime kiln oil consumption using biomass as causticization fuel has also been considered as a sustainable step towards the decarbonization of the pulp and paper production industry [193; 194]. In any case, the integration of better energy conversion technologies in both kraft pulp and fertilizers chemical plants, as well as more efficient cogeneration technologies, will likely increase the overall efficiency and, thus, reduce the exergy destroyed, increasing in turn the Renewability index. Certainly, these breakthrough

approaches would require a detailed economic analysis to weight the advantages and disadvantages in terms of additional investment costs, maintenance and increased complexity.

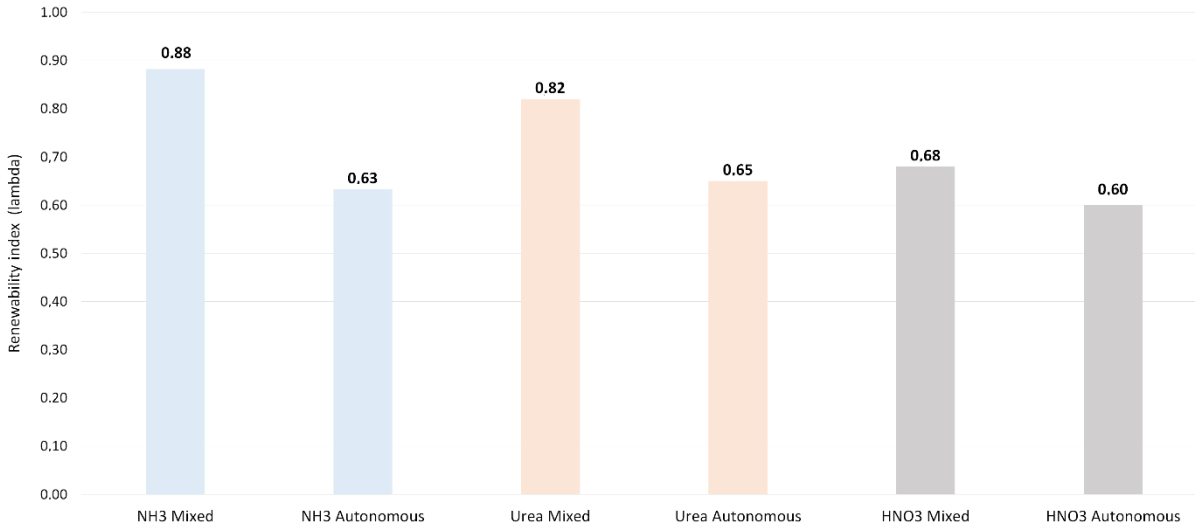

Figure 7.6 Renewability performance indicator for the kraft mill integrated to the fertilizers production plants.

7.5 Economic analysis

Table 7.4 evidences that the integrated pulp and fertilizers production configurations have higher operating revenues compared to the conventional scenario in Table 4.3, due to the complementary value-added CO_2 and fertilizers products, not produced in the conventional route. Even at higher yearly investment cost of the integrated pulp and ammonia plants, net revenues only differ less than 10% compared to the conventional case. For the urea and nitric acid, the net plant revenues can be as higher as 70% compared to the conventional case, due to the higher market selling prices of these commodities.

Table 7.4 Annualized capital costs and net plant revenues for the studied cases.

	Integrated chemical plants					
Chemical plant	**Pulp + NH_3**		**Pulp + Urea**		**Pulp + Nitric acid**	
Operation mode	Mixed	Auto	Mixed	Auto	Mixed	Auto
Operating Incomes (€/ t_{Pulp})	859.72	859.72	1058.31	1058.32	1022.91	1022.91
Operating Costs (€/t_{Pulp})	-214.64	-221.55	-221.56	-206.63	-189.55	-181.74
Operating Revenues (€/t_{Pulp})	645.07	638.17	836.75	851.68	833.36	841.17
Annualized capital cost (€/t_{Pulp})	-318.11	-362.88	-321.95	-369.85	-333.15	-367.17
Net Plant Revenues (€/t_{Pulp})	**326.96**	**275.28**	**514.81**	**481.83**	**500.21**	**474.00**

The breakdown of the capital expenditure for both scenarios of each integrated fertilizer plant (Figure 7.7), depicting the components sizes needed (e.g. refrigeration, furnaces, Rankine cycles, etc.) for each operation mode and chemical plant.

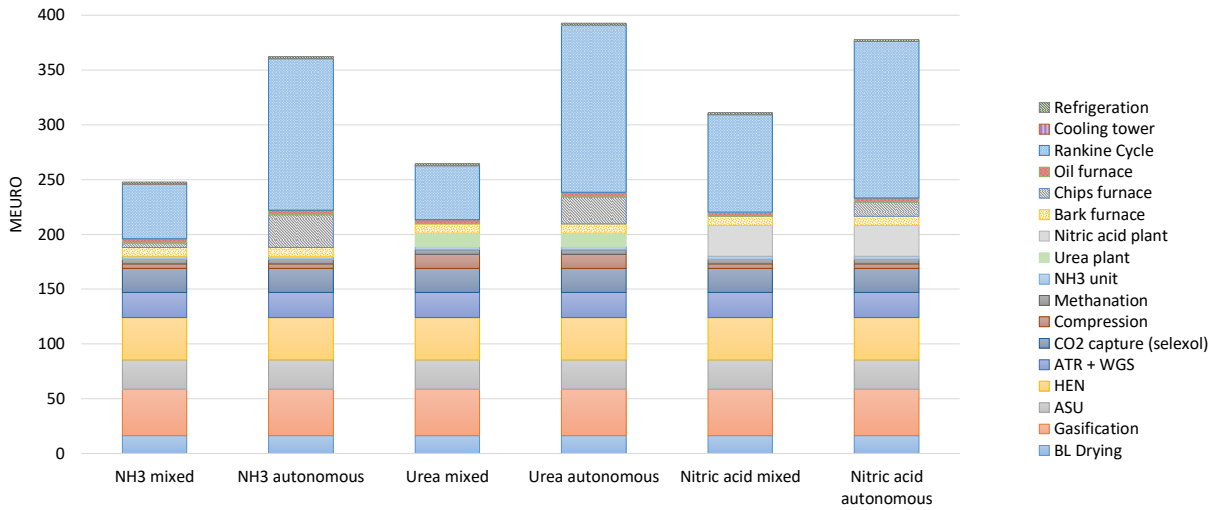

Figure 7.7 Capital expenditure breakdown for the integrated fertilizers plants.

According to Figure 7.8, the ammonia production route with partial electricity import (mixed case in Figure 7.8a) may economically outperform the autonomous setup (Figure 7.8b), depending on the interest rate adopted, for moderate carbon taxations (40-90 EUR/t_{CO2}), nowadays already implemented or planned to be implemented by some countries [176]. The carbon pricing is a measure for economic transformation and recovery, that can improve energy and industrial efficiency, but it still remains politically challenging [176]. On the other hand, for the urea (Figures 7.8c-d) and nitric acid (Figures 7.8e-f) routes, the INPV can achieve positive values for all the carbon taxes evaluated. It can be seen that for the autonomous operation mode, interest rates up to 13% also does not favor to obtain a positive INPV.

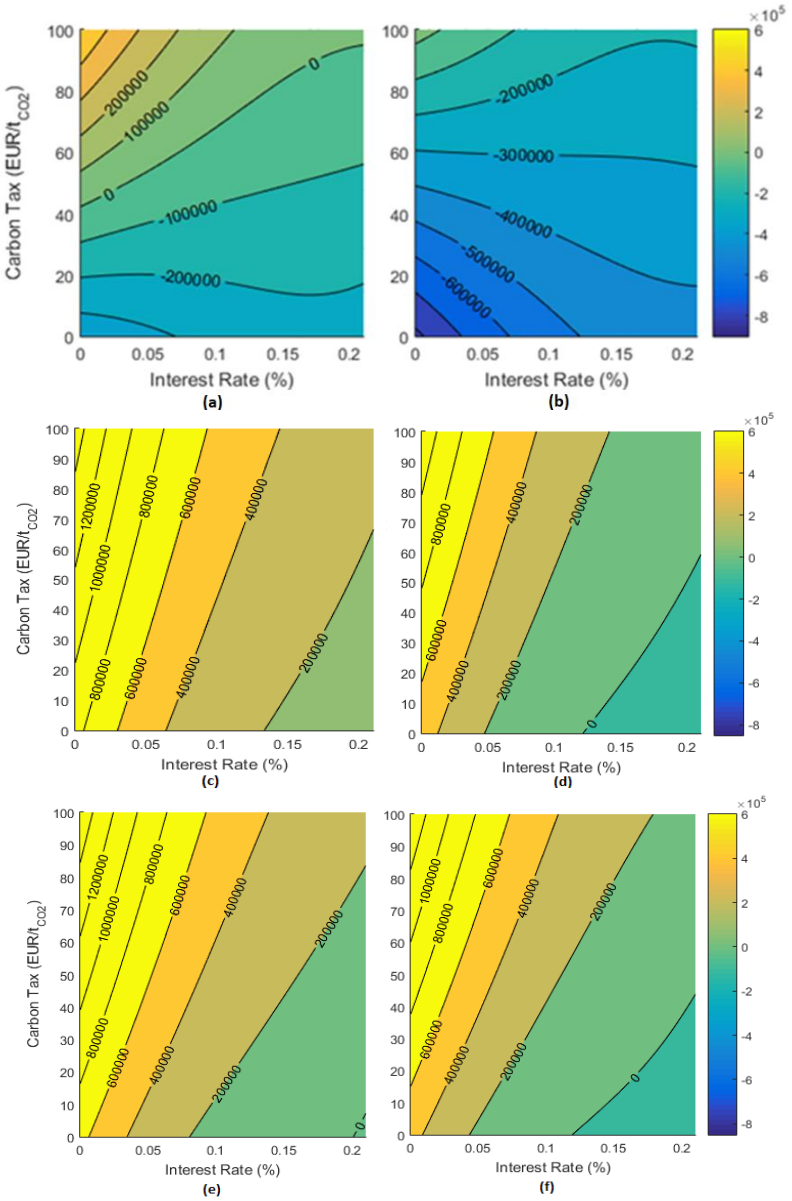

Figure 7.8 Contour plots of INPV (Euro) variation for the integrated kraft pulp process and: Ammonia production under mixed (a) or autonomous (b) operating modes; Urea production under mixed (c) or autonomous (d) operating modes; and Nitric Acid production under mixed (e) or autonomous (f) operating modes.

The heat maps given in Tables 7.5-7.10 summarize the results for each of the integrated fertilizers production obtained for the scenario *i)* DCTIR_SC (see section 3.4.1). Table 7.5 suggests that, for the integrated plant co-producing pulp and ammonia while operating under the mixed mode, and for a region between 60 to 100 EUR/t_{CO2}, there exists a large probability of the INPV being positive, depending on the interest rate adopted. On the other hand, the autonomous mode (Table 7.6), presents relatively unfavorable INPVs, independent of how low interest rates become. As for the urea (Tables 7.7-7.8) and the nitric acid (Tables 7.9-7.10) production, the analysis delivered an even more optimistic scenarios for both operation modes.

Positive INPVs is likely probably to be obtained for all the range of carbon taxes evaluated, depending on the interest rate.

Table 7.5 Probability that INPV is negative (likelihood of loss in %) for scenario DCTIR_SC - ammonia production under the mixed operation mode.

CO_2 tax (EUR/t_{CO2}) → / i (%)	0	10	20	30	40	50	60	70	80	90	100
0%	100.00	100.00	99.90	95.43	63.84	14.94	0.81	0.01	0.00	0.00	0.00
3%	100.00	100.00	100.00	99.56	89.46	44.89	7.41	0.21	0.00	0.00	0.00
6%	100.00	100.00	100.00	100.00	98.59	81.91	34.00	4.64	0.10	0.00	0.00
9%	100.00	100.00	100.00	100.00	99.86	96.60	71.81	26.74	3.46	0.10	0.00
12%	100.00	100.00	100.00	100.00	99.97	99.60	93.54	65.03	22.91	2.70	0.13
15%	100.00	100.00	100.00	100.00	100.00	99.94	99.04	89.60	58.84	19.20	2.31
18%	100.00	100.00	100.00	100.00	100.00	100.00	99.90	97.50	83.99	50.23	15.59
21%	100.00	100.00	100.00	100.00	100.00	100.00	100.00	99.59	96.14	76.60	42.90

Table 7.6 Probability that INPV is negative (likelihood of loss in %) for scenario DCTIR_SC - ammonia production under the autonomous operation mode.

CO_2 tax (EUR/t_{CO2})→ / i (%)	0	10	20	30	40	50	60	70	80	90	100
0%	100.00	100.00	100.00	100.00	100.00	100.00	100.00	99.91	97.26	71.91	22.76
3%	100.00	100.00	100.00	100.00	100.00	100.00	100.00	100.00	99.96	97.39	74.66
6%	100.00	100.00	100.00	100.00	100.00	100.00	100.00	100.00	100.00	99.94	98.41
9%	100.00	100.00	100.00	100.00	100.00	100.00	100.00	100.00	100.00	100.00	100.00
12%	100.00	100.00	100.00	100.00	100.00	100.00	100.00	100.00	100.00	100.00	100.00
15%	100.00	100.00	100.00	100.00	100.00	100.00	100.00	100.00	100.00	100.00	100.00
18%	100.00	100.00	100.00	100.00	100.00	100.00	100.00	100.00	100.00	100.00	100.00
21%	100.00	100.00	100.00	100.00	100.00	100.00	100.00	100.00	100.00	100.00	100.00

Table 7.7 Probability that INPV is negative (likelihood of loss in %) for scenario DCTIR_SC - urea production under the mixed operation mode.

CO_2 tax (EUR/t_{CO2})→ / i (%)	0	10	20	30	40	50	60	70	80	90	100
0%	0.00	0.00	0.00	0.00	0.00	0.00	0.00	0.00	0.00	0.00	0.00
3%	0.00	0.00	0.00	0.00	0.00	0.00	0.00	0.00	0.00	0.00	0.00
6%	0.00	0.00	0.00	0.00	0.00	0.00	0.00	0.00	0.00	0.00	0.00
9%	0.00	0.00	0.00	0.00	0.00	0.00	0.00	0.00	0.00	0.00	0.00
12%	0.03	0.00	0.00	0.00	0.00	0.00	0.00	0.00	0.00	0.00	0.00
15%	0.27	0.06	0.03	0.01	0.00	0.00	0.00	0.00	0.00	0.00	0.00
18%	1.11	0.61	0.17	0.09	0.01	0.00	0.00	0.00	0.00	0.00	0.00
21%	3.47	2.10	0.80	0.27	0.10	0.06	0.00	0.01	0.00	0.00	0.00

Table 7.8 Probability that INPV is negative (likelihood of loss in %) for scenario DCTIR_SC - urea production under the autonomous operation mode.

CO_2 tax (EUR/t_{CO2})→ / i (%)	0	10	20	30	40	50	60	70	80	90	100
0%	0.10	0.01	0.00	0.00	0.00	0.00	0.00	0.00	0.00	0.00	0.00
3%	0.57	0.21	0.04	0.00	0.00	0.00	0.00	0.00	0.00	0.00	0.00
6%	5.13	1.79	0.76	0.26	0.04	0.01	0.00	0.00	0.00	0.00	0.00
9%	20.39	11.70	5.86	2.61	0.73	0.29	0.06	0.01	0.00	0.00	0.00
12%	49.27	35.66	22.13	13.90	6.99	3.20	1.56	0.49	0.13	0.10	0.03
15%	74.10	62.74	48.53	35.40	24.06	13.64	8.14	3.93	1.80	0.81	0.24
18%	90.21	82.20	73.27	61.44	49.10	34.89	25.14	15.11	9.23	5.14	2.23
21%	96.03	93.66	87.89	80.44	72.29	58.97	46.56	35.86	24.94	16.01	9.63

Table 7.9 Probability that INPV is negative (likelihood of loss in %) for scenario DCTIR_SC – nitric acid production under the mixed operation mode.

CO_2 tax (EUR/t_{CO2})→ / i (%)	0	10	20	30	40	50	60	70	80	90	100
0%	0.00	0.00	0.00	0.00	0.00	0.00	0.00	0.00	0.00	0.00	0.00
3%	0.00	0.00	0.00	0.00	0.00	0.00	0.00	0.00	0.00	0.00	0.00
6%	0.07	0.00	0.00	0.00	0.00	0.00	0.00	0.00	0.00	0.00	0.00
9%	0.51	0.06	0.03	0.00	0.00	0.00	0.00	0.00	0.00	0.00	0.00
12%	4.10	1.01	0.30	0.03	0.00	0.00	0.00	0.00	0.00	0.00	0.00
15%	15.49	6.24	1.93	0.34	0.09	0.00	0.00	0.00	0.00	0.00	0.00
18%	33.74	18.17	7.63	2.61	0.77	0.10	0.03	0.00	0.00	0.00	0.00
21%	54.59	35.46	19.79	9.13	3.89	1.34	0.27	0.03	0.00	0.00	0.00

Table 7.10 Probability that INPV is negative (likelihood of loss in %) for scenario DCTIR_SC – nitric acid production under the autonomous operation mode.

CO_2 tax (EUR/t_{CO2})→ / i (%)	0	10	20	30	40	50	60	70	80	90	100
0%	0.00	0.00	0.00	0.00	0.00	0.00	0.00	0.00	0.00	0.00	0.00
3%	0.16	0.00	0.00	0.00	0.00	0.00	0.00	0.00	0.00	0.00	0.00
6%	2.06	0.36	0.07	0.01	0.00	0.00	0.00	0.00	0.00	0.00	0.00
9%	12.39	4.44	0.83	0.16	0.01	0.00	0.00	0.00	0.00	0.00	0.00
12%	39.60	20.50	8.21	2.29	0.51	0.06	0.00	0.00	0.00	0.00	0.00
15%	69.53	48.99	30.19	12.93	4.76	1.37	0.33	0.07	0.03	0.00	0.00
18%	87.39	74.31	56.30	36.56	19.67	8.60	2.94	0.83	0.16	0.06	0.00
21%	95.86	90.26	78.67	63.11	44.10	25.83	12.80	5.31	1.61	0.66	0.09

Meanwhile, the heat map shown in Table 7.11 and in Table 7.12 summarizes the results obtained for scenarios *ii)* LCT_DIR_SC and *iii)* SCTC_DIR, respectively. For both scenarios, similarly to the previous analysis, the integrated chemical plants producing any of the fertilizers while operating under mixed mode presented more favorable results in terms of likelihood of loss, which may contribute for promoting the fertilizers co-production in scenarios with a diversification of the energy inputs and renewable resources. It is important to emphasize that the carbon pricing is an opportunity to drive a sustainable recovery and also finance broader fiscal reforms, that could lead in the achievement of short-term and long-term net zero goals [176].

Table 7.11 Probability that INPV is negative (likelihood of loss in %) as a function of the interest rate for LCT_DIR_SC scenarios.

i (%)	NH_3 mixed	NH_3 auto	Urea mixed	Urea auto	Nitric acid mixed	Nitric acid auto
0%	15.84	100.00	0.00	0.00	0.00	0.00
1%	31.53	100.00	0.00	0.00	0.00	0.00
2%	52.40	100.00	0.00	0.00	0.00	0.00
3%	73.21	100.00	0.00	0.00	0.00	0.00
4%	88.21	100.00	0.00	0.00	0.00	0.00
5%	95.64	100.00	0.00	0.00	0.00	0.00
6%	98.61	100.00	0.00	0.06	0.00	0.00
7%	99.57	100.00	0.00	0.13	0.00	0.01
8%	99.94	100.00	0.00	0.69	0.00	0.04
9%	99.99	100.00	0.00	1.31	0.00	0.14
10%	100.00	100.00	0.00	3.21	0.00	0.66
11%	100.00	100.00	0.00	6.84	0.00	1.79
12%	100.00	100.00	0.00	12.14	0.01	3.64
13%	100.00	100.00	0.00	20.00	0.06	8.64
14%	100.00	100.00	0.00	29.10	0.23	14.87
15%	100.00	100.00	0.06	39.29	0.69	25.94
16%	100.00	100.00	0.03	49.64	1.40	35.74
17%	100.00	100.00	0.17	59.49	2.96	46.87
18%	100.00	100.00	0.30	68.14	4.81	58.29
19%	100.00	100.00	0.56	75.67	8.11	68.79
20%	100.00	100.00	0.91	82.19	12.64	77.49
21%	100.00	100.00	1.56	86.79	18.50	83.21

Table 7.12 Probability that INPV is negative (likelihood of loss in %) as a function of the interest rate for SCTC_DIR scenarios.

i (%)	NH_3 mixed	NH_3 auto	Urea mixed	Urea auto	Nitric acid mixed	Nitric acid auto
0%	20.10	100.00	0.00	0.00	0.00	0.00
1%	28.29	100.00	0.00	0.00	0.00	0.00
2%	37.50	100.00	0.00	0.00	0.00	0.00
3%	47.47	100.00	0.00	0.00	0.00	0.00
4%	58.83	100.00	0.00	0.00	0.00	0.00
5%	69.59	100.00	0.00	0.00	0.00	0.00
6%	78.37	100.00	0.00	0.01	0.00	0.00
7%	86.01	100.00	0.00	0.03	0.00	0.00
8%	90.56	100.00	0.00	0.10	0.00	0.01
9%	94.61	100.00	0.00	0.21	0.00	0.00
10%	96.59	100.00	0.00	0.73	0.00	0.01
11%	98.34	100.00	0.00	1.51	0.00	0.09
12%	99.11	100.00	0.00	3.10	0.00	0.16
13%	99.30	100.00	0.00	6.07	0.00	0.44
14%	99.57	100.00	0.00	10.37	0.00	0.96
15%	99.80	100.00	0.01	15.64	0.01	1.84
16%	99.89	100.00	0.00	21.86	0.11	3.63
17%	99.97	100.00	0.00	29.04	0.14	6.84
18%	100.00	100.00	0.07	36.66	0.23	10.07
19%	100.00	100.00	0.03	44.04	0.56	14.46
20%	100.00	100.00	0.10	53.00	1.01	20.11
21%	100.00	100.00	0.20	59.67	1.89	27.24

7.6 Conclusion

In this work, the upgrade of black liquor from a kraft pulp mill via gasification process in an integrated syngas and different nitrogen fertilizers (i.e., ammonia, urea and nitric acid) production plants are compared with the performance of the conventional conversion route (standalone kraft pulp mill). This approach aims to reduce the amount of non-renewable exergy consumption and net CO_2 emissions, whereas maintains attractive the integrated plant revenues. The combined energy integration and exergy analyses performed allowed spotlighting alternatives that ensure competitive revenues, while maximizing the recovery of the available waste heat exergy. As a result, the exergy efficiencies of the conventional and integrated cases average 40% and 42%, respectively, whereas the overall emission balance varies from 1.97 to -0.79 t_{CO2}/t_{Pulp}, respectively. These negative values point towards the environmental benefits brought about by the production of chemicals through the use of alternative energy sources, such as biomass and electricity. The renewability performance indicator shows that clean electricity import, whether available, may help reducing the extent of the irreversibility and fossil energy resources in the integrated systems, as well as reducing the extended CO_2 emissions. Despite the increased investment cost, due to the complementary value-added CO_2 and fertilizers produced, the operating revenues of the alternative configurations are not be considerably impacted in comparison with the conventional route. In addition, it must be noticed that by defining the extended plant consumption and efficiency concepts, the whole effect of the production process, including the inefficiencies of upstream feedstock supply chain can be evaluated. The results proved to be strongly dependent on the indirect emissions, the energy resources consumed (chips, electricity or black liquor) and the market prices adopted for the resources and products of the integrated plants.

The incremental financial analysis under uncertainty of feedstock costs and carbon taxes allowed to understand the behavior of the integrated systems proposed by considering different market fluctuations. As a result, positive INPVs are achieved when moderate carbon taxes (40-90 EUR/t_{CO2}) are considered for the case of the ammonia production. As for the nitric acid and the urea production, positive INPVs are likely probably in all the range of carbon taxes considered. All in all, even when the systems are subject to linear-increasing or stochastic carbon taxes, the scenario operating under the mixed mode points towards a great potential of decarbonization.

CHAPTER 8: CONCLUDING REMARKS AND SUGGESTIONS FOR FUTURE WORKS

The depletion of the fossil resources has boosted the search for more sustainable industrial and energy processes. Biorefinery technologies offer a great opportunity to expand the portfolio of products of the pulp industry, which has been traditionally based on a monoproduction approach and on the consumption of a large amount of biomass energy resources. The integration of more advanced energy systems, such as mechanical vapor recompression systems, along with entrained flow pressurized gasifiers integrated to different fuels and chemicals production, may help capitalizing on the biorefinery residues, whereas reducing the atmospheric emissions of this industrial sector and also promoting the decarbonization of the supply chains of fossil-based commodities.

Due to its composition and physical properties, the black liquor is a particularly interesting energy feedstock. Although BL combustion is the most typical application in the kraft pulp mills, the BL gasification entails a set of advantages, listed as follows: (i) BL is available in large amounts at the existing pulp and paper mills, rendering it suitable for incremental capacity expansions; (ii) BL is in a liquid form, which allows to be easily pumped and atomized into the pressurized gasifier, transforming it into a fine mist that quickly reacts; (iii) the gasification of the char derived from BL is faster than for any other feedstock, since the inherent inorganics present in its composition (sodium and potassium) act as catalysts; (iv) BL gasification has a potential to reduce greenhouse gas emissions compared with combustion; and (v) BL gasification entails higher overall process efficiency.

This work presented a broad approach for evaluating the co-production of pulp and various chemicals and fuels via black liquor gasification compared with the conventional kraft pulping processes, relying on: (i) the detailed analysis of the simultaneous production of pulp and biofuels; (ii) the implementation of an optimization framework that minimizes energy requirements of the alternative routes proposed; (iii) the consideration of the inefficiencies associated to the different upstream supply chains, and (iv) the use of an incremental financial analysis, which enlightened the influence of the uncertainty related to the feedstock prices and the carbon taxations on the viability of the novel integrated chemical plants.

Figure 8.1 represents the main findings regarding the indicators evaluated and presented in the chapters of this thesis. A first remark is that, due to the specificities of each process, operation mode, market conditions adopted, the relation between the different indicators is not linear, reinforcing the need of this type of study with rigorous simulation

models along with an extensive analysis that takes into account several variables that otherwise are not considered in the early stages of design.

It can be seen from Figure 8.1, that all the mixed cases presented higher efficiencies and renewability performance, except for the nitric acid. The excess of heat coming up from the production of this chemical is used for the internal power generation instead of using other energy resources, which is a less efficient process. As a consequence, the net CO_2 emissions balance has also the lower value, since the indirect emissions are reduced. Thus, there is a tradeoff between higher efficiencies and the importation of different energy resources that come with associated emissions. Despite of this fact, the net CO_2 emissions balance for all the integrated plants studied was negative, ranging between -0.56 to -1.09 t_{CO2}/t_{Pulp}, whereas for the conventional case it achieved 0.26 t_{CO2}/t_{Pulp}. Together with the incremental financial analysis performed to anticipate the future carbon taxation scenarios, the indicators assessed pointed that the integrated biorefineries approach can be a pathway for boosting the bioeconomy and decarbonizing the production of important commodities.

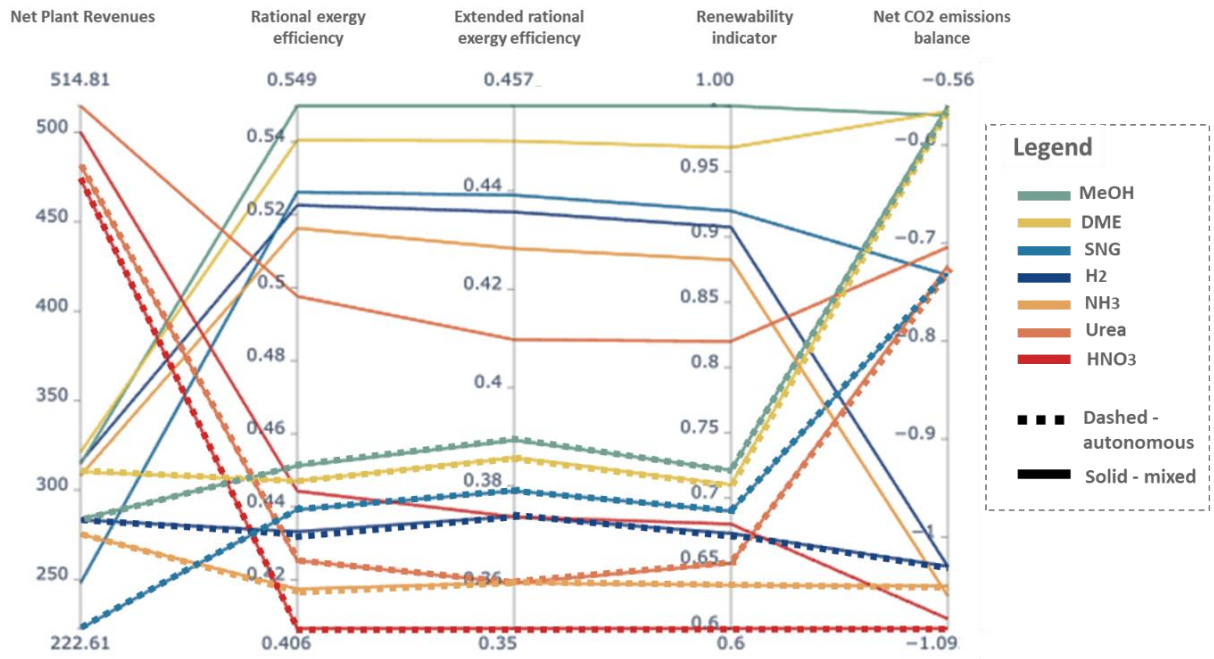

Figure 8.1 Parallel coordinates representationn of the main indicators evaluated in this work.

Aiming to obtain a ranking of the alternative fuels and chemicals with its respective operation modes evaluated in this work, the TOPSIS method is applied. For this analysis, it was considered the same weight (0.2) for each of the indicators displayed in Figure 8.1. Depending on the goal of the decision-maker, this weight can be changed favouring different objectives.

The ranking with the resulted calculation is shown in Table 8.1. It can be observed that hydrogen, ammonia and synthetic natural gas operating under the mixed mode presented the best performance, followed by the same chemicals operating under the autonomous mode. On the other hand, nitric acid and urea occupied the last positions. For all the chemicals, the mixed setup outperformed the autonomous operation mode, which is in compliance with the results presents along the chapters, reinforcing the benefits of the diversification of the energy inputs and also the favourable Brazilian context to the implementation of biorefineries.

Table 8.1 Results of the ranking obtained with the use of the TOPSIS method.

Fuels and chemicals	Results	Rank
H_2 Mixed	0.75	1
NH_3 Mixed	0.73	2
SNG Mixed	0.68	3
H_2 Autonomous	0.61	4
NH_3 Autonomous	0.59	5
SNG Autonomous	0.56	6
MeOH Mixed	0.56	7
DME Mixed	0.54	8
MeOH Autonomous	0.46	9
DME Autonomous	0.42	10
HNO_3 Mixed	0.41	11
HNO_3 Autonomous	0.40	12
Urea Mixed	0.29	13
Urea Autonomous	0.18	14

Suggestions for future works

Certainly, this thesis can be improved and extended, deriving other analyses that can be used as a support to the decision-makers on implementing novel technologies and exploring the biorefinery concept (specially in Brazil, due to its underexploited biomass potential), envisioning the decarbonization of important commodities. Some suggestions for future works are:

- The evaluation of different biomass resources, such as the sugarcane bagasse, applying the biorefinery concept for integrating the fuels and chemicals production considering the novel approaches proposed in this thesis, taking into account the combined exergy and energy integration analysis, the upstream supply chain inefficiencies, and the

uncertainty by using the incremental financial analysis under different market conditions.

- The analysis of multi-time problems considering seasonal demands and storage systems, such as seasonal electricity storage and power-to-gas approach (discussed in appendix D). The CO_2 captured in the gas purification unit in the studied scenarios can be liquefied, compressed, commercialized, injected or stored. Moreover, the CO_2 can be also converted into other chemicals and fuels, such as CH_4, that can also be stored or consumed, depending on the demands.
- The inclusion of new technologies in the biorefinery platform that can widen the product portfolio, and the evaluation of the combination of other technologies for hydrogen production, such as electrolyzers, that may lead to interesting scenarios. This also involves the inclusion of different sources of renewable energy, such as solar and wind, aiming to increase the productivity.
- The application of supply chain analysis: studies considering the biomass supply chain optimization, logistics and seasonal availability, are important to assess the potential for implementing biorefineries.
- The generation of surrogate models for replacing the simulation systems and utilization of those models for evaluating the tradeoffs between conflicting objectives in multiobjective optimization approaches.

PAPERS PUBLISHED AND CONFERENCES ATTENDED

- ***Papers published in international journals.***

DOMINGOS, M. E. G. R., FLOREZ-ORREGO, D., TELES DOS SANTOS, M., OLIVEIRA JR, S. & MARÉCHAL, F. (2022). Techno-economic and environmental analysis of methanol and dimethyl ether production from syngas in a kraft pulp process. **Computers & Chemical Engineering**, 163, 107810.

DOMINGOS, M. E. G. R., FLOREZ-ORREGO, D., TELES DOS SANTOS, M., VELASQUEZ, H. & OLIVEIRA JR, S. (2021). Exergy and environmental analysis of black liquor upgrading gasification in an integrated kraft pulp and ammonia production plant. **International Journal of Exergy**, 35(1), 35-65.

- ***Papers submitted to international journals.***

DOMINGOS, M. E. G. R., FLOREZ-ORREGO, D., TELES DOS SANTOS, M., OLIVEIRA JR, S. & MARÉCHAL, F. Multi-time integration approach for combined pulp and ammonia production and seasonal CO_2 management. *(under review).*

- ***Technical contributions to the proceedings of international conferences.***

DOMINGOS, M. E. G. R., FLOREZ-ORREGO, D., OLIVEIRA JR, S., MARÉCHAL, F., TELES DOS SANTOS, M., (2022). Integrated production of chemicals and fuels in the pulp industry: techno-economic and environmental analysis of black liquor gasification-based processes. **2022 AIChE Annual Meeting,** 13-18 November 2022, United States.

DOMINGOS, M. E. G. R.; FLOREZ-ORREGO, D. A.; SHARMA, S.; SANTOS, M. T.;. MARÉCHAL, F. (2022). Integrated production of urea and nitric acid in the pulp industry: techno-economic and environmental analysis of black liquor gasification-based processes. In: 7th International Conference on Contemporary Problems of Thermal Engineering (**CPOTE 2022**), 20-23 September 2022, Poland.

DOMINGOS, M. E. G. R., FLOREZ-ORREGO, D., TELES DOS SANTOS, M., OLIVEIRA JR, S., MARÉCHAL, F. (2022). Incremental financial analysis of black liquor upgraded gasification in integrated kraft pulp and ammonia production plants under uncertainty of feedstock costs and carbon taxes. **Computer Aided Chemical Engineering**. Vol 51, p. 1315-1320. Elsevier.

DOMINGOS, M. E. G. R., SHARMA, S., FLOREZ-ORREGO, D. A., HEMRLE, J., MARÉCHAL, F., SANTOS, M. T. Efficient exploration of Pareto-optimal designs of a carbon capture process using surrogate models. In: 35th International Conference on Efficiency, Cost, Optimization, Simulation and Environmental Impact of Energy Systems, 2022, Copenhagen. **Proceedings of ECOS 2022**, 2022. p. 931-942.

DOMINGOS, M. E. G. R., FLOREZ-ORREGO, D., TELES DOS SANTOS, M. & OLIVEIRA JR, S. (2021). Comparative assessment of black liquor upgraded gasification in integrated kraft pulp, methanol and dimethyl ether production plants. In **Computer Aided Chemical Engineering.** Vol. 50, pp. 25-30. Elsevier.

DOMINGOS, M. E. G. R., **,** FLÓREZ-ORREGO, D, TELES DOS SANTOS, M., OLIVEIRA JR, S., Exergy and Environmental Analysis of Black Liquor Upgraded Gasification in an Integrated Kraft Pulp and Ammonia Production Plant. 32th International Conference on Efficiency, Cost, Optimization, Simulation and Environmental Impact of Energy Systems, **ECOS 2019**, Wroclaw, Poland, June 23 – 28, 2019. ISBN 978-83-61506-51-5

DOMINGOS, M. E. G. R., FLÓREZ-ORREGO, D, TELES DOS SANTOS, M., OLIVEIRA JR, S. Process integration enhancement via black liquor gasification in the Kraft pulp industry. I Brazilian Congress on Process Systems Engineering – **PSE-BR 2019**, Rio de Janeiro, May 20 – 22, 2019.

- ***Book chapters***

DOMINGOS, M. E. G. R., FLOREZ-ORREGO, D., NOGUEIRA NAKASHIMA, R., TELES DOS SANTOS, M., WON PARK, S. & OLIVEIRA JR, S. Chapter 23. Syngas from black liquor, Volume 1, Section II: Syngas Production Sources**. In book:** Advances in

Synthesis Gas Book Series: Methods, Technologies and Applications. 1ed., 2022, v. 1, p. 475-500.

FLOREZ-ORREGO, D. A., **DOMINGOS, M. E. G. R**., NAKASHIMA, R. N., SANTOS, M. T., OLIVEIRA JUNIOR, S. Chapter 2. Syngas purification by common solvents, Section I: Absorption techniques for Syngas Purification. **In book**: Advances in Synthesis Gas Book Series: Methods, Technologies and Applications. 1ed., 2022, v. 2, p. 27-72.

FLOREZ-ORREGO, D. A., NAKASHIMA, R. N., **DOMINGOS, M. E. G. R**., SANTOS, M. T., OLIVEIRA JUNIOR, S. Chapter 3. Ammonia production from syngas, Section I: Chemicals Production from Syngas. **In book**: Advances in Synthesis Gas: Methods, Technologies and Applications. 1ed., 2022, v. 3, p. 45-92.

NAKASHIMA, R. N., FLOREZ-ORREGO, D. A., **DOMINGOS, M. E. G. R**., SANTOS, M. T., OLIVEIRA JUNIOR, S. Modelling, simulation and optimization of methane production processes. **In book:** Advances in Synthesis Gas: Methods, Technologies and Applications Syngas Process Modelling and Apparatus Simulation. 1ed., 2022, v. 4, p. 345-380.

REFERENCES

[1] IEA; EPE. Pulp and paper industry in Brasil and in the world: an overview. 2022. Available at: < https://www.iea.org/news/iea-deepens-cooperation-with-brazil-with-new-benchmarking-report-on-the-pulp-and-paper-sector >. Accessed in: 01 Mar 2022.

[2] IBÁ. Relatório anual IBÁ 2021. 2021. Available at: < https://www.iba.org/publicacoes/relatorios >. Accessed in: 17 Sep 2022.

[3] HORA, A.; RIBEIRO, L.; MENDES, R. Papel e celulose. 2018. Available at: < https://web.bndes.gov.br/bib/jspui/bitstream/1408/16222/1/PRCapLiv214161_papel%26celulose_%20compl_P.pdf >. Accessed in: 01 Sep 2020.

[4] IEA. Tracking pulp and paper 2020. Paris, 2020. Available at: < https://www.iea.org/reports/tracking-pulp-and-paper-2020 >. Accessed in: 13 Aug 2020.

[5] _____. Tracking industry 2020. Paris, 2020. Available at: < https://www.iea.org/reports/tracking-industry-2020 >. Accessed in: 13 Aug 2020.

[6] MÄKI, E. et al. Drivers and barriers in retrofitting pulp and paper industry with bioenergy for more efficient production of liquid, solid and gaseous biofuels: A review. **Biomass and Bioenergy,** v. 148, n. 106036, p. 1-19, 2021.

[7] BRINCKERHOFF, W. P.; DNV, G. L. **Industrial decarbonisation & energy efficiency roadmaps to 2050: cross-sector summary**. London, UK, p.31. 2015

[8] MOYA, J.; PAVEL, C. **Energy efficiency and GHG emissions: prospective scenarios for the pulp and paper industry**. European Union. Luxembourg, p.73. 2018. (978-92-79-89119-9)

[9] MONGKHONSIRI, G. et al. Integration of the biorefinery concept for the development of sustainable processes for pulp and paper industry. **Computers & Chemical Engineering,** v. 119, p. 70-84, 2018.

[10] FRATTINI, D. et al. A system approach in energy evaluation of different renewable energies sources integration in ammonia production plants. **Renewable Energy,** v. 99, p. 472-482, 2016.

[11] FLÓREZ-ORREGO, D.; SILVA, J. A. M.; OLIVEIRA JR, S. Renewable and non-renewable exergy cost and specific CO2 emission of electricity generation: The Brazilian case. **Energy Conversion and Management,** v. 85, p. 619-629, 2014.

[12] GILBERT, P. et al. Assessing economically viable carbon reductions for the production of ammonia from biomass gasification. **Journal of Cleaner Production,** v. 64, p. 581-589, 2014.

[13] NETL. Gasification background: markets for gasification. 2014. Available at: < https://www.netl.doe.gov/research/coal/energy-systems/gasification/gasifipedia/markets >. Accessed in: 29 Oct 2018.

[14] FLÓREZ-ORREGO, D.; MARÉCHAL, F.; OLIVEIRA JR, S. Comparative exergy and economic assessment of fossil and biomass-based routes for ammonia production. **Energy Conversion and Management,** v. 194, p. 22-36, 2019.

[15] AKBARI, M.; OYEDUN, A. O.; KUMAR, A. Ammonia production from black liquor gasification and co-gasification with pulp and waste sludges: a techno-economic assessment. **Energy,** v. 151, p. 133-143, 2018.

[16] DARMAWAN, A. et al. Black liquor-based hydrogen and power co-production: combination of supercritical water gasification and syngas chemical looping. **Applied Energy,** v. 252, n. 113446, p. 1-11, 2019.

[17] FERNÁNDEZ-DACOSTA, C. et al. Potential and challenges of low-carbon energy options: Comparative assessment of alternative fuels for the transport sector. **Applied energy,** v. 236, p. 590-606, 2019.

[18] IPCC. The evidence is clear: the time for action is now. We can halve emissions by 2030., 2022. Available at: < https://www.ipcc.ch/2022/04/04/ipcc-ar6-wgiii-pressrelease/ >. Accessed in: 17 Sep 2022.

[19] IEA. **Black liquor gasification - summary and conclusions from the IEA Bioenergy ExCo54 Workshop**. International Energy Agency. Rotorua, New Zealand, p.1-12. 2007. (9780081000090)

[20] BÖRJESSON, M.; AHLGREN, E. **Pulp and paper industry - energy technology system analysis oprogram - ETSAP, IEA ETSAP - Technology Brief I07 - May 2015**. International Energy Agency. 2015

[21] ANDERSSON, J.; LUNDGREN, J. Techno-economic analysis of ammonia production via integrated biomass gasification. **Applied Energy,** v. 130, p. 484-490, 2014.

[22] FOELKEL, C. The eucalyptus wood for pulp production - understanding the construction of the indicator of specific consumption of wood for kraft pulp production [In Portuguese]. **Eucalyptus Online Book & Newsletter**, 2017.

[23] MORAES, F. D. A. B. **Model for the evaluation of the specific consumption of wood and energy input in the process of pulp and paper manufacturing [In portuguese].** 2011. 209 p. Dissertation (Master in Production Engineering) Production Engineering Department, Araraquara University Center, Araraquara - SP.

[24] RURAL TECHNOLOGY INITIATIVE. Chapter 8. Pulp and paper. p. 1-10, 2016. Available at: < http://www.ruraltech.org/projects/conversions/briggs_conversions/briggs_ch08/chapter08_combined.pdf >. Accessed in: 17 Sep 2018.

[25] NAQVI, M.; YAN, J.; DAHLQUIST, E. Black liquor gasification integrated in pulp and paper mills: A critical review. **Bioresource Technology,** v. 101, n. 21, p. 8001-8015, 2010.

[26] BACHMANN, D. L. Berchmarking of pulp mill processes. **O Papel,** v. 8, p. 66-70, 2009.

[27] DARMAWAN, A. et al. Energy-efficient recovery of black liquor through gasification and syngas chemical looping. **Applied Energy,** v. 219, p. 290-298, 2018.

[28] GONG, M. Exergy analysis of a pulp and paper mill. **International journal of energy research,** v. 29, n. 1, p. 79-93, 2005.

[29] TRAN, H.; VAKKILAINNEN, E. K. The kraft chemical recovery process. **Tappi Kraft Recovery Short Course**, p. 1-8, 2008. Available at: < https://www.tappi.org/content/events/08kros/manuscripts/1-1.pdf >. Accessed in: 01 Mar 2018.

[30] ONARHEIM, K. **Market and regulatory issues related to Bio-CCUS**. IEA. Belgium: International Energy Agency**:** 20 p. 2018.

[31] ONARHEIM, K. et al. **Techno-economic evaluation of retrofitting CCS in a market pulp mill and an integrated pulp and board mill**. UK: IEAGHG**:** 300 p. 2016.

[32] BELL, G. et al. IEA Bioenergy Task42 Biorefining. 2014. Available at: < http://www.iea-bioenergy.task42-biorefineries.com/en/ieabiorefinery.htm >. Accessed in: 01 Mar 2018.

[33] MARTIN, C. Biorrefinaria industrial. **O Papel: revista mensal de tecnologia em celulose e papel,** v. 72, n. 3, p. 26-32, 2011.

[34] IBÁ. Report 2017. 2017. Available at: < https://iba.org/images/shared/Biblioteca/IBA_RelatorioAnual2017.pdf >. Accessed in: 01 Jul 2020.

[35] HAMAGUCHI, M.; CARDOSO, M.; VAKKILAINEN, E. Alternative technologies for biofuels production in kraft pulp mills—Potential and prospects. **Energies,** v. 5, n. 7, p. 2288-2309, 2012.

[36] BAJPAI, P. **Biorefinery in the pulp and paper industry**. 1. UK, Netherlands, USA: Academic press, Elsevier Inc., 2013. 103 p. ISBN 978-0-12-409508-3.

[37] VALMET. First LignoBoost plants producing large volumes of kraft lignin to the market place. 2020. Available at: < https://www.valmet.com/media/articles/up-and-running/new-technology/PEERS1stLignoBoostPlants/ >. Accessed in: 15 Sep 2020.

[38] RAGAUSKAS, A. J. et al. Lignin valorization: improving lignin processing in the biorefinery. **Science,** v. 344, n. 6185, 2014.

[39] IEA. Innovation gaps: technology report — May 2019. 2019. Available at: < https://www.iea.org/reports/innovation-gaps/industry >. Accessed in: 13 Aug 2020.

[40] BARUAH, D.; BARUAH, D. Modeling of biomass gasification: A review. **Renewable and Sustainable Energy Reviews,** v. 39, p. 806-815, 2014.

[41] PATRICK, K.; SIEDEL, B. Gasification edges closer to commercial reality with three New NA mill startups. **Paper Age,** v. 10, p. 30-33, 2003.

[42] AZZONE, E.; MORINI, M.; PINELLI, M. Development of an equilibrium model for the simulation of thermochemical gasification and application to agricultural residues. **Renewable energy,** v. 46, p. 248-254, 2012.

[43] BEHESHTI, S.; GHASSEMI, H.; SHAHSAVAN-MARKADEH, R. Process simulation of biomass gasification in a bubbling fluidized bed reactor. **Energy Conversion and Management,** v. 94, p. 345-352, 2015.

[44] MUTLU, Ö. Ç.; ZENG, T. Challenges and opportunities of modeling biomass gasification in Aspen Plus: A review. **Chemical Engineering & Technology,** v. 43, n. 9, p. 1674-1689, 2020.

[45] FERREIRA, S. et al. A holistic review on biomass gasification modified equilibrium models. **Energies,** v. 12, n. 160, p. 1-31, 2019.

[46] KIM, C.-H. et al. Global trends and prospects of black liquor as bioenergy. **Journal of Korea TAPPI** v. 51, n. 5, p. 3-15, 2019.

[47] BACKMAN, R.; FREDERICK, W.; HUPA, M. Basic studies on black-liquor pyrolysis and char gasification. **Bioresource technology,** v. 46, n. 1-2, p. 153-158, 1993.

[48] HUANG, H.-J.; RAMASWAMY, S. Thermodynamic analysis of black liquor steam gasification. **BioResources,** v. 6, n. 3, p. 3210-3230, 2011.

[49] LARSSON, A. et al. Influence of black liquor variability, combustion, and gasification process variables and inaccuracies in thermochemical data on equilibrium modeling results. **Energy and Fuels,** v. 20, n. 1, p. 359-363, 2006.

[50] LI, J.; VAN HEININGEN, A. Reaction kinetics of gasification of black liquor char. **The Canadian Journal of Chemical Engineering,** v. 67, n. 4, p. 693-697, 1989.

[51] LI, J.; VAN HEININGEN, A. R. Kinetics of carbon dioxide gasification of fast pyrolysis black liquor char. **Industrial & engineering chemistry research,** v. 29, n. 9, p. 1776-1785, 1990.

[52] LI, J.; VAN HEININGEN, A. Kinetics of gasification of black liquor char by steam. **Industrial & engineering chemistry research,** v. 30, n. 7, p. 1594-1601, 1991.

[53] WHITTY, K. **Gasification of black liquor char with steam at elevated pressures**. Fuel and Energy Abstracts. 1**:** 14 p. 1996.

[54] MARKLUND, M. **Pressurized Entrained-flow High Temperature Black Liquor Gasification: CFD Based Reactor Scale-up Method and Spray Burner Characterization.** 2006. 211 p. Thesis (Doctor of Philosophy). Department of Applied Physics and Mechanical Engineering, Lulea University of Technology, Lulea, Sweden.

[55] MARKLUND, M.; TEGMAN, R.; GEBART, R. CFD modelling of black liquor gasification: Identification of important model parameters. **Fuel,** v. 86, n. 12-13, p. 1918-1926, 2007.

[56] PETTERSSON, K. **Black liquor gasification-based biorefineries–determining factors for economic performance and CO2 emission balances**. 2011. 106 p. Thesis (Doctor of Philosophy). Department of Energy and Environment, Chalmers University of Technology, Goterborg, Sweden.

[57] BAJPAI, P. **Biermann's Handbook of Pulp and Paper**. 3rd ed. Netherlands, UK, USA: Elsevier, 2018. 649 p. ISBN 978-0-12-814240-0.

[58] BAJPAI, P. **Pulp and paper industry: energy conservation**. Netherlands, UK, USA: Elsevier, 2016. 268 p. ISBN 978-0-12-803411-8.

[59] BAJPAI, P. **Black liquor gasification**. UK, USA: Elsevier, 2014. ISBN 978-0-08-100009-0.

[60] CONSONNI, S.; KATOFSKY, R. E.; LARSON, E. D. A gasification-based biorefinery for the pulp and paper industry. **Chemical Engineering Research and Design,** v. 87, n. 9, p. 1293-1317, 2009.

[61] NÄSHOLM, A.-S.; WESTERMARK, M. Energy studies of different cogeneration systems for black liquor gasification. **Energy Conversion and Management,** v. 38, n. 15-17, p. 1655-1663, 2002.

[62] LARSON, E. D. et al. **A cost-benefit assessment of gasification-based biorefining in the kraft pulp and paper industry**. Princeton University. United States, p.145. 2007

[63] EKBOM, T. et al. **Technical and commercial feasibility study of black liquor gasification with methanol/DME production as motor fuels for automotive uses-BLGMF**. Stockholm, Sweden, p.194. 2003

[64] ANDERSSON, E. H., S. System analysis of hydrogen production from gasified black liquor. **Energy,** v. 31, n. 15, p. 3426-3434, 2006.

[65] NAQVI, M.; YAN, J.; FRÖLING, M. Bio-refinery system of DME or CH4 production from black liquor gasification in pulp mills. **Bioresource technology,** v. 101, n. 3, p. 937-944, 2010.

[66] YOO, M. et al. **OSMOSE Lua: a unified approach to energy systems integration with life cycle assessment**. 12th International conference PSE 2015 and 25th International conference ESCAPE 2015. Copenhagen, Denmark 2015.

[67] GRANACHER, J. et al. **Potential of hydrothermal black liquor gasification integrated in pulp production plant**. 32nd international conference on Efficiency, Cost, Optimization, Simulation and Environmental impact of energy systems. Wrocław, Poland, June 23-28: Silesian University of Technology**:** 2299-2309 p. 2019.

[68] PETTERSSON, K.; HARVEY, S. CO2 emission balances for different black liquor gasification biorefinery concepts for production of electricity or second-generation liquid biofuels. **Energy,** v. 35, n. 2, p. 1101-1106, 2010.

[69] YUAN, Z. et al. State-of-the-art and progress in the optimization-based simultaneous design and control for chemical processes. **AIChE Journal,** v. 58, n. 6, p. 1640-1659, 2012.

[70] KOKOSSIS, A. C. et al. Systematic screening of multiple processing paths in biorefineries: the ABC (assessing biomass to chemicals) project and its potential to build process synthesis capabilities. In: (Ed.). **Integrated biorefineries. Design, analysis and optimization**. Boca Raton: CRC Press, Taylor & Francis Group, 2013. p.37-58. ISBN 9780429165771.

[71] MARTIN, M.; GROSSMANN, I. E. On the systematic synthesis of sustainable biorefineries. **Industrial & Engineering Chemistry Research,** v. 52, n. 9, p. 3044-3064, 2013.

[72] HENDRY, J.; RUDD, D.; SEADER, J. Synthesis in the design of chemical processes. **AIChE Journal,** v. 19, n. 1, p. 1-15, 1973.

[73] GROSSMANN, I. E. Mixed-integer programming approach for the synthesis of integrated process flowsheets. **Computers & chemical engineering,** v. 9, n. 5, p. 463-482, 1985.

[74] SEFERLIS, P.; GEORGIADIS, M. C. **The integration of process design and control**. 1st ed. Netherlands, USA, UK: Elsevier, 2004. ISBN 0-444-51557-7.

[75] DOUGLAS, J. M. **Conceptual design of chemical processes**. Singapore: McGraw-Hill New York, 1988. 601 p. ISBN 0-07-100195-6.

[76] LINNHOFF, B., HINDMARSH, E. The pinch design method for heat exchanger networks. **Chemical Engineering Science,** v. 38, n. 5, p. 745-763, 1983.

[77] GROSSMANN, I. E.; CABALLERO, J. A.; YEOMANS, H. Mathematical programming approaches to the synthesis of chemical process systems. **Korean Journal of Chemical Engineering,** v. 16, n. 4, p. 407-426, 1999.

[78] RYAN, J.; HEAVEY, C. Process modeling for simulation. **Computers in industry,** v. 57, n. 5, p. 437-450, 2006.

[79] KLEMEŠ, J. J.; KRAVANJA, Z. Forty years of heat integration: pinch analysis (PA) and mathematical programming (MP). **Current Opinion in Chemical Engineering,** v. 2, n. 4, p. 461-474, 2013.

[80] IBRAHIM, T. K. et al. A comprehensive review on the exergy analysis of combined cycle power plants. **Renewable and Sustainable Energy Reviews,** v. 90, p. 835-850, 2018.

[81] BAKHTIARI, B.; PYLKKANEN, V.; RETSINA, T. Pinch analysis-an essential tool for energy optimization of pulp and paper mills. **O PAPEL,** v. 76, n. 4, p. 51-54, 2015.

[82] KEMP, I. C. **Pinch analysis and process integration: a user guide on process integration for the efficient use of energy**. 2nd ed. UK, USA: Elsevier, 2007. 415 p. ISBN 978 0 75068 260 2.

[83] MARECHAL, F.; KALITVENTZEFF, B. Targeting the minimum cost of energy requirements: a new graphical technique for evaluating the integration of utility systems. **Computers & chemical engineering,** v. 20, p. 225-230, 1996.

[84] SZARGUT, J.; MORRIS, D.; STEWARD, F. **Exergy analysis of thermal, chemical, and metallurgical processes**. New York: Hemisphere Publishing Corporation, 1988.

[85] KOTAS, T. J. **The exergy method of thermal plant analysis**. 2nd ed. Malabar, Florida: Krieger Publishing Company, 1995. ISBN 1483100367.

[86] VELÁSQUEZ, H. et al. Exergo-environmental evaluation of liquid biofuel production processes. **Energy,** v. 54, p. 97-103, 2013.

[87] EL-SAYED, Y. M. Application of exergy to design. **Energy Conversion and Management,** v. 43, n. 9-12, p. 1165-1185, 2002.

[88] LOMBARDO, G. et al. Exergy and pinch analyses of kraft pulp mill. In: (Ed.). **Energy Efficiency in Process Technology**: Springer, 1993. p.1268-1276.

[89] SANTOS, M. T. D. **Análise exergética dos sistemas térmicos em um processo de produção de celulose e papel**. 2007. 190 p. Dissertação (Mestrado em Engenharia Química). Departamento de Engenharia Química, Universidade de Sao Paulo, São Paulo.

[90] PASSINI, R. J. **Análise exergética de um sistema de recuperação química de uma fábrica de papel e celulose**. 2017. 167 p. Dissertação (Mestrado em Engenharia Mecânica). Departamento de Engenharia Mecânica, Universidade de Itajubá, Itajubá, MG.

[91] CAO, C. et al. Evaluation of effect of evaporation on supercritical water gasification of black liquor by energy and exergy analysis. **International Journal of Hydrogen Energy,** v. 43, n. 30, p. 13788-13797, 2018.

[92] DARMAWAN, A. et al. Enhanced process integration of black liquor evaporation , gasification , and combined cycle. **Applied Energy,** v. 204, p. 1035-1042, 2017.

[93] FERREIRA, E. T. D. F.; BALESTIERI, J. A. P. Black liquor gasification combined cycle with CO2 capture - Technical and economic analysis. **Applied Thermal Engineering,** v. 75, p. 371-383, 2015.

[94] RAHMAN, M.; YANG, W. **Thermodynamic analysis of high temperature steam gasification of black liquor ofr power generation**. International Conference on Mechanical Engineering 2009 (ICME 2009) Dhaka, Bangladesh**:** 6 p. 2009.

[95] ASPENTECH. **Aspen Plus V8.8**. Bedford, United States: Aspen technology Inc. 2015.

[96] _____. **Aspen Physical Property System - Physical Property Methods V7.3**. Bedford, United States: Aspen technology Inc. 2011.

[97] FLÓREZ-ORREGO, D. et al. Combined exergy analysis, energy integration and optimization of syngas and ammonia production plants: A cogeneration and syngas purification perspective. **Journal of Cleaner Production,** v. 244, n. 118647, 2020.

[98] KISS, A. A. et al. Novel efficient process for methanol synthesis by CO2 hydrogenation. **Chemical engineering journal,** v. 284, p. 260-269, 2016.

[99] DELLAVEDOVA, M. et al. On the gasification of biomass: Data analysis and regressions. **Process Safety and Environmental Protection,** v. 90, n. 3, p. 246-254, 2012.

[100] PIO, D. T.; TARELHO, L. A. C.; MATOS, M. A. A. Characteristics of the gas produced during biomass direct gasification in an autothermal pilot-scale bubbling fluidized bed reactor. **Energy,** v. 120, p. 915-928, 2017.

[101] BOLOY, R. A. M. et al. Ecological impacts from syngas burning in internal combustion engine: Technical and economic aspects. **Renewable and Sustainable Energy Reviews,** v. 15, n. 9, p. 5194-5201, 2011.

[102] MACEDO, J. C. F. **Thermal and environmental analysis of the primary sludge from pulp and paper making in biomass boiler on the grid [In Portuguese]**. 2006. 196 p. Disssertation (Master in Mechanical Engineering). Department of Mechanical Engineering, Federal University of Itajubá, Itajubá.

[103] GAVRILESCU, D. Energy from biomass in pulp and paper mills. **Environmental Engineering and Management Journal,** v. 7, n. 5, p. 537-546, 2008.

[104] THEIS, M. et al. Fouling tendency of ash resulting from burning mixtures of biofuels. Part 2: Deposit chemistry. **Fuel,** v. 85, n. 14-15, p. 1992-2001, 2006.

[105] HARRIS, A. T. et al. Towards zero emission pulp and paper production : the BioRegional MiniMill. **Journal of Cleaner Production,** v. 16, p. 1971-1979, 2008.

[106] GLOBAL COMBUSTION SYSTEMS. Oil Fuel Properties. 2018. Available at: < http://www.globalcombustion.com/oil-fuel-properties/ >. Accessed in: 20 Dec 2018.

[107] DEMIRBAS, A. Theoretical heating values and impacts of pure compounds and fuels. **Energy Sources, Part A: Recovery, Utilization and Environmental Effects,** v. 28, n. 5, p. 459-467, 2006.

[108] DARMAWAN, A. et al. Enhanced process integration of entrained flow gasification and combined cycle: modeling and simulation using Aspen Plus. **Energy Procedia,** v. 105, p. 303-308, 2017.

[109] SOFRASER. Black liquor recovery (concentration for combustion). 2013. Available at: < https://www.sofraser.com/images/images/applications/InlineControl_Combustion_BlackLiquor_Customer.pdf >. Accessed in: 7 Oct 2018.

[110] VAKKILAINEN, E. K. **Kraft recovery boilers - high dry solids firing:** 254 p. 2006.

[111] UNIDO. Evaluation of technologies on recovery of black liquor chemicals for small and medium size pulp mills using non-wood fibrous raw materials. 1996. ISSN 9992146737. Available at: < https://open.unido.org/api/documents/4808393/download/EVALUATION >. Accessed in: 5 Aug 2018.

[112] HUET, M. **Valorisation hydrothermales de la liqueur noire à des fins énergétiques et de chimie verte**. 2015. 229 p. Thesis (PhD in Engineering). Department de Génie des procédés, Université Grenoble Alpes, Grenoble.

[113] PUIG-GAMERO, M. et al. Three integrated process simulation using aspen plus®: Pine gasification, syngas cleaning and methanol synthesis. **Energy conversion and management,** v. 177, p. 416-427, 2018.

[114] SILVA, F. C. N. et al. Comparative assessment of advanced power generation and carbon sequestration plants on offshore petroleum platforms. **Energy,** v. 203, n. 117737, p. 1-19, 2020.

[115] APPL, M. Ullmann's encyclopedia of industrial chemistry. In: (Ed.). Weinheim: Wiley-VCH Verlag GmbH & Co., v.11, 2012. cap. 2,

[116] FLÓREZ-ORREGO, D. A. **Process synthesis and optimization of syngas and ammonia production in nitrogen fertilizers complexes: energy, energy integration and CO2 emissions assessment**. 2018. 269 p. Thesis (Doctor in Science of Mechanical Engineering). Department of Mechanical Engineering, University of São Paulo, São Paulo.

[117] KIDNAY, A. J.; PARRISH, W. **Fundamentals of natural gas processing**. 1st ed. Boca Raton: CRC Press, 2006. 464 p. ISBN 9780429135644.

[118] DYMENT, J.; WATANASIRI, S. **Acid gas cleaning using DEPG physical solvents: validation with experimental and plant data**. Bedford, MA, USA. 2015

[119] TOUNTAS, A. A. et al. Towards solar methanol: past, present, and future. **Advanced Science,** v. 6, n. 1801903, p. 1-52, 2019.

[120] TOPSØE, H. From solid fuels to substitute natural gas (SNG) using TREMP Topsøe Recycle Energy-efficient Methanation Process. 2009. Available at: < https://www.netl.doe.gov/sites/default/files/netl-file/tremp-2009.pdf >.

[121] COSTA, N. et al. Simulation and analysis of a hydrogen generation unit. **Brazilian Journal of Petroleum and Gas,** v. 12, n. 3, 2018.

[122] VARGAS-MIRA, A.; ZULUAGA-GARCÍA, C.; GONZÁLEZ-DELGADO, A. N. D. A technical and environmental evaluation of six routes for industrial hydrogen production from empty palm fruit bunches. **ACS omega,** v. 4, n. 13, p. 15457-15470, 2019.

[123] ORTIZ, F. G. et al. Methanol synthesis from syngas obtained by supercritical water reforming of glycerol. **Fuel,** v. 105, p. 739-751, 2013.

[124] NAKASHIMA, R. N.; FLÓREZ-ORREGO, D.; OLIVEIRA JUNIOR, S. Integrated anaerobic digestion and gasification processes for upgrade of ethanol biorefinery residues. **Journal of Power Technologies,** v. 99, n. 2, p. 104-114, 2019.

[125] ANTONINI, C. et al. Hydrogen production from natural gas and biomethane with carbon capture and storage–A techno-environmental analysis. **Sustainable Energy & Fuels,** v. 4, p. 2967–2986, 2020.

[126] OTT, J. et al. Methanol. In: (Ed.). **Ullmann's Encyclopedia of Industrial Chemistry; Wiley-VCH Verlag GmbH & Co**. Weinheim, Germany: KGaA, 2012. p.27.

[127] LEONZIO, G. Mathematical modeling of a methanol reactor by using different kinetic models. **Journal of Industrial and Engineering Chemistry,** v. 85, p. 130-140, 2020.

[128] NIMKAR, S. C.; MEWADA, R. K.; ROSEN, M. A. Exergy and exergoeconomic analyses of thermally coupled reactors for methanol synthesis. **International Journal of Hydrogen Energy,** v. 42, n. 47, p. 28113-28127, 2017.

[129] LÜCKING, L. **Methanol production from syngas: process modelling and design utilising biomass gasification and integrating hydrogen supply**. 2017. 113 p. Dissertation (Master of Science). Department of Electrical Engineering, Mathematics and Computer Science, Delft University of Technology, Netherlands.

[130] YANG, Y. et al. Mechanistic studies of methanol synthesis over Cu from CO/CO2/H2/H2O mixtures: The source of C in methanol and the role of water. **Journal of catalysis,** v. 298, p. 10-17, 2013.

[131] AL-MALAH, K. I. **Aspen plus: Chemical Engineering Applications**. New Jersey: John Wiley & Sons, 2017. ISBN 9781119293613.

[132] BANDIERA, J.; NACCACHE, C. Kinetics of methanol dehydration on dealuminated H-mordenite: Model with acid and basic active centres. **Applied catalysis,** v. 69, n. 1, p. 139-148, 1991.

[133] LUYBEN, W. L. **Principles and case studies of simultaneous design**. John Wiley & Sons, 2011. ISBN 1118001648.

[134] INTERNATIONAL DME ASSOCIATION. DME standardization, regulation and safety recommendations. 2011. Available at: < http://aboutdme.org/aboutdme/files/cclibraryfiles/filename/000000001971/7asiandme_ida_bollon.pdf >. Accessed in: 01 Jul 21.

[135] ASPENTECH. **Aspen Plus Urea Synthesis Loop Model**. Aspen technology Inc. Bedford, United States. 2008

[136] GRANDE, C. A. et al. Process Intensification in Nitric Acid Plants by Catalytic Oxidation of Nitric Oxide. **Industrial & Engineering Chemistry Research,** v. 57, n. 31, p. 10180-10186, 2018.

[137] CHANNIWALA, S. A.; PARIKH, P. P. A unified correlation for estimating HHV of solid, liquid and gaseous fuels. **Fuel,** v. 81, n. 8, p. 1051-1063, 2002.

[138] VELÁSQUEZ, H. I.; COLORADO, A. R.; JÚNIOR, S. D. O. Ethanol production from banana fruit and its lignocellulosic residues: Exergy and renewability analysis. **International Journal of Thermodynamics,** v. 12, n. 3, p. 155-162, 2009.

[139] FLÓREZ-ORREGO, D. et al. Renewable and non-renewable exergy costs and CO2 emissions in the production of fuels for Brazilian transportation sector. **Energy,** v. 88, p. 18-36, 2015.

[140] FLÓREZ-ORREGO, D. A. **Thermodynamic and Environmental Comparison (CO2) emissions of the route of the production and end use of vehicle fuels derived from Petroleum, Natural gas, Biofuels, Hydrogen and Electricity [In Portuguese]**. 2014. 229 p. Dissertation (Master in Mechanical Engineering). Department of Mechanical Engineering, University of São Paulo, São Paulo.

[141] KALITVENTZEFF, B.; MARÉCHAL, F.; CLOSON, H. Better solutions for process sustainability through better insight in process energy integration. **Applied Thermal Engineering,** v. 21, n. 13-14, p. 1349-1368, 2001.

[142] INGHAM, A. Reducing the carbon intensity of methanol for use as a transport fuel. **Johnson Matthey Technology Review,** v. 61, n. 4, p. 297-307, 2017.

[143] MARÉCHAL, F.; KALITVENTZEFF, B. Process integration: selection of the optimal utility system. **Computers & Chemical Engineering,** v. 22, n. 98, p. 149-156, 1998.

[144] AEA. Excel Calculation_for_Wood_Fuel_Parameters_16_EN KLIMAACTIV. Vienna, 2008. Available at: < https://www.klimaaktiv.at/erneuerbare/energieholz/werkzeuge-und-hilfsmittel/kenndatenkalkulation.html >. Accessed in: 19 jan 2019.

[145] CELULOSE ONLINE. Preço da celulose cresce em ritmo mais lento. 2018. Available at: < https://www.celuloseonline.com.br/preco-da-celulose-cresce-em-ritmo-mais-lento/ >. Accessed in: 02 Dec 2018.

[146] EUROSTAT. Natural gas price statistics. April 2022 2022. Available at: < https://ec.europa.eu/eurostat/statistics-explained/index.php?title=Natural_gas_price_statistics#Natural_gas_prices_for_non-household_consumers >. Accessed in: 12 Aug 2022.

147 BSE ENGINEERING. Small scale methanol plants a chance for re-industrialisation. International Methanol Conference, 2017. Available at: < http://www.methanol.org/wp-content/uploads/2018/04/Small-Scale-Methanol-Plants-Christian-Schweitzer_bse-Engineering.pdf >. Accessed in: 25 May 2020.

148 FASIHI, M.; BREYER, C. **Synthetic methanol and dimethyl ether production based on hybrid PV-wind power plants**. 11th International Renewable Energy Storage Conference. Düsseldorf 2017.

149 QUINN, R. DTN retail fertilizer trends. 2022. Available at: < https://www.dtnpf.com/agriculture/web/ag/crops/article/2022/06/01/stagnant-retail-fertilizer-prices-2 >. Accessed in: 15 Apr 2022.

150 CEIC. Market price montlhy. 2022. Available at: < https://www.ceicdata.com/en/china/china-petroleum--chemical-industry-association-petrochemical-price-inorganic-chemical-material/cn-market-price-monthly-avg-inorganic-chemical-material-nitric-acid-98-or-above#:~:text=Chemical%20Industry%20Federation-,China%20Market%20Price%3A%20Monthly%20Avg%3A%20Inorganic%20Chemical%20Material%3A%20Nitric,RMB%2FTon%20for%20Jan%202022. >. Accessed in: 15 Apr 2022.

151 FLOREZ-ORREGO, D., SHARMA, S., OLIVEIRA JR, S., MARECHAL, F. **Combined Exergy Analysis and Energy Integration for Design Optimization of Nitrogen Fertilizer Plants**. 30th International Conference on Efficiency, Cost, Optimization, Simulation and Environmental Impact of Energy Systems, ECOS 2017, July 2 - 6 San Diego, United States of America: San Diego State University, 2017. 200 p.

152 COUPER, J. et al. **Chemical process equipment** Third Edition. Boston: Butterworth-Heinemann, 2012. ISBN 978-0-12-396959-0. Disponível em: < http://www.sciencedirect.com/science/article/pii/B9780123969590000318 >.

153 TURTON, R. et al. **Analysis, synthesis, and design of chemical processes**. 3rd ed. Pearson Education Inc., 2018. ISBN 0134177401.

154 RØSSLAND, K. **Feasibility of using Rankine power cycles for utilisation of medium to low temperature heat sources in the industry**. 2016. 94 p. Dissertation (Master of Energy and Environmental Engineering). Department of Energy and Process Engineering, Norwegian University of Science and Technology, Trondheim, Gjøvik.

155 THERMOFLOW. Thermoflow software. 2021. Available at: < https://www.thermoflow.com/ >. Accessed in: 01 Nov 2021.

156 FLEITER, T. et al. Mapping and analyses of the current and future (2020-2030) heating/cooling fuel deployment (fossil/renewables). Work package 2: Assessment of the technologies for the year 2012. 2016.

157 KANGAS, P.; KAIJALUOTO, S.; MÄÄTTÄNEN, M. Evaluation of future pulp mill concepts–Reference model of a modern Nordic kraft pulp mill. **Nordic Pulp & Paper Research Journal,** v. 29, n. 4, p. 620-634, 2014.

158 BLANK, L.; TARQUIN, A. **Engineering Economy**. 7th ed. El Paso, Texas: Mc Graw Hill, 2011. ISBN 978-0-07-337630-1.

[159] DARMAWAN, A.; AZIZ, M.; TOKIMATSU, K. Proposed integrated system from black liquor. In: (Ed.). **Innovative Energy Conversion from Biomass Waste**, 2022. p.107-148.

[160] CONSONNI, S.; LARSON, E. D.; KATOFSKY, R. **An Assessment of Black Liquor Gasification Combined Cycles: Part A—Technological Issues and Performance Comparisons**. Turbo Expo: Power for Land, Sea, and Air, 2004. 1-14 p.

[161] BERGLIN, N.; BERNTSSON, T. CHP in the pulp industry using black liquor gasification: thermodynamic analysis. **Applied thermal engineering,** v. 18, n. 11, p. 947-961, 1998.

[162] JAFRI, Y. et al. Performance of a pilot-scale entrained-flow black liquor gasifier. **Energy & Fuels,** v. 30, n. 4, p. 3175-3185, 2016.

[163] STATISTA. Forecast capital expenditure of a conventional natural gas combustion turbine power plant in the United States from 2022 to 2050. 2022. Available at: < https://www.statista.com/statistics/243704/capital-costs-of-a-typical-us-gas-turbine-power-plant/ >. Accessed in: 15 Oct 2022.

[164] PELLEGRINI, L. F.; DE OLIVEIRA JUNIOR, S. Combined production of sugar, ethanol and electricity: Thermoeconomic and environmental analysis and optimization. **Energy,** v. 36, n. 6, p. 3704-3715, 2011.

[165] BINDER, M. et al. Hydrogen from biomass gasification. **IEA Bioenergy: task 33**, p. 1-82, 2018.

[166] GASSNER, M.; MARÉCHAL, F. Thermo-economic optimisation of the integration of electrolysis in synthetic natural gas production from wood. **Energy,** v. 33, n. 2, p. 189-198, 2008.

[167] GASSNER, M.; MARÉCHAL, F. Thermo-economic optimisation of the polygeneration of synthetic natural gas (SNG), power and heat from lignocellulosic biomass by gasification and methanation. **Energy & Environmental Science,** v. 5, n. 2, p. 5768-5789, 2012.

[168] GASSNER, M.; MARÉCHAL, F. Thermo-economic process model for thermochemical production of Synthetic Natural Gas (SNG) from lignocellulosic biomass. **Biomass and bioenergy,** v. 33, n. 11, p. 1587-1604, 2009.

[169] HARO, P.; JOHNSSON, F.; THUNMAN, H. Improved syngas processing for enhanced Bio-SNG production: A techno-economic assessment. **Energy,** v. 101, p. 380-389, 2016.

[170] IEA. Russian supplies to global energy markets. 2022. Available at: < https://www.iea.org/reports/russian-supplies-to-global-energy-markets >. Accessed in: 18 Aug 2022.

[171] NAQVI, M.; YAN, J.; DAHLQUIST, E. Synthetic gas production from dry black liquor gasification process using direct causticization with CO2 capture. **Applied Energy,** v. 97, p. 49-55, 2012.

[172] D'APRILE, P. et al. **How the European Union could achieve net-zero emissions at net-zero cost**. Chicago, IL, USA. 2020

[173] MESFUN, S.; TOFFOLO, A. Optimization of process integration in a Kraft pulp and paper mill–Evaporation train and CHP system. **Applied energy,** v. 107, p. 98-110, 2013.

[174] VELÁSQUEZ, H.; COLORADO, A. R.; OLIVEIRA JR, S. Ethanol production from banana fruit and its lignocellulosic residues: Exergy and renewability analysis. **International Journal of Thermodynamics,** v. 12, n. 3, p. 155-162, 2009.

[175] WORLD BANK. Carbon pricing dashboard. 2021. Available at: < https://carbonpricingdashboard.worldbank.org/map_data >. Accessed in: 13 Dec 2021.

[176] _____. State and trends of carbon pricing 2022. Washington DC, 2022. Available at: < https://openknowledge.worldbank.org/handle/10986/37455 >. Accessed in: 30 Oct 2022.

[177] LEONZIO, G. State of art and perspectives about the production of methanol, dimethyl ether and syngas by carbon dioxide hydrogenation. **Journal of CO2 Utilization,** v. 27, p. 326-354, 2018.

[178] MEVAWALA, C.; JIANG, Y.; BHATTACHARYYA, D. Plant-wide modeling and analysis of the shale gas to dimethyl ether (DME) process via direct and indirect synthesis routes. **Applied Energy,** v. 204, p. 163-180, 2017.

[179] YANG, S. et al. Biomass-to-methanol by dual-stage entrained flow gasification: design and techno-economic analysis based on system modeling. **Journal of cleaner production,** v. 205, p. 364-374, 2018.

[180] CARVALHO, L. et al. Methanol production via black liquor co-gasification with expanded raw material base–Techno-economic assessment. **Applied energy,** v. 225, p. 570-584, 2018. ISSN 0306-2619.

[181] HÄGGSTRÖM, C. et al. Catalytic methanol synthesis via black liquor gasification. **Fuel processing technology,** v. 94, n. 1, p. 10-15, 2012.

[182] FORNELL, R.; BERNTSSON, T.; ÅSBLAD, A. Techno-economic analysis of a kraft pulp-mill-based biorefinery producing both ethanol and dimethyl ether. **Energy,** v. 50, p. 83-92, 2013. ISSN 0360-5442.

[183] PETTERSSON, K.; HARVEY, S. Comparison of black liquor gasification with other pulping biorefinery concepts–Systems analysis of economic performance and CO2 emissions. **Energy,** v. 37, n. 1, p. 136-153, 2012.

[184] DOMINGOS, M. E. G. R. et al. Exergy and environmental analysis of black liquor upgrading gasification in an integrated kraft pulp and ammonia production plant. **International Journal of Exergy,** v. 34, 2021.

[185] VAN RENS, G. et al. Performance and exergy analysis of biomass-to-fuel plants producing methanol, dimethylether or hydrogen. **Biomass and Bioenergy,** v. 35, p. S145-S154, 2011.

[186] PELLEGRINI, L. F.; DE OLIVEIRA JÚNIOR, S.; BURBANO, J. C. Supercritical steam cycles and biomass integrated gasification combined cycles for sugarcane mills. **Energy,** v. 35, n. 2, p. 1172-1180, 2010.

[187] WBG. **State and trends of carbon pricing 2020**. World bank Group. Washington, DC. 2020

188 MONGE, C. Colombia puts a tax on carbon. **Conservation finance network, Yale Center for Business and Environment, and the Conservation Fund**, 2018. Available at: < https://www.conservationfinancenetwork.org/2018/11/27/colombia-puts-tax-on-carbon >. Accessed in: 01 Oct 2021.

189 IEA. **World energy outlook 2019**. International Energy Agency. Paris: November 2019. 2019

190 YARA. Yara fertilizer industry handbook. 2018. Available at: < https://www.yara.com/siteassets/investors/057-reports-and-presentations/other/2018/fertilizer-industry-handbook-2018-with-notes.pdf/ >. Accessed in: 2 Nov 2020.

191 IEA. **Ammonia technology roadmap: towards more sustainable nitrogen fertiliser production**. International Energy Agency, p.168. 2021

192 ORTIZ, P. A. S.; MACIEL FILHO, R.; POSADA, J. Mass and heat integration in ethanol production mills for enhanced process efficiency and exergy-based renewability performance. **Processes,** v. 7, n. 670, p. 1-31, 2019.

193 TAILLON, J.; HORVATH, A.; OKSMAN, A. Replacement of fossil fuel with biomass in pulp mill lime kilns. **O Papel,** v. 79, n. 3, p. 85-89, 2018.

194 KUPARINEN, K.; VAKKILAINEN, E. Green pulp mill: renewable alternatives to fossil fuels in lime kiln operations. **BioResources,** v. 12, n. 2, p. 4031-4048, 2017.

195 IEA. Global energy review: CO2 emissions in 2021. 2022. Available at: < https://www.iea.org/reports/global-energy-review-co2-emissions-in-2021-2 >. Accessed in: 14 Mar 2022.

196 _____. Global energy review 2021. 2021. Available at: < https://www.iea.org/reports/global-energy-review-2021/co2-emissions >. Accessed in: 14 Mar 2022.

197 ROGELJ, J. et al. Mitigation pathways compatible with 1.5 C in the context of sustainable development. In: (Ed.). **Global warming of 1.5 C**: Intergovernmental Panel on Climate Change, 2018. p.93-174.

198 DOMINGOS, M. E. G. R. et al. Comparative assessment of black liquor upgraded gasification in integrated kraft pulp, methanol and dimethyl ether production plants. In: (Ed.). **Computer Aided Chemical Engineering**: Elsevier, v.50, 2021. p.25-30.

199 ANDREASEN, A. Optimisation of carbon capture from flue gas from a Waste-to-Energy plant using surrogate modelling and global optimisation. **Oil & Gas Science and Technology–Revue d'IFP Energies nouvelles,** v. 76, n. 55, p. 1-11, 2021.

200 YAN, Y. H. et al. Harnessing the power of machine learning for carbon capture, utilisation, and storage (CCUS)–a state-of-the-art review. **Energy & Environmental Science,** v. 14, p. 6122-6157, 2021.

201 CHAN, V.; CHAN, C. Learning from a carbon dioxide capture system dataset: Application of the piecewise neural network algorithm. **Petroleum,** v. 3, n. 1, p. 56-67, 2017.

[202] SIPÖCZ, N.; TOBIESEN, F. A.; ASSADI, M. The use of artificial neural network models for CO2 capture plants. **Applied Energy,** v. 88, n. 7, p. 2368-2376, 2011.

[203] LI, F. et al. Modelling of a post-combustion CO2 capture process using neural networks. **Fuel,** v. 151, p. 156-163, 2015.

[204] PLESU, V. et al. Surrogate model for carbon dioxide equilibrium absorption using aqueous monoethanolamine. **Chemical Engineering Transactions,** v. 70, p. 919-924, 2018.

[205] ZHOU, Q. et al. A statistical analysis of the carbon dioxide capture process. **International Journal of Greenhouse Gas Control,** v. 3, n. 5, p. 535-544, 2009.

[206] XUE, B. et al. A comparative study of MEA and DEA for post-combustion CO2 capture with different process configurations. **International Journal of Coal Science & Technology,** v. 4, n. 1, p. 15-24, 2017.

[207] FLÓREZ-ORREGO, D., OLIVEIRA JUNIOR, S. On the efficiency, exergy costs and CO2 emission cost allocation for an integrated syngas and ammonia production plant. **Energy,** v. 117, Part 2, p. 341-360, 2016.

[208] LEUNG, D. Y. C., CARAMANNA, G., MAROTO-VALER, M. M. An overview of current status of carbon dioxide capture and storage technologies. **Renewable and Sustainable Energy Reviews,** v. 39, p. 426-443, 2014.

[209] DOW. **Gas Sweetening - The Dow Chemical Company. Form No. 170-01395**. The Dow Chemical Company. 1998

[210] BASHEER, I. A.; HAJMEER, M. Artificial neural networks: fundamentals, computing, design, and application. **Journal of microbiological methods,** v. 43, n. 1, p. 3-31, 2000.

[211] SONG, C. et al. Tri-reforming of methane over Ni catalysts for CO2 conversion to syngas with desired H2/CO ratios using flue gas of power plants without CO2 separation. **Studies in Surface Science and Catalysis,** v. 153, p. 315-322, 2004.

[212] KOHL, A. L.; NIELSEN, R. **Gas purification**. Elsevier, 1997. ISBN 0080507204.

[213] CHEMCAD. Power plant carbon capture with CHEMCAD. rev. 031109. Technical Articles. **Engineering advanced**, 2009. Available at: < http://www.chemstations.com/content/documents/Technical_Articles/Power_Plant_Carbon_Capture_with_CHEMCAD.pdf >. Accessed in: 12 Oct 2014.

[214] HASAN, S.; ABBAS, A. J.; NASR, G. G. Improving the carbon capture efficiency for gas power plants through amine-based absorbents. **Sustainability,** v. 13, n. 1, p. 72, 2020.

[215] ALWOSHEEL, A.; VAN CRANENBURGH, S.; CHORUS, C. Is your dataset big enough? Sample size requirements when using artificial neural networks for discrete choice analysis. **Journal of choice modelling,** v. 28, p. 167-182, 2018.

[216] GARUD, S. S. et al. Evaluating smart sampling for constructing multidimensional surrogate models. **Computers & Chemical Engineering,** v. 108, p. 276-288, 2018.

[217] MANGALAPALLY, H. et al. Pilot plant experimental studies of post combustion CO2 capture by reactive absorption with MEA and new solvents. **Energy Procedia,** v. 1, n. 1, p. 963-970, 2009.

[218] RODRÍGUEZ, N.; MUSSATI, S.; SCENNA, N. Optimization of post-combustion CO2 process using DEA–MDEA mixtures. **Chemical engineering research and design,** v. 89, n. 9, p. 1763-1773, 2011.

[219] DYSON, D. C., SIMON, J. M. Kinetic Expression with Diffusion Correction for Ammonia Synthesis on Industrial Catalyst. **Industrial & Engineering Chemistry Fundamentals,** v. 7, n. 4, p. 605-610, 1968.

[220] GILLESPIE, L., BEATTIE, J. A. The thermodynamic treatment of chemical equilibria in systems composed of real gases. I. An approximate equation for the mass action function applied to the existing data on the Haber equilibrium. **Physical Review,** v. 36, n. 4, p. 743-753, 1930.

[221] LARSON, E. D.; CONSONNI, S.; KREUTZ, T. G. Preliminary economics of black liquor gasifier/gas turbine cogeneration at pulp and paper mills. **J. Eng. Gas Turbines Power,** v. 122, n. 2, p. 255-261, 2000.

[222] TOCK, L. **Thermo-environomic optimisation of fuel decarbonisation alternative processes for hydrogen and power production**. 2013. 235 p. Thesis (Doctor in Science). Department of Mechanical Engineering, École Polytechnic Fédérale de Lausanne, Suisse.

[223] WILLIAMS, R. H. et al. Methanol and hydrogen from biomass for transportation. **Energy for Sustainable Development,** v. 1, n. 5, p. 18-34, 1995.

[224] HAMELINCK, C. N.; FAAIJ, A. P. Future prospects for production of methanol and hydrogen from biomass. **Journal of Power sources,** v. 111, n. 1, p. 1-22, 2002.

[225] HOLMGREN, K. **Investment cost estimates for gasification-based biofuel production systems**. IVL Swedish Environmental Research Institute. Stockholm, Sweden, p.25. 2015

[226] HAMELINCK, C. N. et al. Production of FT transportation fuels from biomass; technical options, process analysis and optimisation, and development potential. **Energy,** v. 29, n. 11, p. 1743-1771, 2004.

[227] ZHANG, H. et al. Techno-economic comparison of 100% renewable urea production processes. **Applied Energy,** v. 284, n. 116401, p. 1-15, 2021.

[228] PETERS, M. S.; TIMMERHAUS, K. D.; WEST, R. E. **Plant design and economics for chemical engineers**. McGraw-hill New York, 2003.

[229] TELINI, R. O.; FLÓREZ-ORREGO, D.; OLIVEIRA JUNIOR, S. Techno-economic and environmental assessment of ammonia production from residual bagasse gasification: a decarbonization pathway for nitrogen fertilizers. **Frontiers Energy Research,** v. 10, n. 881263, p. 1-15, 2022.

[230] PETER, S. C. Reduction of CO2 to chemicals and fuels: a solution to global warming and energy crisis. **ACS Energy Letters,** v. 3, n. 7, p. 1557-1561, 2018.

[231] CASTELLANI, B. et al. Flue gas treatment by power-to-gas integration for methane and ammonia synthesis–Energy and environmental analysis. **Energy Conversion and Management,** v. 171, p. 626-634, 2018.

[232] VANDEWALLE, J.; BRUNINX, K.; D'HAESELEER, W. Effects of large-scale power to gas conversion on the power, gas and carbon sectors and their interactions. **Energy Conversion and Management,** v. 94, p. 28-39, 2015.

[233] ZENG, Q. et al. Steady-state analysis of the integrated natural gas and electric power system with bi-directional energy conversion. **Applied Energy,** v. 184, p. 1483-1492, 2016.

[234] JPI URBAN EUROPE. **Strategic research and innovation agenda 2.0**. Vienna, p.1-25. 2019

[235] TRADING ECONOMICS. United States - Producer price index by commodity: lumber and wood products: wood chips, excluding field chips. 2022. Available at: < https://tradingeconomics.com/united-states/producer-price-index-by-commodity-for-lumber-and-wood-products-wood-chips-except-field-chips-fed-data.html >. Accessed in: 01 Jun 2022.

[236] STATISTICS AUSTRIA. Energy prices, taxes. 2018. Available at: < https://www.statistik.at/en/statistics/energy-and-environment/energy/energy-prices-taxes >. Accessed in: 01 Jun 2022.

[237] DOMINGOS, M. E. G. R. et al. Techno-economic and environmental analysis of methanol and dimethyl ether production from syngas in a kraft pulp process. **Computers & Chemical Engineering,** v. 163, n. 107810, p. 1-18, 2022.

[238] DOMINGOS, M. E. G. R. et al. Incremental financial analysis of black liquor upgraded gasification in integrated kraft pulp and ammonia production plants under uncertainty of feedstock costs and carbon taxes. In: (Ed.). **Computer Aided Chemical Engineering**: Elsevier, v.51, 2022. p.1315-1320.

[239] BIROL, F. The future of hydrogen: seizing today's opportunities. **IEA Report prepared for the G,** v. 20, 2019.

[240] BAIER, J.; SCHNEIDER, G.; HEEL, A. A cost estimation for CO2 reduction and reuse by methanation from cement industry sources in Switzerland. **Frontiers in Energy Research**, p. 5, 2018.

[241] PANJESHAHI, M.; ATAEI, A. Application of an environmentally optimum cooling water system design in water and energy conservation. **International Journal of Environmental Science & Technology,** v. 5, n. 2, p. 251-262, 2008.

[242] FLÓREZ-ORREGO, D. et al. Centralized power generation with carbon capture on decommissioned offshore petroleum platforms. **Energy Conversion and Management,** v. 252, n. 115110, p. 1-19, 2022.

[243] FLOREZ-ORREGO, D. et al. **High temperature heat pumps integration in industrial separation and drying processes**. 35th International Conference on Efficiency, Cost, Optimization, Simulation and Environmental Impact of Energy Systems - ECOS 2022. Copenhagen 2022.

[244] THEMA, M.; BAUER, F.; STERNER, M. Power-to-gas: electrolysis and methanation status review. **Renewable and Sustainable Energy Reviews,** v. 112, p. 775-787, 2019.

APPENDIX A: Efficient exploration of Pareto-optimal designs of a carbon capture process using surrogate models

Abstract: Complex industrial processes are often modelled using flow-sheeting software, wherein any change in inputs may require significant computation time. For studying the integration of complex processes into industrial clusters and explore synergies among them, computationally inexpensive surrogate models proved to be a smart solution. This study develops surrogate models for the carbon capture technology using amine absorption considering flue gas as feed. A wide range of CO_2 concentration and moisture content in feed stream, as well as the recirculation flow of the solvent are used as input to simulate the process flowsheet in Aspen® HYSYS software. The artificial neural network-based surrogate is developed to predict the process designs and operations, and error-based performance metrics are used to compare the simulation and the predicted responses (using the surrogates). As a result, the main parameters/variables of the simulation model could be predicted by the surrogate model with a normalized root-mean-square-error below 0.104. Furthermore, for a fixed CO_2 concentration feed, the design and operation of carbon capture plants are optimized to explore trade-offs between CO_2 recovery and reboiler duty. The solutions are represented as a Pareto-optimal front, and each solution represents a particular process design and operating condition. In this way, the surrogate model can be used to explore the Pareto-optimal front by allowing the user to select a solution on the Pareto-optimal front and the developed surrogate determining the corresponding design and operating conditions.

1. Introduction

According to the International Energy Agency (IEA), the global CO_2 emissions from fuel combustion and industrial processes increased around 6% from 2020 to 2021, reaching the highest historical annual level [195]. Flue gases are produced by coal and natural gas power plants, waste incineration plants, internal combustion engines, and boilers, which contribute significantly to CO_2 emissions into environment. For example, the CO_2 emissions from natural gas combustion accounts for 22% of global CO_2 emissions [196]. In this regard, the carbon capture processes are needed in many decarbonization scenarios, either to neutralize emissions from sources with no mitigating measures or to achieve net negative emissions [184; 197; 198].

Due to the complex governing phenomena in absorption, the modelling and simulation of CO_2 capture process can be a cumbersome task, and their solution can be very time consuming and difficult to converge [199]. Moreover, the flue gases contain variable concentrations of CO_2, which affects the design and operation of the carbon capture process. To tackle these issues, several studies have proposed the creation of surrogate models for carbon capture processes [199; 200; 201; 202]. It is crucial to have a reliable method to estimate CO_2 removal rate, as well as the power and energy consumptions associated to the process, provided some known operating conditions. The surrogate modelling technique allows to represent complex systems by generating a simplified mathematical representation based on sampled input-output data, and identifying links between those data that may not be easily identifiable. By these means, it is possible to reduce computational cost by avoiding the repetitive solution of the complete rigorous models. Thus, the surrogate modelling is a powerful tool for studying complex, nonlinear systems.

Li et al (2015) used bootstrap aggregated neural networks to predict the CO_2 capture rate and CO_2 purity by using as inputs the inlet flue gas flow rate; the CO_2 concentration, pressure and temperature of flue gas; the lean solvent flow rate, the MEA concentration and the temperature of lean solvent. The results pointed to accurate predictions for unseen validation data [203]. Sipocz et al (2011) used artificial neural network (ANN) models to develop a surrogate for CO_2 capture plant using MEA (Monoethanolamine) as absorbent. The authors obtained a maximum error equal to 3.1% for the specific reboiler duty prediction, whereas the solvent rich loading and the amount of CO_2 captured had a maximum error lower than 2.8% and 0.17%, respectively [202]. Chan and Chan used a piece-wise linear ANN to investigate and predict the performance of an amine-based CO_2 capture process. They found that the steam flow rate through reboiler, the reboiler pressure and the CO_2 concentration in the flue gas are the most significant parameters governing the CO_2 capture rate [201]. Plesu et al. investigated a surrogate model for the MEA vapour-liquid equilibrium of CO_2 using experimental data and multiple linear regression models [204]. The surrogate model by multiple linear regression was able to represent the CO_2 capture system, however in a limited range of operating parameters. Zhou et al studied the relationships among the parameters involved in the amine-based post combustion CO_2 capture process by applying multiple regression technique. Notwithstanding, their model is not able to represent the non-linear relationship between the parameters [205].

In this work, a surrogate model for a diethanolamine-based CO_2 capture process is built on data generated from Aspen HYSYS model/simulations. Using this commercial software, the process design and operation data for a wide range of CO_2 concentration and

moisture content in feed is generated. Next, an ANN routine in MATLAB is used for developing the surrogate model. The model is validated against several independent simulation tests. As it will be shown, the surrogate model for chemical CO_2 absorption can accurately predict the process design and operation for any CO_2 concentration and moisture in feed. In the second part of this study, for a fixed CO_2 concentration and moisture content in the feed, the design and operation of the carbon capture plant are optimized to explore the trade-off between the CO_2 recovery and the reboiler duty (desorber). The trade-off solutions are collectively represented as Pareto-optimal front, and each solution on the Pareto-optimal front has a distinct process design and operating conditions. Oftentimes, if the user pre-defines the values of the objective functions, the obtainment of the corresponding design and operating conditions becomes a challenging task, as it requires interactive optimization. As an alternate, a surrogate model for the Pareto-optimal front and design/operating conditions has been also developed, which can be used for an easier exploration of the Pareto-optimal front.

2. Methods

In this section, the modelling and simulation of the chemical absorption-based CO_2 capture plant is described. The development of the ANN and its predictive performance are also discussed in the light of the goodness of fit and the error indicators.

2.1. Modelling and simulation of the chemical absorption-based CO_2 capture plant

The process simulation is performed in Aspen HYSYS® v11 using the Amines property package. The CO_2 capture system considered in this work is shown in Figure A.1. It consists of two main units, namely the absorber and desorber columns, which operate with a 40 wt.% aqueous solution of di-ethanolamine (DEA) [206]. Firstly, the flue gases (1000 kmol/h) at atmospheric pressure are cooled down from 270 °C to 25 °C to condense the water present in the feed stream. Thereafter, the flue gases are compressed up to 5 bar and cooled again to 30 °C, before entering to the absorber column. The flue gases enter the absorber at the bottom stage and flow upwards in counter-current with the lean DEA solution, which enters at the top of the absorber. The CO_2 rich solution leaving at the bottoms of the absorption column is expanded up to 1.8 bar and preheated up to 93 °C in a lean-rich heat exchanger to recover a portion of the waste heat [207]. Next, CO_2 rich DEA solution enters in the desorption column, wherein the absorption reaction is reversed at higher temperature and lower pressure. In the

desorption column, a large amount of energy in the form of steam is consumed *(i)* to raise the temperature of the solution up to that of the reboiler, *(ii)* to supply the enthalpy of reaction to break the chemical bond between the acidic gas and the DEA solvent, and *(iii)* to provide the enthalpy of vaporization to produce the vapor that acts as the stripping source [208]. The regenerated solvent, lean in acid gas, leaves the at the bottom of desorption column and it passes through the lean-rich heat exchanger. Subsequently, the solvent is water-cooled and pumped to the top of the absorption column. Makeup water is required to keep the desired concentration of the DEA solution. Meanwhile, the overhead CO_2-enriched gas leaving the desorber is condensed at the top of the desorber column to provide the reflux, and the small amounts of amine is vaporized and lost. Finally, the captured CO_2 gas is cooled and purified (>99 wt.% CO_2) [209].

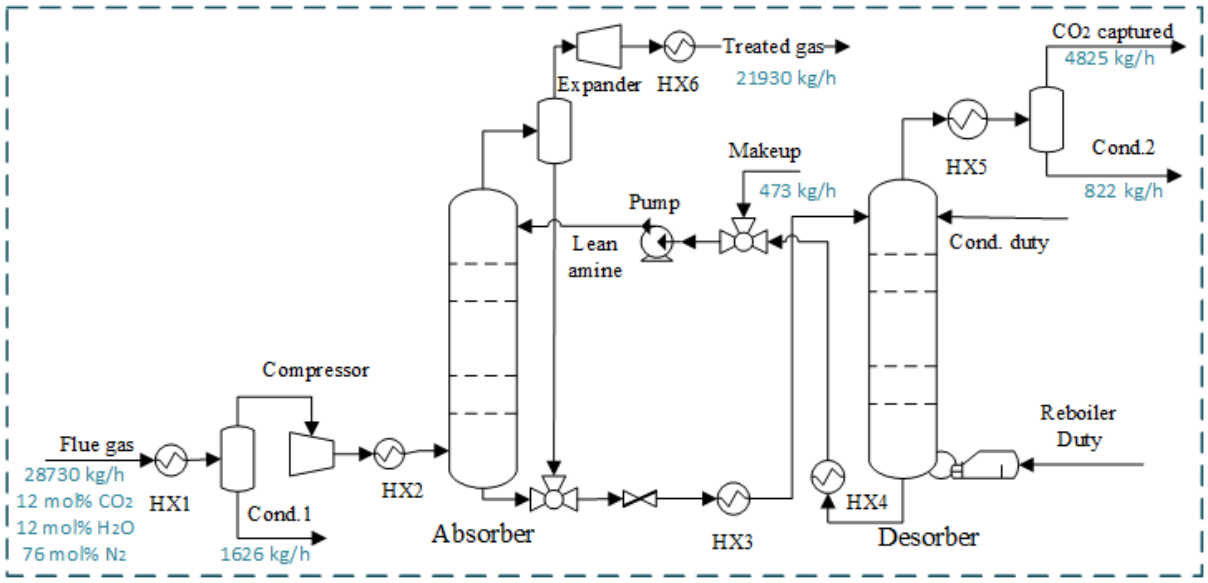

Figure A.1 Flowsheet of the amine-based CO_2 capture plant. The mass flows for a representative inlet flue gas composition are also shown.

2.2. Development of the ANN model

One of the approaches to develop surrogate models is the artificial neural network (ANN). This algorithm is inspired by the biological nervous system and it consists of several layers connected by neurons that perform the input data transformations aiming to obtain the required outputs [210].

In this study, to develop the ANN model, all the data related to the mass flows, heat and power are extracted from the rigorous simulation model developed in Aspen HYSYS®. The feed flow rate is maintained at a constant value of 1000 kmol/h, whereas the CO_2 concentration is varied between 7 and 16 mol%. The water content is also varied in a stochastic

fashion in the range of 8-20 mol%, in order to represent flue gases with different moisture contents [211]. In addition, the solvent recirculation flowrate is also stochastically varied in the simulation model, but still subject to suitable amine concentration (30-40 wt.%) and rich loads (35-45 mol_{CO2}/mol_{DEA}) [212; 213; 214].

The ANN used in this study is a fully connected one with two hidden-layers, as it is schematically illustrated in Figure A.2. There are 3 inputs (namely the CO_2, N_2 and H_2O mol% in the feed stream) and 9 outputs (namely the Cond.2 mass flow, CO_2 captured mass flow, HX3 duty, HX5 duty, Condenser duty, Reboiler duty, Expander, HX6 duty and Treated gas mass flow) variables in the surrogate model. In total, 216 data samples are used, ensuring the 'factor 10' rule-of-thumb [215]. The training of the ANN is carried out in MATLAB® v.2021b using the deep learning and machine learning toolbox. 70% of the samples/data are used for training, whereas 15% is used for validation and other 15% is used for testing the model. The number of neurons in each layer is provided by the neural network algorithm; first hidden layer has 2 neurons, whereas second hidden layer has 9 neurons.

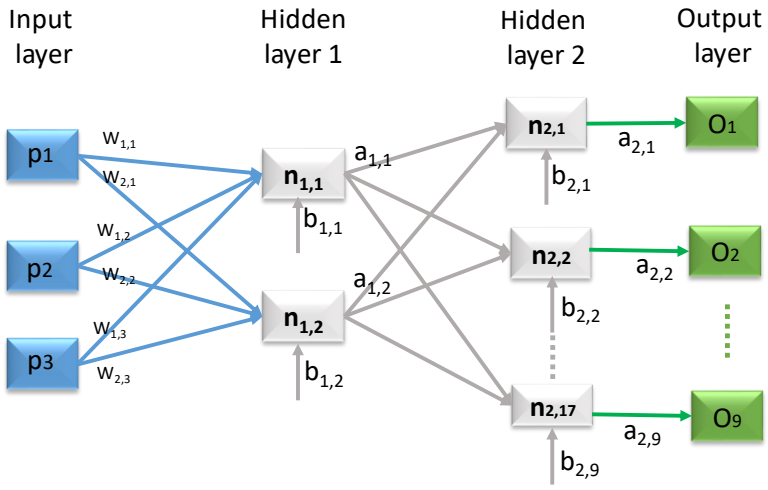

Figure A.2 Schematic diagram of the ANN model, for 3 inputs and 9 outputs.

As mentioned earlier, a Pareto-optimal front is also generated to explore the trade-off between the CO_2 recovery and the reboiler duty for a fixed composition (12 mol% CO_2, 12 mol% H_2O and 76 mol% N_2), by systematically varying the solvent recirculation flow rate. An ANN model for the obtained Pareto-optimal front and corresponding operational parameters is developed, by considering two hidden layers. In total, 229 data samples were used, and 70%, 15% and 15% of the data samples were used for training, validation and testing, respectively. The reboiler duty and the CO_2 recovery are the inputs in the ANN model, whereas the

operational parameters are the outputs. In this way, the surrogate model allows to predict the corresponding design and operating conditions for pre-defined objective functions.

2.3. Performance metrics

In order to measure the quality of the surrogate model, a data set of additional points is generated for testing. The new simulation points are compared against the ANN response using three error-based performance metrics, namely the average absolute error (AAE), the root mean squared error (RMSE), and the pooled error (PE), as suggested in ref. [216]. The AAE (Equation A.1) represents the overall magnitude of the error, while the RMSE (Equation A.2) measures how spread out the data points are from the regression or how well a function fits the available data, inflating or increasing the mean error value due to the square of the error value. The PE (Equation A.3) combines the AAE and the RMSE to provide a single measure of performance.

$$AAE = \frac{\sum_{i=1}^{n} | x_{simul,i} - x_{surr,i} |}{n} \tag{A.1}$$

$$RMSE = \sqrt{\frac{\sum_{i=1}^{n} (x_{simul,i} - x_{surr,i})^2}{n}} \tag{A.2}$$

$$PE = \sqrt{RMSE \cdot AAE} \tag{A.3}$$

where $x_{simul,i}$ is the (Aspen HYSYS) simulation output and $x_{surr,i}$ is the surrogate response for each parameter *i*, and *n* is the number of points in the data set. In order to facilitate the comparison between the dataset with different scales, we compute the relative performance by normalizing the calculated errors using the mean, as described in Equations (A.4-A.6).

$$AAE = \frac{AAE}{\overline{x_{simul,i}}} \tag{A.4}$$

$$RMSE = \frac{RMSE}{\overline{x_{simul,i}}} \tag{A.5}$$

$$PE = \frac{PE}{\overline{x_{simul,i}}} \tag{A.6}$$

where $\overline{x_{simul,i}}$ is the mean of the observed value of the simulation parameter in the considered dataset. The lower the relative error, the better the model.

3. Results and discussion

In this section, the main results related to the performance of the surrogate model developed for variable CO_2 concentration are firstly discussed. Subsequently, the results of the surrogate model developed for the exploration of Pareto-optimal front are presented.

3.1 Surrogate model for variable CO_2 concentration in the feed

Figure A.3 presents the response of some process variables for different CO_2 mole fractions in feed (obtained by simulation). As it can be seen, in general, simple regression models, such as linear regression, are not able to foresee the correct behavior of all process parameters. In addition, the average time for each simulation run in Aspen HYSYS was around 2 minutes. Thus, more accurate surrogate models with less computational time are necessary to represent the complex and non-linear relationships between inputs and outputs of a process.

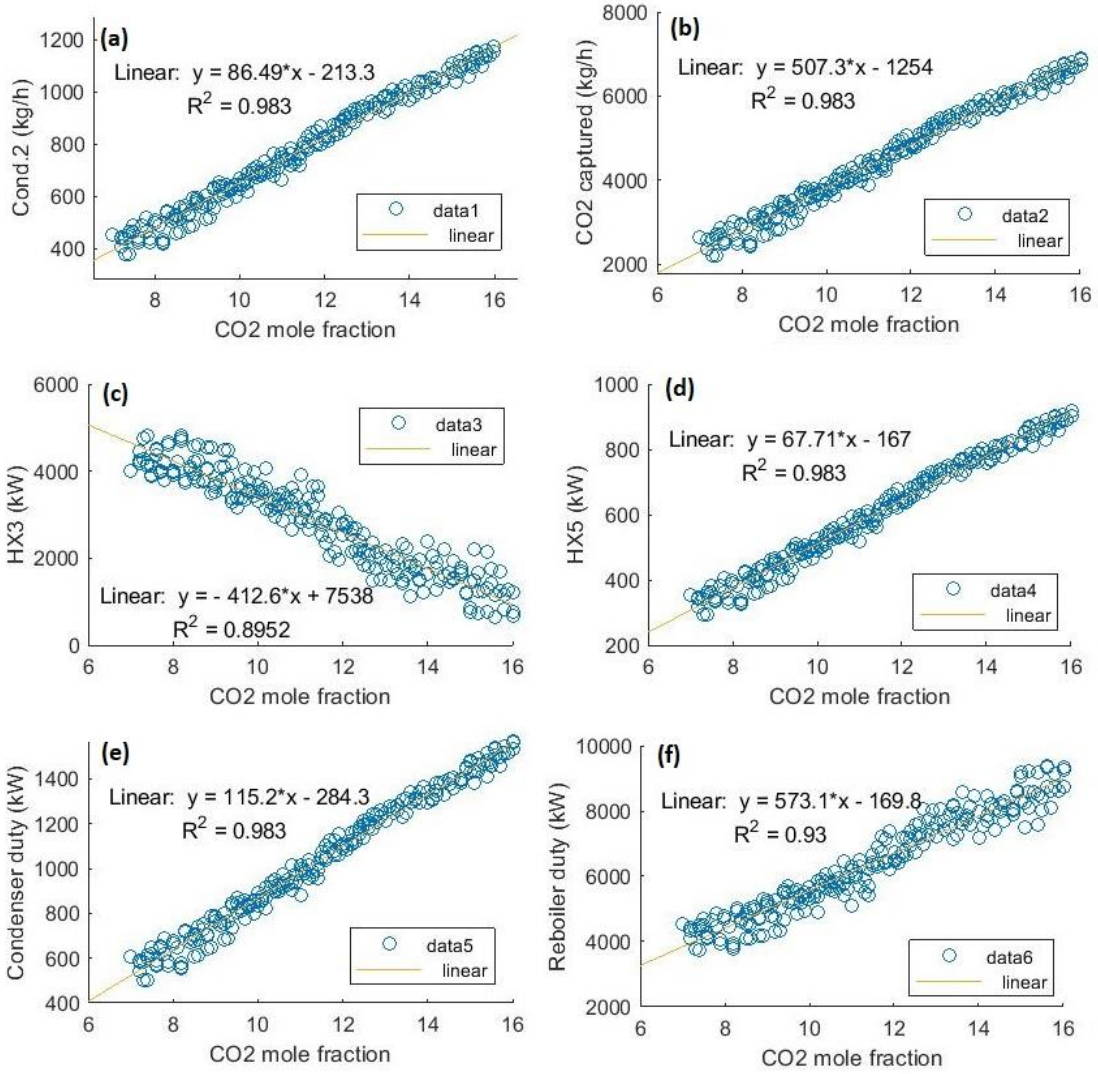

Figure A.3 Responses of the simulation model for different CO_2 mole fractions in the feed: (a) Cond.2 mass flow, (b) CO_2 captured mass flow, (c) HX3 duty, (d) HX5 duty, (e) Condenser duty and (f) Reboiler duty. (Please, refer to Figure A.1 for the details on responses).

In this work, ANN algorithm is used to create a surrogate model for the CO_2 capture system using DEA. The ANN-based surrogate model for the CO_2 capture process requires several weights and bias parameters (*w*, *a* and *b*), and they are reported in Table A.3 in Annex A. The predictions of ANN-based surrogate model are compared to the simulation model outputs based on a test data set (see Table A.1 and Figure A.4). In contrast to the limited performance of the linear regression model presented in Figure A.3, the developed ANN-based surrogate model can accurately predict the essential output parameters, including the process energy requirement and the CO_2 recovery, for a wide range of CO_2 concentrations in the flue gas entering the CO_2 capture system. Considering the statistics reported in Table A.1, the heat exchanger HX3 seems to present the poorest response by the ANN-based surrogate model. The normalized RMSE for this parameter is around 0.104. Another important remark, is that the

average computational time is in the order of 0.04 s, which is 3000 times faster than the simulation model.

Table A.1 Performance comparison between simulation (Aspen HYSYS) and ANN-based surrogate.

Parameter	*AAE*	*RMSE*	*PE*
Cond.2	0.028	0.036	0.032
CO2 Captured	0.028	0.033	0.031
HX3	0.087	0.104	0.095
HX5	0.028	0.035	0.031
Condenser duty	0.028	0.034	0.031
Reboiler duty	0.039	0.049	0.043
Expander	0.005	0.006	0.006
HX6	0.005	0.006	0.006
Treated gas	0.006	0.007	0.006

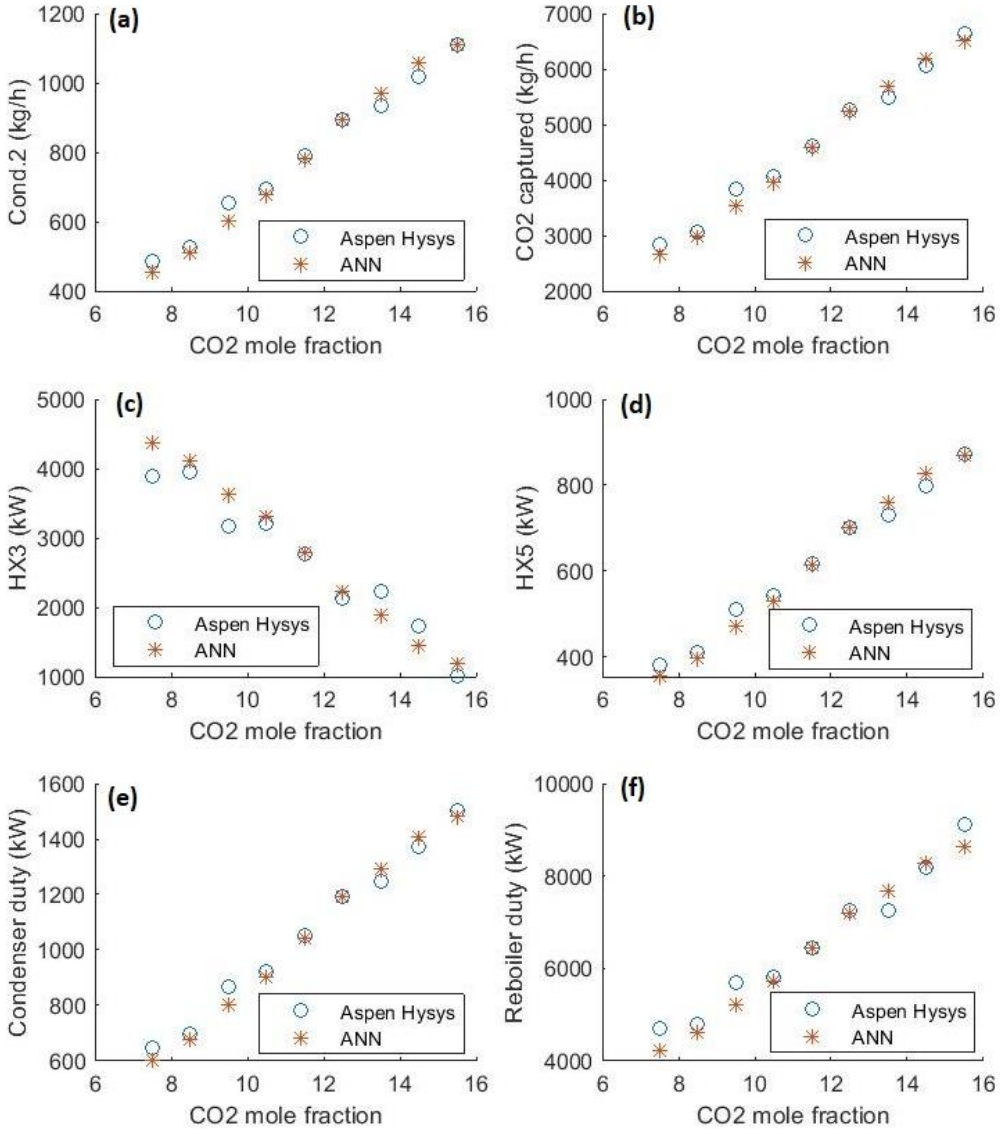

Figure A.4 Comparison between the surrogate model response and the simulation (Aspen HYSYS) output for (a) Cond.2 mass flow, (b) CO_2 captured mass flow, (c) HX3 duty, (d) HX5 duty, (e) Condenser duty and (f) Reboiler duty, as a function of the CO_2 mole fraction in the flue gases.

3.2 Surrogate model for the exploration of Pareto-optimal front

A Pareto-optimal front is generated by the simultaneous optimization of the CO_2 recovery and the reboiler duty of desorber (Figure A.5), to better understand the trade-offs between these conflicting parameters. As expected, an increase in the CO_2 recovery also increases the reboiler duty needed for solvent regeneration. Furthermore, when a certain CO_2 removal rate is exceeded (about 98%), there is a drastic increase in the energy requirements. This behavior is in agreement with experimental findings reported in the literature for amine-based solvents [217]. It is also important to highlight the correlation between the costs and the expected CO_2 recovery, namely the higher the recovery, the higher the total cost, according to ref. [218].

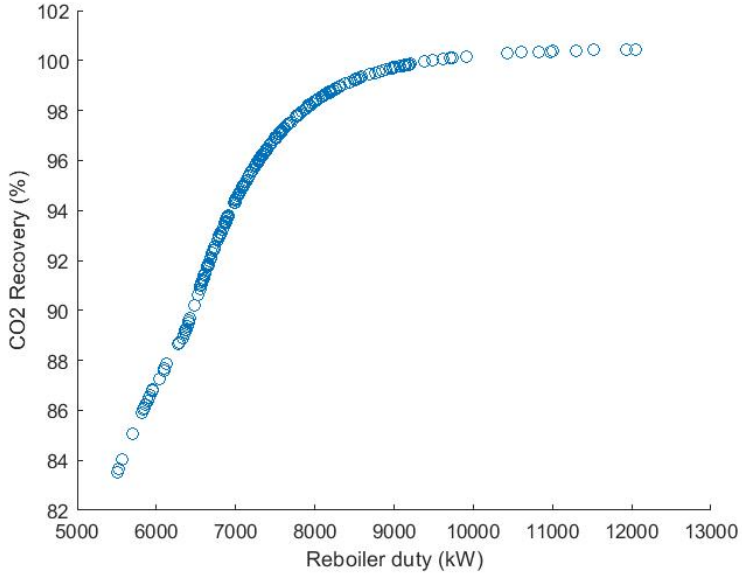

Figure A.5 Pareto-optimal front for simultaneous maximization of CO_2 recovery (%) and minimization of reboiler duty (kW).

Figure A.6 illustrates the relationship between the (Aspen HYSYS) simulation output for the reboiler duty and for selected parameters (related to streams and equipment) reported in Figure A.1, considering a fixed composition (12 mol% CO_2, 12 mol% H_2O and 76 mol% N_2) of flue gases. In general, it can be noticed that the studied parameters are strongly dependent on the reboiler duty, as it is the bulk of energy consumption in the CO_2 capture process. For instance, by analysing Figure A.6c, Figure A.6a, and Figure A.6b, the higher is the reboiler duty, the more CO_2 can be stripped from the rich amine solution, the more is the amount of water condensed and the lesser is the flow of gases leaving the system in the treated gas stream.

An ANN-based surrogate model for the Pareto-optimal front and operational variables is developed, and the obtained parameters for surrogate model are summarized in Table A.4 in Annex A. The surrogate model validation is assessed by the parity plots between a test data set (simulation model) and the ANN model prediction (Figure A.7), and also the statistics reported in Table A.2. From these results, it can be inferred that the ANN-based surrogate model for the Pareto-optimal front can accurately predict the design and operating conditions, allowing user to define values of objective functions on the Pareto-optimal front. The normalized RMSE is smaller than 0.037 (Table A.2).

Table A.2 Validation of the Pareto-optimal front surrogate model performance.

Response	*AAE*	*RMSE*	*PE*
Cond.2	0.0041	0.0059	0.0049
Treated gas	0.0009	0.0014	0.0011
CO_2 captured	0.0041	0.006	0.005
Expander	0.0015	0.0022	0.0018
HX6	0.0016	0.0023	0.0019
HX3	0.0164	0.0372	0.0247
HX4	0.0013	0.0026	0.0019
HX5	0.0041	0.0059	0.0049
Condenser duty	0.0041	0.006	0.005

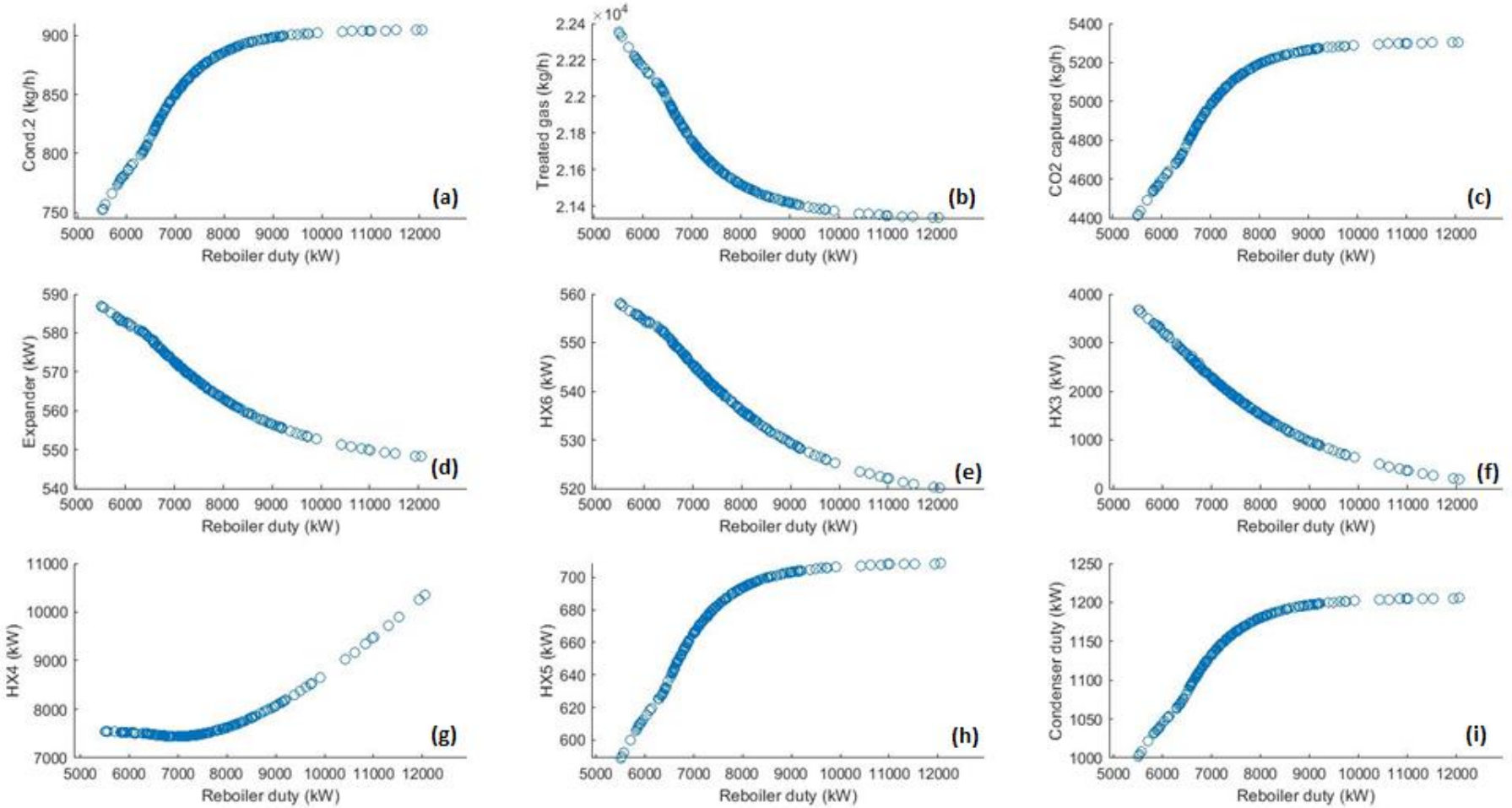

Figure A.6 Influence of the reboiler duty on selected variables of the CO_2 capture system for: a) Cond. 2 stream, b) Treated gas mass flow, c) CO_2 captured mass flow, d) Expander, e) HX6 duty, f) HX3 duty, g) HX4 duty, h) HX5 duty and i) Condenser duty.

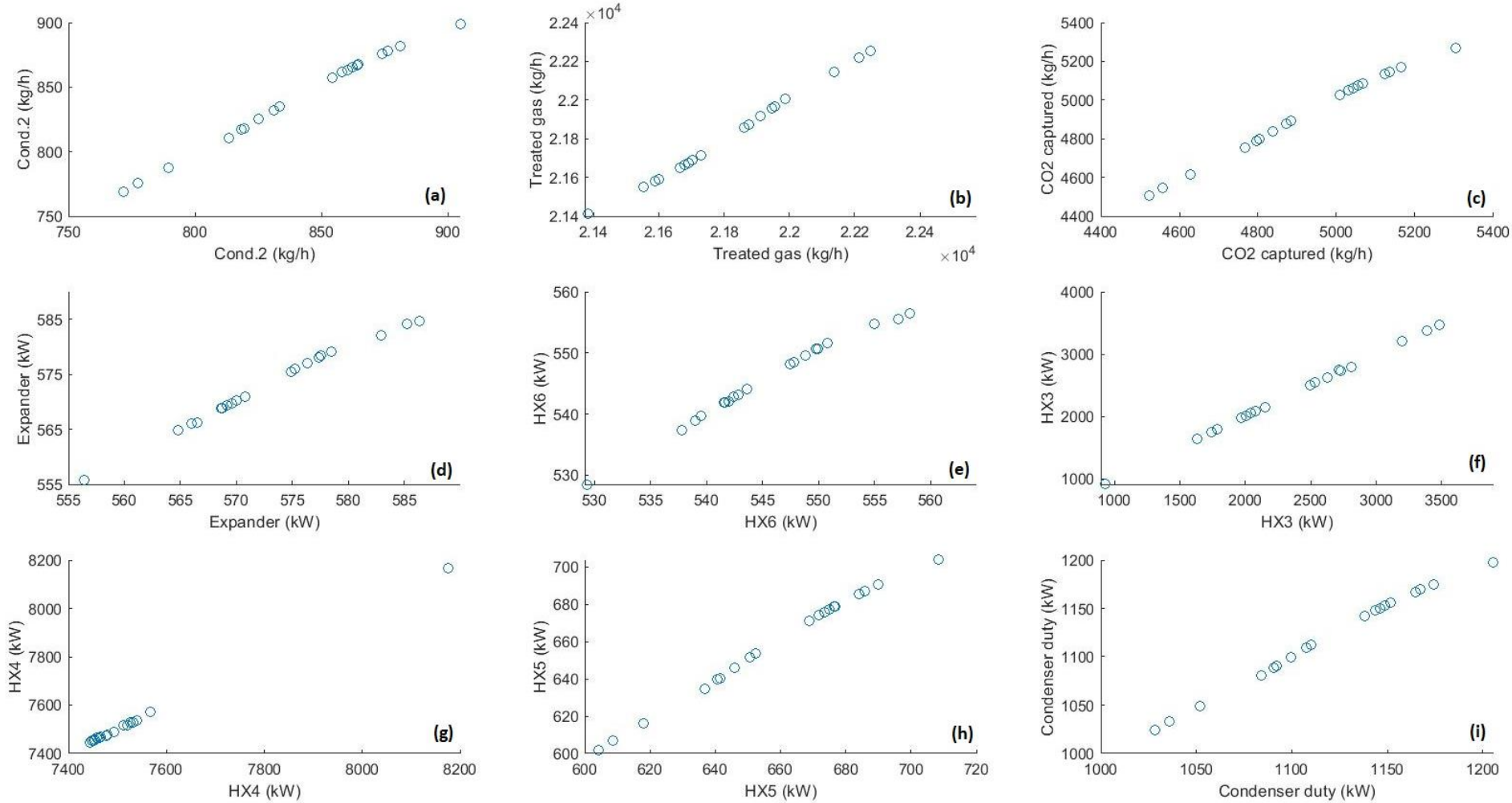

Figure A.7 Parity plots between the ANN model predictions (x axis) and the simulation model output (y axis) for user defined solutions on the Pareto-optimal front: a) Cond. 2 stream, b) Treated gas mass flow, c) CO_2 captured mass flow, d) Expander, e) HX6 duty, f) HX3 duty, g) HX4 duty, h) HX5 duty and i) Condenser duty.

4. Conclusions

The surrogate modelling has proved to be a powerful tool to represent the complex simulation model of the CO_2 capture using amine absorption. The data used for training and validation of the ANN model has been generated using the Aspen HYSYS process simulator. For a wide range of flue gas composition, the correlation derived from the artificial neural network predicted the simulation outputs (obtained by Aspen HYSYS) with a normalized RMSE less than 0.104. The Pareto-optimal front analysis showed the trade-off between the CO_2 recovery and the heat demand in the reboiler, required for the solvent regeneration. In addition, the ANN-based surrogate for the Pareto-optimal front predicted the process designs and operating conditions with errors smaller than 0.037, thus allowing the user to explore the solutions on the Pareto-optimal front. Finally, the developed ANN models could be integrated with other industrial processes or clusters, for exploring synergies and minimizing costs and environmental impacts; different process models can be interlinked with a suitable optimization algorithm.

Annex A

Table A.3 Parameters of the ANN developed considering different flue gas compositions to estimate the operating conditions; Tan-Sigmoid activation function is used.

			Hidden layer 1 a1 = f(IW.p + b1)			
	IW	p1	p2	p3		
a1,1	n1,1	0.053	-0.134	0.311	b1,1	-0.077
a1,2	n1,2	0.636	-0.453	-0.729	b1,2	0.030
			Hidden layer 2 a2 = f(LW.a1 + b2)			
	LW	a1,1	a1,2			
a2,1	n2,1	-0.080	1.167		b2,1	0.006
a2,2	n2,2	1.948	-0.464		b2,2	0.136
a2,3	n2,3	-0.080	1.167		b2,3	0.006
a2,4	n2,4	1.931	-0.476		b2,4	0.135
a2,5	n2,5	1.914	-0.479		b2,5	0.132
a2,6	n2,6	0.096	-1.075		b2,6	0.037
a2,7	n2,7	-0.080	1.167		b2,7	0.006
a2,8	n2,8	-0.080	1.167		b2,8	0.006
a2,9	n2,9	-0.081	1.103		b2,9	-0.052

Table A.4 Parameters of the ANN developed to estimate the operating conditions considering the desired CO_2 recovery and reboiler duty for a fixed flue gas composition; Tan-Sigmoid activation function was used.

			Hidden layer 1 a1 = f(IW.p + b1)		
	IW	p1	p2		
a1,1	n1,1	-0.936	-0.128	b1,1	-0.724
a1,2	n1,2	0.229	-0.007	b1,2	-0.227
			Hidden layer 2 a2 = f(LW.a1 + b2)		
	LW	a1,1	a1,2		
a2,1	n2,1	-2.564	-3.768	b2,1	-1.668
a2,2	n2,2	2.294	2.683	b2,2	1.339
a2,3	n2,3	-2.572	-3.783	b2,3	-1.674
a2,4	n2,4	1.324	-1.210	b2,4	0.158
a2,5	n2,5	1.165	-1.843	b2,5	-0.029
a2,6	n2,6	1.289	-0.983	b2,6	0.176
a2,7	n2,7	1.403	8.843	b2,7	2.346
a2,8	n2,8	-2.564	-3.768	b2,8	-1.669
a2,9	n2,9	-2.565	-3.771	b2,9	-1.669

APPENDIX B: Simulation kinetics data

Methanol synthesis kinetics in Aspen Plus

The generalized rate expression to be used in Aspen Plus is given by Equation B.1:

$$r = \frac{(kinetic\ factor)(driving\ force\ expression)}{(adsorption\ term)} \quad \text{(B.1)}$$

When a reference temperature T_o is not specified, the kinetic factor in Aspen is expressed by a pre-exponential factor and an Arrhenius term:

$$kinetic\ factor = kT^n \exp(-\frac{E_a}{RT}) \quad \text{(B.2)}$$

The methanol kinetics was detailed by Kiss et al. (2016). The reactions for methanol synthesis are:

$$\text{A) } CO + 2H_2 \leftrightarrow CH_3OH \quad \left(\Delta H^o_{298K} = -90.77\, kJ/mol\right) \quad \text{(B.3)}$$

$$\text{B) } CO_2 + H_2 \leftrightarrow CO{+}H_2O \quad \left(\Delta H^o_{298K} = +41.21 kJ/mol\right) \quad \text{(B.4)}$$

$$\text{C) } CO_2 + 3H_2 \leftrightarrow CH_3OH + H_2O \quad \left(\Delta H^o_{298K} = -49.16\, kJ/mol\right) \quad \text{(B.5)}$$

The driving force expressions are as follows:

Reaction A: $K_{CO} f_{CO} f_{H2}^{3/2} - \frac{K_{CO}}{K_A} f_{CH3OH} f_{H2}^{-1/2}$ $[Pa^{3/2}]$ (B.6)

Reaction B: $K_{CO2} f_{CO2} f_{H2} - \frac{K_{CO2}}{K_B} f_{H20} f_{CO}$ $[Pa\ \ ]$ (B.7)

Reaction C: $K_{CO2} f_{CO2} f_{H2}^{3/2} - \frac{K_{CO2}}{K_C} f_{H20} f_{CH3OH} f_{H2}^{-3/2}$ $[Pa^{3/2}]$ (B.8)

In Aspen Plus, the driving force is expressed in a generalized form:

$$K_1\left(\prod c_i^{\upsilon_i}\right) - K_2\left(\prod c_j^{\upsilon_j}\right) \quad \text{(B.9)}$$

When selecting the vapor phase as the reactive phase, and neglecting the difference between partial pressure and fugacity (i.e. assuming ideal gas), the partial pressures are used for the concentration. In Aspen Plus, K_1 and K_2 are expressed in a logarithmic form.

$$\ln(K) = A + \frac{B}{T} \tag{B.10}$$

The adsorption term is the same for all reactions. The expression applied in Aspen Plus is:

$$\sum K_i \left(\prod c_j^{v_j}\right)^m \tag{B.11}$$

Configuring Aspen Plus requires re-writing the adsorption term in the kinetic expression, which is the same for all three reactions:

$$(1 + K_{CO}f_{CO} + K_{CO2}f_{CO2})\left[\sqrt{f_{H2}} + \left(\frac{K_{H2O}}{\sqrt{K_H}}\right)f_{H2O}\right]\left[bar^{\frac{1}{2}}\right] = \sqrt{f_{H2}} + \left(\frac{K_{H2O}}{\sqrt{K_H}}\right)f_{H2O} + K_{CO}f_{CO}\sqrt{f_{H2}} + \left(\frac{K_{CO}K_{H2O}}{\sqrt{K_H}}\right)f_{CO}f_{H2O} + K_{CO2}f_{CO2}\sqrt{f_{H2}} + \left(\frac{K_{CO2}K_{H2O}}{\sqrt{K_H}}\right)f_{CO2}f_{H2O} \tag{B.12}$$

The values for the kinetic factor, the driving force constants and the adsorption term factors are expressed in Tables B.1, B.2, and B.3, respectively.

Table B.1 Kinetic factor for reactions B.3, B.4, B.5 – the units used are [Pa] for fugacity and [mol/$g_{catalyst}$s] for reaction rate [98].

Reaction	*k*	*n*	E_a[J/mol K]
A	4.0638E-6 [kmol/kg_{cat} s Pa]	0	11,695
B	9.0421E+8 [kmol/kg_{cat} s $Pa^{1/2}$]	0	112,860
C	1.5188E-33 [kmol/kg_{cat} s Pa]	0	266,010

Table B.2 Constants for driving force using the Aspen Plus format [98].

	K_1		K_2	
Reaction	A	B	A	B
A	-23.20	14,225	28.895	2385
B	-22.48	9777	-28.12	15,062
C	-22.48	9777	23.974	3222

Table B.3 K_i factors for adsorption term in the Aspen Plus format [98].

Term	Expression	a_i	b_i	$\prod c_j^{v_j}$
1	1	0	0	$\sqrt{f_{H2}}$
2	$\frac{K_{H2O}}{\sqrt{K_H}}$	-26.1568	13,842	f_{H2O}
3	K_{CO}	-23.2006	14,225	$f_{CO}\sqrt{f_{H2}}$
4	$\frac{K_{CO}K_{H2O}}{\sqrt{K_H}}$	-49.3574	28,067	$f_{CO}f_{H2O}$
5	K_{CO2}	-22.4827	9777	$f_{CO2}\sqrt{f_{H2}}$
6	$\frac{K_{CO2}K_{H2O}}{\sqrt{K_H}}$	-48.6395	23,619	$f_{CO2}f_{H2O}$

Dimethyl ether synthesis kinetics in Aspen Plus

The reaction for DME synthesis via methanol dehydration is:

$$2CH_3OH \leftrightarrow CH_3OCH_3 + H_2O \quad \left(\Delta H^o_{298K} = -23.4\, kJ/mol\right) \tag{B.13}$$

The rate equation is given by [132], which was adapted to aspen plus form by [131; 133] (see Tables B.4 and B.5):

$$-r_{CH_3OH} = k_0 \exp(E/RT)\, p_{CH_3OH} \tag{B.14}$$

$$r = \frac{(kinetic\ factor)(driving\ force\ expression)}{(adsorption\ term)} \tag{B.15}$$

Where k_0 = 0.336111 kmol/(m^3.s.Pa), E = 80.48 kJ/mol, and p_{CH3OH} is the partial pressure of methanol.

Table B.4 Constants for driving force using the Aspen Plus format [131; 133].

Driving-force expressions	
Term 1	*Term 2*
Concentration exponents for reactants: CH_3OH = 1	Concentration exponents for reactants: CH_3OH = -1
Concentration exponents for products: DME = 0;	Concentration exponents for products: DME = 1;
H_2O = 0	H_2O = 1
Coefficients: A = 0; B = C = D = 0	Coefficients: A = 2.8086; B = -3061; C = D = 0

Table B.5 Terms for adsorption term in the form of Aspen Plus [131; 133]

Adsorption expression	
Adsorption term exponent = 1	
Concentration exponents	Adsorption constants
Term 1: H_2O = 0	Term 1: A = -0.61395; B = 0; C = 0, D = 0
Term 2: H_2O = 0	Term 2: A = -0.61395; B = 0; C = 0, D = 0

Ammonia synthesis kinetics in Aspen Plus

The kinetics description for ammonia synthesis was taken from Flórez-Orrego (2018). The ammonia synthesis reaction kinetics is given to the reverse reaction, and described as by:

$$\frac{1}{2}N_2 + \frac{3}{2}H_2 \leftarrow NH_3 \tag{B.16}$$

The reaction rate expression in terms of fugacities (or activities) and the corresponding equilibrium constant K_P [219] is:

$$-r_{N_2} = k_b\left[K_P^2 f_{N_2}\left(\frac{f_{H_2}^3}{f_{NH_3}^2}\right)^{\alpha} - \left(\frac{f_{NH_3}^2}{f_{H_2}^3}\right)^{1-\alpha}\right] \tag{B.17}$$

K_P can be determined as a function only of the temperature for a given chemical reaction, regardless of the reactant or product concentrations, total pressure or the presence of catalyst. The value of K_P is calculated by using the Gillespie and Beattie correlation and the constants reported in Table B.6 [220]:

$$\log_{10} K_P = A\cdot\log_{10} T + B\cdot T + C\cdot T^2 + \frac{D}{T} + E \quad \text{with } T \text{ in K} \tag{B.18}$$

Table B.6 Coefficient of the equilibrium constant K_P [220].

Coefficient	**A**	**B**	**C**	**D**	**E**
Value	-2.691122	-5.519265E-5	1.848863E-7	2001.6	2.6899

Additionally, the backward reactions rates constants of the ammonia synthesis is reported as in Table B.7:

Table B.7 Pre-exponential factor and activation energy for backward (b) reaction rate constants.

k_{0b}	Ea_b kJ/kmol	α	**Observations [Reference]**
8.85E+14	170,683	0.5	$k_f = K_P\, k_b$ fugacities in atm Dyson et al. [219]

the reaction rate has units of kmol/(m^3_{cat} h).

The fugacity of the component in the mixture is proportional to the mol fraction of the component at the same temperature of the system. It is worthy to notice that it was assumed $\hat{f}_i = 1$ atm. Finally, the value of f_i° is estimated by using:

$$f_i^{\circ} = \gamma_i \cdot P \tag{B.19}$$

Where γ_i and P are the activity coefficient of the component i and the total pressure of the system respectively. The activity coefficients are calculated by using the following equations [219]:

$$\gamma_{H_2} = \exp\left(e^{-3.8402T^{0.125}+0.541}\cdot P - e^{-0.1263T^{0.5}-15.980}\cdot P^2 + 300\cdot e^{-0.011901T-5.941}\left(e^{-P/300}-1\right)\right) \tag{B.20}$$

$$\gamma_{N_2} = 0.93431737 + 0.3101804E-3\cdot T + 0.295896E-3\cdot P - 0.2707279E-5\cdot T^2 + 0.4775207E-6\cdot P^2 \tag{B.21}$$

$$\gamma_{NH_3} = 0.1438996 + 0.2028538E-2\cdot T - 0.4487672E-3\cdot P - 0.1142945E-5\cdot T^2 + 0.2761216E-6\cdot P^2 \tag{B.22}$$

Where the pressure is given in *atm* and the temperature in K.

APPENDIX C: Equipment cost functions

The equipment cost functions used for estimating the capital expenditure of the main units are expressed in Table C.1.

Table C.1 Equipment cost correlations in MUSD.

Equipment	Function	Unit of the reference variable	Source
Black liquor gasifier	$39.08\left(\frac{P}{381}\right)^{0.6}$	$MW_{Blackliquor}$	221
Air separation unit	$27\left(\frac{\dot{m}}{45833}\right)^{0.6}$	kg_{O2}/h	221
Water gas shift reactor	$1.17*5.77\left(\frac{V}{0.104}\right)^{0.6}$	m^3	222; 223
CO_2 capture unit based on Selexol®	$54.1\left(\frac{\dot{n}}{9909}\right)^{0.7}$	$kmol_{CO2}/h$	224
Methanator	$5.345\left(\frac{P}{175}\right)^{0.67}$, vessel $1.031\left(\frac{P}{175}\right)^{0.67}$, catalyst	MW_{SNG}	225
Pressure swing adsorption unit	$32.6\left(\frac{\dot{n}}{9600}\right)^{0.7}$	$kmol_{feed}/h$	226
Urea plant	$12.96\left(\frac{\dot{m}}{477.34}\right)^{0.65}$	t_{urea}/d	227
Nitric acid plant	$8\left(\frac{\dot{m}}{274}\right)^{0.6}$	t_{HNO3}/d	228

APPENDIX D: Multi-time integration approach for combined pulp and ammonia production and seasonal CO_2 management

Abstract: The exploitation of the industrial residues and the recovery of the waste heat are important strategies for defining pathways to a sustainable economy. The pulp and fertilizers sectors are among the largest global primary energy consumers and generate by-products that can be upgraded for the sake of a better energy management. In this work, the gasification of the black liquor, a residue of the pulping process, is proposed as an alternative ammonia production route. The quantification of the waste heat recovery and the optimization of the energy integration problem is handled by a mixed integer linear programming model. Due to the seasonal variation of the energy prices, a multi-time integration approach that combines different technologies and energy inputs is used to identify the most suitable operating conditions and arrangements that minimize the energy resources consumption. As a result, the integration of technologies such as power-to-gas systems, carbon capture and injection units, along with liquid fuel storage, may help offsetting the intermittency of the renewable energy resources and increasing the economic revenues of the integrated pulp and ammonia plant. The optimal CO_2 management and synthetic natural gas storage may ensure a reliable operation even during the strained periods of the electricity grid. Also, the credits obtained from the injection of biogenic CO_2 emissions may compensate for the investment cost associated to the implementation of these new technologies.

Keywords: Black liquor, Kraft pulp process, Ammonia, CO_2 management, Power-to-gas.

1. Introduction

Ammonia production accounts for around 2% of the total final energy consumption and 1.3% of CO_2 emissions from industry, as it is heavily based on fossil fuels [191]. Pre-combustion CO_2 capture is an inherent part of the ammonia production process, and the CO_2 rich-stream coming from the syngas purification may be reused or permanently stored. In 2020, about 130 Mt of CO_2 were used to produce urea, whereas only 2 Mt of CO_2 were stored [191]. The way in which the electricity consumed is generated also influences the CO_2 emissions of the Haber process. The indirect CO_2 emissions related to the electricity import accounted for 40 Mt of CO_2 in 2020 [191]. Several efforts have been made towards the mitigation of the environmental impacts of this sector. The biomass thermochemical conversion routes for syngas production are among the options to supply feedstock and energy to the ammonia plants, especially in

countries with a long biomass conversion expertise [229]. Other pathways suggested reusing CO_2 for the production of different chemicals and fuels aiming to increase overall process efficiency [230]. The power-to-gas approach is based on water electrolysis for hydrogen production, which combined with CO_2 produces synthetic natural gas via methanation process. This technology is pertinent for CO_2 and energy management purposes, as methane can be produced during periods of inexpensive electricity generation and stored to be used in due time when the energy import is more expensive.

Castellani et al. assessed the potential of using N_2/CO_2 membrane separation of flue gas and water electrolysis to produce ammonia through the Haber process and methane via the Sabatier reaction. The authors found that the electrolysis is responsible for 80% of the energy costs and the CO_2 recycling process is subject to the availability of renewable electricity in order to avoid net emissions [231]. Vandewalle et al. studied the effects of integrating the power-to-gas approach on the power, gas and carbon sectors. This technology directly impacts the final gas price, since it increases the capacity and flexibility of the system, and contributes to enhancing the sustainability of the process [232]. The power-to-gas approach may reduce the need for permanent CO_2 storage, but not the need of short-term storage, since it is necessary to maintain the operation of the system, which may lead to a complex CO_2 network. Other authors also showed that the integration of the power-to-gas technology in the natural gas and electric grids may reduce the total energy loss and maintain a stable operation level [233]. However, the capture and management of the carbon dioxide derived from an integrated pulp and ammonia production plant has not been assessed, neither it has been studied the decarbonization potential on scenarios of carbon taxation and variable energy prices. Thus, in this work, a systematic approach is applied to the analysis of a multi-time problem that considers seasonal energy costs, CO_2 capture technologies, storage systems and power-to-gas to decarbonize the ammonia production and offset the shortcomings of the renewable energy systems, as electricity can be stored or consumed, depending on variable electricity prices.

2. Methods

In this section, the modeling and simulation methods, as well as the optimization problem definition subject to minimum energy requirements, carbon taxation and seasonal

energy cost variation is presented. The key performance indicators to evaluate the two cases are also described in this section. A comparative analysis of two study cases is considered:

Case 1) an integrated pulp and ammonia production plant using black liquor gasification, with typical utility systems (e.g. chips, bark and oil furnaces; steam network; electricity import or export); and

Case 2) an integrated pulp and ammonia production plant using black liquor gasification, with its respective utility systems, and CO_2 management systems (post-combustion CO_2 capture, liquefaction, storage and injection units, and methanation, SNG liquefaction and storage units).

2.1 Process modelling and simulation

Figure D.1 shows the process flowsheet of the kraft pulp mill, where cellulose is extracted from wood under strong alkaline conditions. Around 10% of the biomass input that is lost in log debarking, chipping and chips classification is used in the biomass boiler as fuel. In a standalone pulping mill, the weak black liquor follows to a recovery unit, where it is concentrated in multiple-effect evaporators and burned in the recovery boiler to generate power and steam. The steam produced in the recovery boiler accounts for most of the steam consumption in the pulp mill, whereas the balance is supplied using bark and additional wood chips [23]. Fuel oil or natural gas is also widely used in the lime kilns.

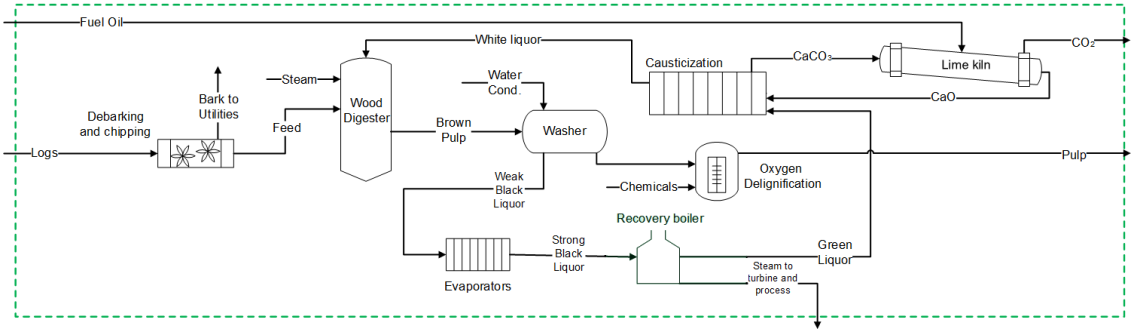

Figure D.1 Process flowsheet of pulp production mill.

The pulp yield is 46.51%wt. of the total amount of digested biomass, whereas black liquor production rate is 1.44 t_{BL}/t_{pulp} [22]. Power and steam demands are adapted for a pulp production of 877.83 t_{ADPulp}/d [23; 93]. According to Figure D.2, in the syngas production unit, the weak black liquor is firstly dried in a mechanical vapor recompression system. Subsequently, the strong black liquor is gasified in a pressurized reactor using oxygen (30 bar, 1000 °C), which

allows to recover the chemicals that are recycled back as green liquor to the digester. Next, the syngas obtained needs to be treated, purified and its composition must be adjusted before it enters to the ammonia loop. To this end, auto-thermal reformer, water gas shift, CO_2 capture and methanation systems are required. Finally, ammonia is produced in an intercooled catalyst bed, before it is chilled and separated for export (see Figure D.2). This process is modeled in Aspen Plus® software and the detailed description of the processes conditions is reported in [184]. For the CO_2 management, a set of option is defined. The CO_2 captured in the syngas purification unit could be dried, compressed and injected to a gas reservoir. It can be also liquefied and stored in a tank at -50 °C and 7 bar (1155 kg/m^3). It can be later fed to a methanation system, in which the hydrogen necessary is provided by a water electrolyzer with a specific electricity consumption of 55 kWh/kg$_{H2}$ [234]. The produced CH_4 is liquefied, stored at -162 °C and 1 bar (423 kg/m^3), and it can be later used in the synthetic natural gas furnace to substitute the consumption of fuel oil in the lime kiln of the kraft pulp mill. Another important CO_2 stream is the one present in the flue gas coming from the furnaces. This CO_2 can be captured in a CO_2 post-combustion system using chemical absorption solvent [97], at the expense of an specific steam consumption of 3.6 MJ/kg$_{CO2}$. Next, the purified CO_2 follows to the dryer and compression system either to be stored again or to be injected.

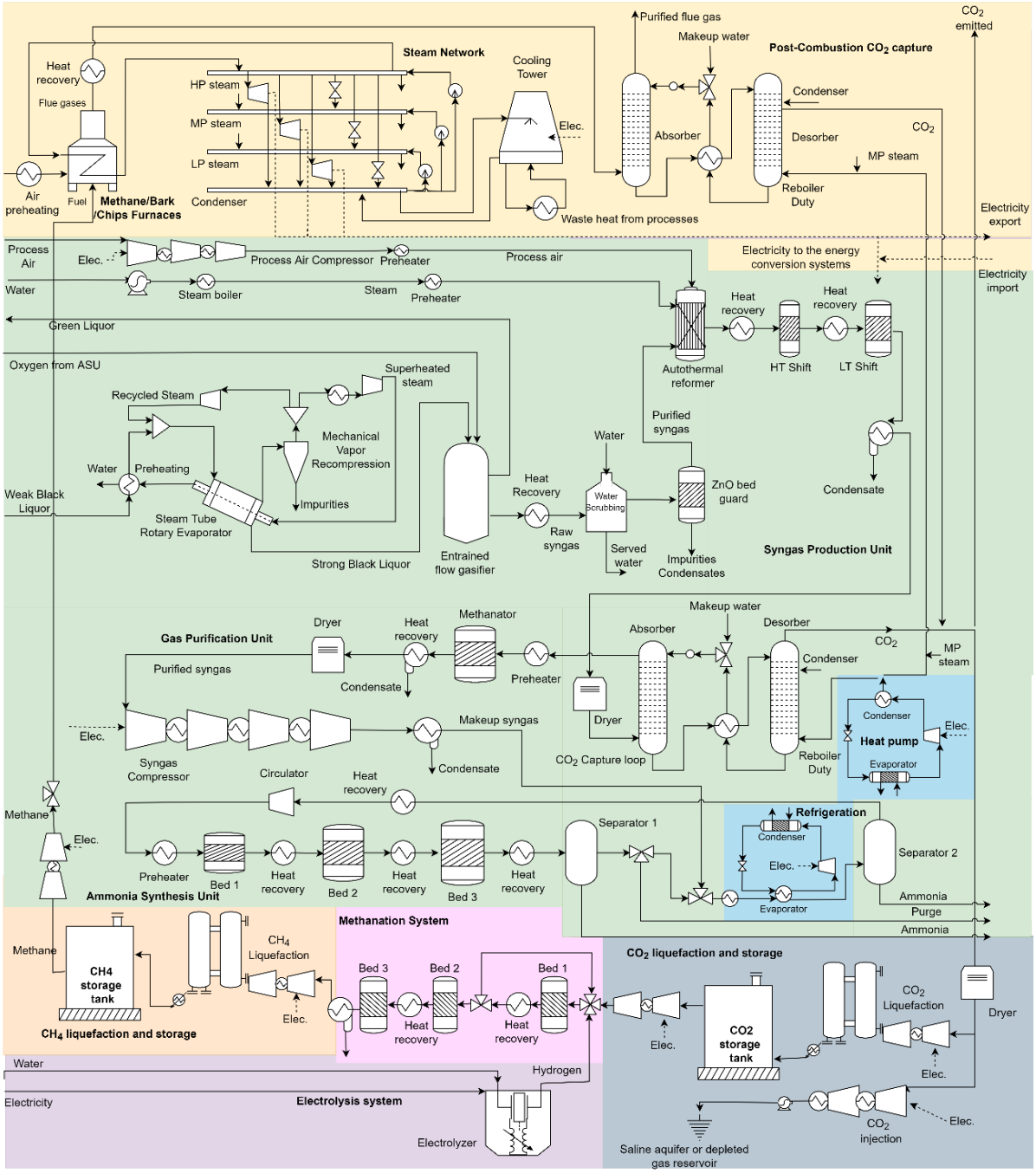

Figure D.2 Superstructure for the ammonia production via black liquor gasification integrated to a utility system, with post-combustion CO_2 capture, power-to-gas devices, liquids storage and injection units.

2.2 Optimization problem definition

The introduction of the new energy technologies shown in Figure D.2 entails the redefinition of the complete energy balance and calls for a systematic method and computational tool to perform a complex energy integration problem. The solution is handled by OSMOSE Lua platform, which finds the most appropriate utility systems and their respective operating conditions that lead to the lowest resources consumption and optimal operating cost

[97]. Data transfer with the ASPEN Plus® software is managed by this framework. The mixed integer linear programming (MILP) problem described in Equations (D.1-D.5) minimizes the objective function, Equation (D.1), and determines the binary variables y_w related to the selection of a given utility unit ω, and its corresponding continuous load factor, f_w.

$$\min_{\substack{f_\omega,\, y_\omega \\ R_r, W}} \left[\begin{array}{l} f_{chips} \times (B \cdot c)_{chips} + f_{wood} \times (B \cdot c)_{wood} + f_{oil} \times (B \cdot c)_{oil} \pm f_{\substack{power \\ grid}} \times (W \cdot c)_{\substack{power \\ grid}} \\ + f_{envEm} \times (m \cdot tax)_{envEm} + f_{water} \times (B \cdot c)_{water} + \dfrac{Z_{equip} * AF}{N_{hours\ per\ year}} \\ - f_{pulp} \times (B \cdot c)_{pulp} - f_{NH_3} \times (B \cdot c)_{NH_3} - f_{\substack{CO_2 market \\ or\ injected}} \times (m \cdot c)_{\substack{CO_2 market \\ or\ injected}} \end{array} \right] \quad \text{(D.1)}$$

Subject to:

Heat balance at the temperature interval *(r)*

$$\sum_{\omega=1}^{N_\omega} f_\omega q_{\omega,r} + \sum_{i=1}^{N} Q_{i,r} + R_{r+1} - R_r = 0 \quad \forall r = 1..N \quad \text{(D.2)}$$

Balance of produced/consumed power

$$\sum_{\omega=1}^{N_\omega} f_\omega W_\omega + \sum_{\substack{chemical \\ units}} W_{net} + W_{imp} - W_{\exp} = 0 \quad \text{(D.3)}$$

Existence and size of the utility unit

$$f_{\min,\omega} y_\omega \le f_\omega \le f_{\max,\omega} y_\omega \quad \forall \omega = 1..N_\omega \quad \text{(D.4)}$$

Feasibility of the solution (MER)

$$R_1 = 0,\ R_{N+1} = 0,\ R_r \ge 0 \ \text{and} \ W_{imp} \ge 0,\ W_{\exp} \ge 0 \quad \text{(D.5)}$$

where:

N is the number of temperature intervals defined by considering the supply and the target temperatures of the entire set of streams;

Q is the heat flow rate exchanged between the process streams ($Q_{i,r} > 0$ for hot stream, $Q_{i,r} < 0$ for cold stream);

R is the heat flow rate cascaded from higher (*r+1*) to lower (*r*) temperature intervals (kW);

N_w is the number of units in the set of utility systems;

B is the exergy flow rate (kW) of the resources going in and out of the plant;

c is the purchasing cost (euro per kWh, m^3 or kg) of the feedstock, electricity consumed and CO_2 taxed, or the selling price of the marketable pulp, ammonia, surplus power and CO_2 produced (marketed or injected);

q is the heating/cooling flow rates supplied by the utility systems (kW);

W is the power produced by either the utility systems, the chemical processes themselves or imported from/exported to the grid (kW).

Equations (D.6) and (D.7) are the balance equations for the amount of liquefied gases stored in the tanks:

$$Storage\,level_t = f_{\tan k,t} \tag{D.6}$$

$$Storage\,level_{t+1} - Storage\,level_t = Mass\ or\ Energy\ Inlet_t - Mass\ or\ Energy\ Outlet_t \tag{D.7}$$

The utility units are modeled via equation-oriented subroutines [66], which requires additional equations for mass and energy balances for water, biomass, syngas, ammonia, pulp, methane, carbon dioxide, power, and heat flows between units. The steam network is responsible for recovering the waste heat produced in the chemical plant, which directly impacts the fuel import. The optimal steam levels are determined by examining the grand composite curve of the chemical process. The choice of importing electricity from the grid or purchasing additional fuel will depend on the performance of the cogeneration systems, and also on the respective cost associated to the electricity and wood chips. The furnace models consider the thermophysical properties of the fuels and the stoichiometric molar air to fuel ratio. The cooling tower assumes supply and return temperatures of 12 °C and 40 °C, respectively, with a consumption of electricity of 0.021 kW_{el}/kW_{th} [152] per unit of cooling duty. The methanation system is based on the intercooled TREMP® process [120].

The market prices of the feedstock and the products considered are summarized in Table D.1. The carbon tax for fossil emissions and the credits for biogenic CO_2 injection are both set as 100 EUR/t_{CO2}, in agreement with the scenario of Net Zero Emissions by 2050 [191].

Table D.1 Market costs and selling prices for feedstock and products.

	Market cost/selling price	**Reference**
Wood	0.013 EUR/kWh	[235]
Chips	0.016 EUR/kWh	[235]
Oil	0.018 EUR/kWh	[236]
Pulp	0.144 EUR/kWh	[145]
Ammonia	0.098 EUR/kWh	[14]
CO_2 exported	0.0084 EUR/kg	[151]

According to Table D.2, cheap electricity prices are considered during the period of March-October as distributed electricity generation by prosumers is higher, whereas expensive electricity costs are considered during November-February periods (dunkelflaute). This assumption allows to simulate not only the seasonal energy costs of intermittent and renewable

energy resources, but also to elucidate the factors that affect the energy and CO_2 management of the integrated pulp and ammonia production system in the second case study. In other words, the optimization routine must work out the best configurations for CO_2 management when capture, storing, injection or power-to-gas approaches for fuel production are adopted.

Table D.2 Monthly electricity costs assumed over a year.

Month	Electricity cost (EUR/kWh)
Jan	0.35
Feb	0.35
Mar	0.001
Apr	0.001
May	0.001
Jun	0.001
Jul	0.001
Aug	0.001
Sep	0.001
Oct	0.001
Nov	0.35
Dec	0.35

2.3 Performance indicators

Thermodynamic, economic and environmental aspects are considered to define suitable indicators to evaluate and compare the case 1 and 2, and they are described next.

2.3.1 Exergy efficiencies

Two exergy efficiency definitions are used to compare the studied scenarios. The rational exergy efficiency, Equation (D.8), considers does not discern the useful output of the integrated energy systems (ammonia and pulp), but considers the total exergy output (*B in kW*) as the product (including CO_2, purge gas, power). This value overestimates the efficiency of the energy conversion system, as it assigns value to residual exergy that otherwise could have been also converted into one of the two main products.

$$\eta_{\text{Rational}} = \frac{B_{useful,output}}{B_{input}} = 1 - \frac{B_{Dest}}{B_{input}} = 1 - \frac{B_{Dest}}{B_{oil/natural\,gas} + B_{wood} + B_{chips} + W_{net}} \quad \text{(D.8)}$$

On the other hand, the relative exergy efficiency, Equation (D.9), quantifies the deviation from the minimum theoretical exergy consumption necessary to make up the main industrial products, i.e. pulp and ammonia:

$$\eta_{\text{Relative}} = \frac{B_{consumed,\,ideal}}{B_{consumed,\,actual}} = \frac{B_{ammonia} + B_{pulp}}{B_{oil/natural\,gas} + B_{wood} + B_{chips} + W_{net}} \quad \text{(D.9)}$$

In Equations (D.8) and (D.9), the total exergy input is the sum of all the energy resources consumed. In Equation(D.9), B_{Dest} stands for the exergy destruction, estimated considering all the subunits that compose each case study. The specific chemical exergy is 21.23 MJ/kg_{dry} for wood, 20.13 MJ/kg_{dry} for bark, 12.08 MJ/kg_{dry} for black liquor, 43.38 MJ/kg_{dry} for oil, 19.80 MJ/kg_{dry} for pulp, and for methane (50 MJ/kg_{CH4}) [237]. In addition, the extended exergy analysis takes into account the efficiency of the electricity generation (55.68%), as well as the oil (95.20%) and biomass (86.13%) supply chains reported in [11; 139].

2.3.2 CO_2 emissions balance

Both overall and net CO_2 emissions balances are calculated according to Equations (D.10) and (D.11), respectively. The former accounts for the total amount of CO_2 emitted, including from fossil or biogenic sources. Meanwhile, the latter considers that the absorption and release of CO_2 during biomass growth and conversion steps is cyclical, thus biogenic emission are neglected. Both balances consider the abated emissions in the capture unit.

$$\text{Overall } CO_{2\text{emissions}} = Oil^{\text{direct}}_{\text{emissions}} + EE^{\text{indirect}}_{\text{emissions}} + Wood^{\text{indirect}}_{\text{emissions}} + Oil^{\text{indirect}}_{\text{emissions}} + Biogenic^{\text{direct}}_{\text{emissions}} - CO_{2\text{captured}} \quad \text{(D.10)}$$

$$\text{Net } CO_{2\text{emissions}} = Oil^{\text{direct}}_{\text{emissions}} + EE^{\text{indirect}}_{\text{emissions}} + Wood^{\text{indirect}}_{\text{emissions}} + Oil^{\text{indirect}}_{\text{emissions}} - CO_{2\text{captured}} \quad \text{(D.11)}$$

The indirect CO_2 emissions associated with the fossil fuel consumption in the upstream supply chains are assumed, respectively, as 0.0029 and 0.0043 gCO_2 per kJ of oil and wood; and 62.09 gCO_2 are indirectly emitted per kWh of electricity [139].

2.3.3 Calculation of investment costs

Equation (D.12) is used to estimate the capital expenditure (CAPEX) of the main plant equipment, by correlating the actual capacity (S_1) of each unit to a reference capacity (S_0) with known capital cost (C_0). A power scaling factors (r) that varies depending on the type of process is considered [153]. The capex for the integrated pulp and ammonia production is retrieved from [238]. For the electrolyzer, an average investment cost price of 1200 USD/kW_e is considered [239]. The specific average investment cost for the methanation system is 300 EUR/kW_{CH4} according to [240]. The capex of the cooling tower is correlated in [241]. The investment cost of the carbon

capture unit is reported in [242], while the cost of heat pumping and refrigeration systems is reported by [243].

$$C_1 = C_0 \left(\frac{S_1}{S_0} \right)^r \quad \text{(D.12)}$$

3. Results and discussion

The results of the optimal processes parameters for case 1 and 2 are summarized in Tables D.3 and D.4, respectively. It must be born in mind that the ammonia and pulp production rates (218.93 t_{NH3}/d and 877.83 t_{Pulp}/d) are fixed for both cases. The power demand of the pulping system alone attains 2.84 GJ/t_{Pulp}, the black liquor treatment and drying processes consume 1.2 GJ/t_{Pulp}, and the syngas conditioning and ammonia synthesis consume 0.58 GJ/t_{Pulp} of power [184].

In case 1, the extended exergy consumption, which considers the upstream supply chain, is 16-21% higher than the plantwide energy consumption. This value varies between 16-25% in the case study 2. The small difference is attributable to the slight increase in energy consumption to drive the additional energy technologies in the case 2. The power generation of the Rankine cycle is also slightly increased in the case 2, if compared to the case 1, especially during the March-October period, in which monthly power generation is as high as twice that of the remaining months, due to the interest in converting surplus CO_2 into synthetic natural gas that will be used in the season of higher electricity costs. For this reason, the electricity export is also reduced in the case 2, aiming to satisfy the internal energy demands, instead of using the waste heat for exporting electricity that could be rather transformed into synthetic natural gas or used to inject more CO_2 to attain a lower emission factor. This is in agreement with a strategy of benefiting from the carbon credits derived from the carbon taxed scenarios. In this regard, the amount of CO_2 injected in the case 2 is for most of the year much larger than the CO_2 vented from the syngas purification unit of the integrated pulp and ammonia production plant of case 1. The seek for a maximum injection is a result of the CO_2 management of the system, which adopts a radical CO_2 abatement approach at the expense of a higher power consumption in the injection compression battery.

Table D.3 Optimal process parameters for case 1, without carbon management and power-to-gas systems.

Process parameter	Jan	Feb	Mar	Apr	May	Jun	Jul	Aug	Sep	Oct	Nov	Dec
Feedstock wood consumption (GJ/t_{Pulp})	41.15	41.15	41.15	41.15	41.15	41.15	41.15	41.15	41.15	41.15	41.15	41.15
Utility chips consumption (GJ/t_{Pulp})	20.72	20.72	0	0	0	0	0	0	0	0	20.72	20.72
Utility electricity consumption (GJ/t_{Pulp})	0	0	4.13	4.13	4.13	4.13	4.13	4.13	4.13	4.13	0	0
Oil consumption (GJ/t_{Pulp})	1.05	1.05	1.05	1.05	1.05	1.05	1.05	1.05	1.05	1.05	1.05	1.05
Overall plant consumption (GJ/t_{Pulp})	62.92	62.92	46.33	46.33	46.33	46.33	46.33	46.33	46.33	46.33	62.92	62.92
Extended plant consumption (GJ/t_{Pulp})	72.93	72.93	56.29	56.29	56.29	56.29	56.29	56.29	56.29	56.29	72.93	72.93
Rankine cycle power generation (GJ/t_{Pulp})	9.13	9.13	1.35	1.35	1.35	1.35	1.35	1.35	1.35	1.35	9.13	9.13
Ancillary power demand (GJ/t_{Pulp})	0.49	0.49	0.22	0.22	0.22	0.22	0.22	0.22	0.22	0.22	0.49	0.49
Biomass consumption ($t_{Wood}/t_{NH3+Pulp}$)	3.88	3.88	2.58	2.58	2.58	2.58	2.58	2.58	2.58	2.58	3.88	3.88
Marketable CO_2 production (kg/h)	50518	50518	50518	50518	50518	50518	50518	50518	50518	50518	50518	50518
Electricity export (kW)	34405.55	34405.55	0	0	0	0	0	0	0	0	34405.55	34405.55

Table D.4 Optimal process parameters for case 2, with carbon management and power-to-gas systems.

Process parameter	Jan	Feb	Mar	Apr	May	Jun	Jul	Aug	Sep	Oct	Nov	Dec
Feedstock wood consumption (GJ/t_{Pulp})	41.15	41.15	41.15	41.15	41.15	41.15	41.15	41.15	41.15	41.15	41.15	41.15
Utility chips consumption (GJ/t_{Pulp})	20.72	20.72	2.64	2.64	2.64	2.64	2.64	2.64	2.64	2.64	20.72	20.72
Utility electricity consumption (GJ/t_{Pulp})	0	0	7.15	7.15	7.15	7.15	4.15	7.15	7.15	7.15	0	0
Overall plant consumption (GJ/t_{Pulp})	61.87	61.87	50.93	50.93	50.93	50.93	47.94	50.93	50.93	50.93	61.87	61.87
Extended plant consumption (GJ/t_{Pulp})	71.83	71.83	63.67	63.67	63.67	63.67	58.29	63.67	63.67	63.67	71.83	71.83
Rankine cycle power generation (GJ/t_{Pulp})	9.15	9.15	2.57	2.57	2.57	2.57	2.19	2.57	2.57	2.57	9.15	9.15
Ancillary power demand (GJ/t_{Pulp})	0.49	0.49	0.22	0.22	0.22	0.22	0.22	0.22	0.22	0.22	0.49	0.49
Biomass consumption ($t_{Wood}/t_{NH3+Pulp}$)	3.88	3.88	2.75	2.75	2.75	2.75	2.75	2.75	2.75	2.75	3.88	3.88
CO_2 injected (kg/h)	46246.47	40416.28	69292.83	69292.83	69292.833	69292.83	59190.95	69292.83	69292.83	69292.83	50518.16	50518.16
Electricity export (kW)	28612.22	28682.18	0	0	0	0	0	0	0	0	28560.96	28560.96

Figures D.3 and D.4 show the breakdown of the monthly energy input (i.e. chips, electricity from grid, and oil) for cases 1 and 2, respectively. As expected, the extent of consumption of each fuel is strongly linked to the seasonal electricity prices defined in Table 2. Interestingly, the fuel oil consumed in case 1 to fire the lime kiln can be replaced by the synthetic natural gas that is produced in the power-to-gas system implemented in case 2. In this way, the new solution adopted in the case 2 represents a change of paradigm with respect to the case 1, as it allows ruling out the only direct fossil emissions associated to the integrated pulp and ammonia production.

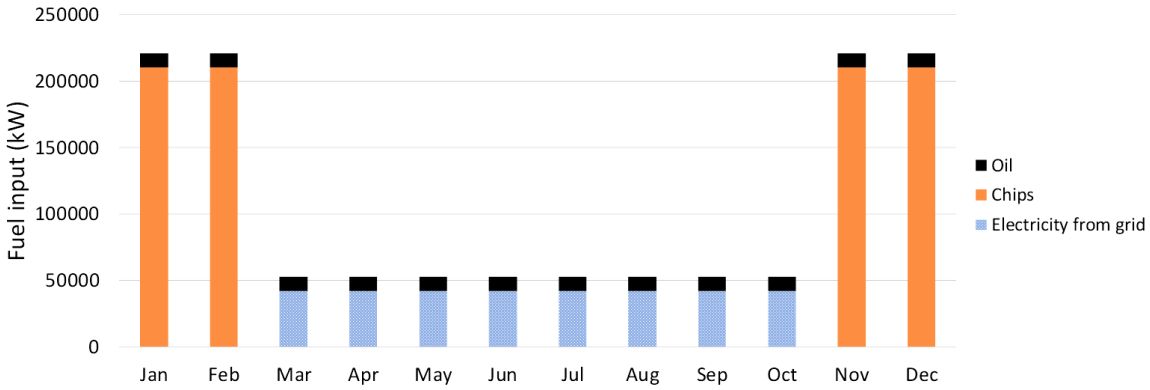

Figure D.3 Monthly fuel and electricity consumption for case 1. Ammonia and pulp production rates are 218.93 t_{NH3}/d and 877.83 t_{Pulp}/d, respectively.

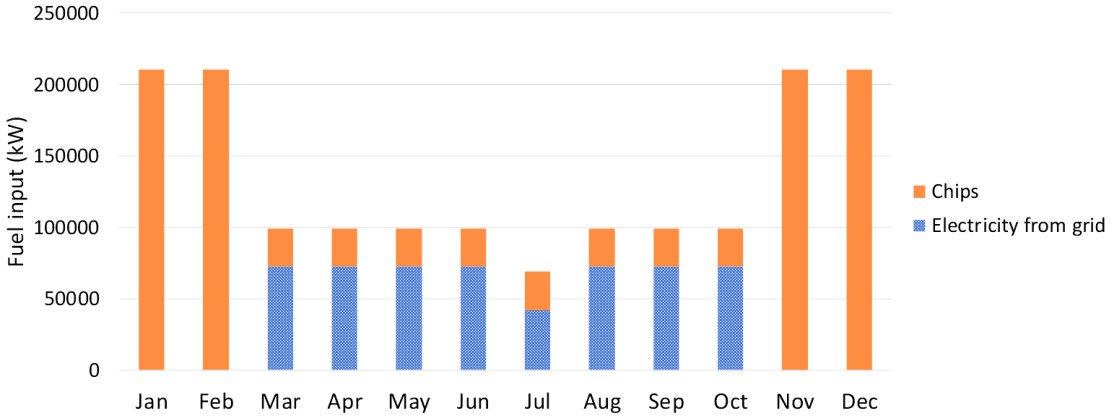

Figure D.4 Monthly fuel and electricity consumption for case 2. Ammonia and pulp production rates are 218.93 t_{NH3}/d and 877.83 t_{Pulp}/d, respectively.

It is also worth noticing an almost invariable consumption of wood chips during the November-February period, mainly as an adaptation to higher electricity prices and more affordable sources of renewable energy, such as biomass. Also, during this period, the synthetic natural gas produced helps reducing the overall energy import, as it can be seen from the monthly variation of methane and carbon dioxide storage, shown in Figure D.5. Advanced

energy conversion technologies, such as the carbon abatement units and the liquid fuel storage, are crucial to ensure a reliable operation of the cogeneration systems, especially when it comes to the reliability of the electricity supply. In this regard, the CO_2 is recirculated and feed to the methanator only during the months in which the electricity price is low enough, so that it barely impacts the overall economic and environmental performances. According to Figure D.5, stored fuel is preferably used in the months in which the electricity price is high, avoiding a large import of costly electricity from the grid.

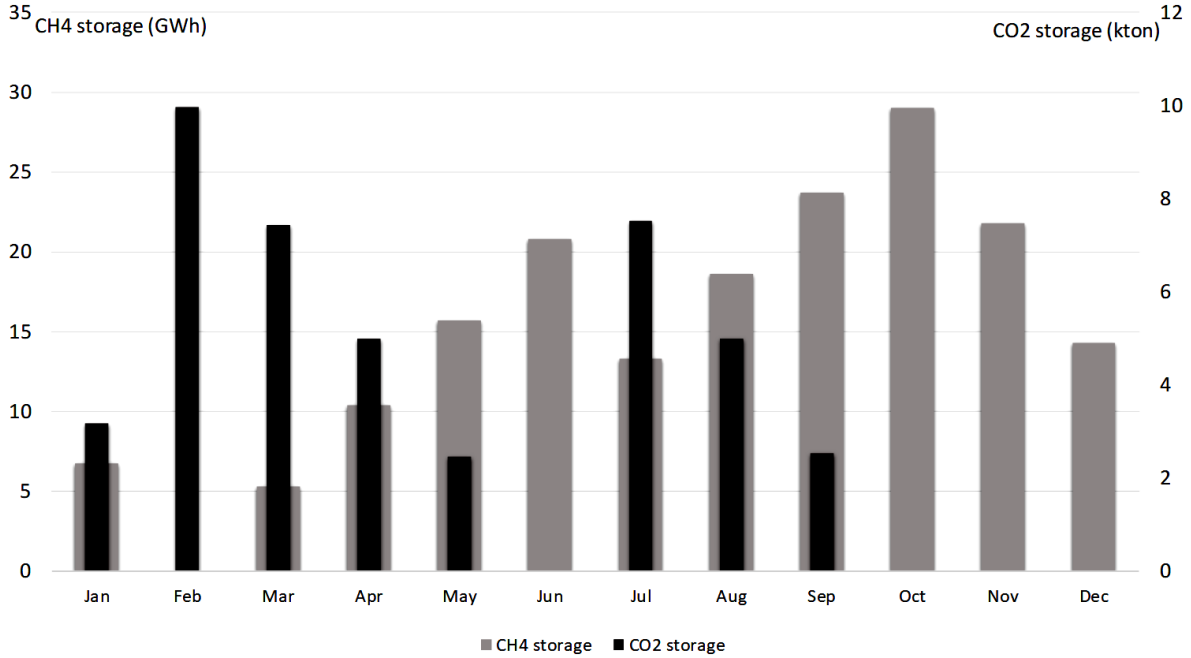

Figure D.5 Monthly variation of methane and carbon dioxide storage for case 2.

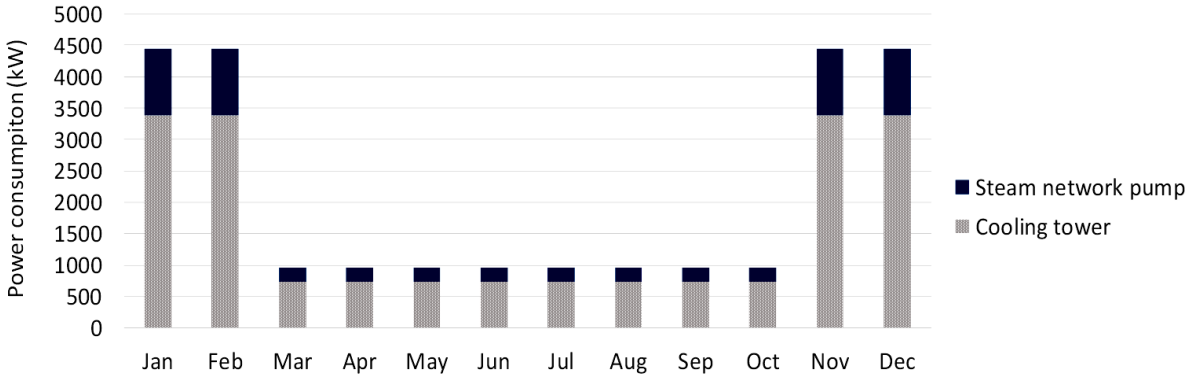

Figure D.6 Monthly power consumption for case 1.

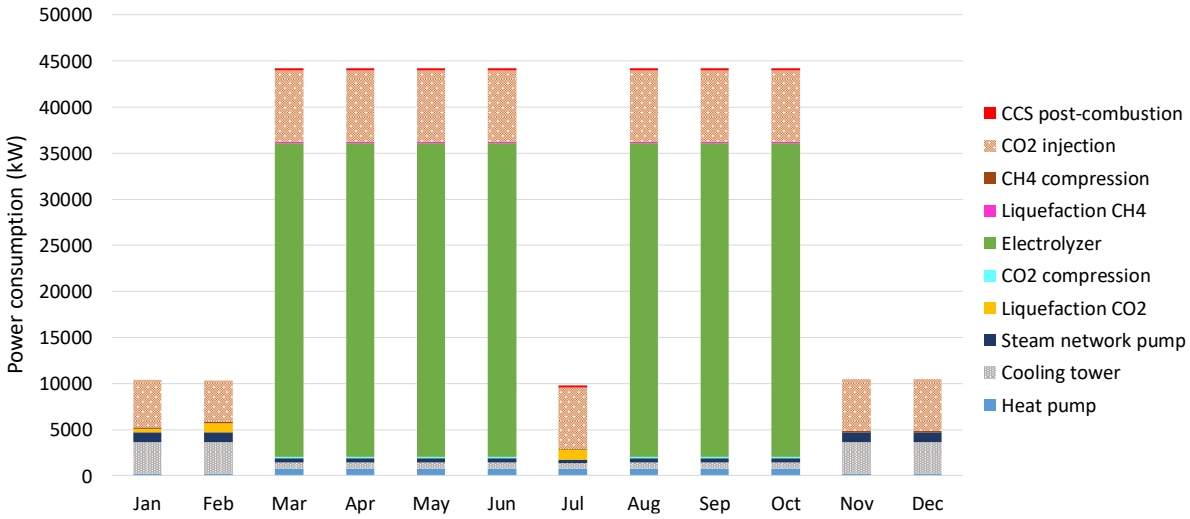

Figure D.7 Monthly power consumption for case 2.

Notwithstanding, for the case 2, larger steam network and cooling units are necessary to recover the waste heat from the chemical processes, to cogenerate the required power for CO_2 and SNG management (i.e. electrolysis, storage, injection) and to evacuate residual heat (see Figures D.6-D.7). The enlarged steam network slightly hinders the overall efficiency of the process studied in case 2, as reported in Tables D.5 and D.6. Meanwhile, by importing electricity from the grid, the exergy efficiencies of both cases can be improved up to five percentage points, compared to the period in which electricity is not substantially imported. In fact, both case studies present higher efficiency when operating during the period of March-October, since the importation of electricity reduces the need for internal cogeneration and, thus, it also reduces the irreversibility of both scenarios. As it concerns the exergy destruction indicator, case 2 presents a slightly better performance, compared to case 1, especially during the months in which electrolysis system is not activated and CO_2 storage is enabled. However, exergy destruction during the period of November-February is comparable in both cases, although the environmental emissions are quite different, being case 2 more environmentally favorable. In addition, the extended exergy analysis shows that, by including the upstream inefficiencies of the supply chains, the performance of the two cases may drop from 13% up to 20% with respect to the plantwide performance only. Thus, the inefficiencies associated with the obtainment of the energy resources should not be neglected in the early stages of the comparative analyses between the traditional and alternative setups that aim to support the decision-making.

The yearly indirect, direct and avoided CO_2 emissions, as well as yearly net and overall CO_2 balances for cases 1 and 2 are presented in Table D.7. Notably, the direct CO_2 emissions from the only fossil resource (i.e. oil combustion in the lime kiln) can be eliminated thanks to

the use of the synthetic natural gas that is produced in the case 2. However, the indirect emissions associated to biomass and electricity supply chains still represent a challenge for the decarbonization of the extended production process. The biomass consumption, either as fuel or feedstock, is responsible for 73% of the indirect CO_2 emissions in the case 2, whereas the electricity import is almost one-fourth of those emissions. Thus, even though both energy resources are typically assumed as renewable in the plantwide scope, it is evident that this fact does not imply that they are emissions-free in a broader scope.

Anyhow, considering the sustainable development scenario for ammonia production, the integration of the advanced energy systems based on renewable energy resources is expected to cut down by 75% the atmospheric emissions of ammonia production until 2050 [191]. In this regard, the integration of the CO_2 management systems not only contributes by already reducing up to 31% the net CO_2 emissions in the case 2, but also may help increasing the financial attractiveness of the alternative setups (see Table D.8). Indeed, additional incomes from the biogenic CO_2 injection occurring in case 2 overcome the incremental investment costs necessary to implement the proposed CO_2 management-based setup. The expectative in the long-term scenarios is that the electrolysis and the methanation technologies become cheaper [244], which could favor further the deployment of those technologies and its integration into the existing biomass-based industrial facilities. In conclusion, the proposed approach capitalizes on the improvement of the scheduling and rational use of the resources, while encourages the recycling and the depletion of the atmospheric carbon, even offsetting the indirect emissions coming from the hard-to decarbonize supply chains (e.g. energy transportation).

Table D.5 Exergy performance indicators for case 1.

Process parameter	Jan	Feb	Mar	Apr	May	Jun	Jul	Aug	Sep	Oct	Nov	Dec
Rational exergy efficiency (%)	43.55	43.55	51.83	51.83	51.83	51.83	51.83	51.83	51.83	51.83	43.55	43.55
Extended rational exergy efficiency (%)	37.57	37.57	42.66	42.66	42.66	42.66	42.66	42.66	42.66	42.66	37.57	37.57
Relative exergy efficiency (%)	36.22	36.22	49.19	49.19	49.19	49.19	49.19	49.19	49.19	49.19	36.22	36.22
Extended relative exergy efficiency (%)	31.24	31.24	40.48	40.48	40.48	40.48	40.48	40.48	40.48	40.48	31.24	31.24
Exergy destruction (GJ/t_{Pulp})	35.52	35.52	22.31	22.31	22.31	22.31	22.31	22.31	22.31	22.31	35.52	35.52
Extended exergy destruction (GJ/t_{Pulp})	45.53	45.53	32.28	32.28	32.28	32.28	32.28	32.28	32.28	32.28	45.53	45.53

Table D.6 Exergy performance indicators for case 2.

Process parameter	Jan	Feb	Mar	Apr	May	Jun	Jul	Aug	Sep	Oct	Nov	Dec
Rational exergy efficiency (%)	43.28	43.17	47.60	47.60	47.60	47.60	50.31	47.60	47.60	47.60	43.36	43.36
Extended rational exergy efficiency (%)	37.28	37.19	38.08	38.08	38.08	38.08	41.38	38.08	38.08	38.08	37.34	37.34
Relative exergy efficiency (%)	36.83	36.83	44.74	44.74	44.74	44.74	47.53	44.74	44.74	44.74	36.83	36.83
Extended relative exergy efficiency (%)	31.72	31.72	35.79	35.79	35.79	35.79	39.09	35.79	35.79	35.79	31.72	31.72
Exergy destruction (GJ/t_{Pulp})	35.09	35.16	26.69	26.69	26.69	26.69	23.82	26.69	26.69	26.69	35.04	35.04
Extended exergy destruction (GJ/t_{Pulp})	45.05	45.12	39.42	39.42	39.42	39.42	34.17	39.42	39.42	39.42	45.00	45.00

Table D.7 Indirect, direct and avoided CO_2 emissions for case 1 and case 2.

	Case 1	**Case 2**
Indirect fossil CO_2 emissions (t_{CO2}/y):	82307	93619
• *electricity (%)*	18.62	26.82
• *wood (%)*	68.87	60.55
• *chips (%)*	11.40	12.63
• *oil (%)*	1.11	
Direct fossil CO_2 emissions (t_{CO2}/y)	24293	-
Direct biogenic emissions (t_{CO2}/y)	281098	236044
CO_2 emissions avoided (t_{CO2}/y):		
• *Captured in the ammonia plant*	442539	442539
• *Captured in post-combustion*	-	110395
• *Injected*	-	535451
Overall CO_2 balance (t_{CO2}/y)	**-54840**	**-205788**
Net CO_2 balance (t_{CO2}/y)	**-335939**	**-441832**

Table D.8 Operating incomes, costs, revenues, capital costs and total cost for cases 1 and 2.

	Case 1	**Case 2**
Operating incomes (MEUR/y)		
Pulp export	228.50	228.50
Ammonia export	43.24	43.24
Electricity export	34.68	28.83
CO_2 marketed [1]	3.72	-
CO_2 injected [2]	-	53.55
Total operating incomes (MEUR/y)	***310.14***	***354.12***
Operating costs (MEUR/y):		
Wood import	-47.61	-47.61
Chips import	-9.70	-12.22
Oil import	-1.57	
Water import	-3.25	-3.29
Electricity import	-0.25	-0.40
CO_2 taxed [3]	-10.66	-9.36
Total operating costs (MEUR/y)	***-73.04***	***-82.40***
Annualized capital cost (MEUR/y)	-19.16	-36.80
Total capital and operating cost (MEUR/y)	***-217.94***	***-234.92***
Total plant revenues (MEUR/y)	***237.10***	***271.71***

1. Considering a CO_2 market price of 8.4 EUR/t_{CO2}. 2. CO_2 injection credit of 100 EUR/t_{CO2}. 3. CO_2 tax price of 100 EUR/t_{CO2}.

4. Conclusions

In this work, a systematic analysis of the integration of a pulp mill and an ammonia plant with CO_2 management systems is presented. The reuse of two common byproducts, one of the pulp mill (i.e. black liquor from the wood digestion process) and other from the ammonia plant (i.e. CO_2 separated at the syngas purification unit) is studied aiming to find synergies that

help increasing the energy integration and waste heat recovery of both chemical processes. In order to offset the intermittency and variable prices associated to the seasonal electricity generation during months of dark doldrums, the CO_2 streams are stored and consumed as a means to produce synthetic natural only when cheap electricity is available, in a power-to-gas approach that benefits from surplus electricity generation by prosumer during the remainder months. The power-to-gas system together with the liquefied gas storage units proved to be a key strategy that can supply the operation in a synergic and reliable way. The overall performance, including thermodynamic, economic and environmental indicators shows to be strongly dependent on the type of energy inputs consumed (either chips or electricity), as it impacts the carbon footprint associated to the supply chains thereof. For instance, up to 80% of the indirect emissions are due to the obtainment of the biomass, which shed lights on the importance of the extended exergy and environmental analyses of the typically known as biomass-based energy conversion systems. Anyhow, the opportunity of injecting biogenic CO_2 emissions actually increased the overall plant revenues by 15%, as the gain in performance with the more advanced energy management technologies allows offsetting the additional investment costs. The avoided CO_2 emissions can be also increased by 31%. Finally, the reliability of the two integrated plants is also increased, as the waste heat recovery potential is improved and the storage technologies behave as buffering systems that can compensate the seasonal intermittency of the renewable electricity generation plants.